

HEATH STEELE WASTE ROCK STUDY
PHASES 1 TO 3

MEND Project 2.31.1(a)

March 1992

HEATH STRELE WASTE ROCK STUDY

1990

REPORT

Our File No. H88113

Submitted to:

Brunswick Mining & Smelting Corporation Limited

by:

Nolan, Davis & Associates (N.S.) Limited
P.O. Box 1021, Armdale
6112 Quinpool Road
Halifax, Nova Scotia B3L 4K9

December 1990

EXECUTIVE SUMMARY

Sulphide ore mining in Northeast New Brunswick has produced waste piles containing acid generating pyritic rock. The generation of acidic drainage from these waste rock piles create immediate environmental control problems in addition to long-term reclamation challenges.

The Heath Steele property, located approximately 50 km northwest of Newcastle, New Brunswick and about 60 km southwest of Bathurst, was developed in the late 1950's. The highly pyritic waste rock at the site continues to pose a challenge to currently available reclamation technology.

A proposal was submitted to various federal and provincial agencies to use several of the waste rock piles at Heath Steele to develop and test strategies for the long-term management of acid generating waste rock. A four phase program was developed, and on December 16, 1988, an agreement to fund the first three phases was signed. This report describes the work comprising the first three phases of the project. Phase IV is the installation of an engineered cover, designed on the basis of the results of Phase III work, on one of the piles and the evaluation of the effect.

Phase I of the study involved the selection of four acid generating waste rock piles most amenable to monitoring and evaluation of remedial measures. Selection criteria and weighting factors were established and the piles were ranked. Piles identified as 18A, 18B, 17 and 7/12 were selected.

Phase II involved the installation of monitoring equipment to define the detailed characteristics and background data for the four piles identified in Phase I.

Piles 18A, 18B and 17 were contoured to provide 3: 1 slopes and ditched to divert surface water and runoff as well as isolating them from surrounding topographic influences. Waste rockpile 7/12 was moved, as part of the ongoing site reclamation program, onto an impermeable

membrane to permit the water balance to be evaluated before and after placement of the cover. **Leachate** collection was not possible at the insitu piles due to the fractured nature of the underlying bedrock. Each pile was instrumented to permit measurement of oxygen and temperature at various points throughout the pile.

In Phase III, the performance characteristics of natural soils in the vicinity of the Heath Steele mine site as potential engineered covers for the waste rock piles were determined. The study also developed the most appropriate cover design scenario for the waste rock piles.

The study involved site exploration for natural soil materials (such as tills, clays, and sand), laboratory geotechnical testing, column fabrication, testing of the soils for their hydraulic characteristics, and measurements of oxygen diffusion coefficients. Laboratory geotechnical testing consisted of measurements for grain size distribution, specific gravity, compaction and consolidation characteristics, and hydraulic conductivity. The hydraulic characteristics (moisture drainage curves) of these natural soils were also determined to assess the potential for their inclusion in composite or layered cover systems. The exploration for the soils was restricted to a 15 km radius of the mine site, since soils located at greater distances would not be economical.

A composite soil cover was designed using natural soil materials. The proposed cover system of a 3-layer composite cover, consisting of a fine-grained saturated till, sandwiched between two coarse-grained layers, will be an effective oxygen barrier. If the till is compacted and placed at a water content slightly wet of optimum, it can be expected to have a low hydraulic conductivity and be an effective water barrier as well. Computer modelling indicated that much lower oxygen fluxes can be expected from this composite system than from a single till layer.

L'extraction de minerais **sulfurés** dans le nord-est du Nouveau-Brunswick a laissé des résidus contenant des roches pyritiques acidogènes. Le drainage acide produit par des tas de stériles crée un problème de pollution de l'environnement en plus de constituer un obstacle à la restauration à long terme.

La propriété Heath Steele, située à environ 50 km au nord-ouest de Newcastle (Nouveau-Brunswick) et à environ 60 km au sud-ouest de Bathurst, a été mise en valeur à la fin des années 1950. Les stériles à forte teneur en roches pyritiques, accumulés au site, continuent de constituer un obstacle pour la technologie de restauration actuelle.

Une proposition a été présentée à différents organismes fédéraux et provinciaux pour que plusieurs tas de stériles accumulés à Heath Steele soient utilisés pour élaborer et mettre à l'essai des stratégies de gestion à long terme des stériles acidogènes. Un programme de quatre phases a été mis sur pied, et le 16 décembre 1988, un accord de financement des trois premières phases a été conclu. Le présent rapport décrit les travaux des trois premières phases du projet. La phase IV consiste à mettre en place une couverture sèche conçue en se basant sur les résultats des travaux de la phase III, sur l'un des tas et évaluer les effets.

La phase I de l'étude consiste à choisir quatre tas de stériles acidogènes qui se prêtent bien à la surveillance et à l'évaluation de mesures correctives. Des critères de sélection et des facteurs de pondération ont été établis et les tas ont été classés. Les quatre tas choisis sont 18A, 18B, 17 et 7/12.

À la phase II, on a installé des instruments de surveillance afin de déterminer les caractéristiques et les données de base des quatre tas choisis à la phase I.

Les tas 18A, 18B et 17 ont été façonnés pour obtenir une pente de 3/1, et des fossés ont été creusés pour faire dévier l'eau superficielle et l'eau de ruissellement et pour isoler les tas des formes de relief environnantes. Le tas 7/12 a été déplacé dans le cadre du programme de

restauration du site, sur une membrane imperméable pour évaluer l'équilibre hydrique avant et après la mise en place de la couverture. Il n'a pas été possible de recueillir les lixiviats issus des tas in situ étant donné que le socle sous-jacent est fracturé. Chaque tas a été instrumenté pour y mesurer la teneur en oxygène et la température en divers points.

À la phase III, les caractéristiques de rendement des sédiments naturels reposant dans le voisinage du site de la mine Heath Steele ont été déterminées en fonction de leur utilisation possible comme couvertures sèches des tas de stériles. L'étude a également permis de concevoir la couverture la plus appropriée aux tas de stériles.

L'étude a notamment comporté une exploration du site pour déterminer les sédiments naturels (till, argile et sable), des essais géotechniques en laboratoire, la fabrication de colonnes, des essais pour déterminer les caractéristiques hydrauliques des sédiments et des mesures des coefficients de diffusion de l'oxygène. Les essais géotechniques en laboratoire ont consisté à mesurer la granulométrie, la densité, les caractéristiques de compaction et de consolidation et la conductivité hydraulique des sédiments. Les caractéristiques hydrauliques (courbes humidité/drainage) de ces matériaux naturels ont également été déterminées pour évaluer la possibilité de les inclure dans les couvertures à système composite ou stratifié. L'exploration des sols s'est limitée à un rayon de 15 km autour du site de la mine, étant donné que l'utilisation de sédiments situés à une plus grande distance ne serait pas économique.

Une couverture de sol composite comportant des sédiments naturels a été conçue. La couverture proposée de trois couches, c'est-à-dire une couche de till saturé à grain fin intercalée entre deux couches de sédiments à grain grossier, servira de barrière efficace de l'oxygène. Si le till est compacté et mis en place à une teneur en eau dépassant légèrement la teneur optimale, il pourrait présenter une conductivité hydraulique faible et servir de barrière d'eau efficace. La modélisation informatique a révélé que l'on peut s'attendre à des flux d'oxygène beaucoup plus faibles dans ce système composite que dans un système à couche de till unique.

TABLE OF CONTENTS

| | Page No. |
|---|----------|
| Table of Contents | ii |
| Acknowledgments | vii |
| | |
| 1.0 INTRODUCTION | 1 |
| 1.1 Historical Review | 1 |
| 1.2 Project Objectives | 3 |
| 1.3 Selection of Study Waste Rock Piles (Phase I) | 4 |
| 1.4 Laboratory Evaluation of Potential Cover Materials (Phase III) | 8 |
| | |
| 2.0 METHODS OF INVESTIGATION | 10 |
| 2.1 Local Meteorology | 10 |
| 2.1.1 Precipitation | 10 |
| 2.1.2 Evaporation | 10 |
| 2.1.3 Temperature | 10 |
| 2.2 Instrumentation and Monitoring of Waste Piles | 11 |
| 2.2.1 General | 11 |
| 2.2.2 Site Preparation | 11 |
| 2.2.2.1 Relocation of Pile 7/12 | 12 |
| 2.2.3 Instrument-Installation | 21 |
| 2.2.3.1 Pore Gas Instrumentation | 21 |
| 2.2.3.2 Temperature Measurement | 26 |
| 2.2.3.3 Seepage and Runoff | 27 |
| 2.2.4 Water and Contaminant Balance | 31 |
| 2.2.5 Waste Rock Pile Characteristics | 31 |
| 2.2.6 Mineralogy and Composition | 32 |
| 2.2.7 Hydraulic Conductivity | 33 |
| | |
| 3.0 RESULTS AND DISCUSSION | 36 |
| 3.1 Local Meteorology | 36 |
| 3.1.1 Precipitation | 36 |
| 3.1.2 Evaporation | 36 |
| 3.1.3 Temperature | 36 |

TABLE OF CONTENTS (contd.)

| | Page No. |
|---|----------|
| 3.2 Pile 18A | 42 |
| 3.2.1 Description of Pile | 42 |
| 3.2.2 Data Presentation | 42 |
| 3.2.3 Interpretation | 43 |
| 3.3 Pile 18B | 51 |
| 3.3.1 Description of Pile | 51 |
| 3.3.2 Data Presentation | 51 |
| 3.3.3 Interpretation | 51 |
| 3.4 Pile 17 | 59 |
| 3.4.1 Description of Pile | 59 |
| 3.4.2 Data Presentation | 59 |
| 3.4.3 Interpretation | 59 |
| 3.5 Pile 7/12 | 69 |
| 3.5.1 Description of Pile | 69 |
| 3.5.2 Data Presentation | 69 |
| 3.5.3 Interpretation | 69 |
| | |
| 4.0 COMPARATIVE REVIEW | 78 |
| 4.1 Comparison to Rum Jungle. | 84 |
| | |
| 5.0 CONCLUSIONS AND RECOMMENDATIONS | 86 |
| | |
| REFERENCES | 87 |

LIST OF TABLES:

| | |
|---|----|
| 1-1 Components of Criteria Used in Waste Rock Pile Assessment | 5 |
| 1-2 Pile Ranking (20 May, 1987) - Initial Assessment of Waste Rock Piles | 6 |
| 1-3 Pile Ranking - Second Review of Sites | 7 |
| 1-4 Summary of Study Pile Characteristics | 9 |
| | |
| 2-1 Analysis of Waste for Acid-Producing Potential | 33 |
| 2-2 Void Ratio Evaluation | 35 |

TABLE OF CONTEXTS (contd.)

| | Page No. |
|--|----------|
| 3-1 Historic Climatological Data | 37 |
| 3-2 Pile 18A - Temperature Data | 45 |
| 3-3 Pile 18A - Oxygen Concentrations | 46 |
| 3-4 Pile 18B - Temperature Data | 53 |
| 3-5 Pile 18B - Oxygen Concentrations | 54 |
| 3-6 Pile 17 - Temperature Data | 61 |
| 3-7 Pile 17 - Oxygen Concentrations | 62 |
| 3-8 Water Quality Data - Pile 17 | 63 |
| 3-9 Pile 7/12 - Temperature Data | 71 |
| 3-10 Pile 7/12 - Oxygen Concentrations | 72 |
| 3-11 Water Quality Data - Pile 7/12 | 73 |

LIST OF FIGURES:

| | |
|---|----|
| 1-1 Waste Rock Disposal Sites Location Map | 2 |
| 2-1 Pile Configuration and Instrument Locations - Piles 18A and 18B | 13 |
| 2-2 Pile Configuration and Instrument Locations - Pile 17 | 14 |
| 2-3 Pile Configuration and Instrument Locations - Pile 7/12 | 15 |
| 2-4 Photograph of Piles - Pile 18A Prior to Contouring | 16 |
| 2-5 Photograph of Piles - Pile 18B Prior to Contouring | 17 |
| 2-6 Photograph of Piles - Pile 18B Recontouring | 18 |
| 2-7 Photograph of Piles - Pile 17 After Contouring | 19 |
| 2-8 Photograph of Piles - Pile 7/12 | 20 |
| 2-9 Photograph of Typical Sampling Station | 22 |
| 2-10 Typical Gas Sampling and Piezometer Installation - Heath Steele Mines | 23 |
| 2-11 Photograph of Typical Piezometer/Gas Sampling Array Prior to Installation | 24 |
| 2-12 Photograph of Pore Gas Monitoring | 25 |
| 2-13 Typical Thermocouple Installation | 28 |
| 2-14 Photograph of Temperature Monitoring | 29 |
| 2-15 Photograph of Water Sampling Arrangement at Pile 7/12 | 30 |
| 3-1 Rose Diagram of Wind Direction Percentage Frequency | 38 |
| 3-2 Comparison of Historical and Study Monthly Precipitation | 39 |
| 3-3 Estimated Evaporation Potential | 40 |

PART ONE

INTRODUCTION

1.0 INTRODUCTION

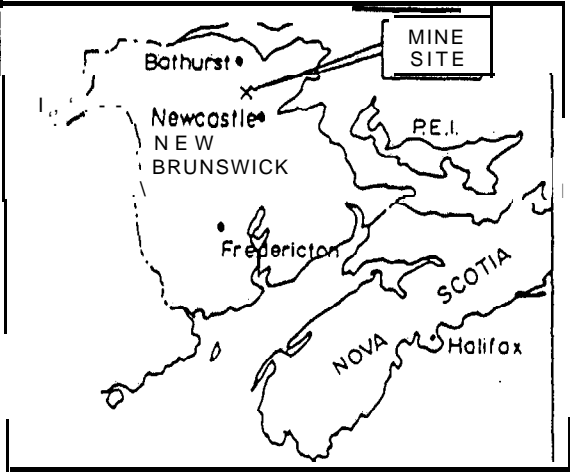
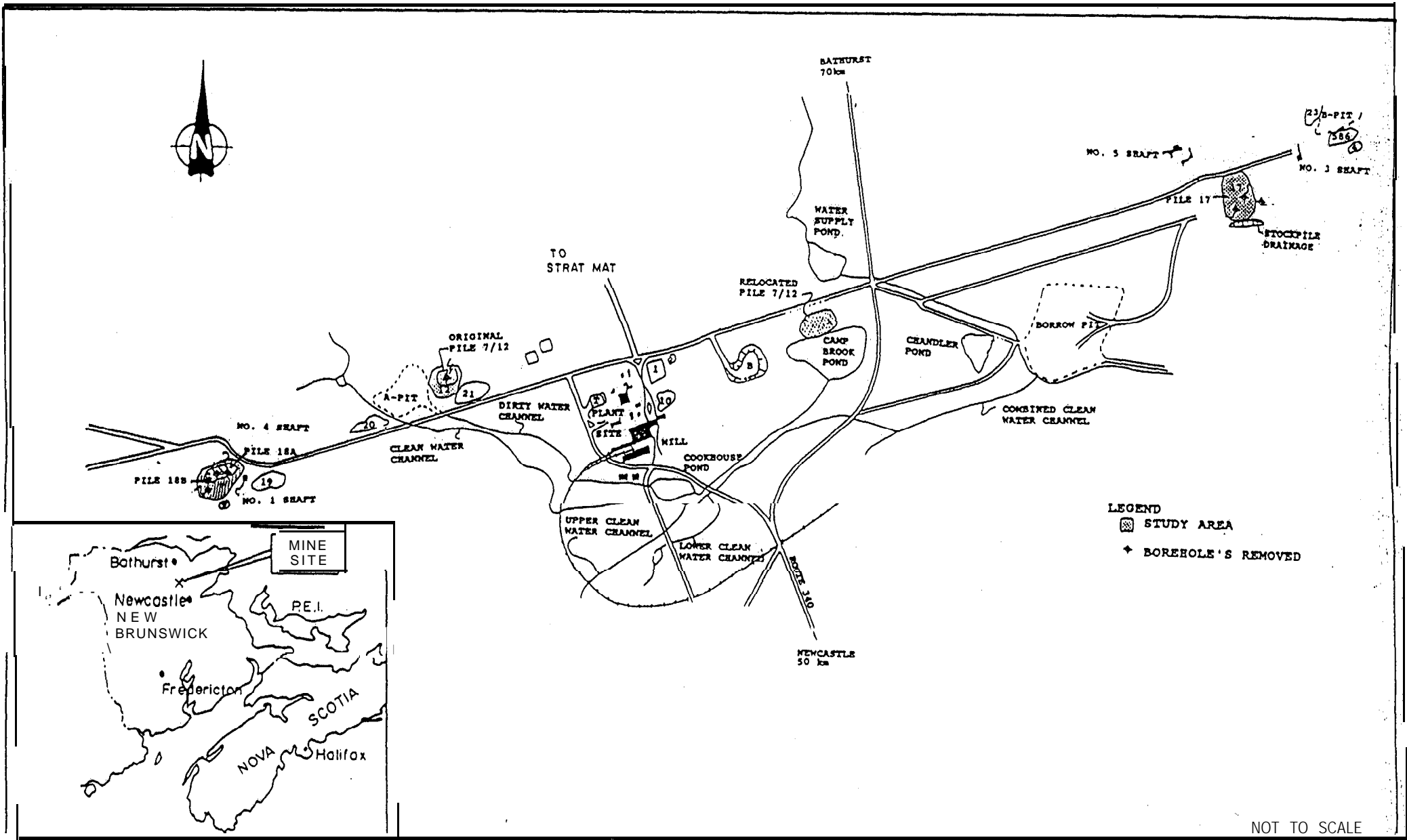
The Heath Steele site provides a unique opportunity to evaluate management techniques for acid generating waste rock under practical field conditions. The mine is located approximately 50 km northwest of Newcastle, New Brunswick, and about 60 km southwest of Bathurst, within the drainage basin of the Northwest Mirimachi River (see Figure 1-1).

1.1 Historical Review

The massive sulphide deposits at Heath Steele were discovered in 1953. Mine development and plant construction started in 1955, and ore beneficiation commenced in 1957. The operation closed in May 1958 as a result of low metal prices and metallurgical problems with oxidized portions of the ore zones.

Production was resumed in 1960 and the capacity of the mill was steadily increased through the 1960s reaching 3000 tpd in 1969. In 1977, it was further increased to 4000 tpd.

In May 1983, the sulphide ore operation was again shut down due to low metal prices. However, the mill was modified and operated until October 1984 to treat the gold-silver gossan ore that had been stockpiled on site for over 20 years, since the development of the B-Zone open pit. The collection and treatment of both surface water and mine drainage was maintained, and continues to operate in essentially the same manner today. The system involves the operation of a comprehensive site drainage collection scheme which allows contaminated drainage to be pumped to the tailings pond for treatment. Lime slurry is mixed with the drainage to neutralize acid and precipitate heavy metals from solution.



ND NOLAN, DAVIS & ASSOCIATES

FIGURE 1-1
WASTE ROCK DISPOSAL SITES LOCATION MAP
HEATH STEELE MINES

In 1989, production commenced at the new Stratmat mine and was reinstated at the existing B-Zone underground mine. The Stratmat site is located approximately 4.5 km northwest of the mill complex.

In total, at least 756,000 tonnes of pyritic waste rock and reject ore are stockpiled in more than 20 piles at the Heath Steele site. Pyritic waste rock was also used in the development of mine haulage roads, **railbeds** and other site infrastructure. The widely dispersed nature of this acid-generating material poses a particular challenge to currently available reclamation technology.

A recent study on acid waste rock management at Canadian base-metal mines (Nolan, Davis, 1987) identified the need for field performance data on waste rock pile covers and other management systems. The Heath Steele project is designed to address this need, as well as to aid in the development of practical reclamation measures for mine sites in Northeastern New Brunswick where the combination of massive sulphide ore bodies and the sensitive local **salmonid** environment pose an especially challenge to mine reclamation.

1.2 Project Objectives

During the spring of 1987, Brunswick Mining and Smelting Corporation Limited developed a proposal to various federal and provincial agencies to use several of the waste rock piles at the Heath Steele mine site to develop and test strategies for the long-term management of acid-generating waste rock. After an extended period of discussion, a four phase program was developed and on December 16, 1988, an agreement to fund the initial three phases was signed by the New Brunswick Department of Natural Resources and Energy, the New Brunswick Department of Commerce and Technology, and Brunswick Mining and Smelting Corporation.

The four phases of the overall project are as follows:

- Phase I Selection of four piles to be used for specific field trials.

- Phase II Installation of monitoring equipment to define the characteristics and background data for the four piles identified in Phase I.

- Phase III Column tests to evaluate the performance characteristics of potential covers.

- Phase IV Application of covers and performance monitoring under field conditions.

This report describes the work comprising Phase II of the project with a brief overview of Phase I included so as to reduce the need to refer to the progress report for that phase.

1.3 Selection of Study Waste Rock Piles (Phase I)

Phase I of the Study involved the selection of four acid-generating waste rock piles most amenable to monitoring and evaluation of remedial measures.

The Heath Steele site contains at least 20 identifiable waste rock piles. Selection criteria (Table 1-1) and weighting factors were established in consultation with regulatory and mine personnel, and the fifteen most promising waste rock piles were ranked (Table 1-2). The most favourable piles from this initial ranking were examined in greater detail, and were again ranked using a revised weighting and scoring (Table 1-3). Waste rock Pile 17, which had been initially screened out as being too large, was reconsidered as a possible candidate for further investigation. The locations of the waste rock piles selected for further characterization are shown in Figure 1-1.

TABLE 1-1

Criteria-used in Waste Rock Pile Assessment
Heath Steele Mines

| Criteria | Components |
|------------------------------|--|
| Morphology | Size of Pile Shape of Pile |
| Material Gradation & Type | Size Gradation Mineral Composition (including acid-base characteristics and particle surface chemistry) Moisture Content Permeability Surface Infiltration Rate Void Ratio |
| Segregation | Isolation of Piles Boundary Effects and Interactions |
| Ease of Monitoring | Accessibility Ability to Install Instrumentation Anticipated Effectiveness of Instrumentation and Monitoring |
| Background Data | Available Data on History, Materials, Mine Records and Other Studies of Waste Rock Piles |

TABLE 1-2

File Ranking (20 May, 1987)
Initial Assessment of Waste Rock Piles
Heath Steele Mines

| Pile No. | Size & Shape | Segregation | Material Grade & Type | Ease of Monitoring | Background Data | Weighted Score | Rank Order |
|----------|--------------|-------------|-----------------------|--------------------|-----------------|----------------|------------|
| | (25) | (25) | (25) | (15) | (10) | (100) | |
| 5 & 6 | 6 | 0 | 7 | 0 | 0 | 32.5 | 11 |
| 4* | 10 | 8 | 6 | 6 | 0 | 69 | 6 |
| 23 | | | | | | N/S | |
| 22 | | | | | | N/S | |
| 17 | 4 | 8 | 8 | | 10 | 72 | 3 |
| 1 & 2 | | | | | | N/S | |
| 10* | 8 | 9 | 7 | | 0 | 70.5 | 4 |
| 15 | | | | | | N/S | |
| 14* | 8 | 7 | 7 | 7 | | 65.5 | 7 |
| 21 | 2 | 2 | 7 | 5 | 2 | 37.0 | 10 |
| 7 & 12* | 9 | 6 | 10 | 7 | 2 | 75 | 2 |
| 20* | 8 | 8 | 1 | 5 | 6 | 56 | 8 |
| 18* | 9 | 9 | 5 | 8 | 0 | 69.5 | 5 |
| 9 | 2 | 8 | 2 | 8 | 0 | 42 | 9 |
| 19* | 10 | 7 | 9 | 8 | 0 | 77 | 1 |

* - Sites selected for second review.
N/S - Not suitable

TABLE 1-3

**Pile Ranking - Second Review of Sites
Heath Steele Mines**

| Pile No. | Size & Shape | Segregation | Material Grade & Type | Ease of Monitoring | Total |
|---------------------|-----------------|-------------|--------------------------|-----------------------|-------|
| Weighting | (10) | (10) | (10) | (10) | (40) |
| 4 | 8 | 0 | 8 | 2 | 18 |
| 10 | 3 | 2 | 5 | 3 | 13 |
| 14 | 6 | 8 | 8 | 7 | 29 |
| 7 & 12 ^a | 8 | 8 | 9 | 7 | 32 |
| 20 | | | | | N/S |
| 18 ^b | 9 | 9 | 7 | 8 | 33 |
| 19 | 8 | 4 | 8 | 5 | 25 |
| 17 ^c | | | | - | 28 |

a - Piles selected for Field Reconnaissance

b - Pile can be segregated into two: A & B

N/S - Not suitable

C - Pile 17, with weighted score of 28, was subsequently added to the list selected for field reconnaissance.

A field reconnaissance program was defined to characterize the piles selected as best candidates. The characteristics examined included the vertical profile through the centre of each pile into bedrock; composition/ mineralogy of material; acid producing/consuming ratio; geophysical characteristics; and topography. A CME 55 auger and diamond drill rig was used to bore exploratory holes through each of the piles and into the underlying bedrock.

Two additional holes were drilled beside Piles **18B** and 17 to further investigate overburden and bedrock characteristics. Waste rock and bedrock samples were collected, permeability tests were conducted, and piezometers were

installed to monitor water levels. A seismic geophysical survey was undertaken to define the base profile of each rock pile. The key characteristics of each pile are summarized in Table 1-4.

Waste rock Piles 17, 7/12, 18A, and 18B were selected as being most suitable for the study. Pile 7/12 could be moved as part of the ongoing site reclamation program, and it was decided to take this opportunity to reconstruct the pile on an impermeable synthetic membrane base. This would permit the water balance to be evaluated before and after placement of the cover. Relocation of the pile was planned for the fall of 1988, but early freezing conditions forced a postponement until May 1989.

1.4 Laboratory Evaluation of Potential Cover Materials (Phase III)

An evaluation of potential cover materials was undertaken concurrently with Phase II of the study. The work was being conducted by the Mining and Environment Laboratory of the Noranda Technology Centre at Pointe-Claire, Quebec. A separate report has been issued to describe this phase of the study.

TABLE I-4
Summary of Study Pile Characteristics
Heath Steele Waste Rock Study

| Pile | Surface Area (m ²) | Average Depth (m) | Maximum Depth (m) | Estimated Volume (m ³) | Estimated Tonnes [a] | Foundation Condition [b] | Mineralogy | | Sulphides Present | Percent |
|---------|--------------------------------|-------------------|-------------------|------------------------------------|----------------------|---------------------------|--------------------|-----|---|---|
| | | | | | | | AP / AC (kg/tonne) | [c] | | |
| 18A | 1,210 | 1.6 | 3.4 | 1,900 | 3,250 | Thin over rock | 79.6 | 1.5 | Pyrite Galena Sphalerite | 5 - 7 <1 <1 |
| 18B | 3,570 | 2.3 | 6.7 | 8,300 | 19,500 | Thin over rock | 158.4 | 0.5 | Pyrite Fe-S Sphalerite Galena Chalcopyrite | 7 - 10 7 - 10 <1 <1 <1 |
| 17 | 25,640 | 3.9 | 10.5 | 100,300 | 235,700 | Thin over rock | 35.7 | 0.8 | Sphalerite Pyrite Arsenopyrite Chalcopyrite Galena Silver | 7 - 10 <1 <1 <1 <1 <<1 |
| 7/12[d] | 2,100 | 2.9 | 5.0 | 6,200 | 14,700 | Impermeable Membrane Base | 210.7 | 0.4 | Pyrite Fe-S Galena Chalcopyrite Arsenopyrite Sphalerite Pyrrhotite | 7 - 10 5 - 7 <1 <1 <1 <1 <1 |

[a] Based on assumed waste rock density of 2.35 tonnes/m³
[b] Based on geophysical, **borehole** and field observations
[c] AP/AC represents Theoretical Acid Production / Acid-Consumed
[d] Pile as relocated (June 1989)

PART TWO

METHODS OF INVESTIGATION

2.0 METHODS OF INVESTIGATION

2.1 Local Meteorology

Temperature and precipitation data were measured at an AES climate station at Heath Steele from 1956 to 1983, with the exception of a two year gap from 1958 to 1960. Wind data was collected from 1974 to 1983. The station was reactivated for this study and an evaporation pan was added to the monitoring equipment. The weather information gathered at the station, which is located at the mine security gate, has been provided to Environment Canada for addition to their weather database. Available historical data is presented in Part 3 of the report (Figure 3-1 and Table-3-1).

2.1.1 Precipitation

Precipitation was measured in a standard AES rain gauge located at the climate station. The gauge was checked twice daily, the rainfall recorded, and the gauge emptied and reset. Snowfall was also measured and recorded. The instrumentation was established at the site in July 1989. For data prior to this time, the AES stations in Bathurst and Chatham should be used.

2.1.2 Evaporation

A standard Class A, 1.2 metre diameter evaporation pan was set up at the weather station. Daily records of water additions and removals were made. These data, with the temperature and rainfall data, permit the evaporation potential to be estimated.

2.1.3 Temperature

Minimum and maximum temperatures were recorded twice daily. The thermometers were housed in a Stevenson Screen at the weather station and were reset twice daily. The current temperature was also recorded at the time of reading.

2.2 Instrumentation and Monitorins of Waste Piles

2.2.1 General

It was decided that the waste rock piles should be monitored over a period of at least one year to adequately characterize the background conditions, and thereby enable the performance of the covers to be applied in Phase IV to be fully evaluated relative to seasonal variations. The parameters that best reflect the dynamics of waste rock acid generation were considered to be pore gas oxygen levels, the temperature profile within the pile, and the characteristics of any pore water and/or **leachate** associated with the pile. The instrumentation and monitoring of the study piles was therefore designed to assess these characteristics.

2.2.2 Site Preparation

Site preparation consisted of re-contouring each of the waste rock piles to maximum side slopes of approximately **3:1** (H:V). Each pile was also isolated from the influence of any neighbouring topographical or other local features. The objective was to provide side slopes that could easily accommodate equipment required for placement of the covers in Phase IV of the study. The more uniform shape resulting from re-contouring of the waste rock piles would also reduce any shape-induced effects on the monitoring results.

Investigations in-Phase I indicated that the bedrock near the surface is highly fractured and therefore of relatively high permeability.

Mounding of pore water within the piles is, therefore, highly unlikely. Monitoring of pore water quality and the determination of water and contaminant balances for the existing piles was therefore impractical. Diversion and collection ditches were constructed around the piles to minimize the inflow of surface water and to collect any surface runoff once the piles have been covered in Phase IV.

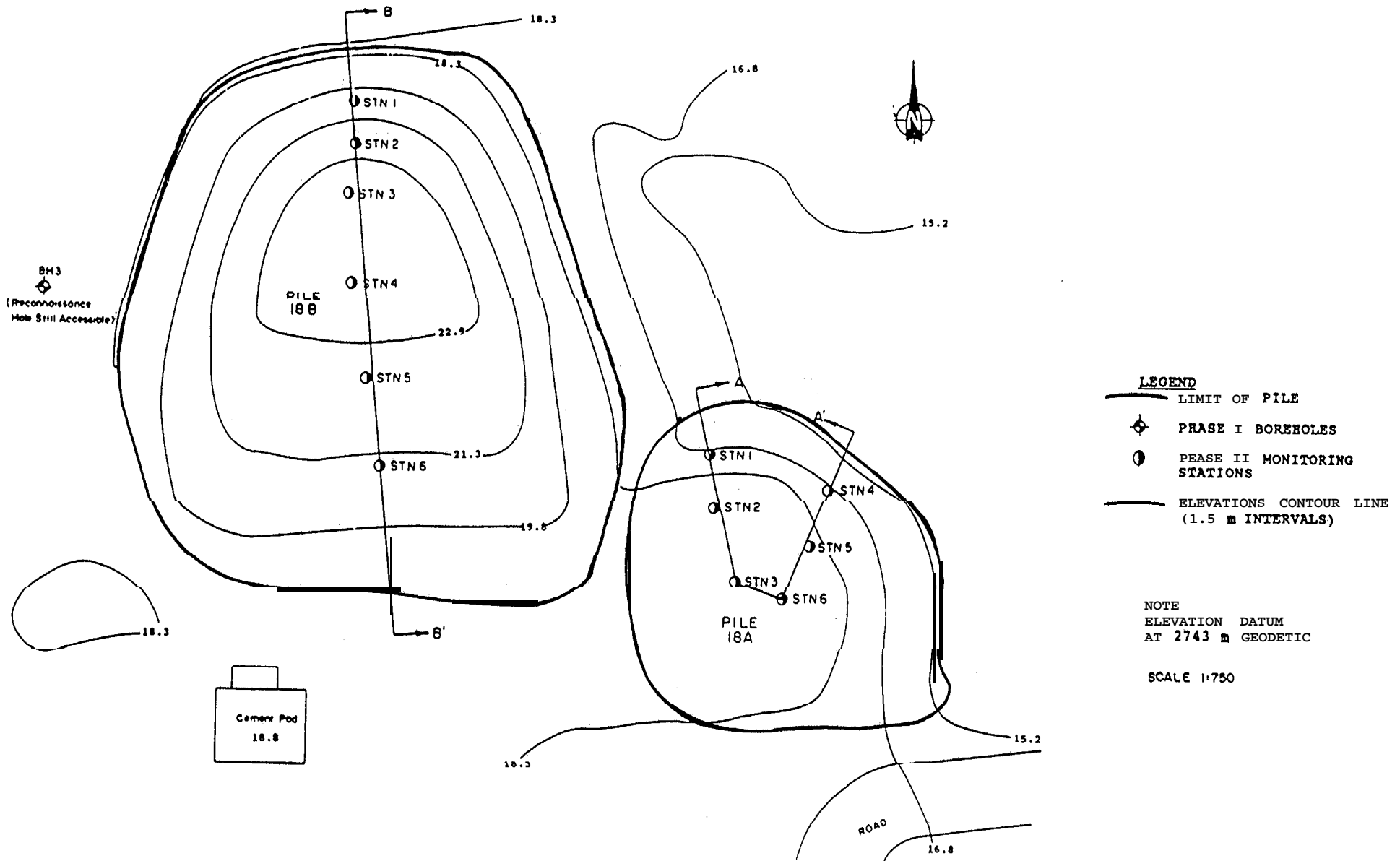
After re-contouring the piles, drilling was completed for the installation of instrumentation in Piles 18A, 18B and 17. The Phase I investigations determined that auger drilling was very slow and unable to penetrate boulders or gravelly sections which occurred frequently and unpredictably within the piles. Diamond drilling was impractical because of anticipated high water losses, distances to water sources in the winter conditions, and rough terrain. It was therefore decided to use an air track percussion drill to prepare the holes for instrument installation. There was some concern that the gas balance in the piles might be modified. However, it was felt that equilibrium conditions would be rapidly re-established due to the high permeability of the piles.

Instrumentation was installed Piles 18A, 18B and 17 in November and December 1988. Waste rock Pile 7/12 was instrumented in June 1989 as described in the following sub-section. Figures 2-1, 2-2 and 2-3 show the pile configurations and instrumentation locations. Photographs of the piles are presented as Figures 2-4 to 2-8. The characteristics of the instruments are described in Section 2.2.3.

2.2.2.1 Relocation of Pile 7/12

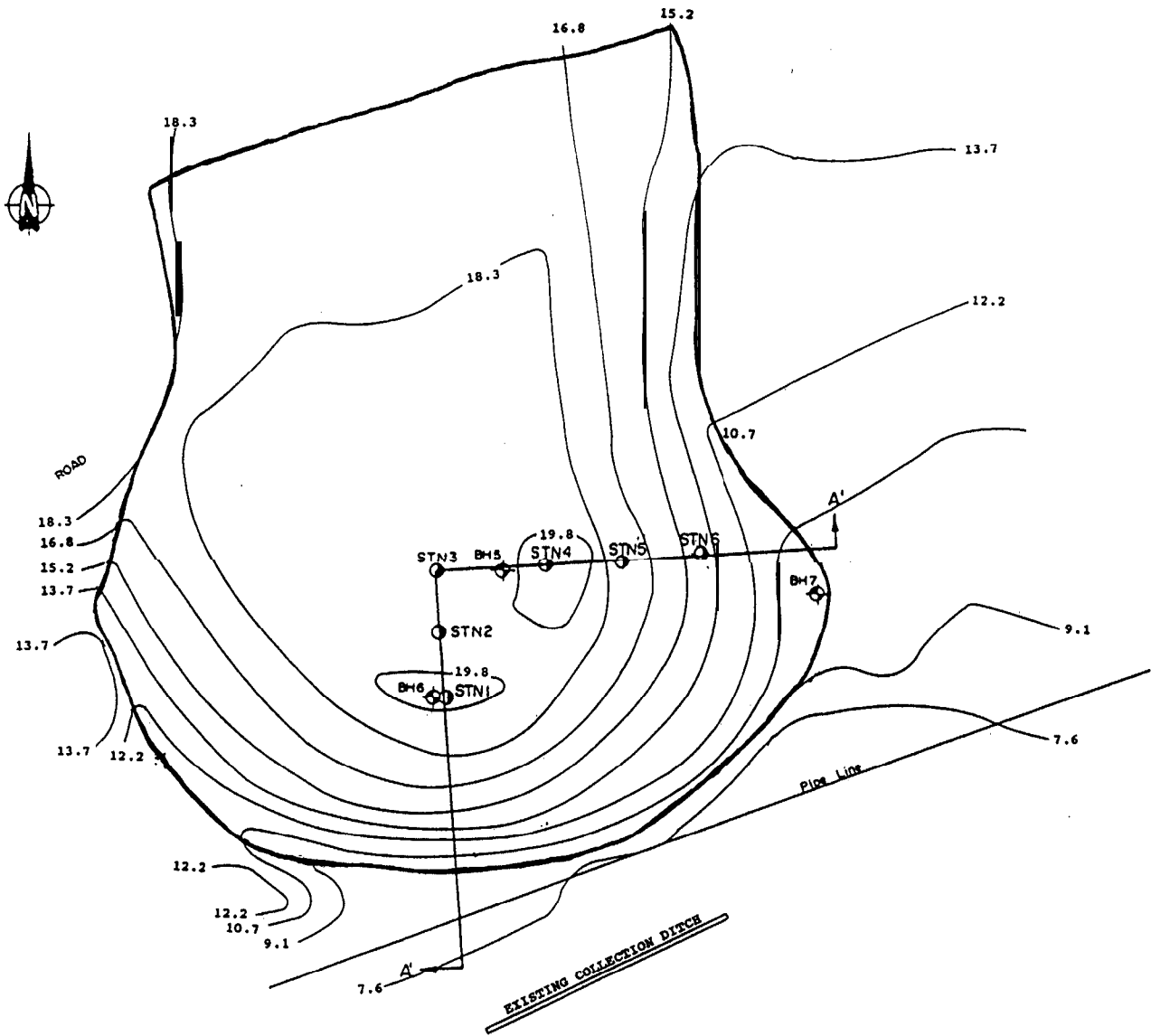
Waste rock Pile 7/12 was to be moved as part of an ongoing reclamation program at Heath Steele Mines. This provided a unique opportunity to place the pile on an impermeable liner and thereby provide for the collection of leachate before and after placement of the cover in Phase IV. Reconstruction would also provide for a more homogeneous rock pile and more favourable placement of the instrumentation. Installation of the pad and impermeable membrane and relocation of Pile 7/12 was completed in June 1989.





The impermeable membrane was fabricated from Fabrene fabric strips which were glued together into three large panels in the mill shop. When the weather was favourable, the panels were assembled at the site on a prepared pad and glued together. The pad was a compacted sand base, free of any protrusions which could puncture or damage the membrane. The membrane was folded over itself for 2 foot strips in several places to allow for some expansion or movement so



NOLAN, DAVIS
& ASSOCIATES

FIGURE 2-1
PILE CONFIGURATION AND INSTRUMENT LOCATIONS
PILE 18A AND 18B
HEATH STEELE MINES



- LEGEND**
-  **LIMIT OF PILE**
 -  **PHASE I BOREHOLES**
 -  **PHASE II MONITORING STATIONS**
 -  **ELEVATION CONTOUR LINE (1.5m INTERVALS)**

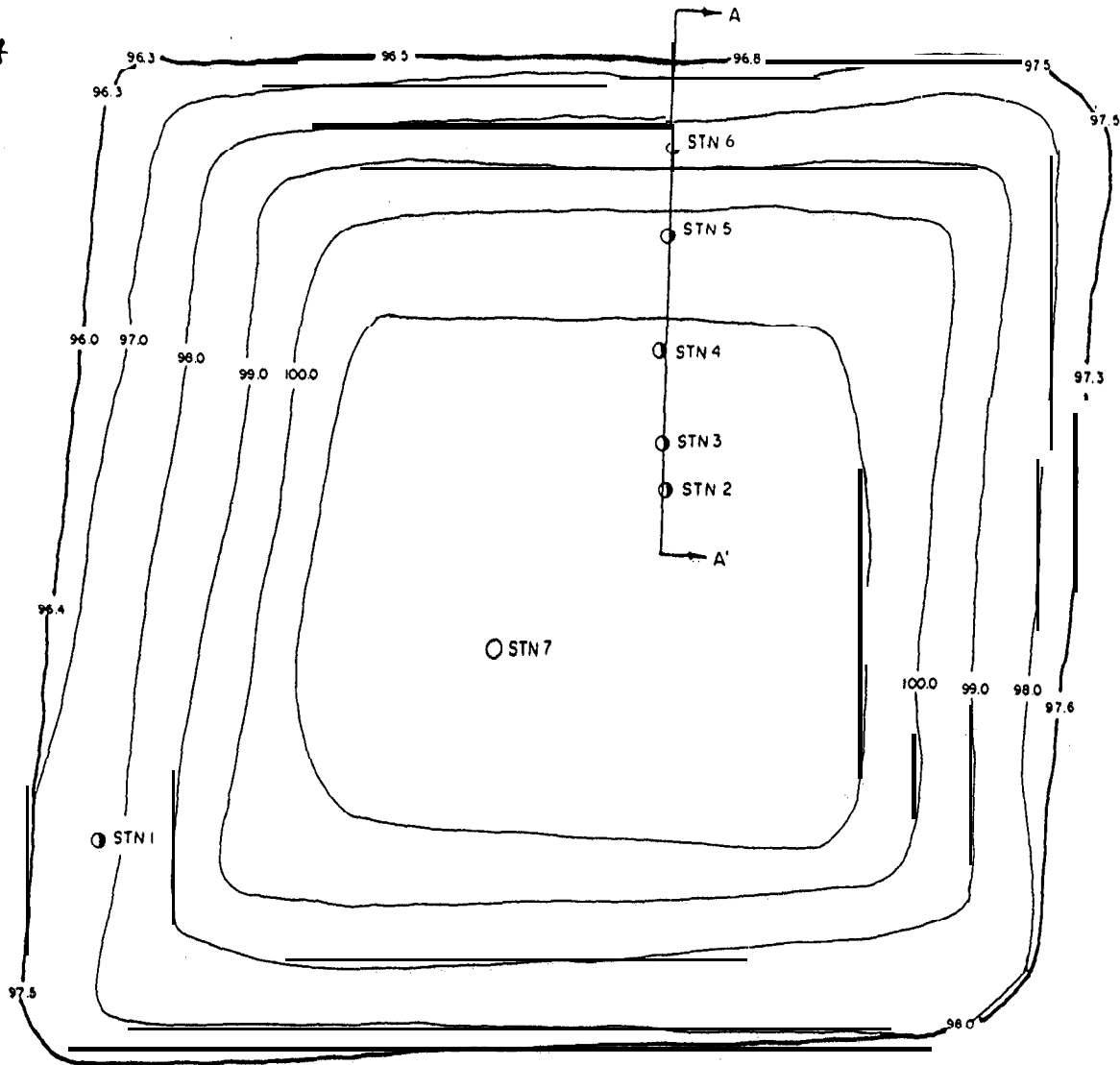
NOTE
 ELEVATION DATUM AT
 2713m GEODETIC




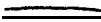
SCALE 1:1500



**NOLAN, DAVIS
 & ASSOCIATES**

FIGURE 2-2
 PILE CONFIGURATION AND INSTRUMENT LOCATIONS
 PILE '17
 HEATH STEELE MINES



- LEGEND
-  LIMIT OF PILE
 -  PHASE I BOREHOLES
 -  PHASE II MONITORING STATIONS
 -  ELEVATION CONTOUR LINE (1.0m INTERVALS)

NOTE
ELEVATION DATUM ASSUMED
100.0m
SCALE 1:275



NOLAN, DAVIS
& ASSOCIATES

FIGURE 2-3
PILE CONFIGURATION AND INSTRUMENT LOCATIONS
PILE 7/12
HEATH STEELE MINES



FIGURE 2-4

PILE 18A PRIOR TO CONTOURING
HEATH STEELE MINES

May 1987



FIGURE 2-5

**PILE 18B PRIOR TO CONTOURING
HEATH STEELE MINES**

May 1987



FIGURE 2-6

RECONTOURING OF PILE 18B
HEATH STEELE MINES

October 1988

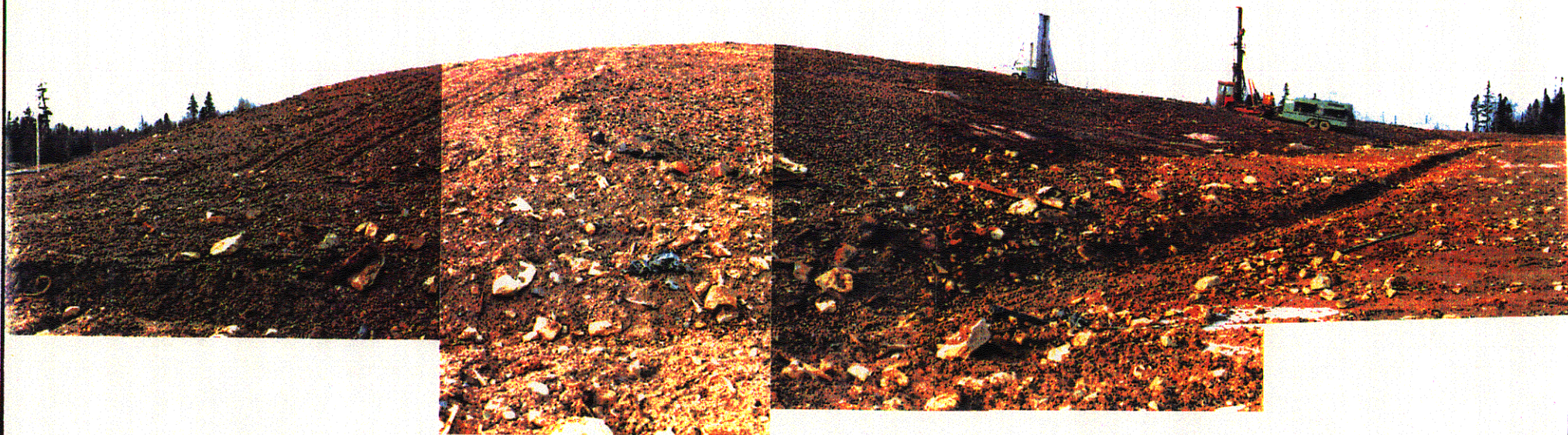


FIGURE 2-7

PILE 17 AFTER CONTOURING
HEATH STEELE MINES

October 1988



FIGURE 2-8

PILE 7/12 AFTER RELOCATION
HEATH STEELE MINES

July 1989

as to relieve any tension which might develop due to settling or traffic during placement of the waste rock.

A 150 mm thick layer of sand was placed on top of the membrane to act as a protective filter for the underdrain system, and to protect the liner itself from penetration by the rock fill.

An underflow drainage collection system consisting of 50 mm diameter Schedule 80 PVC drain pipe was installed within the upper sand filter. The outlet of this system was installed with a 'U-bend' water trap to prevent air from being drawn into the base of the waste pile.

The rock was placed on the pad to a height of approximately 5 metres, with the sides shaped to 3:1 slopes. During construction, vertical pipes of 150 mm diameter were set into the rock fill. After shaping the pile, these pipes were pulled out, thus creating a vertical hole into which the instrumentation was placed using the general installation procedures described in the following sections.

2.2.3 Instrument Installation

The typical instrumentation cluster assembled at each sampling location consists of a piezometer installed to bedrock or a maximum 5 metres depth. It was constructed of 38 mm internal diameter PVC tubing. A series of pore gas monitoring tubes were installed on the piezometer, and an adjacent series of temperature probes installed in a separate hole within one metre of the piezometer. Due to space limitations on Pile 7/12, both pore gas and temperature probes are mounted on the piezometer. A typical sampling station is shown in Figure 2-9. The specific details of these installations are as follows:

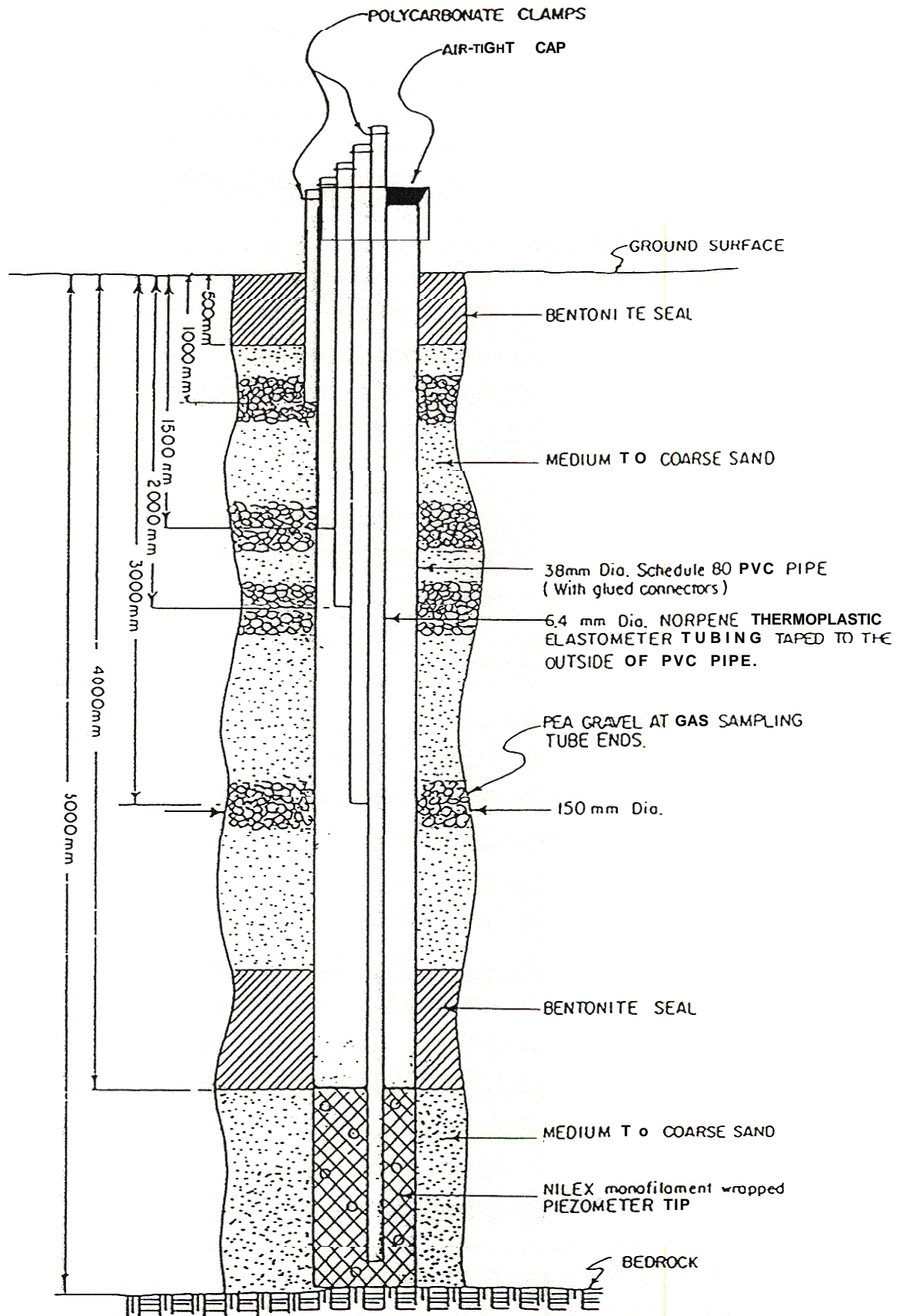
2.2.3.1 Pore Gas Instrumentation

The general instrument configuration for sampling pore gases is shown in Figure 2-10. Sampling ports were established at depths of approximately 1.0, 1.5, 2.0, 3.0, 4.0 and 5.0 metres by taping non-collapsing tubes of norprene



FIGURE 2-9

TYPICAL SAMPLING STATION
HEATH STEELE MINES



NOT TO SCALE



NOLAN, DAVIS
& ASSOCIATES

FIGURE 2-10
TYPICAL GAS SAMPLING AND
PIEZOMETER INSTALLATION
HEATH STEELE MINES

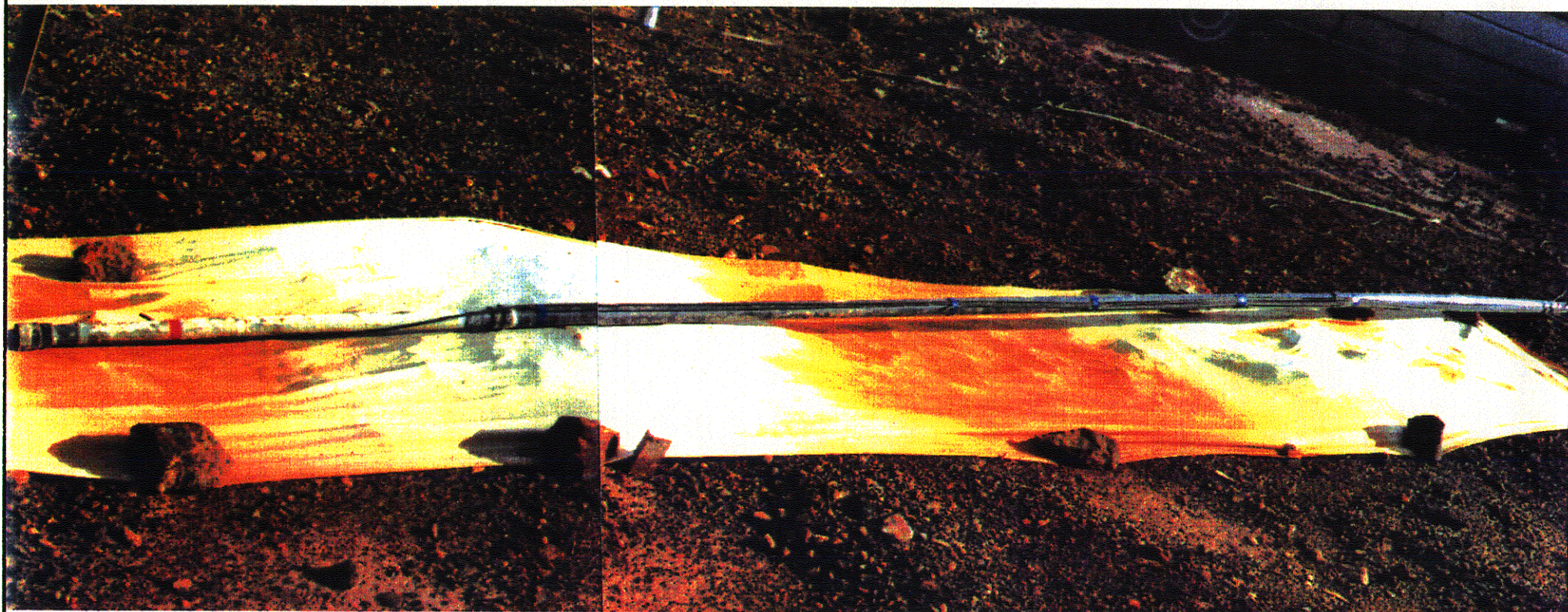


FIGURE 2-11

TYPICAL PIEZOMETER/GAS SAMPLING ARRAY PRIOR TO INSTALLATION
HEATH STEELE MINES

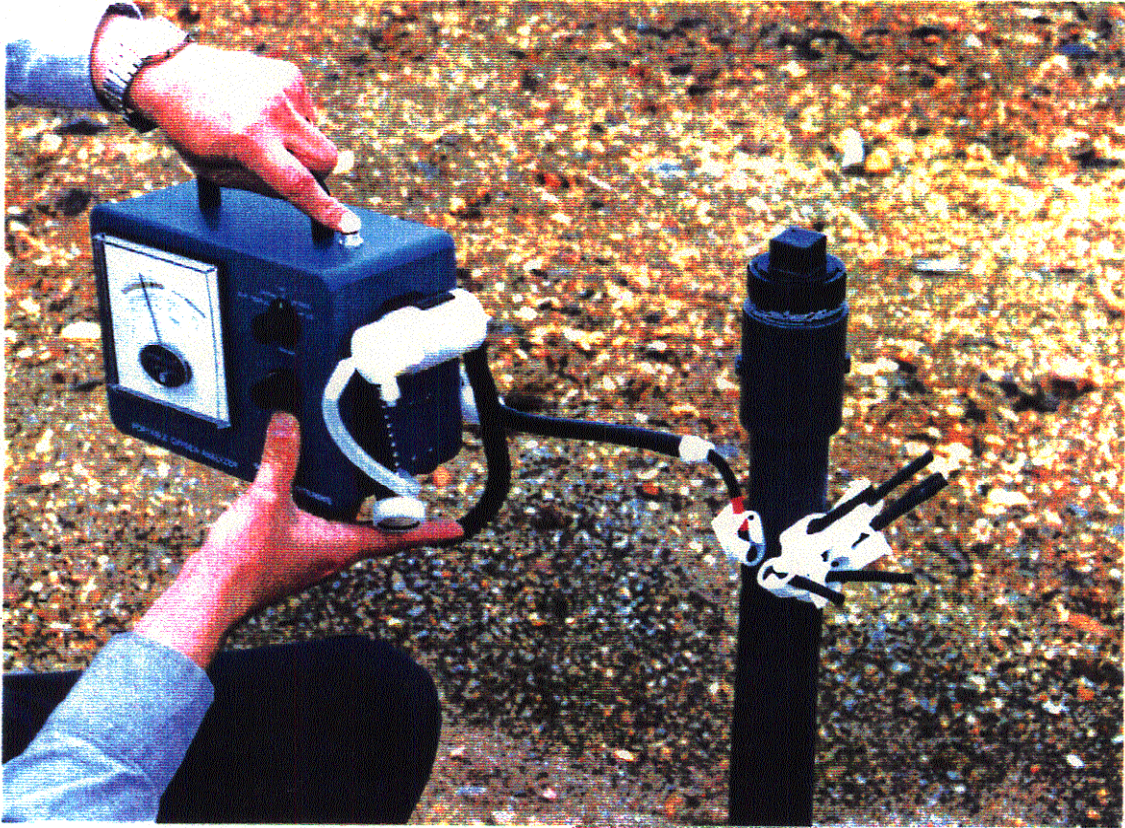


FIGURE 2-12

**PORE GAS MONITORING
HEATH STEELE MINES**

rubber, a flexible, acid resistant material, to the PVC piezometer tube prior to installation in the drilled holes. A typical sampling array prior to installation is shown in Figure 2-11. Once in the hole, a layer of sand/gravel was placed around each sample point and the upper ends clamped at all times other than during sampling. The system was designed to use a low-volume portable oxygen analyzer (Teledyne 320A). When the instrument is connected and the tube clamp is released, the instrument draws air through the tubing to the sensors located within the analyzer.

The sampling protocol required determination of the volume of pore gas to be extracted to ensure that interstitial pore gas was sampled and analyzed, and to reject gas contained in the tubing. Because of the minimum volume of air extracted from the area around the sampling point and the high porosity of the surrounding materials, less than 200 cc of interstitial gas needed to be evacuated during sampling. The neighbouring gas sampling tubes would be unaffected by this procedure. Bentonite seals were not used between the various sampling levels due to a concern that the bentonite might migrate and obstruct the gas sampling ports. The exceptions to this rule were the placement of seals at the surface and above the piezometer tip, but, in these cases, a sand filter was placed between the backfill and the bentonite sealer to prevent any piping. Reliable operation of the analyzer requires the unit to be warmer than -5°C . This was sometimes a problem during the winter months.

2.2.3.2 Temperature Measurement

In order to monitor temperature profiles within each of the piles, type K thermocouples were installed at depths of approximately 0.3, 1.5 and 4.6 metres.

The configuration of a typical thermocouple station is shown in Figure 2-13. The thermocouples were assembled with the given separations; the base of the 150 mm diameter hole was filled to approximately 4.6 metres; approximately 0.1 m of sand or fine waste rock was set at the base to minimize the potential for damage to the thermocouples. The deepest thermocouple was placed using a pole. Approximately 0.1 m of sand or fine waste rock was placed

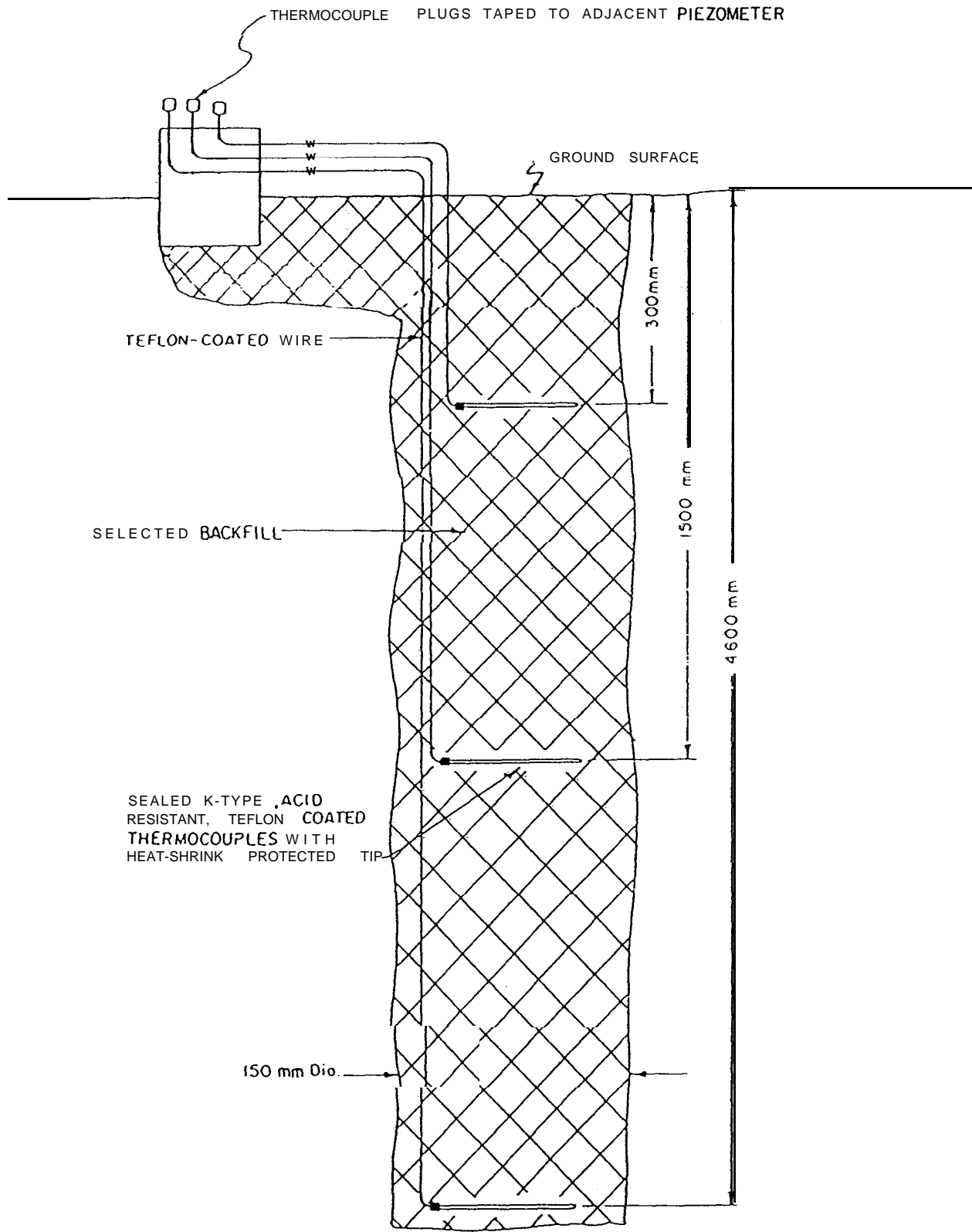
around the thermocouple and the pole was withdrawn. The thermocouple lead was then backfilled with waste rock and sand to the next thermocouple level. Fine materials were again backfilled around the thermocouple tip. Backfilling continued to the surface with a protective zone around each tip.

The thermocouples were fabricated by the manufacturer to meet specific requirements for acid resistance and are specified as long-lasting for burial in contact with water. The type **K** thermocouple is well-suited to operate within the temperature conditions expected at the site. Readings were made by attaching a hand-held thermocouple thermometer (**Digi** Sense Model BA 8528-40) to the surface contacts, using colour-coded thermocouple plugs as shown in Figure 2-14.

2.2.3.3 Seepage and Runoff

The Phase I evaluation of the waste rock piles indicated that the base underlying all four sites is permeable fractured bedrock. Routine collection and monitoring of water in the unsaturated pile would be impractical unless a bottom seal could be developed as in the case of Pile **7/12**. Despite this limitation, piezometers were installed into the bedrock in case saturation and mounding of pore water might occur under extreme conditions. Provision was also made to collect surface runoff from the piles by ditching the perimeter where feasible at Piles **18A** and **18B**. At Pile 17, due to its size and layout, limited ditching was completed with a view to improving drainage around the pile. An existing toe ditch on the low side of the pile (ref. Figure 2-2) was expected to reflect combined seepage and surface runoff quality.

Due to the high permeabilities of the piles prior to placement of the covers, no surface runoff was anticipated for Piles **18A** and **18B** during Phase II, but provision was made to monitor the volume and quality of runoff subsequent to the placement of the covers by installing flow measuring devices in the ditches. On Pile **7/12**, both seepage and surface runoff can be independently monitored for flow and quality. Automated water samplers (ISCO Model 2900 with water level sampler activator Model 1640) and automated water level recorders (Richards type) were installed at the outlet weirs (see Figure 2-15). Collected water samples



NOT TO SCALE



NOLAN, DAVIS
& ASSOCIATES

FIGURE 2-13

TYPICAL THERMOCOUPLE INSTALLATION
HEATH STEELE MINES

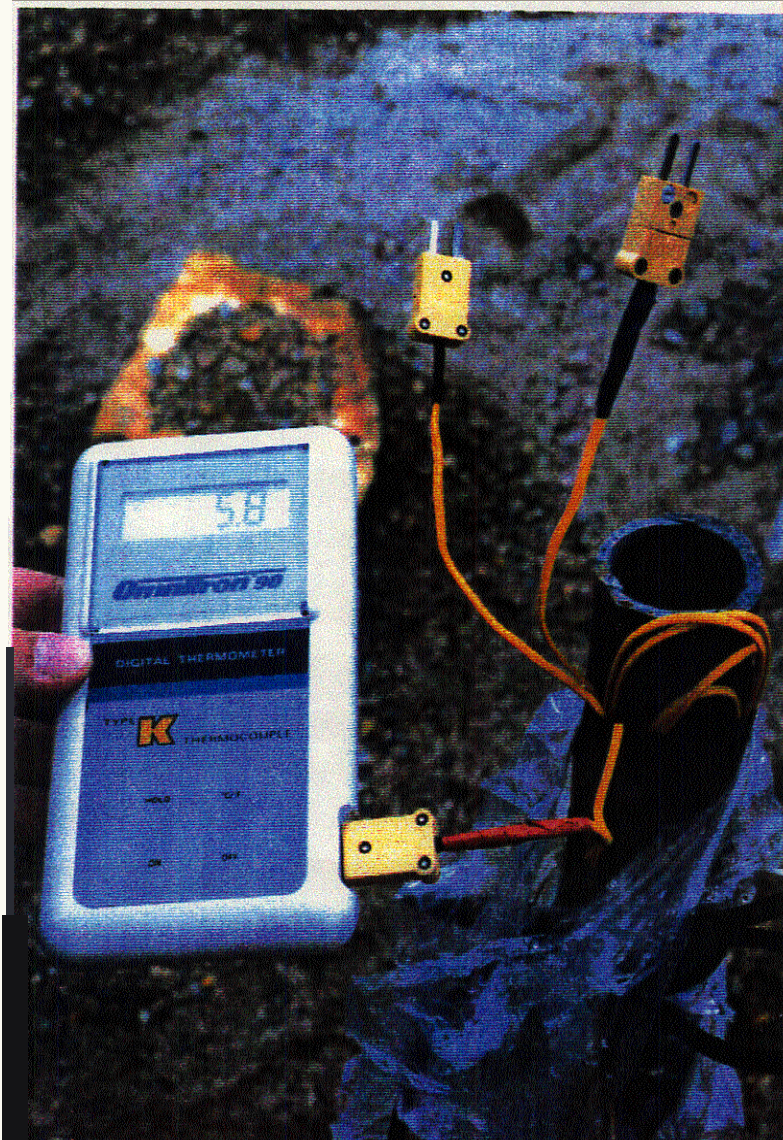


FIGURE 2-14

**TEMPERATURE MONITORING
HEATH STEELE MINES**



FIGURE 2-15

WATER SAMPLING ARRANGEMENT AT PILE 7/12
HEATH STEELE MINES

have been analyzed for the following parameters: **pH**, acidity, iron, copper, zinc and sulphate. Supplementary analyses for lead and total solids have also been conducted.

2.2.4 Water and Contaminant Balance

As previously described, the Phase I assessment indicated that the high permeability of the bedrock would preclude the development of meaningful water and contaminant balances as a measure of cover performance except for Pile **7/12**. Thus, for Piles **18A, 18B** and 17, reliance on the evaluation of gas and temperature characteristics will be necessary to determine the effectiveness of the cover. Only on Pile **7/12** will the impact of the cover on water and contaminant balances be susceptible to quantitative analysis.

2.2.5 Waste Rock Pile Characteristics

The pile characteristics, size, shape and tonnage of the waste rock, are important to the interpretation of the monitoring data. All of the study piles were surveyed once the monitoring wells were installed. The base of the piles was characterized from the geophysical investigation, **borehole** contacts and field observations.

A refraction seismograph was employed to determine the nature of the pile foundations. Using the seismic velocity contrast between the pile, overburden and bedrock, the bottom profile could be developed, although the coarseness of the pile, hillside effects, and the low contrast with the underlying fractured bedrock limited the sensitivity of this survey.

The pile sizes, in order of increasing volume, are **18A, 7/12, 18B** and 17, with volumes of 1900, 6000, 8300, and 10,300 **m³**, respectively.

The tonnage of waste rock piles was estimated based on the volume of the piles, and the typical bulk density of the material. The bulk density for broken waste rock was assumed to be approximately 2.35 **tonnes/m³**. The tonnages of Piles **18A, 7/12, 18B** and 17 were estimated to be 3000, 14,000, 19,000

and 234,000 tonnes, respectively. These figures closely match estimates made by mine engineering staff in 1970.

2.2.6 Mineralogy and Composition

The mineralogy was determined from grab samples obtained during Phase I. Samples were sent to the Research and Productivity Council in Fredericton, New Brunswick, and the mineralogy and sulphide contents of each sample was evaluated. Visual observations confirmed similar conditions and materials during placement of monitoring instrumentation and pile preparation during Phase II.

The acid producing and acid consuming potential was determined by static testing of grab samples from various depths in each rock pile. Analyses were conducted by the Research and Productivity Council and are summarized in Table 2-1.

The particle size distribution within the waste rock piles varies considerably from silt and clay sizes to coarse stone and boulders. The method of pile construction affects the size distribution. End dumping tends to segregate coarse material at the base of the dump face, while layered dumping results in less segregation. In addition, shaping of the pile tends to segregate surface materials, with smaller, more easily packing particles remaining on the surface, and large coarse stones and boulders tending to be moved to the edges. As a result, a survey of the-surface or sides of the waste rock piles can be misleading. A fresh cut into Pile 7/12 during reclamation provided an opportunity to examine the physical properties of the pile. The exposed face was divided in three blocks, and the intermediate axis of exposed-particles and area coverages were measured. The resulting distribution is therefore based on area, not weight (Table 2-2). A void ratio of 31 percent was estimated and is considered to be typical for piles of blasted rock.

TABLE 2-1

Analysis of Waste for Acid-Producing Potential

| Sample | Sulphur (%) | Theoretical Acid Production (kg/tonne) | Acid Consumed (kg/tonne) | A-B (kg/tonne) | Theoretical Acid Producer |
|--------------------------------|-------------|--|--------------------------|----------------|---------------------------|
| Pile 18A | | | | | |
| BH 1 9'6"-10' Waste Rock | 2.60 | 79.6 | 1.47 | 78.1 | Yes |
| BH 1 10'-12' Bedrock | 0.22 | 6.8 | 1.47 | 5.3 | Yes |
| Pile 18B | | | | | |
| BH 2 5'-7' Waste Rock | 3.94 | 120.7 | <0.5 | 120.4 | Yes |
| BH 2 15'-17' Waste Rock | 6.40 | 196.0 | 0.74 | 195.3 | Yes |
| Beside Pile 18B ("PAD") | | | | | |
| BH 3 0-1' Outwash | 0.15 | 4.6 | 0.5 | 4.1 | Yes |
| Pile 7/12 | | | | | |
| BH 4 4'-5' Waste Rock | 6.69 | 204.9 | <0.3 | 204.6 | Yes |
| BH 4 14'6"-15'9" Waste Rock | 7.07 | 216.5 | 0.49 | 216.0 | Yes |
| Beside Pile 7/12 | | | | | |
| Bedrock Sample 0-1' | 4.98 | 152.5 | 1.72 | 150.8 | Yes |
| Pile 17 | | | | | |
| BH 5 15'-17' Waste Rock | 1.28 | 39.2 | 1.23 | 38.0 | Yes |
| BH 6 5'-7' Waste Rock | 1.05 | 32.2 | <0.3 | 31.9 | Yes |

Analyses by RPC

Refer to Table 1-4 for Mineralogy

2.2.7 Hydraulic Conductivity

The hydraulic conductivity, or permeability, of the rock piles is difficult to quantify. The conditions within the piles make slug testing

inapplicable. Field infiltration measurements were conducted in the reconnaissance boreholes. From these tests, apparent conductivities of 10^{-2} to 10 cm/second were measured. In coarse soils, the approximate value of hydraulic conductivity can be estimated by:

$$K = 10^{-2} D_{10}^2 \text{ (m/s)}$$

where 10 percent by weight of the material is finer than D_{10} in **millimeters**.

Although D_{10} is, by definition, based on weight not area, as described in Table 2-2, a value of 1 mm was estimated and the conductivity calculated at 1 cm/second. The spatial variation of grain sizes, and loose compaction **may** result in variations in conductivity by 2 or 3 orders of magnitude.

PART THREE

RESULTS AND DISCUSSION

TABLE 2-2

Void Ratio Evaluation

| Description | Size (mm) | Block Area (cm ²) | | | Average | Distribution % |
|-------------------------------|--------------------|-------------------------------|------|------|---------|-------------------|
| | | 1 | 2 | 3 | | |
| Fines | < 0.06 | 450 | 2.50 | 0 | 2.33 | 3 |
| Sand | 0.062 | 800 | 700 | 0 | 500 | 7 |
| Gravel | 2-60 | moo | 1800 | 750 | 1517 | 22 |
| Cobbles | 60-200 | 2600 | 3400 | 900 | 2300 | 33 |
| Boulders | >200 | 2100 | 0 | 4900 | 2333 | 34 |
| Total Area (cm ²) | | 7950 | 6150 | 6550 | 6883 | 100 |
| Voids | | 2050 | 3850 | 3450 | 3117 | |
| Voids (%) | | 21 | 39 | 35 | 31 | |

Note: Particles generally blocky to angular.

Weathered state varied from relatively unstained to decomposing soft residue

3.0 RESULTS AND DISCUSSION

Due to the volume of data presented in this section, it has been organized so that the relevant tables and figures appear together at the end of each sub-section, ie., 3.1 for climate data, after 3.2 for Pile 8A, after 3.3 for Pile 8B and so forth.

3.1 Local Meteorology

The climate at the Heath Steele site can be described as Maritime continental, with hot, relatively dry summers, and cold, snowy winters. Mean annual precipitation at the Little River Mine AES Station is 1134 mm, of which 762 mm is rainfall. The station records an average of 93 days per year with rain and 47 with snowfall. The coldest months are January and February with mean daily temperatures of -12.5°C and -11.5°C , respectively. July is the warmest month with a daily mean of 17.9°C . Winds are predominantly from the northwest. Historical climate data are presented in Table 3-1 and Figure 3-1.

3.1.1 Precipitation

Precipitation during the Phase II period followed the general seasonal trends for the early months as illustrated in Figure 3-2, although the winter of 1988/89 recorded dry months in December, February and March relative to long-term averages. During the latter part of the study, and particularly the summer of 1990, several wetter than average months were recorded.

3.1.2 Evaporation

Evaporation was measured at the site from July through November 1989. The data for these months is shown in Figure 3-3. Evaporation is a function of the wind velocity, air and water surface temperatures, and humidity;

3.1.3 Temperature

The instrumentation to record ambient temperatures at the site was established only at the end of June 1989. Data to October 1990 is presented in Figure 3-4 and compared to the monthly mean values. Air temperatures during the fall and winter of 1989/90 were significantly lower than normal.

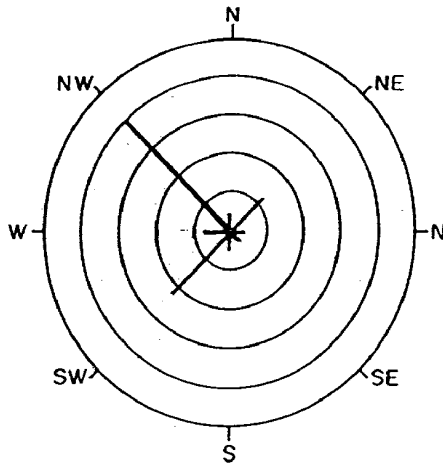
TABLE 3-1

Historical Climatological Data

LITTLE RIVER MINE

47° 17'N 66° 4'W 351 m

| | | | | | | | | | | | | | | | |
|---|-------|-------|-------|-------|-------|------|-------|------|------|-------|-------|-------|--------|---|--|
| Daily Maximum Temperature (°C) | -7.4 | -5.9 | -0.1 | 5.8 | 13.5 | 20.7 | 23.3 | 22.2 | 18.8 | 10.2 | 2.8 | -4.2 | 8.1 | 8 | Température Maximale Quotidienne |
| Daily Minimum Temperature (°C) | -17.5 | -17.0 | -10.5 | -4.3 | 2.0 | 9.0 | 12.5 | 10.9 | 6.0 | 0.7 | -5.1 | -13.2 | -2.2 | 8 | Température Minimale Quotidienne |
| Daily Temperature (°C) | -12.5 | -11.5 | -5.3 | 0.7 | 7.8 | 14.9 | 17.9 | 16.6 | 11.4 | 5.5 | -1.2 | -8.7 | 3.0 | 8 | Température Quotidienne |
| Standard Deviation, Daily Temperature | 2.2 | 1.8 | 2.0 | 1.1 | 1.8 | 1.2 | 1.6 | 1.2 | 1.4 | 1.4 | 1.9 | 2.6 | 0.7 | 3 | Écart Type de la Température Quotidienne |
| Extreme Maximum Temperature (°C) | 12.2 | 10.0 | 20.0 | 21.7 | 31.7 | 33.3 | 33.3 | 35.0 | 30.0 | 24.5 | 19.4 | 13.3 | 35.0 | | Température Maximale Extrême |
| Years of Record | 20 | 21 | 21 | 22 | 22 | 21 | 20 | 21 | 20 | 20 | 20 | 20 | 20 | | Années de Relèves |
| Extreme Minimum Temperature (°C) | -37.2 | -35.0 | -29.4 | -19.4 | -15.0 | -5.0 | 1.1 | -1.1 | -6.7 | -10.6 | -20.0 | -29.0 | -37.2 | | Température Minimale Extrême |
| Years of Record | 21 | 21 | 22 | 22 | 23 | 21 | 20 | 21 | 20 | 21 | 21 | 21 | 21 | | Années de Relèves |
| Rainfall (mm) | 16.4 | 9.9 | 23.9 | 43.5 | 90.4 | 85.6 | 100.7 | 83.9 | 95.5 | 104.7 | 74.0 | 33.8 | 782.3 | 8 | Chutes de Pluie |
| Snowfall (mm) | 76.0 | 58.1 | 72.3 | 43.3 | 5.7 | 0.0 | 0.0 | 0.0 | 0.0 | 4.2 | 35.8 | 81.0 | 376.2 | 3 | Chutes de Neige |
| Total Precipitation (mm) | 91.1 | 68.0 | 96.1 | 86.8 | 96.4 | 85.6 | 100.7 | 83.9 | 95.5 | 108.8 | 105.8 | 115.6 | 1134.3 | 3 | Précipitations Totales |
| Standard Deviation, Total Precipitation | 45.9 | 26.7 | 36.3 | 51.0 | 49.3 | 47.4 | 48.5 | 41.7 | 43.0 | 47.3 | 45.9 | 42.7 | 184.3 | 3 | Écart Type des Précipitations Totales |
| Greatest Rainfall in 24 hours (mm) | 49.3 | 42.9 | 44.5 | 78.2 | 68.8 | 50.5 | 55.4 | 99.6 | 99.3 | 86.6 | 52.8 | 58.4 | 99.6 | | Chute de Pluie Record en 24 heures |
| Years of Record | 19 | 22 | 20 | 23 | 21 | 22 | 22 | 22 | 21 | 22 | 18 | 22 | 22 | | Années de Relèves |
| Greatest Snowfall in 24 hours (mm) | 43.2 | 34.8 | 35.6 | 50.8 | 20.3 | T | 0.0 | 0.0 | T | 17.8 | 35.6 | 48.3 | 50.8 | | Chute de Neige Record en 24 heures |
| Years of Record | 22 | 20 | 21 | 21 | 23 | 22 | 23 | 22 | 22 | 22 | 22 | 22 | 22 | | Années de Relèves |
| Greatest Precipitation in 24 hours (mm) | 49.3 | 42.9 | 44.5 | 78.2 | 68.8 | 50.5 | 55.4 | 99.6 | 99.3 | 86.6 | 52.8 | 58.4 | 99.6 | | Précipitation Record en 24 heures |
| Years of Record | 22 | 21 | 21 | 22 | 21 | 22 | 22 | 22 | 21 | 22 | 21 | 23 | 22 | | Années de Relèves |
| Days with Rain | 2 | 1 | 4 | 6 | 12 | 12 | 13 | 11 | 11 | 11 | 7 | 3 | 93 | 8 | Jours de Pluie |
| Days with Snow | 9 | 8 | 9 | 5 | 1 | 0 | 0 | 0 | 0 | 1 | 5 | 9 | 47 | 3 | Jours de Neige |
| Days with Precipitation | 10 | 9 | 12 | 11 | 13 | 12 | 13 | 11 | 11 | 11 | 11 | 11 | 135 | 8 | Jours de Précipitation |



LITTLE RIVER MINE* DATA (6yr.s)
 CONTOUR FREQUENCY = 10 %

LITTLE RIVER MINE N.B.

PERIOD 1974-80 PERIODE

Lat. 47°17'N Long 066°04'W

Elevation 351 m Altitude

JAN FEB MAR APR MAY JUN JUL AUG SEP OCT NOV DEC YEAR
 JANV FEV MARS AVR MAI JUIN JUL AOUT SEPT OCT NOV DEC ANNUEL

PERCENTAGE FREQUENCY
 FRÉQUENCE EN %

| | | | | | | | | | | | | | | |
|------|------|------|------|------|------|------|------|------|------|------|------|------|------|------|
| N | 3.8 | 4.2 | 4.4 | 6.1 | 4.7 | 3.7 | 2.2 | 3.1 | 3.1 | 3.1 | 3.3 | 3.2 | 3.7 | N |
| NE | 12.6 | 11.5 | 15.9 | 19.2 | 17.2 | 16.1 | 6.6 | 7.1 | 6.3 | 6.9 | 7.9 | 11.2 | 11.5 | NE |
| E | 1.8 | 1.2 | 1.5 | 1.9 | 2.4 | 2.2 | 1.5 | 1.2 | 1.1 | 1.7 | 2.3 | 1.3 | 1.7 | E |
| SE | 4.9 | 4.7 | 8.4 | 11.2 | 11.6 | 8.5 | 7.7 | 7.4 | 5.7 | 5.8 | 6.0 | 5.8 | 7.3 | SE |
| S | 5.2 | 4.7 | 3.6 | 3.4 | 4.0 | 4.6 | 4.2 | 4.0 | 3.4 | 3.3 | 5.2 | 4.4 | 4.2 | S |
| SW | 17.4 | 11.3 | 18.2 | 12.1 | 22.5 | 31.8 | 34.3 | 27.8 | 31.2 | 26.9 | 22.5 | 15.5 | 22.6 | SW |
| W | 9.1 | 7.6 | 7.3 | 6.3 | 6.7 | 8.3 | 10.0 | 13.4 | 8.1 | 9.0 | 11.2 | 9.5 | 8.9 | W |
| NW | 45.0 | 54.6 | 40.6 | 39.7 | 30.8 | 24.8 | 33.4 | 36.0 | 41.0 | 43.1 | 41.5 | 49.0 | 40.0 | NW |
| Calm | 0.2 | 0.2 | 0.1 | 0.1 | 0.1 | 0.0 | 0.1 | 0.0 | 0.1 | 0.2 | 0.1 | 0.1 | 0.1 | Calm |

MEAN WIND SPEED IN KILOMÈTRES PER HOUR
 VITESSE MOYENNE DES VENTS EN KILOMÈTRES PAR HEURE

| | | | | | | | | | | | | | | |
|----|------|------|------|------|------|------|------|------|------|------|------|------|------|----|
| N | 8.8 | 8.5 | 11.9 | 7.8 | 8.2 | 10.2 | 7.3 | 6.9 | 8.3 | 7.9 | 8.1 | 8.8 | 8.6 | N |
| NE | 13.7 | 12.5 | 14.8 | 12.2 | 11.7 | 11.9 | 11.3 | 9.6 | 11.2 | 10.9 | 13.1 | 12.6 | 12.1 | NE |
| E | 6.4 | 6.9 | 6.4 | 7.8 | 7.4 | 7.3 | 9.1 | 5.8 | 5.3 | 6.5 | 7.5 | 7.0 | 7.0 | E |
| SE | 10.2 | 8.5 | 11.2 | 10.1 | 9.7 | 11.1 | 9.9 | 8.9 | 9.8 | 10.3 | 8.9 | 11.1 | 10.0 | SE |
| S | 6.8 | 6.7 | 7.1 | 6.1 | 6.4 | 8.4 | 6.8 | 6.4 | 6.4 | 7.6 | 6.0 | 6.1 | 6.7 | S |
| SW | 15.4 | 15.8 | 16.2 | 14.3 | 15.0 | 16.4 | 14.8 | 14.1 | 15.6 | 15.3 | 15.0 | 13.5 | 15.1 | SW |
| W | 13.3 | 11.5 | 12.0 | 13.0 | 11.8 | 11.5 | 12.0 | 11.4 | 10.5 | 11.1 | 13.4 | 14.3 | 12.2 | W |
| NW | 19.8 | 19.1 | 20.4 | 16.6 | 16.7 | 15.3 | 14.8 | 14.8 | 15.2 | 16.9 | 18.5 | 20.7 | 17.4 | NW |

All Directions / Toutes directions

15.9 15.7 16.3 13.4 13.3 13.7 13.3 12.7 13.7 14.3 14.9 16.3 14.5

Maximum Hourly Speed / Vitesse horaire maximale

50 51 50 42 37 39 35 37 48 47 48 60 60
 NW SVL NW NW SVL SVL SW SW NW NW NW W W

Height of anemometer 14.5 m hauteur de l'anémomètre

SOURCE: ENVIRONMENT CANADA

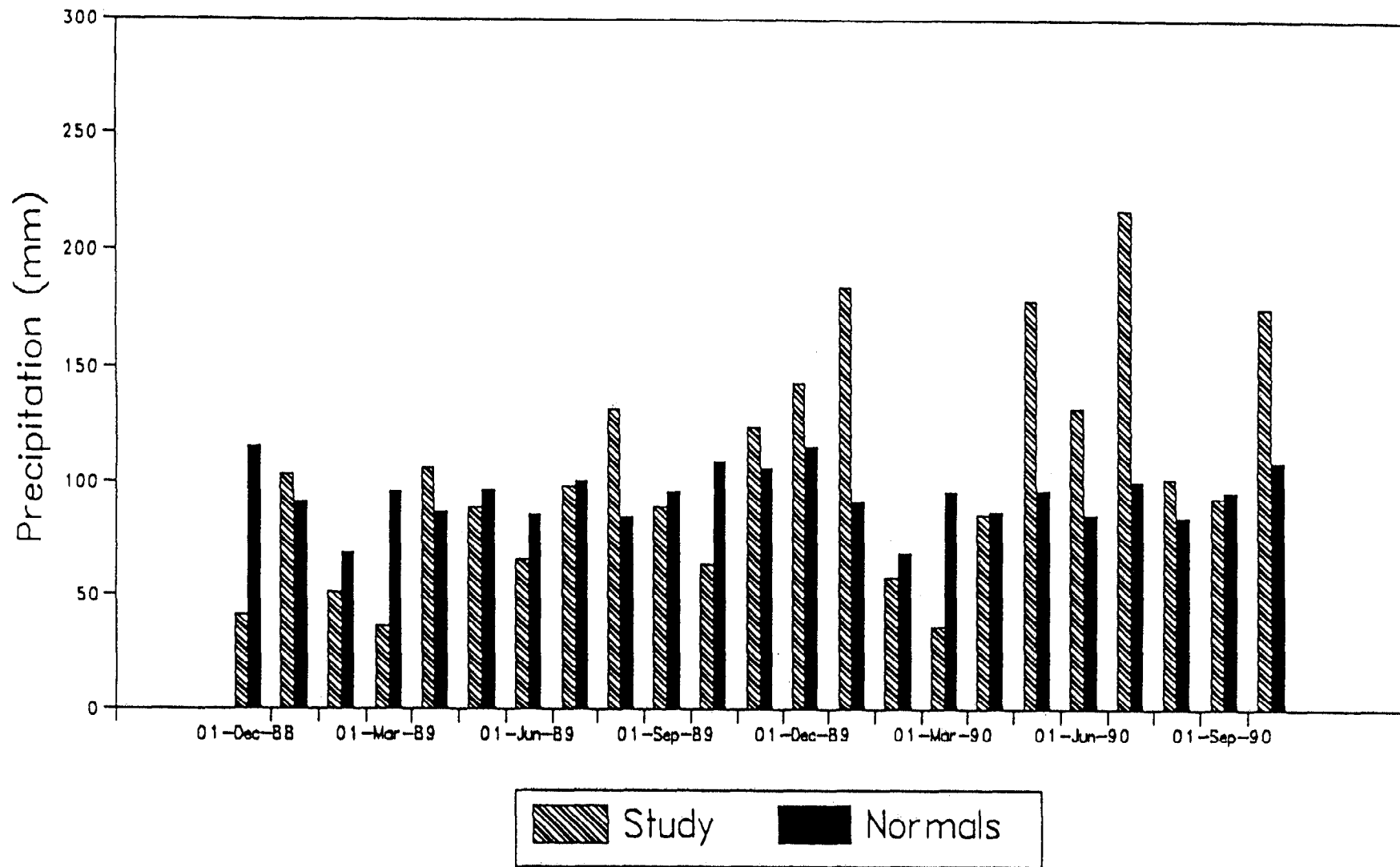
* LITTLE RIVER MINE station is located at Heath Steele Mine, NB.



**NOLAN, DAVIS
 & ASSOCIATES**

FIGURE 3-1

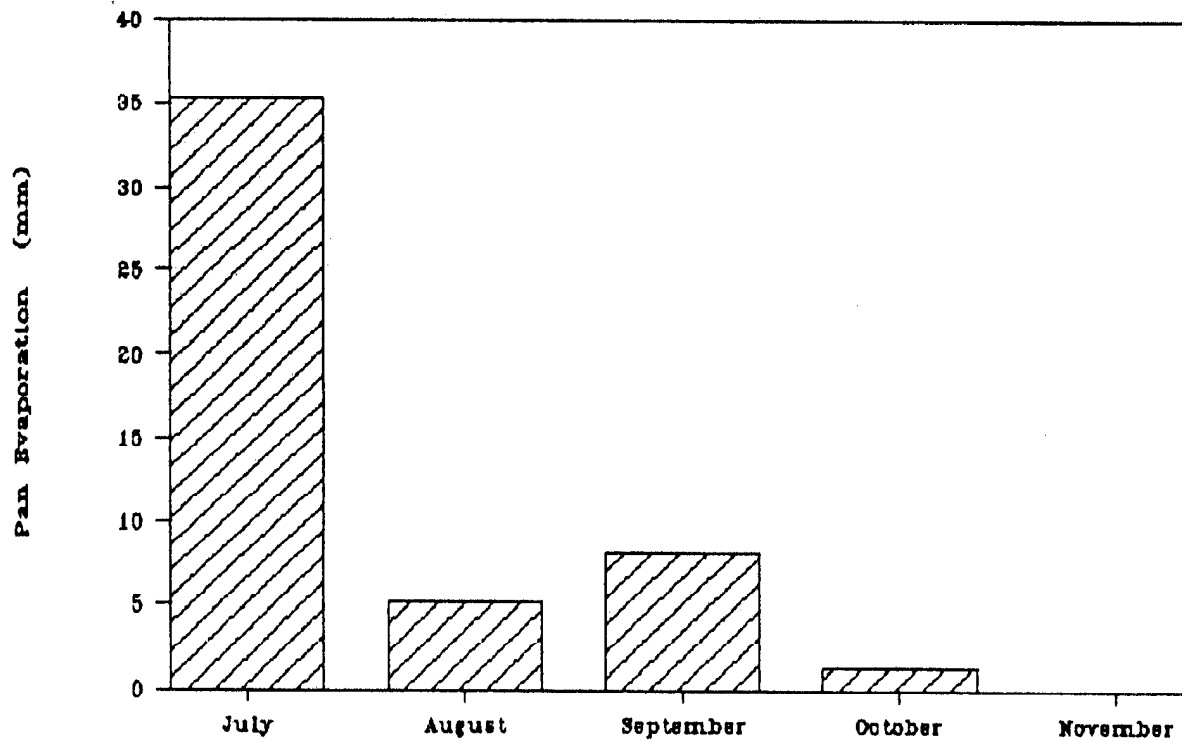
ROSE DIAGRAM OF WIND DIRECTION
 PERCENTAGE FREQUENCY AND
 MEAN WIND SPEED



NOLAN, DAVIS
& ASSOCIATES

FIGURE 3-2

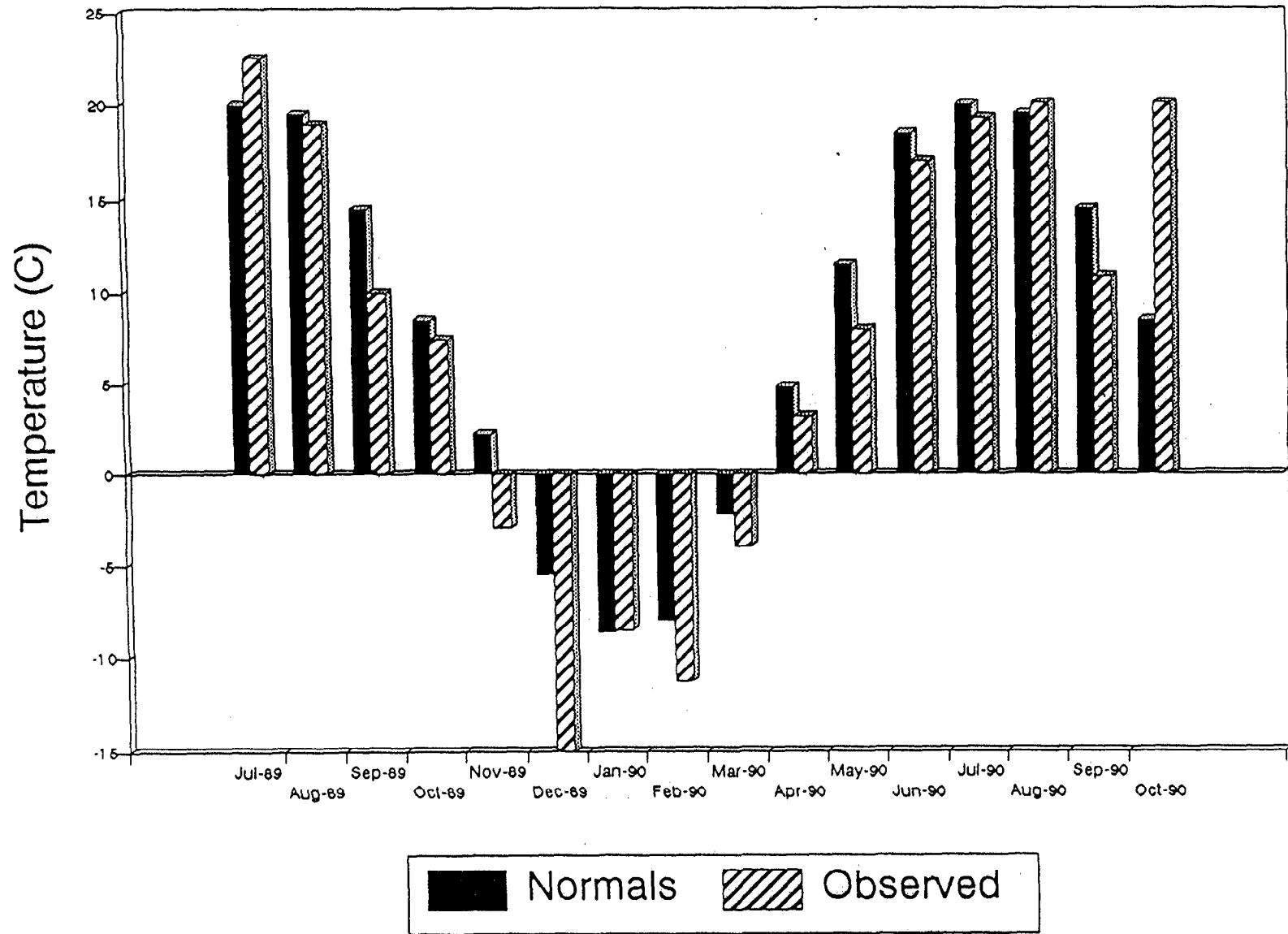
COMPARISON OF HISTORICAL AND STUDY MONTHLY PRECIPITATION
HEATH STEELE MINES



NOLAN, DAVIS
& ASSOCIATES

FIGURE 3-3

ESTIMATED EVAPORATION POTENTIAL
HEATH STEELE MINES



NOLAN, DAVIS
& ASSOCIATES

FIGURE 3-4

AIR TEMPERATURE RECORD
HEATH STEELE MINES

3.2 Pile 18A

3.2.1 Description of Pile

Pile 18A is the smallest of the four piles instrumented and has an estimated volume of 3,250 tonnes of highly acid-generating sulphidic waste rock situated on fractured bedrock. The maximum depth of the pile is 3.4 m. It was initially joined to the adjacent pile (18B) but was isolated in the course of the grading activities described in Section 1.3.

The pile was instrumented with six sets of thermocouples and gas ports to provide two angled profiles through the pile as shown in Figure 2-1.

3.2.2 Data Presentation

Temperature and oxygen data was collected monthly from November 1988 through to October 1990 (23 data sets). During some winter sampling trips, it was impossible to record oxygen levels as the meter was inoperative at air temperatures below -5°C . Thus, not all data sets include both temperature and oxygen readings. The available raw data, along with minimum, maximum and average values is presented in Tables 3-2 and 3-3.

To aid in the interpretation of this data, a typical longitudinal profile of temperatures in the pile in December 1989 is presented (Figure 3-5) along with a bar chart showing the seasonal variation in temperature for sampling location No. 3, which is the deepest hole in the pile (Figure 3-6).

A similar bar chart and profile is presented for oxygen concentration (Figures 3-6 and 3-7) together with a matched depth profile of temperature and oxygen (Figure 3-8).

Water quality and flow measurements could not be made at this site due to the high permeability of the waste rock pile and the underlying overburden and bedrock.

3.2.3 Interpretation

The longitudinal plot of temperature data for December (Figure 3-5) clearly indicates a relatively uniform temperature gradient with depth throughout the pile, with bottom temperatures of approximately 12°C compared to surface temperatures of -14°C . Similar gradients were observed in the pile during the other winter months.

The seasonal variation in temperature within the pile (Figure 3-6) shows the temperature at the bottom of the pile warming in response to increased summer surface temperatures to the point where the gradient is reversed from May through October. During the August 1989 sampling period, the bottom of the pile was recorded as having a temperature of 17.3°C compared to a surface temperature of 32°C .

The longitudinal profile of oxygen levels for November 1989 (Figure 3-7) indicates a far less uniform distribution than for the temperature data, but in general, oxygen levels are depleted towards the bottom of the pile. It is not clear whether the low values shown at Station 2 reflect a local low due to a zone of low permeability or a local region of particularly active pyrite oxidation. Similar irregularities have been observed at the Rum Jungle and Mount Washington sites as described in Section 4.1.

Seasonal variations in oxygen levels (Figure 3-6) show that the depletion of oxygen at depth is observed year-round, although concentrations are considerably higher in late winter and spring than during the fall. At Station 3, the variation at 3.7 m depth (i.e. the bottom of the pile) is from 13 percent in May to a low of 0.5 percent in October. The change in oxygen concentration at depth appears to follow a reasonably regular cycle evident in Figure 3-6. There would appear to be a reversed correlation between the temperature and oxygen levels with the lowest oxygen levels associated with the highest temperatures.

Corresponding depth profiles for temperature and oxygen at Station 3 are shown in Figure 3-8 and confirm the general depletion of oxygen with depth, as well as the stabilizing effect of depth on temperature. The time record of

oxygen concentrations and temperatures at this station suggests that the rate of oxygen consumption was reduced when the temperature was below about 10°C. The heat released in oxidation might delay the reduction of temperature at the onset of winter, but by December the winter temperatures had significantly reduced the temperature at 3 m and appears to have stopped the consumption of oxygen.

The fact that there is a temperature difference of 25⁰ C between the surface and bottom of the pile over a depth of only 3.4 m, despite its obviously high permeability, provides strong evidence of the ongoing exothermic oxidation process within the pile. The temperature within the pile is still very much influenced by ambient air temperatures, and it appears from the pore gas data that the oxidation reaction is moderated as the pile temperature drops on a seasonal basis to a low in April. At this time, pore gas oxygen concentrations are at their highest.

Near the edge of pile 18A (stations 2 and 4) low oxygen concentrations (2.2% and 0.5%) occurred only 0.1 and 0.2 m below the top surface. Low oxygen concentrations so close to the surface implies the existence of a crust, although it is possible that an upward air flow could overwhelm the downwards diffusion from the top surface.

Between August and November 1989 the oxygen concentration at station 2 was low at the surface and increased to close to atmospheric values at the base. The high oxygen concentrations at depth indicate that convective or advective transport was bringing oxygenated air into the lower parts of the pile. Wind could enhance the transport of air as this pile faces north. Temperatures in the pile were relatively low but thermal convection could occur in the winter when the temperature difference between the surrounding air and the material within the pile is highest.

TABLE 3-2

Heath Steele Waste Rock Study
Pile 18A

Temperature (C)

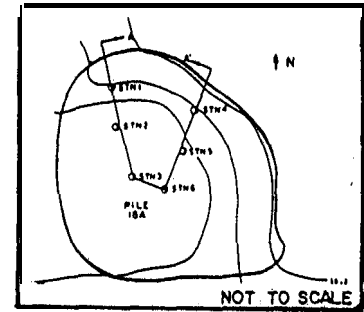
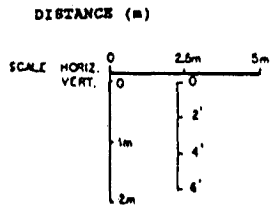
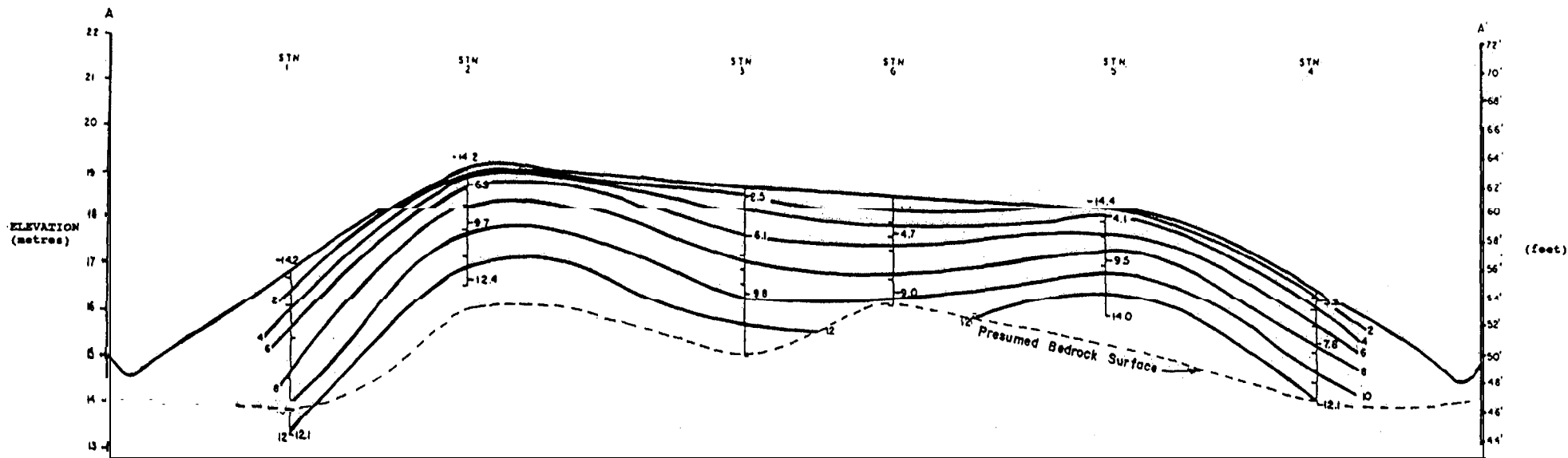
| St | Port | Depth (m) | Min. | Max. | Avg. | 1988 | | | | | 1989 | | | | | 1990 | | | | | | | | | |
|----|---------|--------------|-------|------|------|--------|--------|--------|--------|--------|--------|--------|--------|------|--------|--------|--------|--------|--------|--------|--------|--------|--------|--------|--------|
| | | | | | | 10-Nov | 10-Dec | 14-Jan | 04-Apr | 30-Apr | 15-May | 04-Jul | 03-Aug | **** | 22-Sep | 12-Oct | 22-Nov | 29-Dec | 25-Apr | 25-May | 14-Jun | 20-Jul | 16-Aug | 28-Sep | 12-Oct |
| 1 | Red | 3.6 | 2.5 | 20.5 | 11.4 | 13.0 | 12.6 | 8.8 | 5.0 | 2.5 | 3.9 | 9.2 | 11.8 | 20.5 | 20.1 | 18.3 | 15.7 | 12.1 | 6.5 | 9.0 | 8.6 | 14.8 | 18.0 | 18.6 | 17.2 |
| | Blue | 2.4 | 0.8 | 21.9 | 10.6 | 10.5 | 9.5 | 4.6 | 1.4 | 0.8 | 5.5 | 14.9 | 17.3 | 20.1 | 21.9 | 16.9 | 12.1 | 8.2 | 5.2 | 8.3 | 11.8 | 19.7 | 22.1 | 18.6 | 16.1 |
| | Black | 1.5 | -0.1 | 23.4 | 9.2 | 6.5 | 3.7 | 1.1 | -0.1 | 0.3 | 8.0 | 19.3 | 23.4 | 19.8 | 19.8 | 10.3 | 5.0 | 6.8 | 5.5 | 6.3 | 16.9 | 23.0 | 20.4 | 15.1 | 11.5 |
| | Surface | 0.0 | -14.2 | 32.5 | 9.2 | 3.2 | -7.5 | -12.9 | 7.7 | 15.0 | 17.7 | 29.3 | 32.5 | 20.3 | 21.8 | 10.7 | -4.5 | -14.2 | 10.3 | 21.8 | 20.3 | 26.4 | 24.8 | 20.9 | 17.1 |
| 2 | Red | 2.4 | 3.9 | 20.4 | 10.7 | 12.7 | 13.6 | 9.0 | 4.7 | 4.0 | 3.9 | 8.7 | 12.0 | 20.4 | 13.8 | 14.1 | 14.1 | 12.4 | 6.4 | 7.4 | 7.7 | 11.4 | 12.2 | 14.2 | 14.4 |
| | Blue | 1.2 | 1.6 | 20.4 | 10.5 | 10.6 | 10.7 | 5.8 | 1.6 | 2.5 | 5.4 | 13.7 | 17.6 | 20.4 | 17.2 | 14.8 | 12.5 | 9.7 | 5.0 | 8.1 | 10.4 | 15.9 | 19.0 | 16.5 | 15.2 |
| | Black | 0.3 | -0.7 | 21.2 | 9.7 | 8.6 | 7.6 | 2.4 | -0.7 | 0.3 | 6.9 | 17.7 | 21.2 | 18.8 | 18.8 | 13.1 | 10.0 | 6.9 | 4.8 | 7.3 | 13.5 | 20.0 | 22.2 | 16.0 | 14.0 |
| | Surface | 0.0 | -14.2 | 32.0 | 8.8 | 3.2 | -7.3 | -12.9 | 7.7 | 15.0 | 17.7 | 29.0 | 32.0 | 17.0 | 17.1 | 11.4 | -4.0 | -14.2 | 10.9 | 19.0 | 22.6 | 24.8 | 25.0 | 21.8 | 17.0 |
| 3 | Red | 2.3 | 2.2 | 17.3 | 9.6 | 9.8 | 9.9 | 5.7 | 3.1 | 2.2 | 5.6 | 13.0 | 17.3 | 14.8 | 13.5 | 12.4 | 11.8 | 9.8 | 5.1 | 7.5 | 8.4 | 11.2 | 14.6 | 12.9 | 12.8 |
| | Blue | 1.1 | 0.3 | 22.7 | 9.2 | 7.3 | 7.3 | 2.3 | 0.3 | 0.7 | 6.7 | 18.4 | 22.7 | 16.1 | 15.8 | 11.3 | 9.1 | 6.1 | 4.2 | 7.3 | 12.1 | 16.9 | 19.5 | 12.8 | 12.2 |
| | Black | 0.2 | -3.4 | 24.2 | 8.0 | 4.4 | 3.7 | -3.4 | 0.1 | -0.1 | 8.3 | 20.0 | 24.2 | 17.8 | 17.2 | 7.8 | 4.4 | 2.5 | 5.6 | 6.6 | 20.4 | 23.1 | 19.9 | 12.0 | 9.8 |
| | Surface | 0.0 | -14.2 | 32.0 | 8.9 | 3.2 | -7.2 | -12.9 | 7.7 | 15.0 | 17.7 | 29.0 | 32.0 | 17.0 | 16.4 | 11.7 | -5.1 | -14.2 | 13.6 | 21.8 | 24.1 | 27.3 | 30.0 | 22.8 | 16.9 |
| 4 | Red | 2.4 | 4.6 | 18.1 | 10.8 | 12.8 | 11.5 | 7.4 | 4.9 | 5.8 | 4.6 | 10.1 | 13.6 | 18.1 | 15.7 | 14.8 | 13.9 | 12.1 | 6.1 | 7.7 | 9.2 | 12.3 | 14.0 | 15.7 | 15.7 |
| | Blue | 1.2 | 0.9 | 20.0 | 9.6 | 4.6 | 7.3 | 1.8 | 0.9 | 2.8 | 6.2 | 17.2 | 20.0 | 18.8 | 18.6 | 13.6 | 10.2 | 7.8 | 4.3 | 7.2 | 13.2 | 18.8 | 20.1 | 16.1 | 14.6 |
| | Black | 0.2 | -2.0 | 23.1 | 8.2 | 5.4 | 2.5 | -2.0 | -0.9 | 1.9 | 7.8 | 19.0 | 23.1 | 18.5 | 18.3 | 8.3 | 4.1 | 3.3 | 4.8 | 5.6 | 19.1 | 22.7 | 19.6 | 13.7 | 10.7 |
| | Surface | 0.0 | -12.9 | 31.8 | 9.8 | 3.2 | -7.2 | -12.9 | 7.7 | 15.0 | 17.7 | 28.4 | 31.8 | 18.3 | 18.6 | 9.7 | -3.8 | - | 10.1 | 14.8 | 24.8 | 21.6 | 24.6 | 21.3 | 17.1 |
| 5 | Red | 2.4 | 3.9 | 18.9 | 10.6 | 12.8 | 10.8 | 7.4 | 3.9 | 4.5 | 3.9 | 10.3 | 13.7 | 18.9 | 15.4 | 14.7 | 13.2 | 14.0 | 5.4 | 7.8 | 9.5 | 12.6 | 15.1 | 16.3 | 15.5 |
| | Blue | 1.2 | 0.3 | 20.1 | 9.8 | 9.2 | 6.1 | 2.8 | 0.3 | 2.3 | 5.1 | 16.8 | 20.1 | 18.6 | 18.3 | 14.0 | 9.8 | 9.5 | 3.9 | 7.5 | 13.5 | 18.9 | 21.0 | 16.7 | 14.6 |
| | Black | 0.3 | -3.4 | 23.1 | 7.9 | 5.0 | 0.3 | -3.4 | -0.3 | 1.4 | 7.8 | 20.1 | 23.1 | 18.0 | 17.4 | 9.0 | 3.2 | 4.1 | 4.3 | 6.9 | 20.2 | 23.1 | 19.0 | 14.7 | 11.4 |
| | Surface | 0.0 | -14.4 | 32.7 | 9.3 | 3.2 | -7.2 | -12.9 | 7.7 | 15.0 | 17.7 | 28.6 | 32.7 | 20.3 | 21.9 | 9.9 | -3.6 | -14.4 | 11.0 | 17.5 | 26.1 | 24.1 | 29.6 | 21.5 | 17.1 |
| 6 | Red | 2.1 | 0.7 | 17.9 | 8.3 | 8.6 | 6.9 | 3.3 | 0.7 | 2.0 | 2.6 | 11.6 | 14.7 | 17.9 | 14.4 | 12.0 | 9.6 | 9.0 | 2.8 | 6.7 | 9.5 | 13.3 | 16.9 | 14.2 | 13.0 |
| | Blue | 0.9 | 0.2 | 19.5 | 7.9 | 6.6 | 2.2 | 1.8 | 0.2 | 1.5 | 4.9 | 16.2 | 19.5 | 18.0 | 15.9 | 9.5 | 6.4 | 4.7 | 2.6 | 6.3 | 14.3 | 19.2 | 20.4 | 13.6 | 11.4 |
| | Black | 0.3 | -6.8 | 21.8 | 6.9 | 4.7 | -2.1 | -6.8 | 0.8 | 2.1 | 6.8 | 18.1 | 21.8 | 18.7 | 16.8 | 7.7 | 3.3 | 1.1 | 3.2 | 6.2 | 18.8 | 21.7 | 19.9 | 13.7 | 10.3 |
| | Surface | 0.0 | -12.9 | 33.0 | 10.4 | 3.2 | -7.2 | -12.9 | 7.7 | 15.0 | 17.7 | 29.0 | 33.0 | 20.3 | 25.1 | 10.3 | -4.2 | - | 8.2 | 21.1 | 25.0 | 23.2 | 25.5 | 25.2 | 17.1 |

TABLE 3-3

Heath Steele Waste Rock Study
Pile 18 A

Oxygen Concentration (% of pore gas)

| Stn | Port | Depth (m) | Min. | Max. | Avg. | 1988 | | | | | 1989 | | | | | 1990 | | | | | | |
|-----|------|--------------|------|------|------|--------|--------|--------|--------|--------|--------|--------|--------|--------|--------|--------|--------|--------|--------|--------|--------|--------|
| | | | | | | 10-Dec | 14-Jan | 30-Apr | 15-May | 04-Jul | 03-Aug | 04-Sep | 22-Sep | 13-Oct | 22-Nov | 25-Apr | 25-May | 14-Jun | 20-Jul | 16-Aug | 28-Sep | 12-Oct |
| 1 | 1 | 2.4 | 3.6 | 19.5 | 11.1 | 19.5 | 15.6 | 13.0 | 3.6 | 10.8 | 6.0 | 5.2 | 9.0 | 11.7 | 9.5 | 16.8 | 16.5 | 14.0 | 9.5 | 4.4 | 10.0 | 13.0 |
| | 2 | 1.3 | 7.5 | 20.6 | 16.0 | 20.6 | 17.7 | 16.0 | 7.5 | 18.6 | 13.0 | 14.8 | 14.0 | 15.1 | | 19.5 | 18.5 | 18.8 | 16.7 | 13.7 | 15.0 | 17.0 |
| | 3 | 0.8 | 8.8 | 19.2 | 14.6 | 19.2 | 17.2 | 15.0 | 18.0 | 16.5 | 10.3 | 12.0 | 9.0 | 14.0 | 14.0 | 18.6 | 17.5 | 17.7 | 14.7 | 8.8 | 12.0 | 15.5 |
| | 4 | 0.2 | 2.2 | 18.7 | 11.5 | 18.7 | 15.6 | 18.7 | 18.5 | 8.3 | 2.2 | 5.7 | 5.8 | 10.0 | | 19.5 | 15.0 | 12.5 | 8.0 | 3.5 | 7.6 | 12.0 |
| 2 | 1 | 2.6 | 18.8 | 20.8 | 6.7 | 20.8 | 20.6 | - | 18.8 | - | - | - | - | - | - | - | - | - | - | 20.7 | 20.5 | 20.5 |
| | 2 | 2.0 | 15.5 | 18.6 | 17.7 | 18.6 | 18.6 | 15.5 | 17.6 | 18.0 | 18.0 | 18.2 | 16.8 | 18.2 | 17.5 | 17.5 | 16.2 | 19.0 | 17.1 | 17.5 | 20.0 | 16.5 |
| | 3 | 1.3 | 12.4 | 18.6 | 15.4 | 18.6 | 18.6 | 15.0 | 12.4 | 16.0 | 15.5 | 14.0 | 12.8 | 16.0 | | 16.9 | 15.2 | 17.7 | 14.9 | 15.5 | 15.5 | 14.5 |
| | 4 | 0.7 | 5.2 | 17.0 | 10.7 | 17.0 | 17.0 | | 12.5 | 8.0 | 6.5 | 8.5 | 5.2 | 10.5 | 9.0 | 14.8 | 17.0 | 10.9 | 14.4 | 5.2 | 6.0 | 8.5 |
| | 5 | 0.4 | 2.8 | 16.4 | 9.7 | 16.4 | 16.4 | 14.0 | 13.5 | 7.3 | 4.2 | 5.0 | 2.8 | 8.0 | 8.3 | 16.3 | 17.0 | 8.9 | 5.5 | 16.0 | 6.7 | 8.0 |
| | 6 | 0.1 | 2.2 | 17.0 | 9.6 | 17.0 | 16.4 | 17.0 | | 8.0 | 4.1 | 4.8 | 2.2 | 7.5 | 9.5 | 18.4 | 20.0 | 9.0 | 12.2 | 6.2 | 8.6 | 9.3 |
| 3 | 1 | 3.7 | 0.4 | 13.0 | 4.6 | 4.2 | 11.5 | | 13.0 | 2.9 | 1.8 | 0.6 | 2.5 | 0.5 | 1.3 | 11.5 | 7.0 | 0.4 | 7.0 | 5.9 | 9.0 | 14.0 |
| | 2 | 3.0 | 0.1 | 17.8 | 8.1 | 7.4 | 14.4 | 14.6 | 17.8 | 15.0 | 1.3 | 0.8 | 0.1 | 1.5 | 2.0 | 7.3 | 8.2 | 6.5 | 5.5 | 6.4 | 19.5 | 3.0 |
| | 3 | 2.4 | 8.0 | 18.8 | 14.8 | 17.5 | 18.8 | 17.5 | 16.0 | 17.5 | 14.0 | 12.7 | 8.0 | 11.5 | 10.8 | 17.4 | 12.0 | 16.4 | 14.0 | 13.0 | 13.0 | 14.0 |
| | 4 | 2.1 | 12.1 | 19.4 | 15.7 | 18.5 | 19.4 | 18.0 | 12.1 | 17.5 | 15.0 | 15.2 | 13.5 | 12.2 | | 17.6 | 17.5 | 18.6 | 16.0 | 14.5 | 18.1 | 18.5 |
| | 5 | 1.8 | 12.7 | 18.6 | 16.0 | 18.6 | | 18.2 | 12.7 | 18.0 | 14.5 | 14.7 | 13.3 | 17.6 | 15.8 | 17.6 | 17.0 | 18.3 | 15.5 | 14.0 | 17.5 | 18.5 |
| | 6 | 1.5 | 13.0 | 20.8 | 16.9 | 18.8 | 19.0 | 17.1 | 20.8 | 16.8 | 13.5 | 15.2 | 13.0 | 17.6 | 17.0 | 17.6 | 17.5 | 18.7 | 15.0 | 13.5 | 17.5 | 18.5 |
| 4 | 1 | 2.0 | 16.8 | 18.5 | 13.9 | 18.5 | 16.8 | | 12.2 | 7.9 | | | | | | | | | | 20.0 | 19.0 | 19.0 |
| | 2 | 1.4 | 0.2 | 16.2 | 8.9 | 15.0 | 16.2 | 12.0 | 12.0 | 7.7 | 0.7 | 7.8 | 0.8 | 7.5 | 8.0 | 10.6 | 4.5 | 4.3 | 1.2 | 0.3 | 0.2 | 0.2 |
| | 3 | 0.8 | 0.1 | 15.0 | 6.8 | 12.8 | 15.0 | 10.5 | 9.5 | 4.3 | 0.5 | 3.8 | 0.4 | 4.2 | 7.0 | 8.5 | 3.0 | 4.5 | 1.1 | 0.7 | 0.5 | 0.1 |
| | 4 | 0.5 | 0.1 | 14.4 | 6.2 | 12.4 | 14.4 | 12.0 | 8.5 | 2.5 | 0.5 | 1.7 | 0.8 | 2.8 | | 7.8 | 2.5 | 3.5 | 0.7 | 0.2 | 0.1 | 0.7 |
| | 5 | 0.2 | 0.3 | 14.6 | 7.0 | 11.0 | 13.6 | 10.0 | 9.5 | 14.6 | 0.5 | 0.6 | 0.9 | 2.4 | 3.5 | 6.8 | 2.5 | 4.0 | 0.4 | 0.7 | 0.3 | 0.5 |
| 5 | 1 | 1.9 | 4.8 | 19.0 | 16.1 | 17.2 | 18.4 | 16.5 | 19.0 | 17.7 | 15.7 | 13.5 | 14.5 | 12.2 | 15.5 | 17.2 | 13.5 | 18.0 | 16.8 | 4.8 | 7.0 | 8.9 |
| | 2 | 1.3 | 4.2 | 19.2 | 11.6 | 16.8 | 18.0 | 14.6 | 19.2 | 10.1 | 4.6 | 8.1 | 4.2 | 9.0 | | 15.6 | 19.5 | 11.5 | 6.5 | 6.8 | 4.6 | 6.7 |
| | 3 | 0.7 | 3.3 | 19.5 | 11.7 | 16.6 | 18.0 | 14.6 | 19.5 | 10.6 | 4.6 | 8.1 | 3.3 | 10.0 | 12.5 | 15.1 | 19.5 | 11.8 | 6.0 | 7.1 | 4.6 | 6.4 |
| | 4 | 0.4 | 3.2 | 19.3 | 10.9 | 16.6 | | 15.0 | 19.3 | 10.7 | 4.5 | 8.1 | 3.2 | 9.5 | | 15.1 | 19.5 | 11.0 | 6.3 | 13.0 | 14.0 | 7.5 |
| | 5 | 0.1 | 16.5 | 17.6 | 17.1 | 16.5 | 17.6 | | 17.2 | | | | | | | | | | | | | |
| 6 | 1 | 2.5 | 15.5 | 19.5 | 16.8 | 17.1 | 18.2 | | 19.5 | 15.8 | 15.5 | 16.4 | 16.0 | 16.0 | 17.0 | 19.4 | 18.5 | 17.5 | 18.2 | 17.3 | 16.2 | 17.0 |
| | 2 | 1.9 | 16.6 | 20.0 | 18.4 | 18.0 | 19.2 | | 20.0 | 18.4 | 17.0 | 18.4 | 17.5 | 18.5 | | 19.8 | 18.5 | 19.0 | 16.6 | 17.2 | 18.5 | 18.5 |
| | 3 | 1.3 | 17.0 | 20.8 | 19.6 | 19.0 | 20.0 | 20.8 | 20.5 | 20.0 | 17.0 | 19.9 | 18.5 | 20.5 | 20.8 | 20.3 | 19.0 | 19.8 | 19.5 | 18.5 | 19.5 | 19.5 |
| | 4 | 1.0 | 16.2 | 20.8 | 19.1 | 19.2 | 20.0 | 20.8 | 20.5 | 19.1 | 17.5 | 18.4 | 17.0 | 19.5 | | 19.8 | 19.0 | 19.3 | 18.1 | 16.2 | 18.3 | 19.0 |
| | 5 | 0.7 | 10.5 | 20.5 | 18.2 | 19.0 | | | 20.5 | 19.5 | 16.0 | 17.6 | 15.5 | 19.2 | | 20.6 | 19.0 | 18.2 | 16.5 | 16.0 | 17.5 | 10.5 |
| | 6 | 0.4 | 16.9 | 20.8 | 19.6 | 19.5 | | 20.8 | 20.5 | 20.2 | 19.5 | 18.6 | 18.0 | 20.0 | 20.5 | 20.8 | 19.4 | 19.2 | 16.9 | 17.5 | 20.5 | 20.0 |



NOLAN, DAVIS
& ASSOCIATES

FIGURE 3-5
 TEMPERATURE PROFILE
 PILE 18A - DEC. 1989
 HEATH STEELE MINES

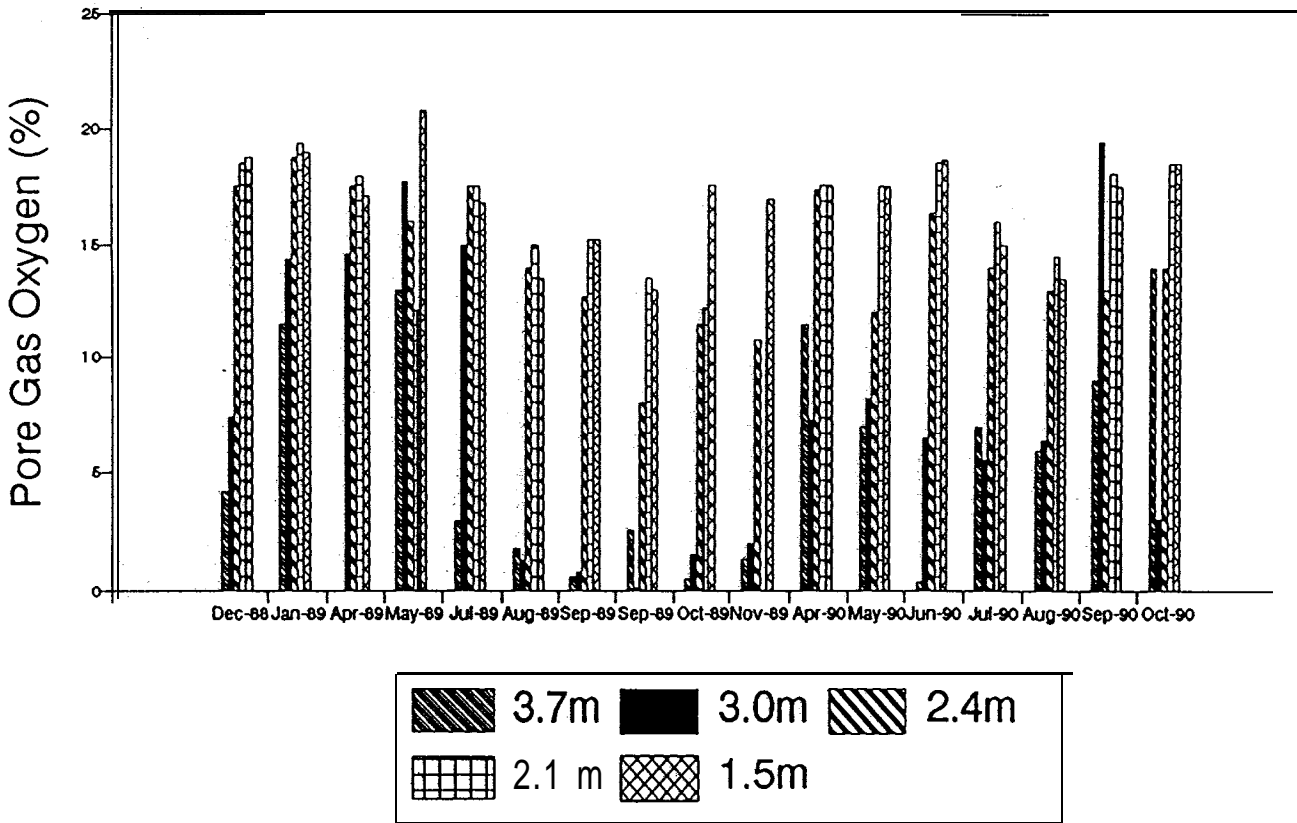
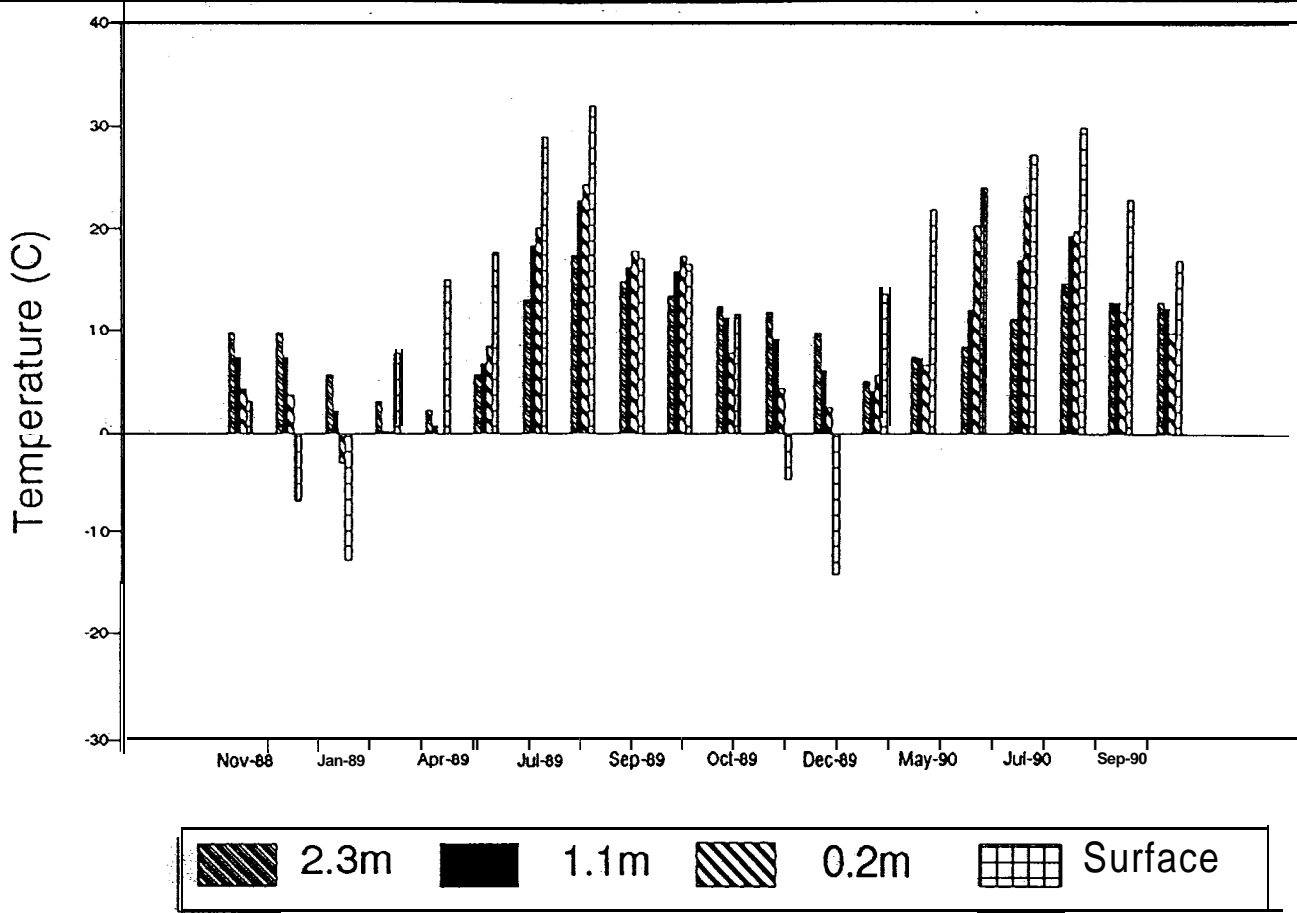
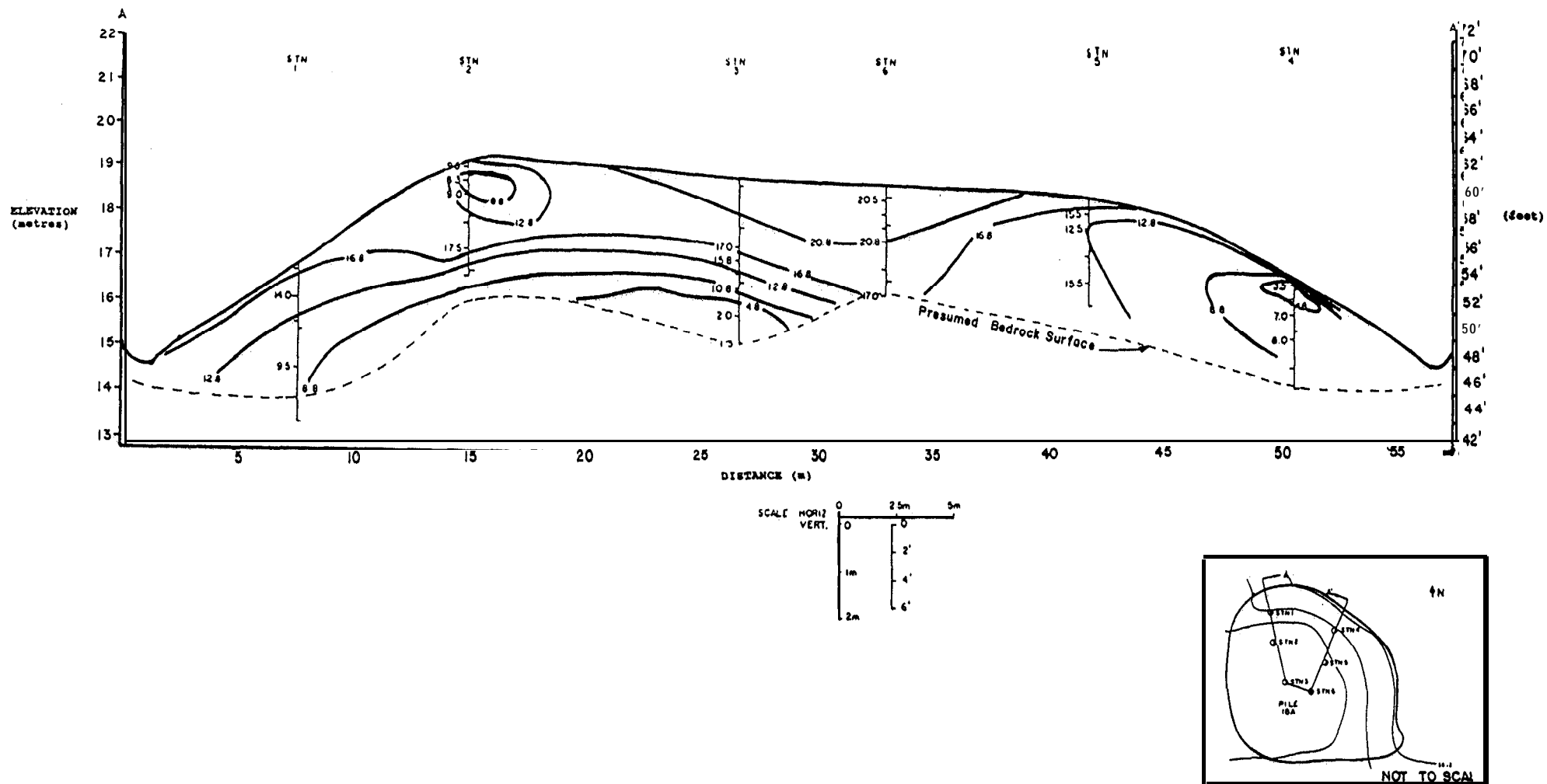
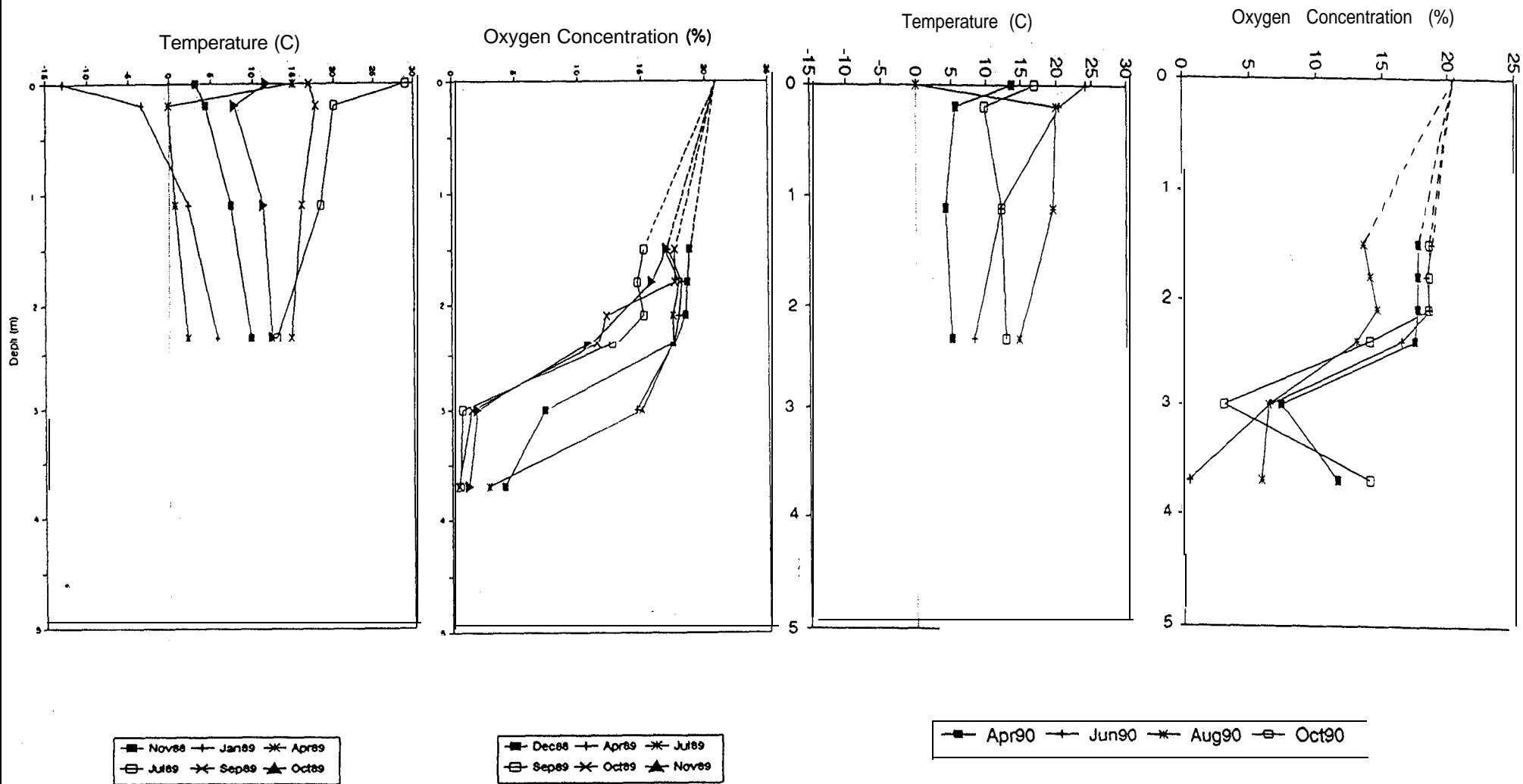


FIGURE 3-6
 SEASONAL VARIATION IN TEMPERATURE AND OXYGEN
 PILE 18A
 HEATH STEELE MINES



NOLAN, DAVIS
& ASSOCIATES

FIGURE 3-7
OXYGEN PROFILE
PILE 18A - NOV. 1989
HEATH STEELE MINES



**NOLAN, DAVIS
& ASSOCIATES**

FIGURE 3-8

MATCHED TEMPERATURE AND OXYGEN DEPTH PROFILES
PILE 18A, STATION 3
HEATH STEELE MINES

3.3 Pile 18B

3.3.1 Description of Pile

Pile 18B is immediately adjacent to 18A but is significantly larger at an estimated 19,500 tonnes of acid generating waste rock (ref. Table 1-4) containing pyrite, pyrrhotite, sphalerite, galena and chalcopyrite. Its maximum depth is 6.7 m. The pile is instrumented with six sets of thermocouples and gas ports to provide a single longitudinal profile (ref. Figure 2-1).

3.3.2 Data Presentation

As described for Pile 18A, temperature and oxygen data were collected monthly for all site monitoring locations, except in extreme winter conditions when the oxygen meter was inoperative. The raw data for the pile is presented in Tables 3-4 and 3-5. Similar profile presentations, as described for Pile 18A, are also presented to aid in the interpretation of the data.

Water quality and flow measurements could not be made at this site due to the high permeability of the waste rock pile and the underlying overburden and bedrock.

3.3.3 Interpretation

The data for this pile follows a single profile through the centre of the pile and provides for a comparison of the effects of its greater depth (6.7 m) compared to Pile 18A (3.4 m).

The general seasonal trends for both temperature and oxygen described for the smaller Pile 18A are reflected in Pile 18B with a temperature difference of 30°C in December 1989 and the lowest internal temperatures occurring in May. Like Pile 18A, the highest oxygen levels at depth occur in April/May (Figure 3-10).

The oxygen profile (Figure 3-11) for November 1989 indicates a zone of oxygen depletion around Station 5 but very little depletion around Station 4. This pattern is also reflected in the data sets at other times and must represent spatial variations in the air permeability and/or rate of oxidation of the waste rock within the pile. Similarly, the region of oxygen depletion at Station 3 appears to expand in size during the summer months.

The difference between the north and the south side of this pile could be due to differences in material properties, or due to advection caused by the wind. The prevailing northwest wind would tend to generate air flow in the pile from the north to the south and could explain the presence of high oxygen levels near the base on the northern side but not on the south.

The observed temperature and oxygen pattern in pile 18B can be explained by a combination of oxidation near the surface when temperatures were high enough, continuous oxidation at depth, thermal convection in the winter, prevailing wind from the north and, perhaps, variability in distribution of oxidizable material.

TABLE 3-4

Heath Steele Waste Rock Study
Pile 18B

Temperature Data (C)

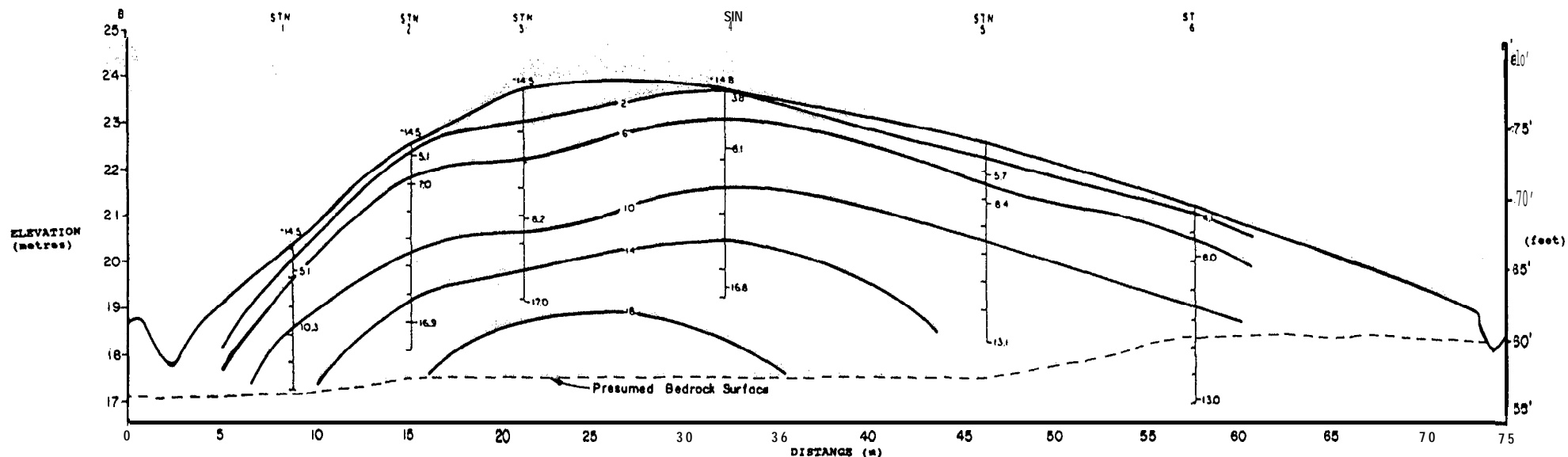
| Stn | Port | Depth (m) | 1988 | | | | 1989 | | | | | | | | 1990 | | | | | | | | | | |
|-----|---------|--------------|-------|------|------|--------|--------|--------|--------|--------|--------|--------|--------|--------|--------|--------|--------|--------|--------|--------|--------|--------|--------|--------|--------|
| | | | Min. | Max. | Avg. | 10-Nov | 10-Dec | 14-Jan | 17-Feb | 30-Apr | 15-May | 04-Jul | 03-Aug | 04-Sep | 22-Sep | 12-Oct | 22-Nov | 29-Dec | 25-Apr | 25-May | 14-Jun | 20-Jul | 16-Aug | 28-Sep | 12-Oct |
| 1 | Red | 1.8 | 4.7 | 15.2 | 9.5 | 8.8 | 6.8 | 7.0 | 8.0 | 5.4 | 4.7 | 9.7 | 12.4 | 15.2 | 13.5 | 12.1 | 10.0 | 10.3 | 5.7 | 6.7 | 7.3 | 10.4 | 14.5 | 12.8 | 12.7 |
| | Blue | 0.6 | 1.8 | 19.2 | 8.6 | 6.0 | 2.5 | 2.5 | 4.9 | 1.8 | 6.9 | 16.6 | 19.2 | 17.2 | 15.7 | 8.9 | 4.9 | 5.1 | 3.2 | 5.1 | 12.8 | 18.7 | 20.7 | 11.8 | 10.4 |
| | Surface | 0.0 | -20.1 | 28.3 | 5.6 | 3.2 | -7.2 | -12.9 | -20.1 | 7.7 | 17.7 | 26.7 | 28.3 | 19.9 | 18.1 | 9.5 | -4.0 | -14.5 | 10.5 | 19.6 | 22.3 | 23.0 | 26.4 | 23.6 | 16.6 |
| 2 | Red | 4.0 | 6.9 | 18.5 | 13.6 | 16.2 | 13.4 | 12.4 | 13.0 | 8.4 | 6.9 | 9.7 | 12.4 | 18.5 | 16.2 | 16.4 | 16.4 | 16.9 | 10.2 | 9.5 | 9.8 | 11.6 | 14.7 | 16.6 | 17.0 |
| | Blue | 0.9 | -0.2 | 22.0 | 10.1 | 9.1 | 3.9 | 0.7 | 2.7 | -0.2 | 6.2 | 19.2 | 22.0 | 19.9 | 19.3 | 12.8 | 8.1 | 7.0 | 5.9 | 7.0 | 15.3 | 21.1 | 22.5 | 16.2 | 13.8 |
| | Black | 0.3 | -0.7 | 23.3 | 9.3 | 7.7 | 2.1 | -0.7 | 1.4 | -0.6 | 6.9 | 19.8 | 23.3 | 19.8 | 19.1 | 10.7 | 5.8 | 5.1 | 6.1 | 6.5 | 17.5 | 22.8 | 22.5 | 15.3 | 12.0 |
| | Surface | 0.0 | -20.0 | 28.7 | 6.7 | 3.2 | -7.2 | -12.9 | -20.0 | 7.7 | 17.7 | 26.7 | 28.7 | 25.1 | 24.9 | 10.7 | -3.4 | -14.5 | 13.3 | 19.9 | 27.3 | 26.3 | 31.0 | 22.9 | 16.5 |
| 3 | Red | 4.6 | 8.0 | 17.7 | 14.1 | 16.9 | 15.1 | 13.8 | 14.4 | 9.5 | 8.0 | 10.0 | 12.7 | 17.7 | 15.7 | 15.7 | 16.6 | 17.0 | 10.4 | 9.0 | 9.6 | 11.4 | 14.2 | 15.5 | 16.2 |
| | Blue | 2.8 | 6.6 | 20.1 | 13.6 | 16.1 | 12.8 | 10.0 | 11.5 | 6.6 | 6.9 | 13.0 | 16.8 | 20.1 | 19.5 | 18.6 | 16.6 | 8.2 | 8.4 | 8.7 | 10.2 | 14.3 | 17.8 | 18.9 | 18.6 |
| | Black | 1.6 | 0.0 | 20.3 | 11.2 | 11.5 | 6.4 | 5.0 | 6.5 | 2.7 | 7.4 | 17.3 | 20.1 | 20.3 | 19.8 | 16.2 | 12.2 | - | 6.1 | 7.4 | 12.3 | 18.0 | 21.0 | 17.8 | 16.3 |
| | Surface | 0.0 | -20.0 | 28.5 | 6.4 | 3.2 | -7.3 | -12.9 | -20.0 | 7.7 | 17.7 | 27.3 | 28.5 | 25.1 | 22.7 | 10.4 | -4.1 | -14.5 | 11.5 | 19.6 | 25.3 | 21.9 | 26.5 | 24.4 | 16.6 |
| 4 | Red | 4.3 | 7.4 | 18.8 | 13.3 | 15.1 | 13.5 | 11.8 | | 7.7 | 7.4 | 10.2 | 12.9 | 18.8 | 15.0 | 15.5 | 15.0 | 16.8 | 9.2 | 9.3 | 10.0 | 11.7 | 14.9 | 15.9 | 15.5 |
| | Blue | 1.3 | 0.2 | 21.0 | 10.8 | 9.5 | 4.7 | 1.2 | | 0.2 | 8.0 | 18.3 | 21.0 | 19.9 | 17.9 | 12.8 | 8.3 | 8.1 | 5.7 | 7.6 | 14.4 | 19.6 | 21.9 | 15.7 | 13.4 |
| | Black | 0.1 | -5.2 | 24.7 | 9.1 | 5.3 | -5.2 | -3.1 | | 0.0 | 9.9 | 23.8 | 24.7 | 20.8 | 18.1 | 9.9 | 1.5 | 3.8 | 5.8 | 7.8 | 20.2 | 23.8 | 21.5 | 14.2 | 11.3 |
| | Surface | 0.0 | -14.8 | 28.2 | 8.6 | 3.2 | -7.2 | -12.9 | | 7.7 | 17.7 | 27.3 | 28.2 | 20.9 | 27.9 | 10.7 | -5.1 | -14.8 | 15.2 | 20.9 | 29.8 | 26.2 | 26.6 | 26.1 | 16.9 |
| 5 | Red | 4.4 | 7.2 | 17.9 | 12.3 | 14.6 | 12.5 | 10.9 | | 8.0 | 7.2 | 9.6 | 11.8 | 17.9 | 14.1 | 14.2 | 14.1 | 13.1 | 8.4 | 8.8 | 10.0 | 10.7 | 13.3 | 14.7 | 14.3 |
| | Blue | 1.3 | 0.5 | 20.4 | 10.8 | 9.9 | 4.5 | 1.9 | | 0.5 | 7.8 | 17.7 | 20.4 | 18.7 | 18.0 | 12.9 | 8.4 | 8.4 | 5.1 | 7.3 | 14.0 | 18.8 | 21.3 | 15.8 | 12.9 |
| | Black | 0.7 | -1.5 | 22.2 | 9.5 | 8.3 | 1.1 | -1.5 | | -0.2 | 8.6 | 19.1 | 22.2 | 18.3 | 17.8 | 9.8 | 5.2 | 5.7 | 5.6 | 6.3 | 16.9 | 21.6 | 21.5 | 14.7 | 10.7 |
| | Surface | 0.0 | -12.9 | 29.3 | 10.0 | 3.2 | -7.2 | -12.9 | | 7.7 | 17.7 | 28.6 | 27.3 | 20.9 | 29.3 | 9.9 | -5.0 | - | 11.6 | 28.8 | 31.2 | 26.7 | 31.5 | 23.8 | 16.7 |
| 6 | Red | 4.2 | 4.1 | 15.5 | 10.2 | 12.4 | 8.7 | 7.0 | | 4.1 | 6.5 | 8.1 | 10.2 | 15.5 | 12.5 | 12.4 | 12.1 | 13.0 | 7.2 | 7.4 | 8.0 | 9.1 | 11.4 | 12.8 | 11.5 |
| | Blue | 1.1 | -0.5 | 19.0 | 10.1 | 10.1 | 5.2 | 0.8 | | -0.5 | 5.7 | 14.4 | 17.8 | 19.0 | 17.3 | 13.9 | 9.4 | 8.0 | 3.1 | 7.1 | 10.7 | 15.1 | 18.5 | 16.1 | 13.4 |
| | Black | 0.2 | -3.3 | 20.6 | 9.2 | 9.4 | 1.5 | -3.3 | | -0.8 | 7.7 | 17.8 | 20.6 | 19.2 | 17.3 | 10.6 | 5.8 | 4.1 | 3.6 | 5.8 | 13.7 | 19.7 | 20.7 | 14.5 | 10.7 |
| | Surface | 0.0 | -12.9 | 28.6 | 9.6 | 3.2 | -7.2 | -12.9 | | 7.7 | 17.7 | 28.6 | 27.3 | 20.9 | 25.1 | 10.0 | -5.0 | - | 12.4 | 25.1 | 27.6 | 24.9 | 30.0 | 24.5 | 16.5 |

TABLE 3-5

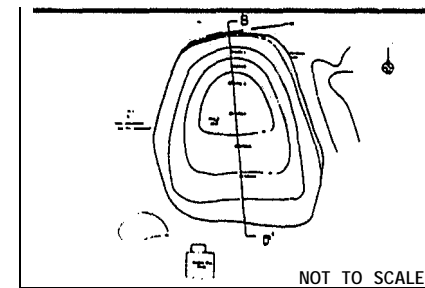
Heath Steele Waste Rock Study
Pile 18 B

Oxygen Concentration (% of pore gas)

| Sun | Port | Depth (m) | Min. | Max. | Avg. | 1988 | | | | | 1989 | | | | | 1990 | | | | | | | |
|-----|------|--------------|------|------|------|--------|--------|--------|--------|--------|--------|--------|--------|--------|--------|--------|--------|--------|--------|--------|--------|--------|--------|
| | | | | | | 10-Dec | 14-Jan | 17-Feb | 30-Apr | 15-May | 04-Jul | 03-Aug | 04-Sep | 22-Sep | 13-Oct | 22-Nov | 25-Apr | 25-May | 14-Jun | 20-Jul | 16-Aug | 28-Sep | 12-Oct |
| 1 | 1 | 3.2 | 0.0 | 20.5 | 19.5 | 19.8 | | 20.5 | | 19.2 | 18.8 | | | 19.0 | 19.5 | | | | 19.8 | 20.5 | 20.7 | | |
| | 2 | 2.6 | 18.6 | 20.5 | 19.8 | 19.8 | 19.8 | 19.9 | 19.6 | 19.6 | 20.0 | 19.5 | 20.0 | 19.2 | 19.8 | | 20.5 | 20.5 | 19.8 | 19.0 | 18.6 | 19.5 | 20.0 |
| | 3 | 2.0 | 18.5 | 20.5 | 19.8 | 19.4 | 19.6 | 19.6 | 19.5 | 19.6 | 20.4 | 19.0 | 20.0 | 19.5 | 20.0 | 20.5 | 20.5 | 20.5 | 19.8 | 19.4 | 18.5 | 19.3 | 20.0 |
| | 4 | 1.4 | 18.6 | 20.6 | 19.8 | 19.4 | 19.6 | 19.2 | 19.7 | 19.6 | 20.5 | 19.5 | 20.2 | 19.5 | 20.2 | | 20.6 | 20.5 | 19.8 | 19.4 | 18.6 | 19.5 | 20.0 |
| | 5 | 0.8 | 18.5 | 20.7 | 19.9 | 19.6 | 19.6 | 19.6 | 20.0 | 19.8 | 20.4 | 19.5 | 20.1 | 19.5 | 20.4 | | 20.7 | 20.8 | 19.8 | 19.2 | 18.5 | 19.3 | 20.0 |
| | 6 | 0.2 | 18.5 | 20.8 | 20.1 | 19.6 | 20.2 | 19.4 | 20.0 | | 20.3 | 19.5 | 20.5 | 20.0 | 20.6 | 20.8 | 20.7 | 20.8 | 20.0 | 19.0 | 18.5 | 19.3 | 20.2 |
| 2 | 1 | 4.6 | 11.5 | 20.0 | 16.5 | 18.6 | 18.6 | 19.6 | | 18.8 | 17.1 | 12.0 | 13.5 | 11.7 | 15.5 | 16.0 | 20.0 | 20.5 | 19.6 | 17.2 | 11.5 | 17.5 | 18.7 |
| | 2 | 4.0 | 11.2 | 20.0 | 16.4 | 18.4 | 18.6 | 18.7 | 18.0 | 19.0 | 16.4 | 11.5 | 13.3 | 11.2 | 15.5 | | 20.0 | 20.2 | 19.2 | 16.0 | 12.0 | 17.7 | 18.5 |
| | 3 | 3.4 | 9.5 | 20.0 | 16.7 | 18.4 | 19.2 | 18.7 | 18.0 | 18.8 | 16.6 | 9.5 | 13.5 | 10.5 | 18.7 | 18.0 | 20.0 | 20.0 | 19.0 | 14.1 | 10.3 | 17.7 | 18.5 |
| | 4 | 2.7 | 9.4 | 20.3 | 16.8 | 18.5 | 19.4 | 18.6 | 19.2 | 18.8 | 16.6 | 9.4 | 14.5 | 11.0 | 18.5 | | 20.3 | 20.2 | 19.3 | 15.0 | 10.5 | 17.5 | 18.5 |
| | 5 | 2.1 | 7.6 | 20.0 | 16.0 | 18.5 | 17.8 | 18.5 | 18.5 | 18.5 | 13.6 | 7.6 | 14.5 | 10.0 | 18.2 | | 20.0 | 20.1 | 17.5 | 11.7 | 9.7 | 16.5 | 18.0 |
| | 6 | 1.5 | 4.2 | 19.9 | 14.3 | 18.4 | 16.5 | 17.5 | 17.0 | 17.6 | 7.7 | 4.2 | 12.5 | 7.0 | 17.4 | 15.8 | 19.9 | 19.9 | 14.0 | 7.9 | 8.5 | 15.5 | 17.0 |
| | 7 | 0.9 | 2.8 | 19.6 | 11.4 | | | | | | 5.9 | 2.8 | 15.9 | 7.0 | 17.4 | | 19.6 | 19.0 | 9.8 | 4.0 | 6.7 | 14.0 | 16.0 |
| 3 | 1 | 4.6 | 11.0 | 20.0 | 17.4 | 18.5 | | | 19.6 | 19.0 | 19.5 | 14.0 | 17.1 | 14.5 | 14.5 | 17.0 | 20.0 | 20.5 | 20.0 | 17.5 | 11.0 | 13.0 | 16.2 |
| | 2 | 4.0 | 10.9 | 20.1 | 16.2 | 18.5 | | 19.6 | | 19.3 | 18.7 | 11.5 | 12.0 | 12.7 | 13.5 | | 20.1 | 20.5 | 19.8 | 17.4 | 10.9 | 13.0 | 18.0 |
| | 3 | 3.4 | 9.0 | 20.0 | 16.1 | 18.3 | 19.0 | 19.4 | 19.2 | 19.0 | 18.2 | 9.0 | 12.0 | 15.0 | 12.7 | 11.8 | 20.0 | 20.5 | 19.8 | 16.2 | 10.0 | 17.0 | 18.0 |
| | 4 | 2.7 | 8.0 | 19.9 | 15.4 | 17.8 | 17.6 | 18.3 | 18.5 | 18.5 | 16.0 | 8.0 | 11.0 | 10.7 | 12.7 | | 19.9 | 20.0 | 19.0 | 15.5 | 9.0 | 11.0 | 17.0 |
| | 5 | 2.1 | 4.9 | 19.7 | 12.8 | 17.6 | 16.5 | 16.5 | 17.6 | 17.1 | 10.2 | 4.9 | 9.0 | 6.6 | 11.2 | 10.5 | 19.7 | 19.5 | 17.7 | 16.0 | 7.0 | 10.5 | 16.5 |
| | 6 | 1.5 | 0.9 | 19.3 | 10.3 | 15.4 | 11.2 | 11.5 | 16.7 | 15.8 | 5.5 | 0.9 | 6.7 | 3.1 | 7.5 | | 19.3 | 19.0 | 13.5 | 7.1 | 4.2 | 10.7 | 15.5 |
| | 7 | 0.9 | 0.2 | 18.9 | 8.6 | 15.5 | 9.8 | 8.0 | | 13.9 | 5.2 | 0.2 | | 2.6 | 4.5 | 7.7 | 18.9 | 18.5 | 9.0 | 2.8 | 1.9 | 11.0 | 15.0 |
| 4 | 1 | 4.6 | 1.5 | 18.5 | 11.4 | 1.5 | | | 16.6 | 17.6 | 9.6 | 5.1 | 10.1 | 6.6 | 15.2 | 13.0 | 18.5 | 19.3 | 13.2 | 9.0 | 8.2 | 10.5 | 14.0 |
| | 2 | 4.0 | 5.1 | 19.0 | 13.2 | 14.4 | | | 18.0 | 18.0 | 12.8 | 5.1 | 10.4 | 6.3 | 15.2 | | 19.0 | 19.1 | 13.3 | 9.0 | 7.3 | 9.8 | 13.5 |
| | 3 | 3.4 | 4.8 | 19.6 | 13.3 | 16.5 | | | 18.6 | 18.3 | 8.0 | 4.8 | 9.9 | 6.3 | 15.0 | 15.5 | 19.6 | 19.0 | 10.8 | 6.0 | 6.2 | 9.4 | 12.5 |
| | 4 | 2.7 | 3.6 | 19.7 | 12.8 | 17.5 | 16.6 | | 18.5 | 18.2 | 6.8 | 3.6 | 8.8 | 4.8 | 13.5 | | 19.7 | 17.0 | 9.5 | 6.5 | 6.5 | 8.4 | 12.0 |
| | 5 | 2.1 | 0.0 | 19.2 | 11.7 | 16.5 | 16.4 | | 17.5 | 17.5 | 5.1 | 0.0 | 6.0 | 3.0 | 13.5 | 14.5 | 19.2 | 15.0 | 9.3 | 2.5 | 1.8 | 6.4 | 10.5 |
| | 6 | 1.5 | 0.1 | 17.1 | 9.0 | 16.4 | | | 14.6 | 13.8 | 1.1 | 0.1 | 1.0 | 0.2 | 14.5 | 11.3 | 17.1 | 13.0 | 5.5 | 1.0 | 2.1 | 1.2 | 5.3 |
| 5 | 1 | 3.7 | 0.3 | 7.4 | 1.9 | 1.1 | 0.9 | | 3.9 | 1.7 | 0.5 | 1.3 | 0.3 | 1.0 | 1.0 | 7.4 | 5.0 | 16.5 | 4.0 | 10.5 | 1.7 | 2.9 | |
| | 2 | 3.1 | 1.9 | 9.7 | 4.5 | 1.9 | | | 7.8 | 8.7 | 4.1 | 2.0 | 2.8 | 2.3 | 3.0 | 2.5 | 9.7 | 7.0 | 8.5 | 4.0 | 4.3 | 3.8 | 4.5 |
| | 3 | 2.5 | 0.6 | 9.9 | 4.3 | 3.2 | 6.8 | | 7.0 | 6.6 | 3.1 | 1.2 | 2.5 | 0.6 | 2.5 | | 9.9 | 10.0 | 10.1 | 3.7 | 4.2 | 4.2 | 4.5 |
| | 4 | 1.9 | 0.1 | 12.2 | 5.5 | 3.4 | 11.5 | | 8.6 | 8.8 | 1.5 | 0.1 | 1.4 | 2.0 | 6.0 | 5.0 | 12.2 | 15.2 | 11.5 | 5.5 | 3.6 | 7.2 | 7.1 |
| | 5 | 1.2 | 3.2 | 15.0 | 9.3 | 10.2 | 15.0 | | 12.0 | 11.5 | 4.6 | 3.2 | 8.0 | 4.2 | 10.5 | | 14.1 | 15.8 | 11.5 | 6.3 | 6.5 | 10.5 | 9.2 |
| | 6 | 0.6 | 2.4 | 15.7 | 9.9 | 11.5 | 15.0 | | 14.0 | 15.7 | 2.7 | 2.4 | 8.3 | 3.8 | 10.2 | 11.5 | 14.0 | 18.0 | 10.0 | 6.0 | 5.4 | 9.6 | 8.9 |
| | 7 | 0.1 | 11.5 | 20.8 | 18.6 | 11.5 | 20.0 | | 20.5 | 20.8 | 20.5 | 17.0 | 19.4 | 15.2 | 19.0 | 20.0 | 20.5 | 20.5 | 20.8 | 20.8 | 20.0 | 19.7 | 19.5 |
| 6 | 1 | 4.3 | 1.0 | 8.0 | 4.0 | 2.7 | 7.7 | | 4.1 | 8.0 | 3.2 | 1.0 | 2.7 | 1.5 | 4.2 | 5.0 | | 5.0 | 9.8 | 5.2 | 1.5 | 13.7 | 4.4 |
| | 2 | 3.7 | 1.9 | 9.9 | 5.5 | 3.7 | 8.8 | | 5.0 | 9.9 | 5.5 | 3.0 | 5.0 | 1.9 | 4.5 | | 7.5 | 6.0 | 10.5 | 5.6 | 3.4 | 7.6 | 4.3 |
| | 3 | 3.0 | 3.7 | 11.8 | 8.0 | 6.0 | 11.8 | | 5.6 | 11.8 | 7.6 | 4.1 | 9.0 | 5.4 | 9.5 | 8.0 | 9.6 | 11.2 | 9.8 | 6.6 | 3.7 | 12.0 | 8.1 |
| | 4 | 2.4 | 4.0 | 18.2 | 11.3 | 17.0 | 18.2 | | 10.0 | 12.0 | 8.0 | 4.8 | 11.0 | 4.0 | 15.0 | | 12.6 | 15.5 | 10.0 | 7.5 | 4.5 | 13.5 | 12.0 |
| | 5 | 1.8 | 4.5 | 18.6 | 12.9 | 16.0 | 18.6 | | 13.0 | 15.5 | 12.0 | 4.5 | 11.0 | 7.6 | 14.5 | 15.5 | 13.5 | 16.5 | 10.5 | 7.4 | 8.7 | 14.0 | 11.5 |
| | 6 | 1.2 | 5.0 | 18.6 | 14.0 | 16.8 | 18.6 | | 14.0 | 15.8 | 15.0 | 7.1 | 13.0 | 9.5 | 15.5 | | 15.0 | 17.5 | 17.5 | 10.0 | 5.0 | 14.7 | 13.5 |
| | 7 | 0.6 | 0.0 | 18.8 | 15.2 | 16.5 | 18.8 | | 15.0 | 15.5 | 13.9 | 9.5 | 14.9 | 14.2 | 16.5 | 16.8 | 16.0 | 17.8 | 14.5 | 10.0 | | | 14.0 |

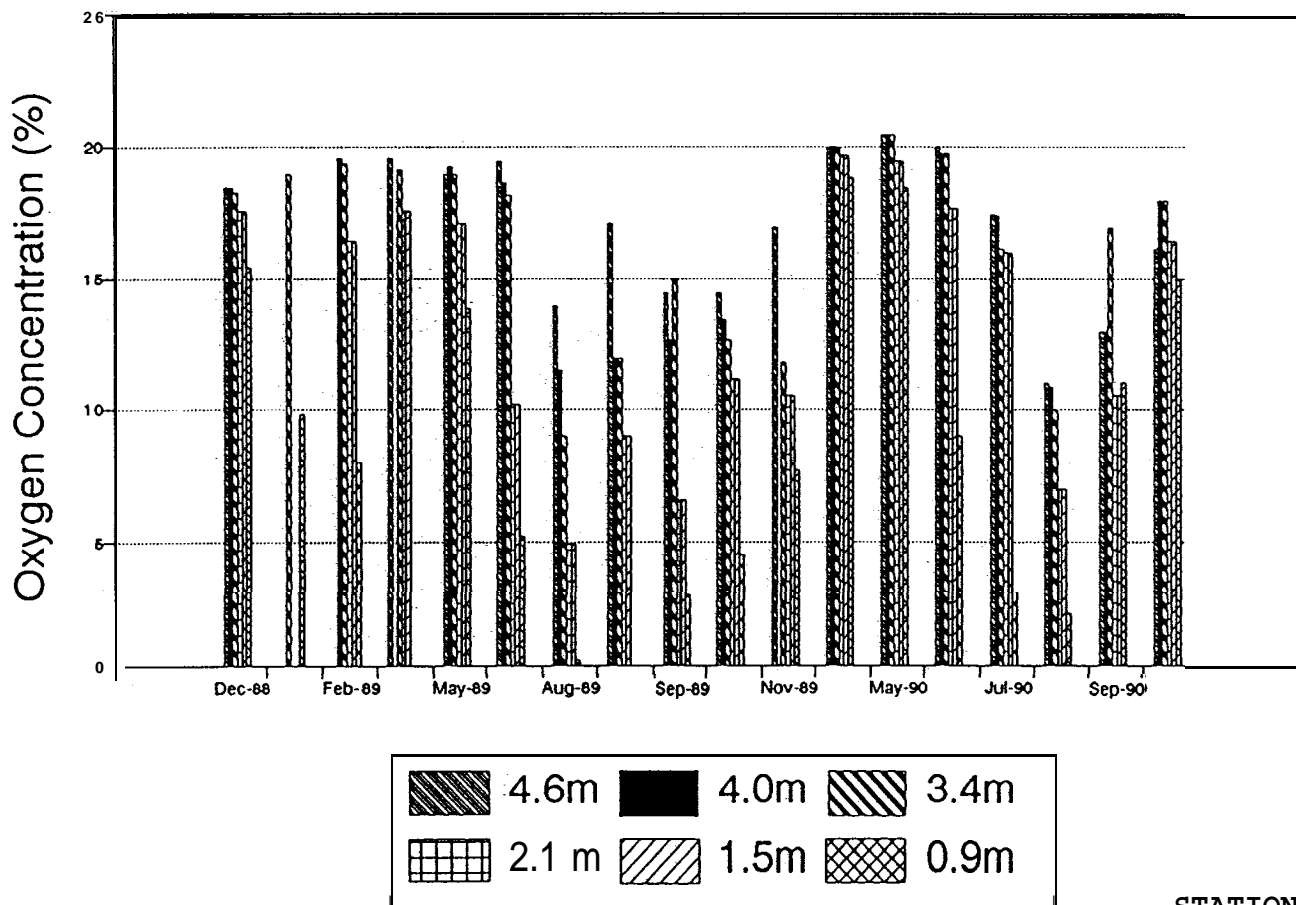
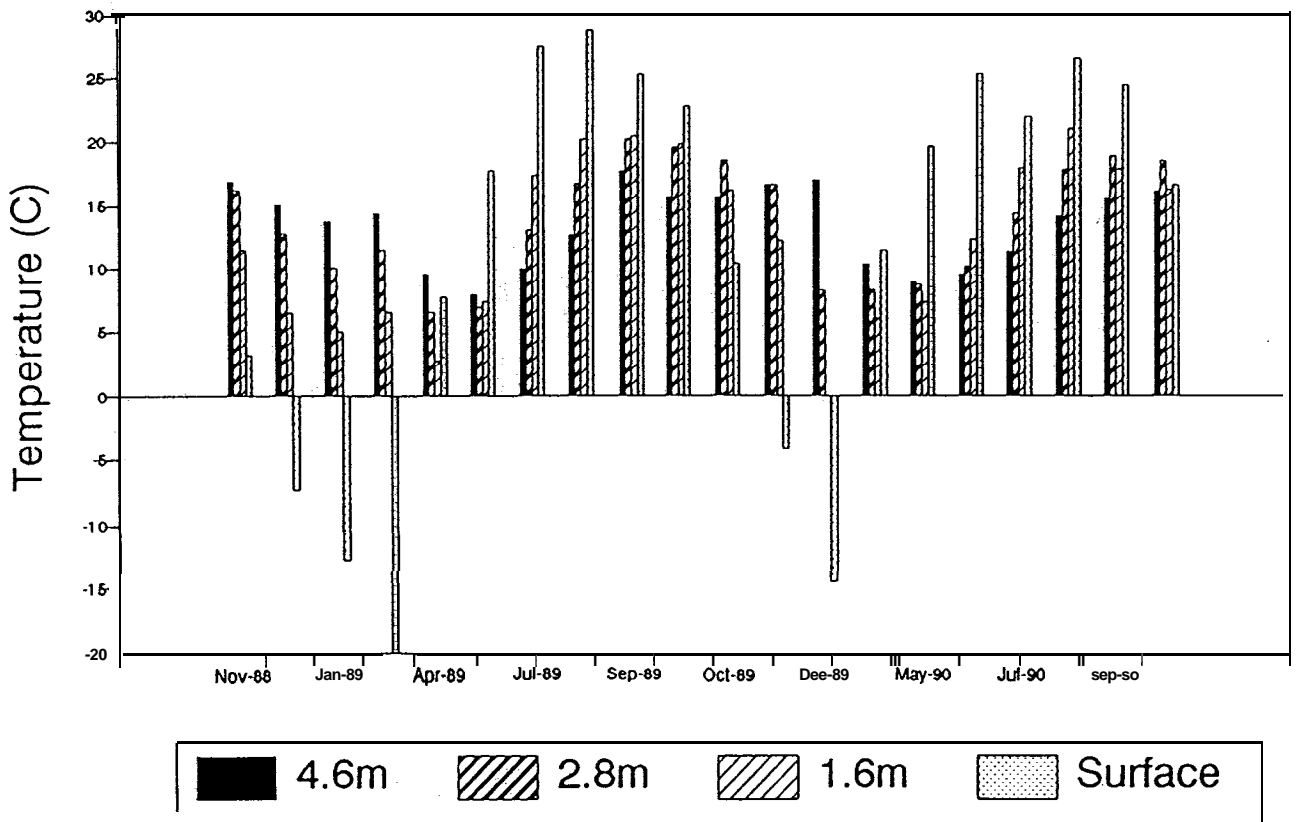


PILE 18B (looking grid north)
 SCALE HORIZ. 0 1m 2.5m 5m
 VERT. 0 0.5m 1m 2m
 0 1' 2' 3' 4' 5' 6'



NOLAN, DAVIS
& ASSOCIATES

FIGURE 3-9
 TEMPERATURE PROFILE
 PILE 18B - DEC. 1989
 HEATH STEELE MINES



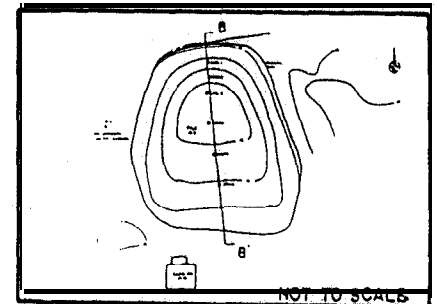
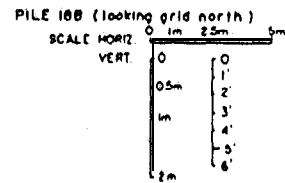
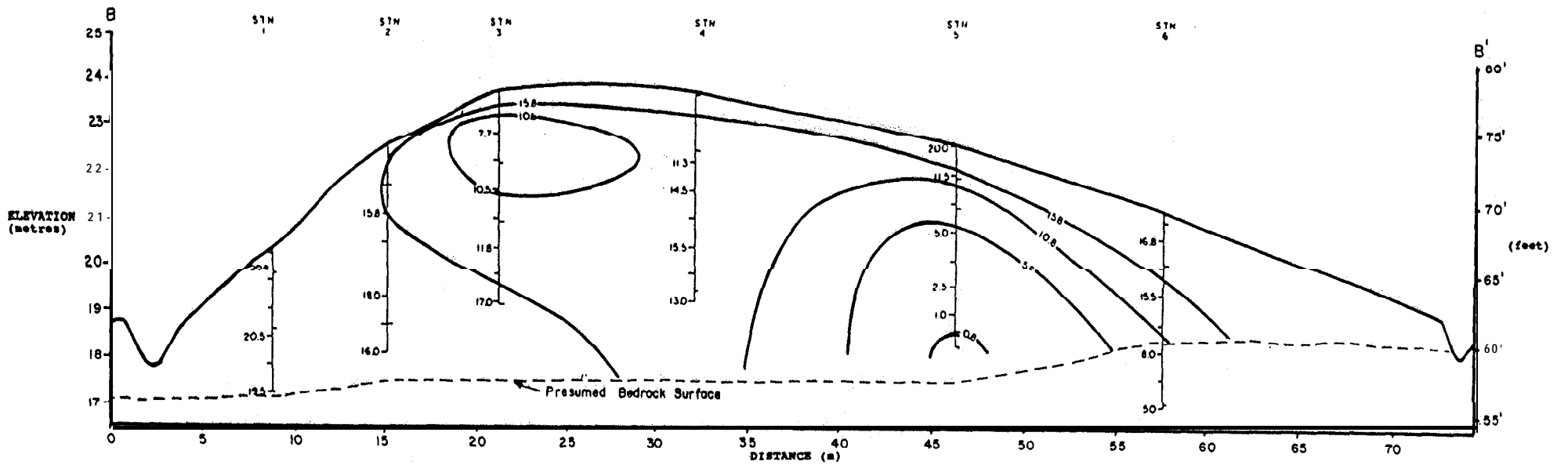
STATION 3



NOLAN, DAVIS
& ASSOCIATES

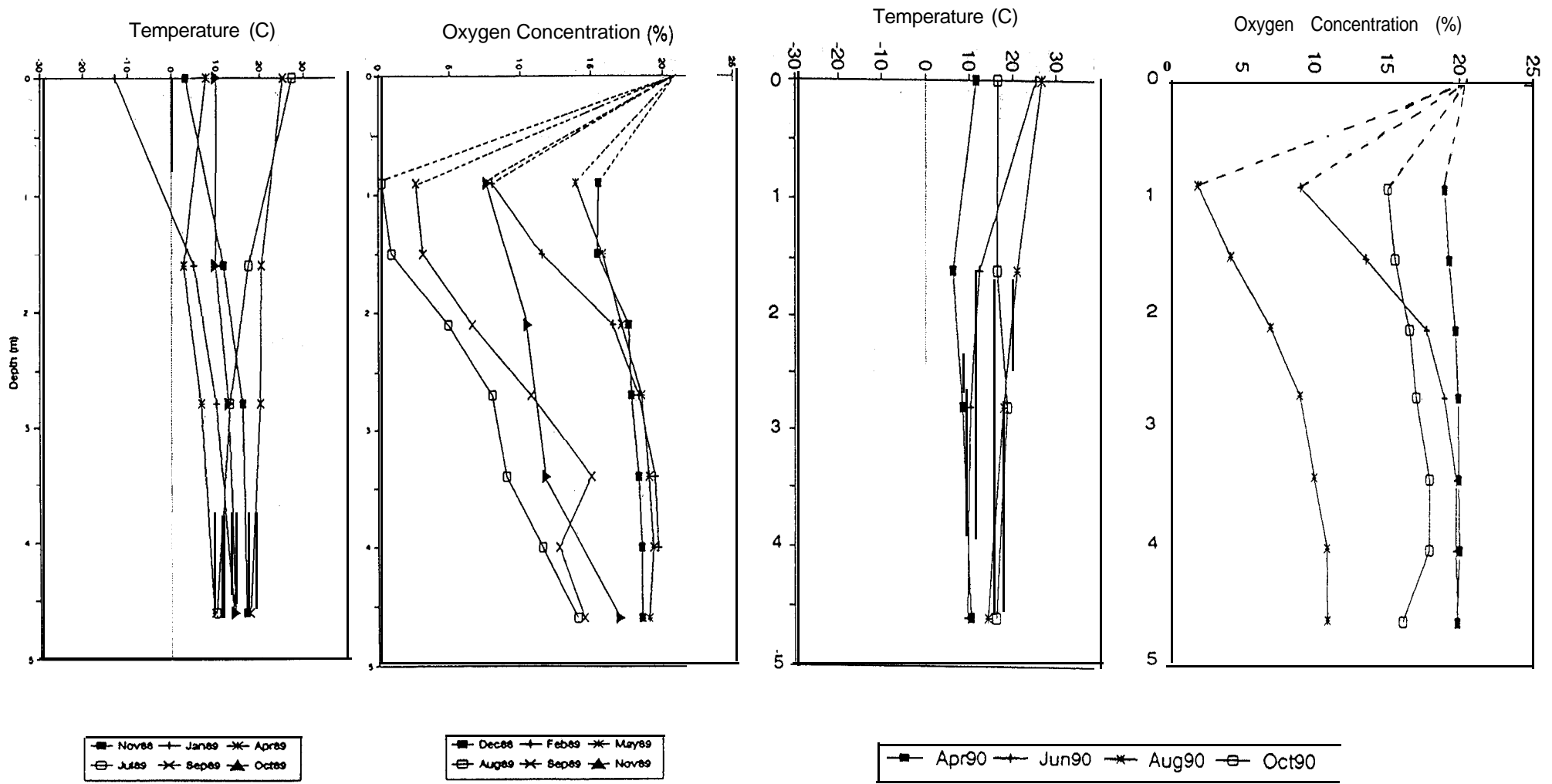
FIGURE 3-10

SEASONAL VARIATION IN TEMPERATURE AND OXYGEN
PILE 18B
HEATH STEELE MINES



NOLAN, DAVIS
& ASSOCIATES

FIGURE 3-11
OXYGEN PROFILE
PILE 18B - NOV. 1989
HEATH STEELE MINES



**NOLAN, DAVIS
& ASSOCIATES**

FIGURE 3-12

MATCHED TEMPERATURE AND OXYGEN DEPTH PROFILES
PILE 18B, STATION 3
HEATH STEELE MINES

3.4 Pile 17

3.4.1 Description of Pile

Pile 17 is the largest of the four piles monitored with approximately 236,000 tonnes of sphalerite bearing waste (Table 1-4). Its maximum depth is 10.5 m. As outlined in Section 2.2.5, it was impractical to segregate the pile with perimeter ditching, but it is situated on a slope with an existing collection ditch at the downstream toe.

The pile was instrumented with six sets of thermocouples and gas ports arranged on two perpendicular axes as shown in Figure 2-2.

3.4.2 Data Presentation

Temperature and oxygen measurements were made at each of the six sampling locations on a monthly basis as described for Pile **18A**. The raw data for temperature and oxygen, along with calculated averages, are presented in Tables 3-6 and 3-7, respectively. Profiles similar to those for Piles **18A** and **18B** are also included to aid interpretation.

Water quality in the downslopetoe ditch was monitored throughout the project as part of the ongoing site monitoring program. Available data for the period from February 1987 to July 1989 is presented in Table 3-8, with **pH** and zinc levels shown diagrammatically in Figure 3-17.

3.4.3 Interpretation

Pile 17 has a maximum depth of 10.5 metres in the area monitored and thus provides a further opportunity to assess the effects of pile depth and size, although the instrumentation was installed to a maximum depth of only 4.8 metres.

The spatial and seasonal variations in both temperature and oxygen described for Piles **18A** and **18B** appear also to exist in Pile 17.

Although measured data are not available, it would appear by extrapolation that the bottom temperature of the pile in December would be in excess of 20°C , thus giving a 40°C difference with the surface. As with the piles described earlier, the lowest internal temperatures occur in May.

The oxygen data for this pile show far less variation than for the other piles described and in many instances greater concentrations were found at depth than at the surface, with the greatest contrast in this regard being in the central sampling stations (Nos. 3, 2 and 4). An explanation for this phenomenon could be the fact that the surface of the pile consists of hard packed fine material and the primary mechanism for the transport of air to the interior of the pile is through diffusion from the sides. The surface condition may be the result of end dumping on the slope coupled with weathering and compaction of the surface material.

Water quality data for the downgradient collection ditch provides some indication of the combined surface runoff and **leachate** from the pile, although it must be kept in mind that drainage from neighbouring areas also reports to the ditch. Since January 1988, the **pH** has been fairly constant at about 2.1 and over the study period copper has averaged **120.5 mg/L**, lead **0.36 mg/L** and zinc **258.1 mg/L**. The metal levels generally decrease during the winter months, and demonstrate a sharp peak during April/May, and more prolonged elevated levels during late summer and fall. This pattern is typical of local runoff characteristics from acid-generating areas.

TABLE 3-6

Heath Steele Waste Rock Study
Pile 17

Temperature (C)

| n | Port | Depth (m) | Min. | Max. | Avg. | 1988 | | | | | | | | | | | | | | | | 1989 | | | | 1990 | | | |
|---|---------|--------------|-------|------|------|--------|--------|--------|--------|--------|--------|--------|--------|--------|--------|--------|--------|--------|--------|--------|--------|--------|--------|--------|--|------|--|--|--|
| | | | | | | 10-Dec | 14-Jan | 04-Apr | 30-Apr | 15-May | 04-Jul | 03-Aug | 04-Sep | 22-Sep | 12-Oct | 22-Nov | 29-Dec | 25-Apr | 25-May | 14-Jun | 20-Jul | 16-Aug | 28-Sep | 12-Oct | | | | | |
| 1 | Red | 4.6 | 4.9 | 14.2 | 8.9 | 10.1 | 10.0 | 6.1 | 4.9 | 5.4 | 5.6 | 7.0 | 8.9 | 9.9 | 11.3 | 14.2 | 12.8 | 5.1 | 4.7 | 5.5 | 6.1 | 8.7 | 10.9 | 9.5 | | | | | |
| | Blue | 1.5 | -1.0 | 16.3 | 8.4 | 5.1 | 1.4 | -1.0 | 4.9 | 0.0 | 12.9 | 16.3 | 15.2 | 15.5 | 12.6 | 9.8 | 5.7 | 0.4 | 3.3 | 8.7 | 13.8 | 18.0 | 14.7 | 10.9 | | | | | |
| | Black | 0.3 | -7.7 | 21.7 | 6.2 | -3.0 | -7.2 | -0.4 | -1.0 | 6.2 | 18.1 | 21.7 | 18.2 | 17.1 | 8.3 | 3.7 | -7.7 | 2.0 | 4.9 | 17.5 | 20.4 | 19.7 | 13.9 | 8.1 | | | | | |
| | Surface | 0.0 | -20.5 | 22.2 | 6.5 | -7.0 | -5.5 | 7.7 | 1.5 | 17.7 | 20.5 | 22.2 | 20.2 | 17.3 | 10.0 | -6.2 | -20.5 | 12.9 | 25.4 | 30.3 | 22.2 | 29.9 | 21.8 | 14.0 | | | | | |
| 2 | Red | 4.6 | 4.2 | 15.0 | 8.7 | 9.9 | 7.5 | 5.3 | 4.2 | 4.3 | 6.1 | 8.0 | 8.2 | 11.0 | 11.6 | 13.5 | 15.0 | 5.8 | 5.6 | 6.5 | 7.2 | 10.0 | 11.2 | 10.3 | | | | | |
| | Blue | 1.5 | -0.9 | 16.4 | 7.9 | 5.2 | -0.9 | -0.6 | -0.7 | 2.5 | 13.9 | 16.4 | 14.3 | 16.2 | 12.4 | 9.4 | 6.8 | 0.8 | 6.5 | 10.2 | 14.3 | 18.0 | 14.5 | 11.4 | | | | | |
| | Black | 0.3 | -10.0 | 21.9 | 6.2 | -4.5 | -10.0 | -0.2 | 0.0 | 7.5 | 19.7 | 21.9 | 19.7 | 8.0 | 7.8 | 2.6 | 1.3 | 1.5 | 5.6 | 18.8 | 21.3 | 18.8 | 12.3 | 8.0 | | | | | |
| | Surface | 0.0 | -8.2 | 22.0 | 7.8 | -8.2 | -5.5 | 7.7 | 2.0 | 17.7 | 20.5 | 22.0 | 20.2 | 16.0 | 9.4 | -7.9 | - | 12.8 | 21.1 | 29.9 | 19.4 | 32.9 | 21.9 | 14.1 | | | | | |
| 3 | Red | 4.6 | 3.0 | 15.2 | 8.2 | 9.6 | 8.4 | 4.9 | 4.5 | 3.0 | 5.4 | 7.3 | 7.4 | 9.6 | 10.2 | 12.9 | 15.2 | 4.4 | 4.8 | 5.5 | 6.7 | 10.9 | 11.2 | 9.4 | | | | | |
| | Blue | 1.5 | -0.4 | 16.7 | 7.7 | 3.9 | 0.0 | -0.4 | 0.4 | 1.7 | 14.0 | 16.7 | 15.5 | 15.1 | 11.3 | 8.2 | 5.8 | 0.6 | 5.3 | 10.4 | 14.6 | 18.3 | 14.5 | 10.0 | | | | | |
| | Black | 0.3 | -7.4 | 21.3 | 6.3 | -3.7 | -7.4 | 0.0 | 1.4 | 6.5 | 17.8 | 21.3 | 18.8 | 15.9 | 7.3 | 1.3 | -3.2 | 3.2 | 6.2 | 17.8 | 20.8 | 19.0 | 12.3 | 8.0 | | | | | |
| | Surface | 0.0 | -9.0 | 22.0 | 7.8 | -9.0 | -5.5 | 7.7 | 1.5 | 17.0 | 21.4 | 22.0 | 20.2 | 14.4 | 9.4 | -5.2 | - | 12.7 | 21.7 | 30.5 | 20.2 | 31.4 | 21.9 | 14.4 | | | | | |
| 4 | Red | 4.0 | 2.7 | 16.8 | 9.1 | 9.8 | 8.3 | 3.7 | 3.8 | 2.7 | 6.4 | 9.3 | 8.8 | 12.4 | 12.8 | 13.9 | 16.8 | 4.0 | 5.0 | 6.5 | 8.2 | 7.8 | 13.5 | 11.8 | | | | | |
| | Blue | 0.9 | -1.5 | 16.9 | 8.2 | 3.9 | -1.5 | -0.5 | 0.5 | 3.7 | 14.5 | 16.9 | 15.7 | 15.9 | 11.7 | 9.4 | 8.0 | -0.1 | 5.4 | 11.3 | 15.8 | 18.1 | 14.6 | 10.9 | | | | | |
| | Black | 0.3 | -9.0 | 21.3 | 7.1 | -4.7 | -9.0 | 0.4 | 3.6 | 7.3 | 18.5 | 21.3 | 20.1 | 16.8 | 7.3 | 3.5 | 0.1 | 1.8 | 5.7 | 18.7 | 21.4 | 19.4 | 13.4 | 9.1 | | | | | |
| | Surface | 0.0 | -10.5 | 21.8 | 7.8 | -10.5 | -5.5 | 7.7 | 1.5 | 17.0 | 21.4 | 21.8 | 20.4 | 16.4 | 9.1 | -6.0 | - | 11.7 | 16.5 | 28.1 | 21.0 | 33.4 | 20.8 | 14.5 | | | | | |
| 5 | Red | 4.6 | 1.0 | 14.2 | 8.1 | 7.1 | 6.5 | 3.3 | 2.8 | 1.0 | 6.8 | 9.9 | 8.8 | 12.6 | 11.9 | 11.7 | 14.2 | 2.8 | 4.4 | 6.4 | 8.6 | 13.6 | 13.4 | 11.0 | | | | | |
| | Blue | 1.5 | -0.3 | 17.2 | 8.4 | 3.6 | -0.3 | 1.4 | 1.4 | 0.1 | 15.0 | 17.2 | 16.8 | 16.8 | 11.2 | 8.8 | 8.9 | 0.6 | 5.0 | 11.9 | 16.2 | 20.4 | 14.1 | 10.2 | | | | | |
| | Black | 0.3 | -8.6 | 20.8 | 6.9 | -6.9 | -8.6 | 1.6 | 2.0 | 7.3 | 19.1 | 20.8 | 19.6 | 15.7 | 7.7 | 1.7 | 3.3 | 2.3 | 7.4 | 19.7 | 21.3 | 20.0 | 13.4 | 8.3 | | | | | |
| | Surface | 0.0 | -10.5 | 20.8 | 7.8 | -10.5 | -5.5 | 7.7 | 2.0 | 17.7 | 20.6 | 20.8 | 20.0 | 17.1 | 9.3 | -5.2 | - | 14.8 | 19.8 | 33.8 | 19.6 | 31.7 | 21.6 | 14.6 | | | | | |
| 6 | Red | 4.7 | 4.5 | 14.6 | 7.7 | 7.5 | 8.0 | 6.8 | 5.1 | 4.5 | 5.0 | 5.8 | 6.0 | 8.6 | 9.1 | 10.8 | 14.6 | 5.2 | 5.3 | 6.3 | 5.9 | 11.7 | 9.0 | 7.9 | | | | | |
| | Blue | 1.6 | 0.9 | 14.9 | 7.6 | 2.2 | 1.2 | 1.5 | 0.9 | 2.2 | 12.1 | 14.9 | 13.9 | 14.8 | 10.7 | 7.1 | 9.6 | 0.5 | 4.8 | 10.9 | 14.3 | 19.2 | 13.3 | 9.9 | | | | | |
| | Black | 0.7 | -0.4 | 19.5 | 8.0 | -0.4 | -0.1 | 1.3 | 3.3 | 4.8 | 15.5 | 17.8 | 19.5 | 15.4 | 8.3 | 4.5 | 5.6 | 0.8 | 4.8 | 15.0 | 19.0 | 19.4 | 12.7 | 8.0 | | | | | |
| | Surface | 0.0 | -20.5 | 20.6 | 6.1 | -10.7 | -5.5 | 7.7 | 1.5 | 17.7 | 20.3 | 20.6 | 19.8 | 19.3 | 8.6 | -5.2 | -20.5 | 12.2 | 21.5 | 26.2 | 21.6 | 29.5 | 21.1 | 14.4 | | | | | |

TABLE 3-7

Heath Steele Waste Rock Study
Pile 17

Oxygen Concentration (% of pore gas)

| Stn | Port | Depth (m) | 1988 | | | 1989 | | | | | | | 1990 | | | | | | | | | |
|-----|------|--------------|------|------|------|--------|--------|--------|--------|--------|--------|--------|--------|--------|--------|--------|--------|--------|--------|--------|--------|------|
| | | | Min. | Max. | Avg. | Dec-88 | Jan-89 | Apr-89 | May-89 | Jul-89 | Aug-89 | Sep-89 | Oct-89 | Nov-89 | 25-Apr | 25-May | 14-Jun | 20-Jul | 16-Aug | 28-Sep | 12-Oct | |
| 1 | 1 | 4.8 | 17.8 | 20.5 | 19.1 | 17.8 | 19.8 | 20.0 | 20.5 | 19.0 | 18.0 | 18.0 | 18.7 | 19.2 | 19.5 | 20.5 | 20.0 | 19.8 | 17.6 | 17.0 | 18.2 | 19.0 |
| | 2 | 3.8 | 18.3 | 20.0 | 19.0 | 18.4 | | 20.0 | | 19.0 | 18.3 | 19.3 | 19.0 | 19.2 | | 20.8 | 20.0 | 20.0 | 18.1 | 17.7 | 18.0 | 19.0 |
| | 3 | 2.6 | 17.5 | 20.8 | 19.1 | 17.8 | 19.8 | 20.0 | 20.8 | 17.5 | 17.7 | 19.4 | 18.7 | 19.5 | 19.8 | 20.5 | 20.5 | 18.0 | 16.0 | 18.0 | 18.5 | 19.0 |
| | 4 | 1.5 | 17.5 | 20.5 | 19.2 | 17.5 | | 20.0 | 20.5 | 18.3 | 20.0 | 19.5 | 18.3 | 19.5 | | 20.5 | 20.8 | 18.5 | 18.4 | 17.7 | 18.7 | 19.2 |
| | 5 | 0.2 | NA | NA | NA | | | | | | | | | | | | | | | | | |
| 2 | 1 | 4.9 | 18.7 | 20.8 | 19.4 | 20.0 | 19.6 | 20.0 | 20.8 | 18.7 | 18.7 | 19.5 | 19.0 | 19.0 | 18.7 | 20.5 | 20.0 | 20.0 | 18.7 | 18.7 | 17.2 | 17.5 |
| | 2 | 4.0 | 18.5 | 20.8 | 19.3 | 19.6 | 19.6 | 20.0 | 20.8 | 18.5 | 18.5 | 19.5 | 18.5 | 19.0 | | 20.1 | 20.0 | 19.9 | 18.5 | 18.0 | 16.5 | 17.5 |
| | 3 | 2.7 | 16.3 | 20.8 | 18.3 | 19.6 | 19.6 | 20.0 | 20.8 | 17.0 | 16.3 | 18.3 | 16.5 | 17.0 | 17.5 | 20.5 | 20.0 | 17.7 | 16.2 | 15.6 | 15.7 | 14.0 |
| | 4 | 1.5 | 12.0 | 20.8 | 16.2 | 19.8 | 19.6 | | 20.8 | 12.6 | 12.9 | 14.5 | 12.0 | 17.2 | | 20.0 | 20.0 | 14.2 | 13.0 | 12.6 | 13.7 | 14.2 |
| | 5 | 0.3 | 15.0 | 20.5 | 17.8 | 20.0 | | 20.0 | 20.5 | 17.0 | 17.0 | 16.0 | 15.0 | 17.5 | 17.0 | 20.0 | 20.3 | 19.6 | 18.1 | 15.0 | 14.7 | 13.2 |
| 3 | 1 | 4.8 | 18.3 | 20.5 | 19.3 | 19.6 | 19.6 | 19.8 | 20.5 | 18.7 | 18.5 | 19.5 | 19.0 | 18.3 | 19.3 | 20.1 | 20.0 | 19.3 | 18.7 | 17.9 | 18.0 | 18.2 |
| | 2 | 3.8 | 15.8 | 20.5 | 18.3 | 18.6 | 19.2 | 19.5 | 20.5 | 18.5 | 18.0 | 15.8 | 17.7 | 17.3 | | 20.0 | 19.0 | 19.0 | 18.0 | 17.1 | 16.2 | 15.7 |
| | 3 | 2.6 | 12.5 | 19.2 | 16.4 | 16.5 | 18.6 | 19.2 | 18.7 | 16.4 | 14.0 | 18.8 | 12.5 | 13.5 | 15.5 | 18.6 | 18.0 | 17.5 | 15.0 | 14.4 | 12.5 | 10.2 |
| | 4 | 1.4 | 11.0 | 19.2 | 15.0 | 16.0 | 18.4 | 19.2 | 18.4 | 13.8 | 12.0 | 13.0 | 11.0 | 13.5 | | 18.9 | 17.0 | 15.7 | 13.0 | 14.2 | 14.0 | 10.2 |
| | 5 | 0.2 | 12.5 | 19.5 | 15.6 | 17.0 | | 19.5 | 19.5 | 16.0 | 13.7 | 13.1 | 12.5 | 14.5 | 14.8 | 18.6 | 17.5 | 19.3 | 11.2 | 14.4 | 13.0 | 10.0 |
| 4 | 1 | 4.3 | 18.3 | 20.8 | 19.8 | 20.8 | 19.5 | 19.6 | 20.5 | 20.6 | 20.3 | 18.6 | 18.3 | 20.0 | 20.0 | 20.0 | 20.0 | 19.8 | 18.5 | | 19.7 | 20.0 |
| | 2 | 3.4 | 19.0 | 20.7 | 19.9 | 20.1 | 19.3 | 20.0 | 20.5 | 20.7 | 20.7 | 19.8 | 19.0 | 19.5 | 19.5 | 20.0 | 20.8 | 20.3 | 19.0 | | 20.0 | 19.0 |
| | 3 | 2.1 | 16.7 | 20.8 | 19.4 | 19.6 | 19.5 | 20.2 | 20.8 | 20.0 | 19.7 | 18.6 | 16.7 | 19.8 | | 20.0 | 20.8 | 19.5 | 17.8 | | 20.2 | 19.2 |
| | 4 | 0.9 | 13.0 | 20.8 | 18.4 | 20.0 | | 20.2 | 20.8 | 19.7 | 19.5 | 13.0 | 13.5 | 20.0 | 18.7 | 20.4 | 20.0 | 19.5 | 17.2 | | 16.7 | 15.7 |
| 5 | 1 | 4.6 | 19.6 | 20.8 | 20.5 | 20.2 | 19.6 | 20.5 | 20.8 | 20.8 | 20.7 | 20.5 | 20.2 | 20.8 | 20.5 | 20.8 | 20.8 | 20.5 | 20.5 | 19.1 | 20.8 | 20.5 |
| | 2 | 3.7 | 19.5 | 20.8 | 20.4 | 20.2 | 19.5 | | 20.8 | 20.7 | 20.8 | 20.5 | 20.2 | 20.8 | | 20.8 | 20.8 | 20.6 | 20.5 | 19.0 | 20.5 | 20.8 |
| | 3 | 2.4 | 19.6 | 20.8 | 20.5 | 20.2 | 19.6 | 20.5 | 20.8 | 20.7 | 20.8 | 20.8 | 20.2 | 20.8 | 20.5 | 20.6 | 20.8 | 20.7 | 20.0 | 19.0 | 20.5 | 20.5 |
| | 4 | 1.8 | 19.6 | 20.8 | 20.4 | 20.2 | 19.6 | | 20.8 | 20.6 | 20.8 | 20.6 | 20.0 | 20.8 | | 20.8 | 20.8 | 20.8 | 19.8 | 18.3 | 20.0 | 20.5 |
| | 5 | 1.2 | 19.5 | 20.8 | 20.3 | 20.2 | 19.8 | 20.5 | 20.8 | 20.6 | 20.5 | 20.0 | 19.5 | 20.8 | 20.0 | 20.8 | 20.8 | 20.5 | 19.5 | | 20.5 | 20.5 |
| | 6 | 0.6 | 19.5 | 20.8 | 20.3 | 20.2 | | 20.5 | 20.8 | 20.5 | 20.2 | 20.1 | 19.5 | 20.8 | 20.5 | 20.8 | 20.8 | 20.8 | 19.8 | 18.0 | 20.5 | 20.5 |
| 6 | 1 | 4.0 | 18.0 | 20.7 | 19.5 | 20.2 | 20.3 | 18.8 | 19.0 | 18.0 | 18.7 | 20.0 | 19.0 | 20.7 | 20.5 | 19.8 | 19.0 | 19.2 | 20.0 | 16.0 | 19.5 | 19.0 |
| | 2 | 3.1 | 17.8 | 20.7 | 19.2 | 19.8 | 20.3 | 18.8 | 17.8 | 18.2 | 18.0 | 20.0 | 17.8 | 20.7 | 20.5 | 19.6 | 19.3 | 19.0 | 20.0 | 15.0 | 19.5 | 18.5 |
| | 3 | 1.9 | 17.5 | 20.5 | 19.6 | 19.8 | 20.3 | 20.0 | 20.0 | 19.2 | 18.5 | 20.0 | 17.5 | 20.5 | 20.0 | 20.2 | 20.5 | 19.0 | 19.8 | 18.4 | 19.7 | 19.5 |
| | 4 | 1.2 | 18.0 | 20.5 | 19.6 | 19.8 | 20.3 | 20.0 | 20.2 | 19.0 | 18.5 | 20.1 | 18.0 | 20.5 | | 20.4 | 20.5 | 19.2 | 19.7 | 18.7 | 20.0 | 15.0 |
| | 5 | 0.6 | 18.5 | 20.8 | 19.9 | 19.6 | 20.3 | 20.0 | 20.5 | 19.3 | 19.5 | 20.2 | 18.5 | 20.8 | 20.0 | 20.5 | 20.8 | 20.5 | 20.0 | 19.0 | 20.2 | 20.5 |
| | 6 | 0.1 | 20.6 | 20.8 | 20.8 | 20.8 | 20.8 | 20.8 | 20.8 | 20.8 | 20.8 | 20.8 | 20.8 | 20.6 | 20.8 | | 20.8 | 20.8 | | 20.8 | 20.3 | 20.0 |

TABLE 3-8

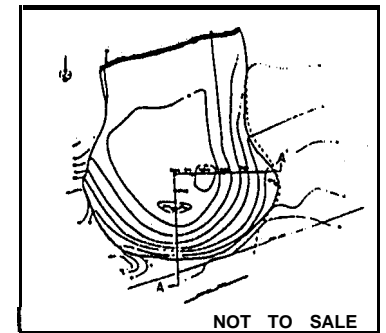
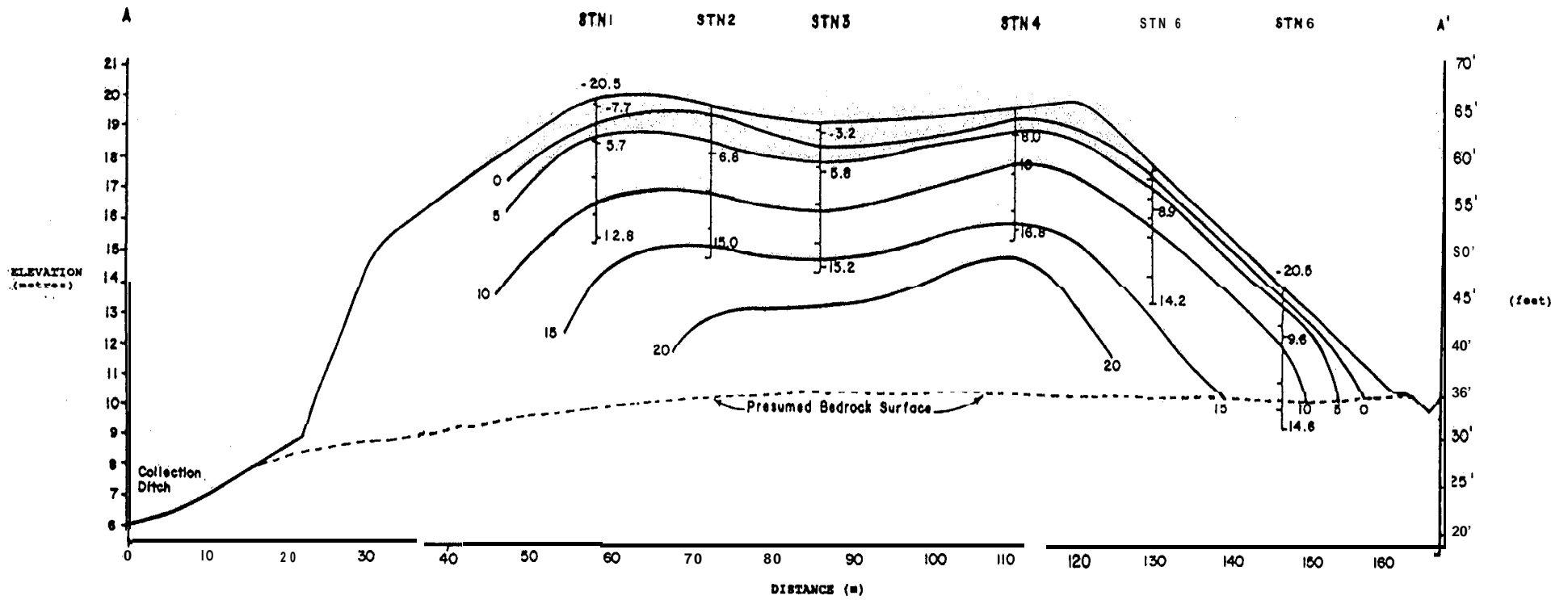
Water Quality at
Pile 17 Collection Ditch

| Date | pH | Cu | Pb | Zn | Date | pH | Cu | Pb | Zn |
|-----------|-----|-------|-------|-------|-----------|-----|-------|-------|-------|
| 04-Feb-87 | 2.8 | 81.0 | 0.140 | 139.2 | 05-May-88 | 2.0 | 77.2 | 0.256 | 203.6 |
| 12-Feb-87 | 2.7 | 84.4 | 0.235 | 161.2 | 13-May-88 | 2.0 | 79.8 | 0.326 | 218.2 |
| 20-Feb-87 | 2.9 | 84.2 | 0.207 | 157.6 | 21-May-88 | 2.1 | 148.8 | 0.358 | 410.0 |
| 28-Feb-87 | 3.0 | 83.8 | 0.206 | 155.8 | 29-May-88 | 2.1 | 128.2 | 0.370 | 368.8 |
| 06-Mar-87 | 2.8 | 94.2 | 0.230 | 168.6 | 06-Jun-88 | 2.2 | 141.2 | 0.379 | 370.0 |
| 17-Mar-87 | 3.3 | 90.1 | 0.189 | 155.2 | 14-Jun-88 | 2.0 | 174.0 | 0.373 | 411.4 |
| 24-Mar-87 | 3.8 | 3.1 | 0.095 | 4.4 | 22-Jun-88 | 2.1 | 168.0 | 0.359 | 341.2 |
| 02-Apr-87 | 2.9 | 3.4 | 0.172 | 6.9 | 30-Jun-88 | 2.2 | 39.6 | 0.214 | 99.8 |
| 09-Apr-87 | 2.7 | 116.6 | 0.123 | 232.4 | 10-Jul-88 | 2.2 | 57.4 | 0.005 | 109.0 |
| 17-Apr-87 | 2.9 | 79.2 | 0.222 | 147.8 | 18-Jul-88 | 2.2 | 93.0 | 0.005 | 187.2 |
| 25-Apr-87 | 2.8 | 102.6 | 0.520 | 305.6 | 27-Jul-88 | 2.2 | 92.2 | 0.005 | 188.8 |
| 03-May-87 | 2.9 | 91.4 | 0.209 | 190.0 | 03-Aug-88 | 2.1 | 124.0 | 0.005 | 240.8 |
| 11-May-87 | 2.9 | 55.6 | 0.160 | 100.6 | 11-Aug-88 | 2.1 | 42.0 | 0.190 | 118.2 |
| 19-May-87 | 2.8 | 107.7 | 0.273 | 220.6 | 18-Aug-88 | 2.1 | 101.6 | 0.256 | 257.6 |
| 27-May-87 | 2.9 | 116.0 | 0.209 | 229.6 | 25-Aug-88 | 2.0 | 207.8 | 0.339 | 404.2 |
| 04-Jun-87 | 3.0 | 124.2 | 0.275 | 256.8 | 02-Sep-88 | 2.0 | 133.0 | 0.337 | 344.2 |
| 12-Jun-87 | 3.0 | 128.2 | 0.241 | 235.0 | 10-Sep-88 | 2.0 | 141.8 | 0.343 | 343.6 |
| 20-Jun-87 | 2.8 | 136.4 | 0.376 | 251.2 | 18-Sep-88 | 2.2 | 162.4 | 0.441 | 380.0 |
| 28-Jun-87 | 3.4 | 70.3 | 0.100 | 268.0 | 26-Sep-88 | 2.2 | 148.2 | 0.323 | 393.8 |
| 06-Jul-87 | 3.1 | 35.8 | 0.005 | 70.8 | 04-Oct-88 | 2.2 | 128.4 | 0.305 | 374.2 |
| 15-Jul-87 | 3.2 | 42.4 | 0.020 | 97.6 | 12-Oct-88 | 2.2 | 131.2 | 0.398 | 346.0 |
| 22-Jul-87 | 3.0 | 75.6 | 0.005 | 166.6 | 20-Oct-88 | 2.2 | 104.0 | 0.179 | 315.0 |
| 30-Jul-87 | 3.0 | 59.8 | 0.030 | 128.0 | 28-Oct-88 | 2.1 | 218.2 | 0.936 | 422.0 |
| 07-Aug-87 | 3.1 | 76.6 | 0.152 | 143.2 | 05-Nov-88 | 2.2 | 181.4 | 0.505 | 409.0 |
| 15-Aug-87 | 3.0 | 78.0 | 0.157 | 137.6 | 10-Jan-89 | 2.0 | 183.6 | 0.403 | 397.4 |
| 23-Aug-87 | 3.2 | 57.6 | 0.133 | 138.4 | 18-Jan-89 | 2.1 | 175.2 | 0.360 | 371.2 |
| 31-Aug-87 | 3.1 | 45.0 | 0.127 | 88.0 | 26-Jan-89 | 2.3 | 166.8 | 0.463 | 390.4 |
| 08-Sep-87 | 3.0 | 39.4 | 0.148 | 72.8 | 03-Feb-89 | 2.1 | 188.2 | 0.553 | 443.4 |
| 16-Sep-87 | 3.0 | 88.2 | 0.353 | 138.0 | 11-Feb-89 | 2.1 | 155.8 | 0.475 | 383.2 |
| 24-Sep-87 | 3.1 | 49.8 | 0.158 | 76.6 | 19-Feb-89 | 2.2 | 147.4 | 0.445 | 379.7 |
| 02-Oct-87 | 3.1 | 100.6 | 0.317 | 185.0 | 25-Feb-89 | 2.0 | 200.2 | 0.581 | 358.6 |
| 10-Oct-87 | 3.1 | 109.2 | 0.339 | 191.6 | 05-Mar-89 | 2.2 | 195.1 | 0.510 | 344.7 |
| 18-Oct-87 | 3.1 | 143.2 | 0.425 | 269.0 | 13-Mar-89 | 2.2 | 222.4 | 0.492 | 400.8 |
| 26-Oct-87 | 3.1 | 87.6 | 0.236 | 163.6 | 21-Mar-89 | 2.4 | 30.4 | 0.181 | 143.1 |
| 03-Nov-87 | 2.6 | 84.2 | 0.262 | 169.4 | 29-Mar-89 | 2.1 | 48.2 | 0.262 | 51.2 |
| 11-Nov-87 | 2.5 | 123.0 | 0.278 | 237.0 | 06-Apr-89 | 2.4 | 20.5 | 0.220 | 212.0 |
| 19-Nov-87 | 2.4 | 120.4 | 0.239 | 189.0 | 14-Apr-89 | 2.1 | 88.8 | 0.311 | 144.8 |
| 27-Nov-87 | 2.4 | 139.4 | 0.302 | 260.0 | 21-Apr-89 | 2.1 | 56.0 | 0.286 | 70.8 |
| 05-Dec-87 | 2.4 | 127.6 | 0.244 | 216.2 | 30-Apr-89 | 2.1 | 60.8 | 0.428 | 84.6 |
| 13-Dec-87 | 2.5 | 180.0 | 0.295 | 414.0 | 08-May-89 | 2.2 | 62.7 | 0.400 | 91.5 |
| 22-Dec-87 | 2.4 | 177.0 | 0.278 | 406.8 | 16-May-89 | 2.0 | 110.2 | 0.452 | 266.8 |
| 30-Dec-87 | 2.4 | 170.8 | 0.348 | 376.4 | 24-May-89 | 2.1 | 117.8 | 0.365 | 267.1 |
| 06-Jan-88 | 2.4 | 159.2 | 0.227 | 352.0 | 30-May-89 | 2.0 | 131.6 | 0.437 | 286.4 |
| 14-Jan-88 | 2.3 | 149.6 | 0.202 | 272.0 | 05-Jun-89 | 2.1 | 112.4 | 0.473 | 226.2 |
| 22-Jan-88 | 2.5 | 38.6 | 0.154 | 76.2 | 15-Jun-89 | 2.0 | 116.6 | 0.561 | 253.4 |
| 30-Jan-88 | 2.2 | 81.0 | 0.271 | 182.4 | 19-Jun-89 | 2.1 | 88.4 | 0.451 | 207.0 |
| 07-Feb-88 | 2.5 | 38.4 | 0.251 | 72.6 | 26-Jun-89 | 2.0 | 88.0 | 0.419 | 177.6 |
| 15-Feb-88 | 2.3 | 63.2 | 0.233 | 132.8 | 03-Jul-89 | 2.0 | 95.4 | 0.040 | 196.0 |
| 23-Feb-88 | 2.2 | 108.2 | 0.337 | 267.6 | 10-Jul-89 | 2.1 | 92.6 | 0.060 | 195.0 |
| 02-Mar-88 | 2.2 | 94.6 | 0.410 | 235.4 | 17-Jul-89 | 2.1 | 113.2 | 0.010 | 212.8 |
| 10-Mar-88 | 2.3 | 105.0 | 0.362 | 266.8 | 31-Jul-89 | 2.1 | 124.0 | 0.010 | 261.6 |
| 18-Mar-88 | 2.1 | 125.6 | 0.408 | 302.8 | | | | | |
| 26-Mar-88 | 2.7 | 15.4 | 0.047 | 55.2 | | | | | |
| 03-Apr-88 | 2.6 | 4.8 | 0.108 | 6.4 | | | | | |
| 10-Apr-88 | 2.3 | 31.0 | 0.105 | 69.6 | | | | | |
| 19-Apr-88 | 2.6 | 10.8 | 0.071 | 20.8 | | | | | |
| 27-Apr-88 | 2.1 | 31.6 | 0.242 | 55.8 | | | | | |

pH Cu Pb Zn

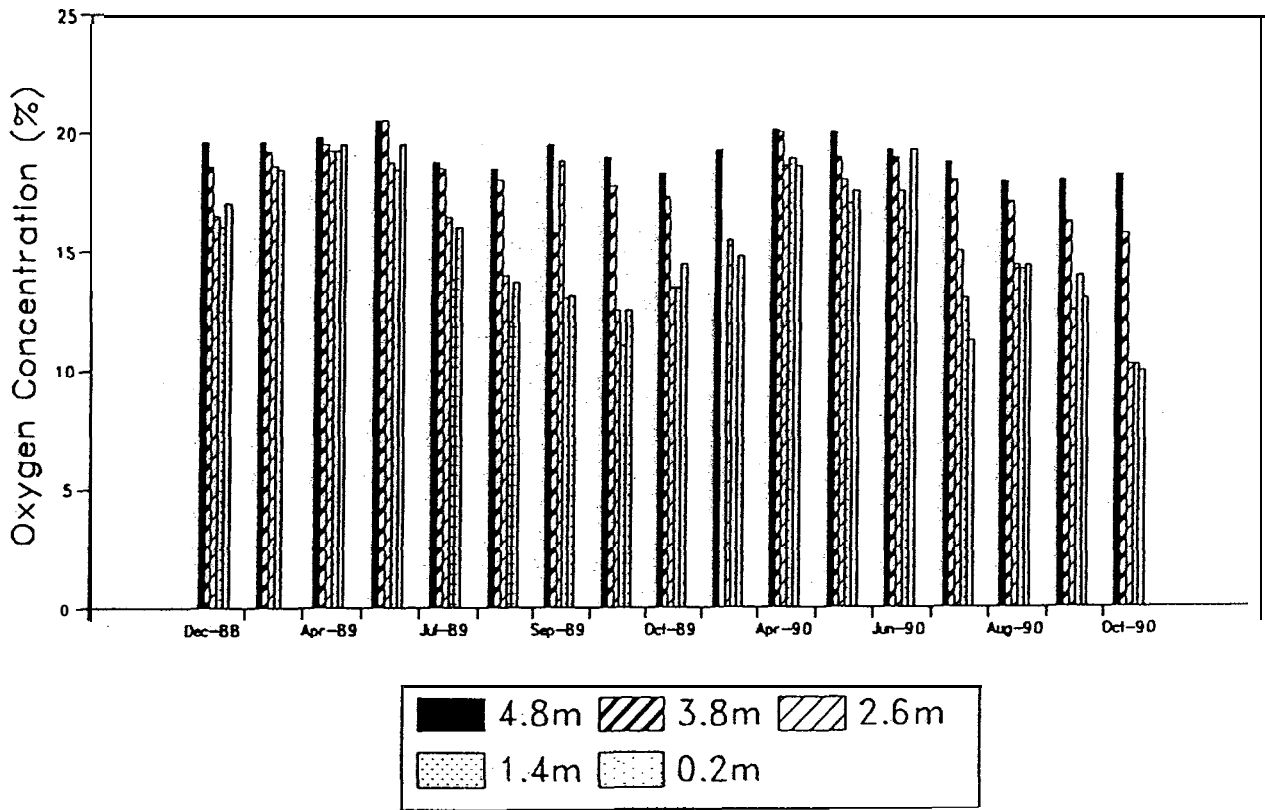
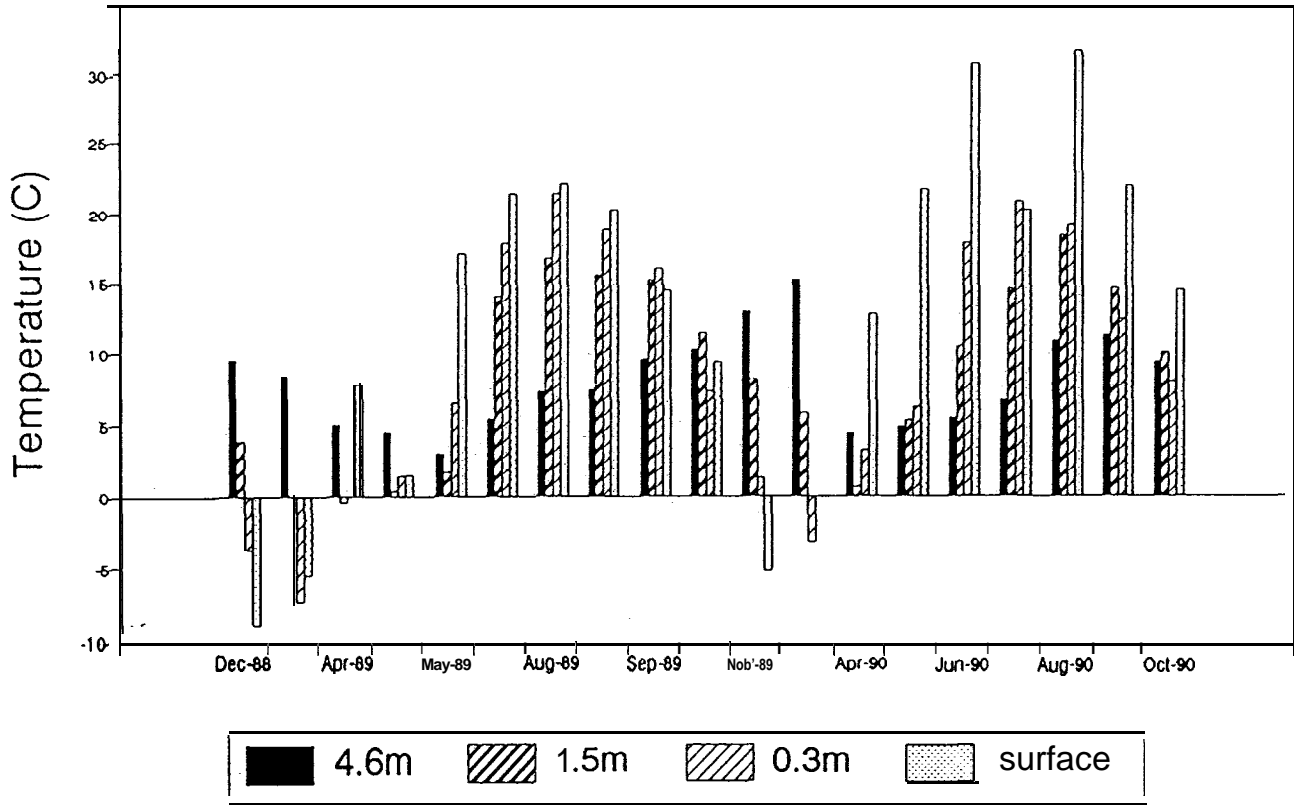
Average 2.5 103.1 0.272 223.7

Average since
Nov. 1988 2.1 120.5 0.363 258.1



NOLAN, DAVIS
& ASSOCIATES

FIGURE 3-13
TEMPERATURE PROFILE
PILE 17 - DEC. 1989
HEATH STEELE MINES

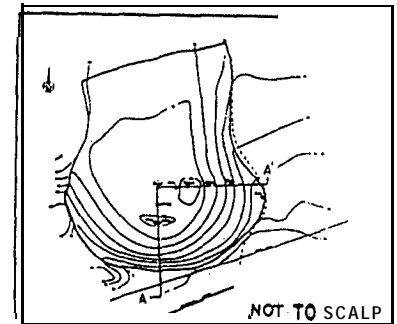
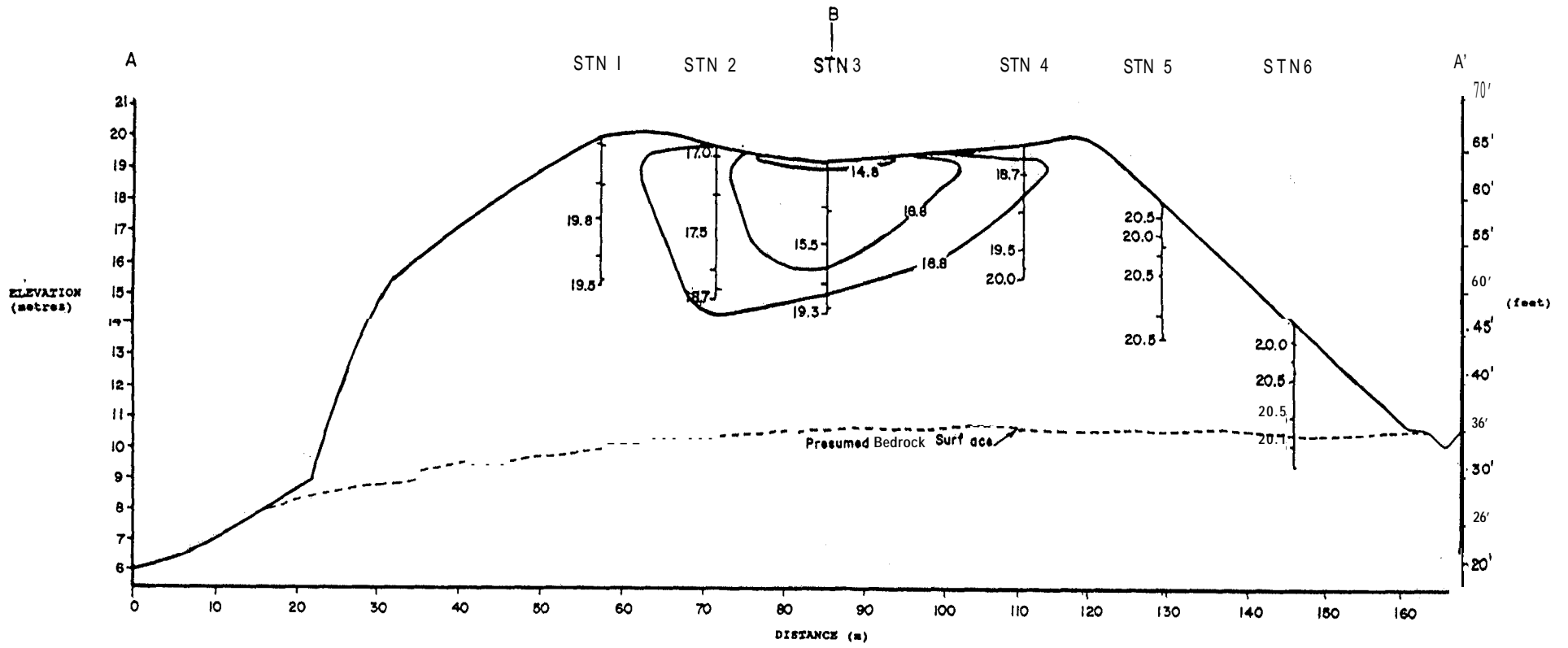


STATION 3



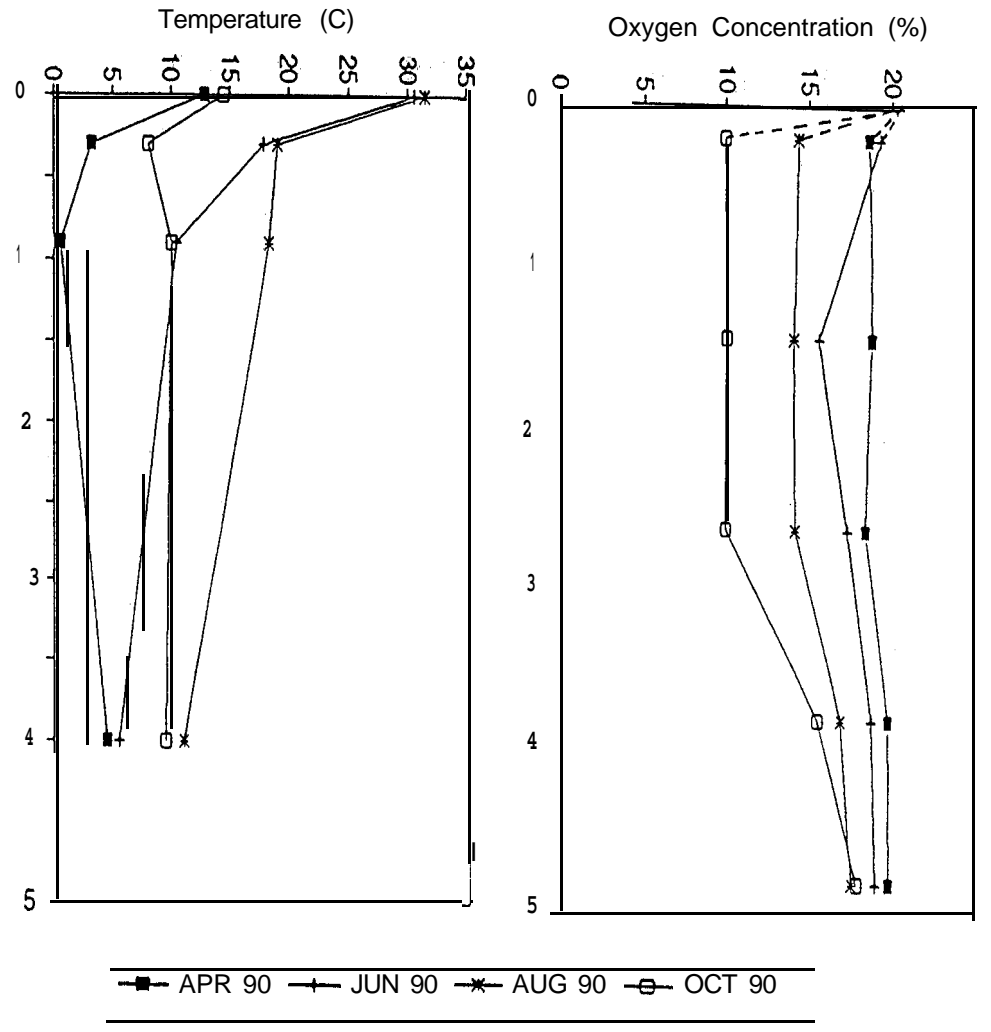
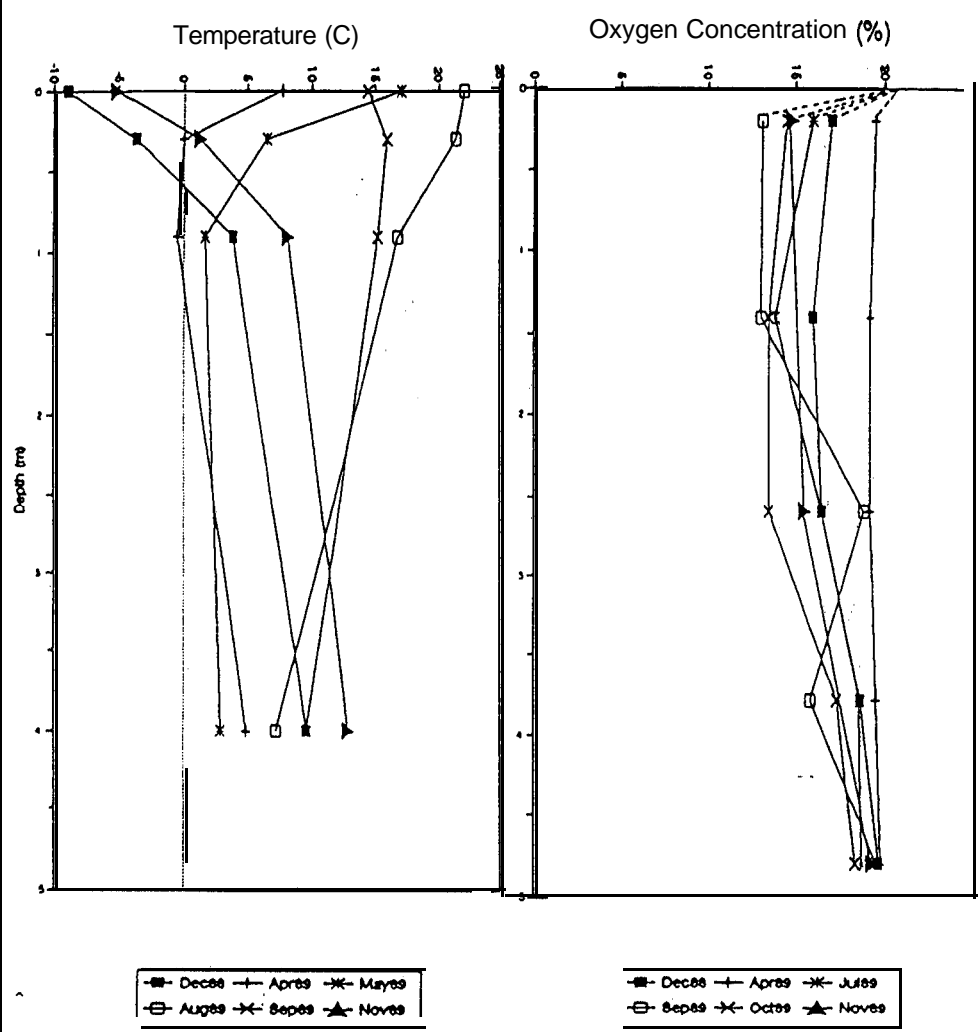
NOLAN, DAVIS & ASSOCIATES

FIGURE 3-14
SEASONAL VARIATION IN
TEMPERATURE AND OXYGEN
PILE 17
HEATH STEELE MINES



NOLAN, DAVIS
& ASSOCIATES

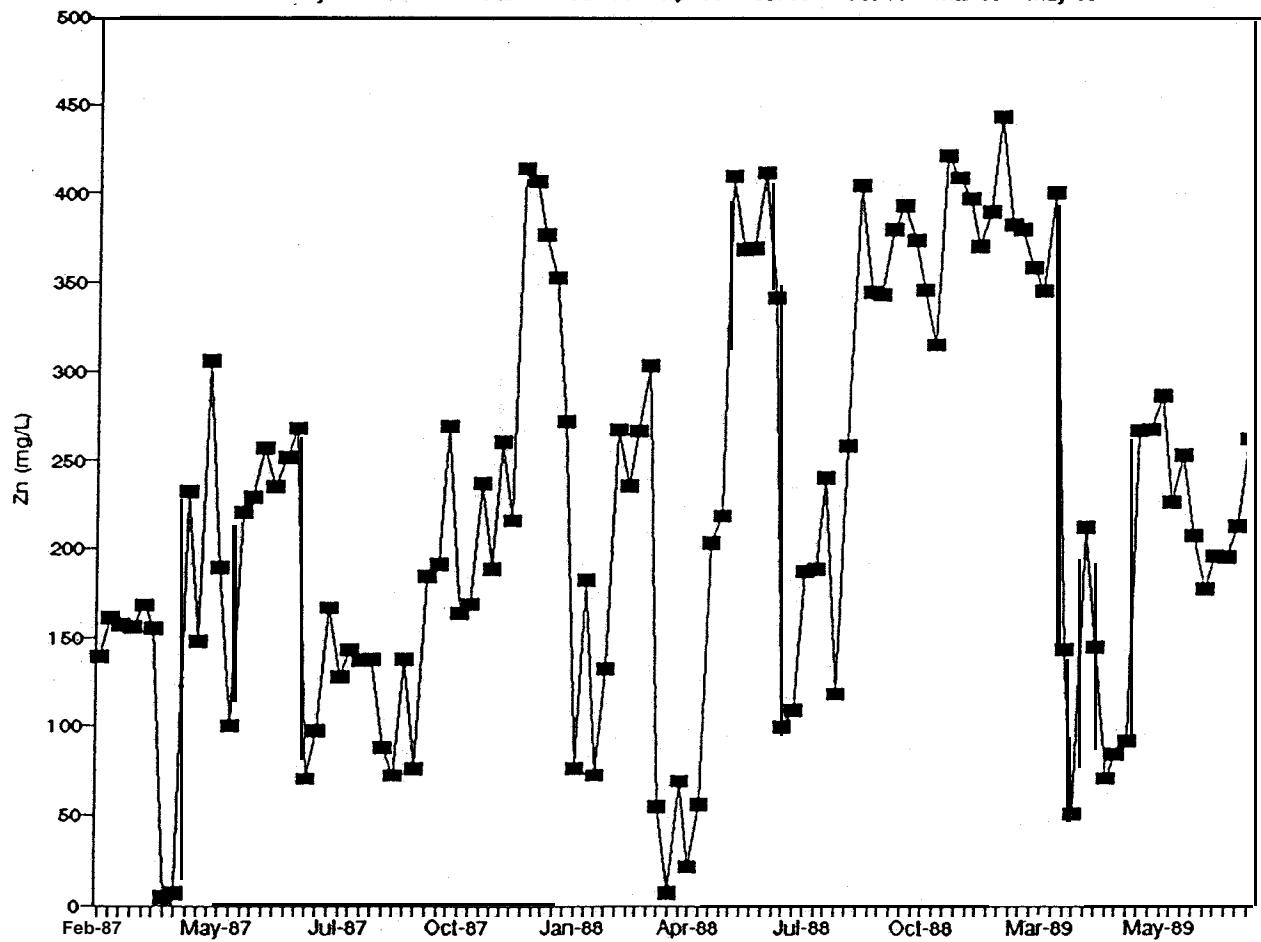
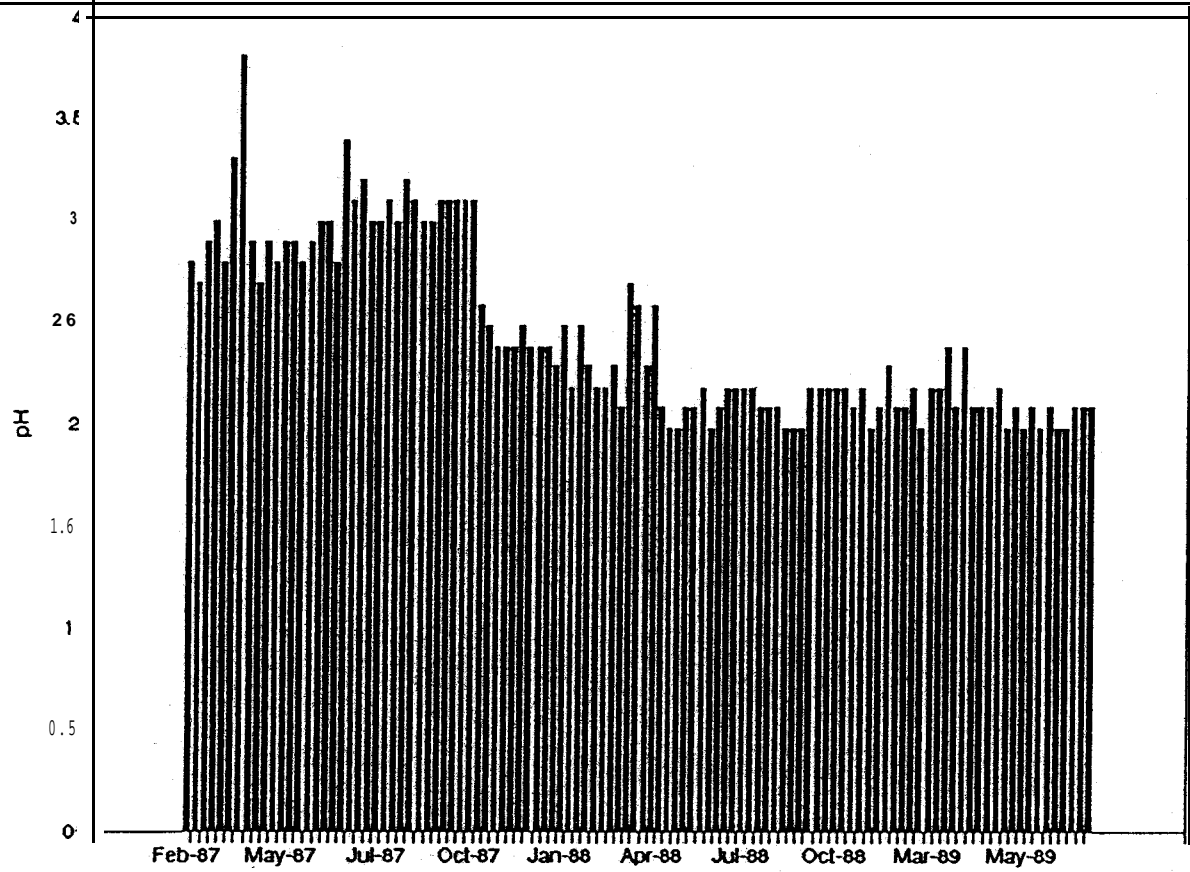
FIGURE 3-15
OXYGEN PROFILE
PILE 17 - NOV. 1989
HEATH STEELE MINES



NOLAN, DAVIS
& ASSOCIATES

FIGURE 3-16

MATCHED TEMPERATURE AND OXYGEN DEPTH PROFILES
PILE 17, STATION 3
HEATH STEELE MINES



NOLAN, DAVIS
& ASSOCIATES

FIGURE 3-17
WATER QUALITY
PILE 17
HEATH STEELE MINES

3.5 Pile 7/12

3.5.1 Description of Pile

Pile 7/12 was reconstructed on a prepared base with an impermeable membrane as described in Section 2.2.2.1. It contains approximately 14,000 tonnes of pyritic waste and was instrumented with seven sets of thermocouples and six sets of gas ports as shown in Figure 2-3. Its maximum depth is 5.0 m. The perimeter ditching and membrane placement is arranged to allow for separate collection of surface runoff and underdrain flow, thus making it the only pile for which a water and contaminant balance can be determined once the cover is in place (Phase IV).

3.5.2 Data Presentation

A lesser number of data sets are available for this pile as compared to the other three due to the fact that construction of the pile and installation of the instrumentation was not completed until July 1989. Seventeen monthly temperature and oxygen data sets are presented in Tables 3-9 and 3-10, respectively. Profile and bar charts similar to those presented for the other piles are also included.

Water quality and quantity measurements were made at this site for both the water collected in the underdrain system and the perimeter ditch collecting surface runoff. This data is presented in Table 3-11. No water left the underdrain system until late July 1989, presumably due to the unsaturated nature of the newly placed material and the low rainfall experienced at that time.

3.5.3 Interpretation

From the more limited data available for Pile 7/12 (July to October, 1990), the temperature at depth appears to be more constant relative to the other piles monitored. During the initial months, temperatures at the centre were typically over 40°C, resulting in a temperature difference over the 5 metres depth of the pile in December 1990 of almost 60°C. However, in 1990 the average

temperature at depth had dropped to 25⁰C resulting in an average temperature difference relative to surface over the sampling period of approximately 2⁰C. This would appear to indicate the very rapid establishment of the exothermic oxidation process after placement of the pile followed by a period of stabilization. This conclusion is consistent with the observation of strong air drafts in the instrumentation holes prior to packing. Snow cover appeared to melt from the bottom up during the winter of 1989/90.

The oxygen profiles for this pile do not reflect the patterns observed in the other three. Levels were initially very low at the bottom of the centre sampling station (No. 2) for the July and August 1989 sampling times but then increased rapidly to much higher values (14 to 17.6 percent) during the fall. A possible explanation might be that very high levels of oxidation existed immediately after placement and were quickly consumed due to the availability of fresh reaction sites. As temperatures in the pile increased, thermal convection of air into the pile increased oxygen levels with time. Oxygen levels at the surface would tend to decrease in winter due to the inhibiting effect of sub-zero temperatures on the oxidation reaction. During 1990, lower levels of oxygen were observed in June, July and October with relatively high levels in April and August.

An assessment of the water quality data collected to date indicates the following:

- . New precipitation is initially stored within the pile and does not necessarily result in water leaving the pile.
- . Concentrations of contaminants can be very high in both the surface runoff and underdrainage. Acidity concentrations of over 30,000 mg/l are characteristic of the collected water.
- . Concentrations of contaminants in the waters leaving the pile often increase with time following the precipitation event.
- . Surface runoff from the pile may be as high as 30 percent during a storm event.

TABLE 3-9

Heath Steele Waste Rock Study
Pile 7 / 12

Temperature (C)

| Stn | Port | Depth (m) | Min. | Max. | Avg. | 1988 | | | 1989 | | | 1990 | | | | | | | |
|-----|---------|--------------|-------|------|------|--------|--------|--------|--------|--------|--------|--------|--------|--------|--------|--------|--------|--------|--------|
| | | | | | | 04-Jul | 03-Aug | 04-Sep | 22-Sep | 12-Oct | 22-Nov | 29-Dec | 25-Apr | 25-May | 14-Jun | 20-Jul | 16-Aug | 28-Sep | 12-Oct |
| 1 | Red | 1.4 | 5.2 | 32.3 | 18.9 | 26.2 | 32.3 | 28.6 | 25.2 | 17.0 | 10.9 | 6.1 | 5.2 | 8.3 | 13.9 | 21.9 | 27.4 | 20.0 | 15.7 |
| | Blue | 0.1 | -5.4 | 35.2 | 15.3 | 35.2 | 34.6 | 20.3 | 21.8 | 10.0 | -0.9 | -5.4 | 6.4 | 8.9 | 22.6 | 26.9 | 26.6 | 16.9 | 11.8 |
| | Surface | 0.0 | -14.0 | 43.9 | 16.5 | 38.3 | 43.9 | 21.8 | 22.6 | 11.0 | -4.7 | -14.0 | 12.8 | 29.0 | 30.3 | 24.6 | 33.5 | 19.6 | 15.3 |
| 2 | Red | 3.9 | 23.2 | 45.6 | 39.1 | 23.2 | 38.3 | 44.1 | 44.6 | 45.0 | 44.5 | 45.6 | 27.1 | 24.8 | 23.8 | 23.7 | 27.7 | 27.3 | 26.8 |
| | Blue | 0.9 | 14.5 | 42.1 | 32.2 | 27.3 | 42.1 | 42.1 | 41.9 | 37.0 | 26.7 | 25.6 | 14.5 | 14.9 | 21.9 | 26.4 | 28.6 | 22.1 | 18.7 |
| | Black | 0.3 | 10.3 | 37.5 | 24.7 | 28.9 | 37.5 | 30.9 | 33.2 | 26.9 | 14.5 | 15.5 | 10.3 | 10.9 | 22.1 | 25.7 | 24.3 | 18.1 | 14.2 |
| | Surface | 0.0 | -14.2 | 43.8 | 17.6 | 39.3 | 43.8 | 24.2 | 25.5 | 13.5 | -4.7 | -14.2 | 13.7 | 32.2 | 34.7 | 24.8 | 36.3 | 23.1 | 15.6 |
| 3 | Red | 4.1 | 21.1 | 46.5 | 37.0 | 21.1 | 34.0 | 39.2 | 41.5 | 42.6 | 43.5 | 46.5 | 27.5 | 25.6 | 24.0 | 23.1 | 24.7 | 27.0 | 26.6 |
| | Blue | 1.4 | 18.1 | 48.4 | 37.4 | 32.9 | 46.7 | 48.1 | 48.4 | 44.2 | 35.6 | 25.5 | 18.1 | 20.6 | 23.7 | 27.1 | 29.7 | 26.1 | 23.2 |
| | Black | 0.4 | 10.1 | 40.1 | 21.6 | 31.4 | 40.1 | 13.8 | 32.4 | 23.8 | 10.1 | 10.5 | 10.4 | 13.9 | 24.1 | 25.9 | 23.9 | 18.0 | 14.0 |
| | Surface | 0.0 | -13.1 | 43.8 | 17.6 | 39.3 | 43.8 | 24.2 | 25.9 | 11.8 | -5.1 | -13.1 | 13.7 | 24.7 | 34.7 | 22.8 | 30.8 | 23.1 | 16.3 |
| 4 | Red | 4.3 | 25.8 | 43.1 | 36.8 | 25.8 | 35.1 | 36.9 | 42.2 | 43.1 | 42.7 | 42.8 | 25.8 | 24.0 | 25.2 | 24.1 | 27.3 | 29.2 | 29.3 |
| | Blue | 1.3 | 19.5 | 45.4 | 38.0 | 35.2 | 42.9 | 39.4 | 45.4 | 43.0 | 40.5 | 38.2 | 19.5 | 21.0 | 25.2 | 28.6 | 31.9 | 30.0 | 28.3 |
| | Black | 0.3 | 11.5 | 38.4 | 24.4 | 33.5 | 38.4 | | 32.7 | 25.1 | 14.1 | 15.8 | 11.5 | 14.6 | 26.4 | 27.5 | 27.3 | 20.5 | 16.3 |
| | Surface | 0.0 | -12.3 | 43.0 | 17.6 | 37.8 | 43.0 | 24.1 | 25.4 | 14.1 | -5.0 | -12.3 | 13.7 | 25.4 | 36.0 | 24.1 | 33.8 | 22.0 | 16.3 |
| 5 | Red | 3.7 | 21.0 | 40.7 | 34.6 | 29.7 | 40.7 | 39.2 | 40.6 | 38.2 | 33.7 | 33.8 | 21.0 | 23.0 | 25.1 | 28.7 | 32.5 | 38.6 | 36.6 |
| | Blue | 0.7 | 13.8 | 42.5 | 30.4 | 34.9 | 42.5 | 35.4 | 37.8 | 29.5 | 22.8 | 26.4 | 13.8 | 15.3 | 26.6 | 33.3 | 36.9 | 31.4 | 26.3 |
| | Black | 0.2 | 10.0 | 40.2 | 23.4 | 33.6 | 40.2 | 27.9 | 31.9 | 22.0 | 10.5 | 11.2 | 10.0 | 13.0 | 26.3 | 30.4 | 31.4 | 25.0 | 18.8 |
| | Surface | 0.0 | -11.0 | 43.0 | 17.9 | 38.0 | 43.0 | 21.8 | 23.8 | 14.9 | -0.1 | -11.0 | 13.1 | 23.6 | 33.5 | 21.8 | 36.6 | 23.3 | 17.8 |
| 6 | Red | 2.0 | 9.3 | 27.4 | 19.4 | 21.1 | 27.4 | 24.8 | 26.3 | 20.0 | 13.9 | 12.5 | 9.3 | 14.0 | 20.3 | 27.1 | 32.8 | 26.3 | 23.3 |
| | Blue | 0.4 | 7.4 | 35.9 | 20.3 | 27.4 | 35.9 | 27.2 | 28.1 | 17.6 | 9.0 | 9.7 | 7.4 | 11.0 | 23.8 | 31.4 | 33.4 | 24.8 | 20.2 |
| | Surface | 0.0 | -15.5 | 43.8 | 16.6 | 38.3 | 43.8 | 21.8 | 22.8 | 10.7 | -0.4 | -15.5 | 11.3 | 22.5 | 38.3 | 25.4 | 25.4 | 21.3 | 17.4 |
| 7 | Black | 0.7 | 30.8 | 49.2 | 41.6 | 30.8 | 44.5 | 48.0 | 49.2 | 46.2 | 39.3 | 33.1 | | | | | | | |
| | Surface | 0.0 | -10.5 | 43.9 | 19.8 | 39.3 | 43.9 | 24.2 | 29.9 | 14.6 | -2.9 | -10.5 | | | | | | | |

TABLE 3-10

Heath Steele Waste Rock Study
Pile 7/12

Oxygen Concentration (% of pore gas)

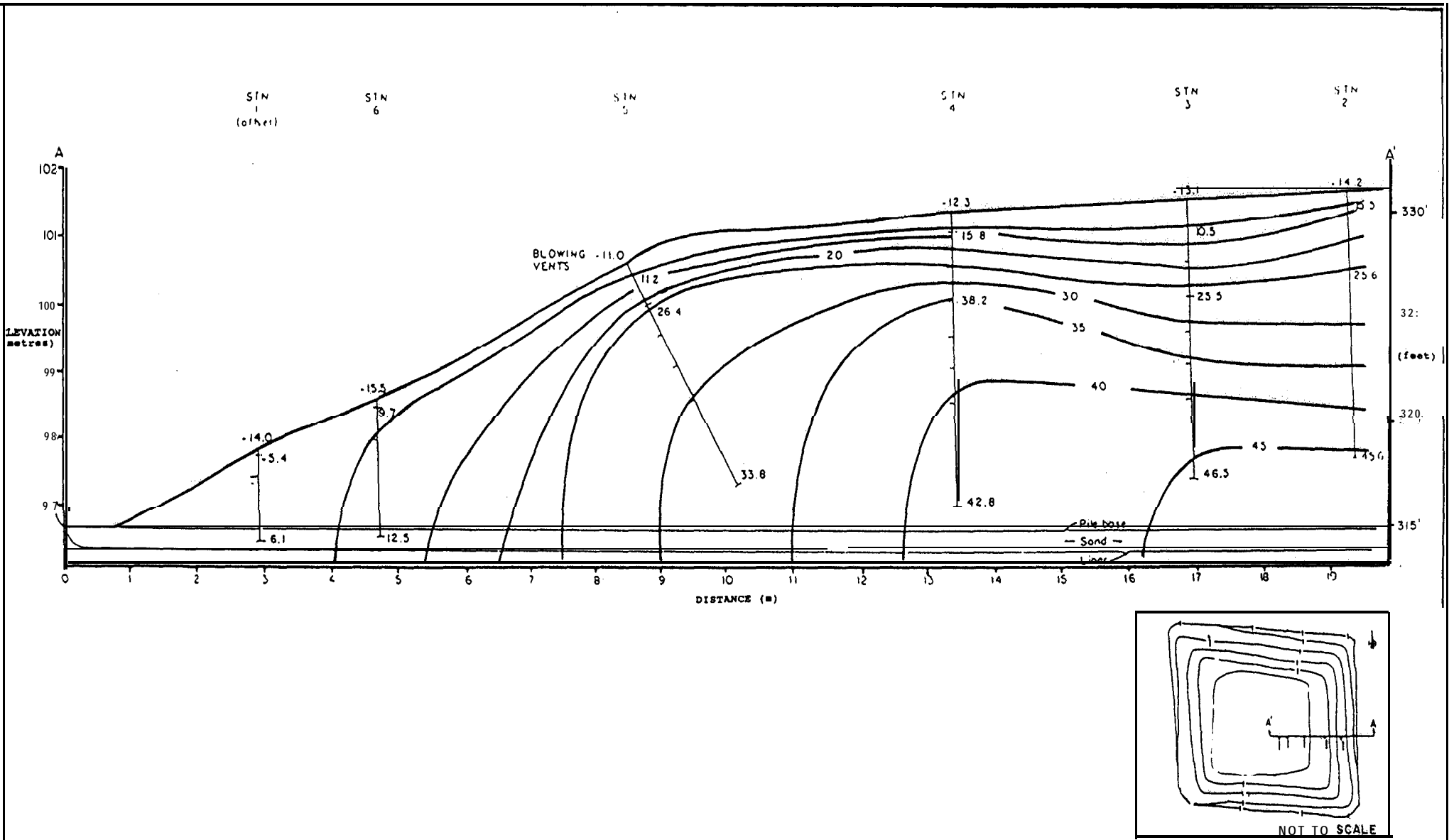
| Stn | Port | Depth (m) | 1988 | | | 1989 | | | | | | 1990 | | | | | | |
|-----|------|--------------|------|------|------|--------|--------|--------|--------|--------|--------|--------|--------|--------|---------|--------|--------|--------|
| | | | Min. | Max. | Avg. | 04-Jul | 03-Aug | 04-Sep | 22-Sep | 13-Oct | 22-Nov | 25-Apr | 25-May | 14-Jun | 20-July | 16-Aug | 28-Sep | 12-Oct |
| 1.0 | 1.0 | 1.4 | 15.2 | 20.8 | 19.3 | 18.4 | 19.0 | 20.4 | 20.3 | 20.8 | 19.9 | 20.8 | 20.5 | 15.2 | 17.7 | 19.5 | 19.5 | 18.0 |
| | 2.0 | 0.5 | 14.3 | 20.8 | 18.9 | 17.8 | 19.0 | 20.1 | 20.3 | 20.8 | 19.0 | 19.6 | 20.5 | 14.3 | 17.5 | 19.0 | 19.5 | 18.0 |
| | 3.0 | 0.4 | 14.5 | 20.8 | 19.1 | 18.0 | 18.5 | 20.4 | 19.8 | 20.8 | 20.0 | 20.6 | 20.5 | 14.5 | 17.5 | 18.5 | 19.2 | 17.5 |
| 2.0 | 1.0 | 3.9 | 0.5 | 17.9 | 11.8 | 0.5 | 0.5 | 16.6 | 17.6 | 14.1 | | 17.9 | 15.0 | 12.7 | 11.0 | 17.2 | 13.5 | 11.5 |
| | 2.0 | 2.4 | 5.0 | 17.5 | 12.1 | 5.0 | 5.4 | 12.5 | 14.8 | 14.5 | 15.3 | 17.5 | 15.2 | 11.6 | 9.1 | 14.0 | 10.5 | 10.5 |
| | 3.0 | 1.9 | 5.0 | 15.9 | 10.8 | 5.0 | 5.2 | 10.3 | 13.3 | 13.0 | | 15.9 | 14.0 | 11.3 | 9.0 | 12.6 | 11.5 | 9.2 |
| | 4.0 | 1.4 | 4.7 | 16.8 | 11.0 | 5.0 | 4.7 | 12.0 | 12.5 | 12.5 | 11.0 | 16.2 | 16.8 | 10.0 | 9.5 | 13.5 | 10.5 | 9.3 |
| | 5.0 | 0.9 | 3.9 | 20.5 | 11.8 | 6.3 | 3.9 | 10.5 | 11.0 | 13.5 | | 16.6 | 20.5 | 8.5 | 15.5 | 13.5 | 15.5 | 9.3 |
| | 6.0 | 0.4 | 3.2 | 20.9 | 13.6 | 5.8 | 3.2 | 12.5 | 10.7 | 18.7 | 15.8 | 15.5 | 20.9 | 13.0 | 19.8 | 19.5 | 19.0 | 8.5 |
| 3.0 | 1.0 | 4.1 | 6.0 | 18.8 | 14.6 | 6.0 | 6.4 | 14.8 | 16.5 | 18.0 | 17.0 | 18.8 | 18.0 | 14.0 | 16.7 | 16.4 | 15.0 | 13.5 |
| | 2.0 | 2.9 | 7.1 | 20.4 | 14.7 | 7.3 | 7.1 | 14.0 | 16.0 | 17.5 | | 20.4 | 20.0 | 14.2 | 16.0 | 16.6 | 14.0 | 13.0 |
| | 3.0 | 2.4 | 7.2 | 18.9 | 14.2 | 7.3 | 7.2 | 13.5 | 14.8 | 17.7 | 15.0 | 18.9 | 18.0 | 13.5 | 15.6 | 16.0 | 14.5 | 13.0 |
| | 4.0 | 1.9 | 6.5 | 16.6 | 11.6 | 7.0 | 6.5 | 11.5 | 12.3 | 16.0 | | 16.6 | 13.5 | 10.5 | 10.4 | 10.3 | 10.0 | 8.4 |
| | 5.0 | 1.4 | 7.5 | 17.0 | 13.1 | 7.8 | 7.5 | 13.2 | 13.3 | 16.2 | 15.5 | 17.0 | 15.0 | 11.3 | 13.8 | 12.2 | 12.5 | 11.0 |
| | 6.0 | 0.9 | 7.1 | 17.9 | 13.3 | 7.5 | 7.1 | 13.4 | 14.2 | 15.2 | | 17.9 | 17.5 | 11.7 | 14.8 | 14.2 | 15.0 | 12.0 |
| | 7.0 | 0.4 | 0.0 | 20.8 | 13.0 | 7.0 | 6.6 | 14.5 | | 15.2 | 14.8 | 18.0 | 20.8 | r | 19.8 | | | |
| 4.0 | 1.0 | 4.3 | 8.6 | 19.5 | 15.8 | 9.0 | 8.6 | 15.5 | 17.5 | 19.0 | 17.8 | 19.5 | 18.0 | 15.5 | 17.5 | 20.5 | 16.2 | 15.5 |
| | 2.0 | 2.8 | 10.5 | 19.5 | 16.7 | 11.0 | 10.5 | 17.8 | 19.5 | 19.5 | | 19.5 | 18.0 | 16.1 | 18.4 | 16.2 | 18.5 | 16.5 |
| | 3.0 | 2.3 | 10.5 | 19.9 | 16.9 | 11.0 | 10.5 | 17.6 | 19.3 | 19.8 | 19.0 | 19.9 | 17.5 | 16.0 | 18.5 | 16.4 | 18.2 | 16.2 |
| | 4.0 | 1.8 | 10.2 | 19.6 | 16.5 | 11.2 | 10.2 | 17.6 | 19.3 | 19.6 | | 19.4 | 17.1 | 15.6 | 18.5 | 16.0 | 18.0 | 16.5 |
| | 5.0 | 1.3 | 10.0 | 19.5 | 16.6 | 10.5 | 10.0 | 17.5 | 18.9 | 19.5 | 19.5 | 19.4 | 17.2 | 15.4 | 18.2 | 15.5 | 17.5 | 16.0 |
| | 6.0 | 0.8 | 10.0 | 19.4 | 16.0 | 10.5 | 10.0 | 17.0 | 17.6 | 19.4 | | 19.1 | 17.2 | 15.0 | 18.2 | 15.5 | 17.5 | 15.2 |
| | 7.0 | 0.3 | 9.8 | 19.5 | 16.4 | 10.0 | 9.8 | 17.0 | 17.5 | 19.5 | 19.0 | 19.1 | 18.0 | 16.0 | 18.2 | 15.7 | 17.5 | 15.5 |
| 5.0 | 1.0 | 3.7 | 16.6 | 20.8 | 19.5 | 19.5 | 19.5 | 20.8 | 20.5 | 20.0 | 20.0 | 20.5 | 17.7 | 16.6 | 19.5 | 13.6 | 19.5 | 18.5 |
| | 2.0 | 2.3 | 12.5 | 20.8 | 19.1 | 20.0 | 20.0 | 20.8 | 20.5 | 20.7 | | 20.5 | 12.5 | 17.0 | 20.2 | 16.6 | 20.0 | 20.0 |
| | 3.0 | 1.7 | 17.0 | 20.8 | 19.8 | 20.5 | 20.0 | 20.8 | 20.4 | 20.0 | 19.5 | 20.5 | 19.0 | 17.0 | 20.0 | 16.7 | 18.0 | 17.5 |
| | 4.0 | 1.2 | 16.8 | 20.7 | 19.5 | 20.0 | 20.0 | 20.7 | 20.3 | 20.7 | | 20.5 | 16.8 | 16.9 | 19.8 | 15.9 | 18.2 | 17.7 |
| | 5.0 | 0.7 | 16.5 | 20.8 | 19.6 | 20.8 | 20.0 | 20.5 | 20.2 | 20.5 | 20.5 | 20.5 | 16.5 | 16.8 | 19.8 | 15.9 | 18.5 | 17.5 |
| | 6.0 | 0.2 | 16.2 | 20.8 | 19.1 | 20.8 | 19.0 | 20.8 | 18.8 | 20.1 | 19.5 | 20.4 | 16.5 | 16.2 | 19.1 | 15.5 | 18.0 | 17.5 |
| 6.0 | 1.0 | 2.1 | 18.0 | 20.8 | 20.5 | 20.8 | 20.8 | 20.8 | 20.8 | 20.8 | 20.8 | 20.8 | 18.0 | 20.8 | 20.5 | 20.6 | 20.5 | 20.5 |
| | 2.0 | 0.6 | 17.3 | 20.8 | 20.2 | 20.8 | 20.5 | 20.5 | 20.3 | 20.7 | 20.8 | 20.5 | 17.3 | 20.4 | 20.5 | 20.4 | 20.2 | 20.2 |
| | 3.0 | 0.1 | 20.0 | 20.8 | 20.5 | 20.8 | 20.5 | 20.5 | 20.0 | 20.7 | 20.8 | 20.4 | 20.8 | 20.0 | 20.8 | 19.7 | 20.2 | 20.0 |

TABLE 3-11

Average Water Quality
Pile 7/12

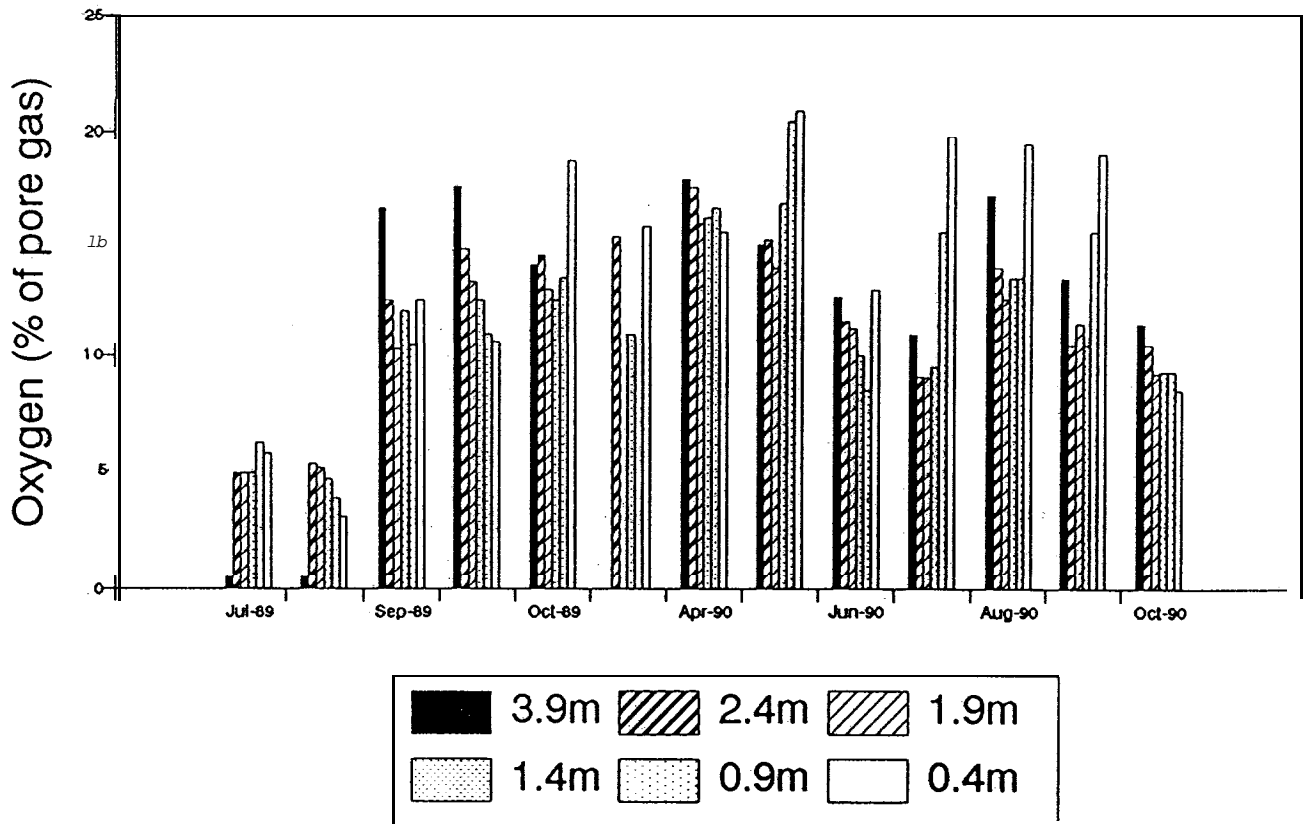
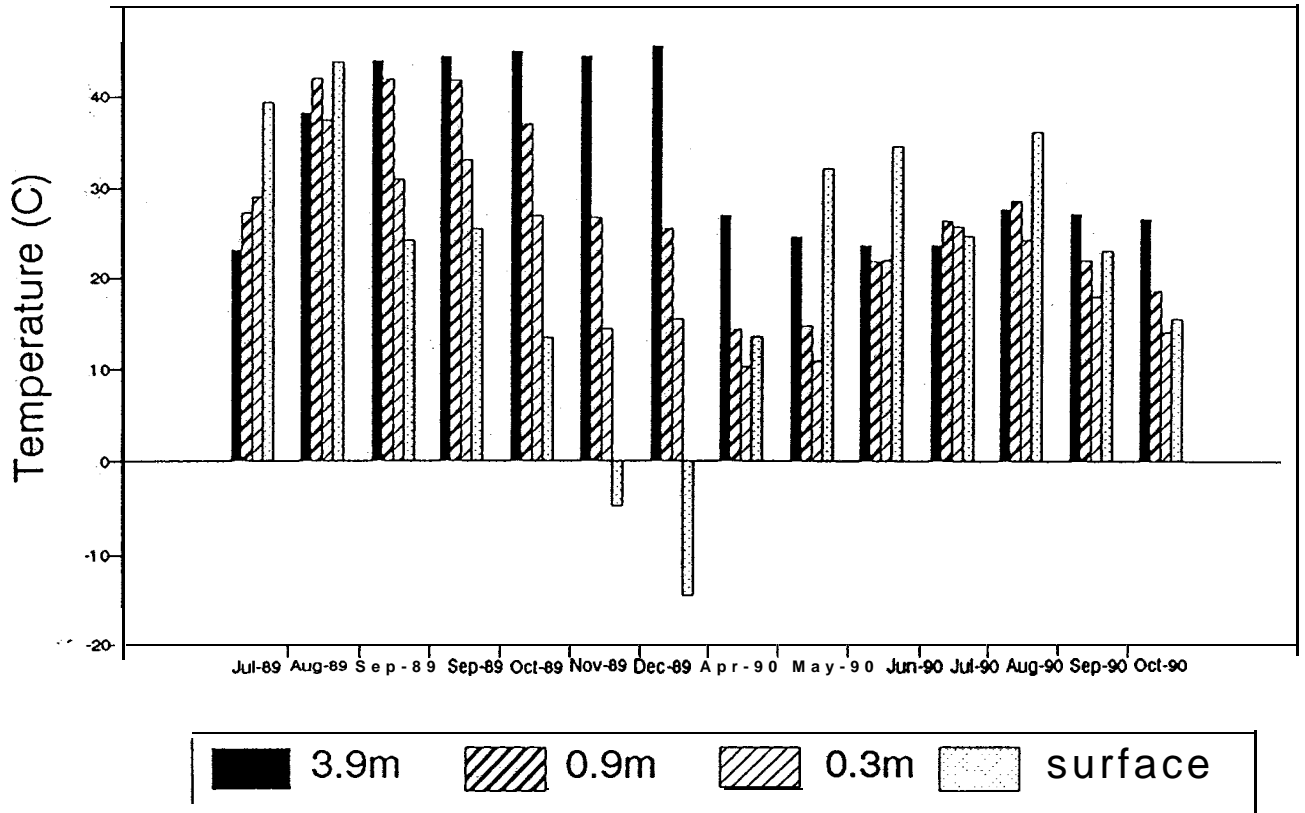
| Date | pH | Acidity | Sulfate | Lead | Iron | Copper | Zinc | Aluminum | Total Solids |
|-----------------|-----|---------|-----------|--------|-------|--------|-------|----------|--------------|
| Surface Runoff | | | | | | | | | |
| July 1989 | 2.8 | 22000 | 22970 | 0.029 | 1700 | 320 | 8000 | | |
| August 1989 | 2.0 | 45500 | 54285 | 0.002 | 9810 | 430 | 13350 | | |
| September 1989 | 3.0 | 40100 | 47500 | | 6590 | 420 | 11000 | | 79300 |
| April 1990 | 2.4 | 48500 | 70500 | | 10600 | | | | |
| May 1990 | 2.4 | 44700 | 40000 | | 16900 | | | | |
| August 1990 | 2.1 | 62000 | | | 18800 | | 6930 | 2160 | 118000 |
| September 1990 | 2.2 | 67850 | 55165 | | 11924 | | | | |
| October 1990 | 2.2 | 56500 | | | 3600 | | | 246 | 101000 |
| Overall Average | 2.4 | 48394 | 48403.333 | 0.0155 | 9991 | 390 | 9820 | 1203 | 99433.333 |
| Underdrains | | | | | | | | | |
| July 1989 | 2.4 | 44000 | 43440 | 0.186 | 5100 | 970 | 12700 | | |
| August 1989 | 2.2 | 15800 | 21328 | 0.002 | 3550 | 615 | 7895 | | |
| September 1989 | 2.8 | 30500 | 28000 | | 2800 | 910 | 8000 | | 53100 |
| April 1990 | 2.5 | 16400 | 17000 | | 3510 | | | | |
| May 1990 | 2.4 | 16400 | 12700 | | 5510 | | | | |
| August 1990 | 2.1 | 44800 | | | 13767 | | | | 81300 |
| September 1990 | 2.2 | 73250 | 32970 | | 7920 | | 9730 | 3150 | |
| October 1990 | 2.1 | 64400 | | | 3700 | | 8700 | 2820 | 11200 |
| Overall Average | 2.3 | 38194 | 25906 | 0.094 | 5732 | 832 | 9405 | 2985 | 48533 |

* Values in mg/L, except pH.



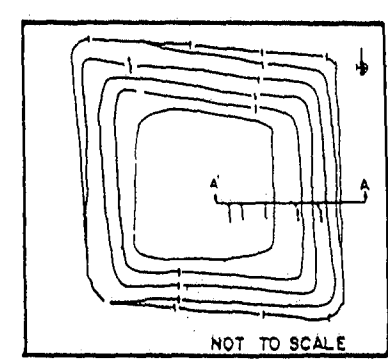
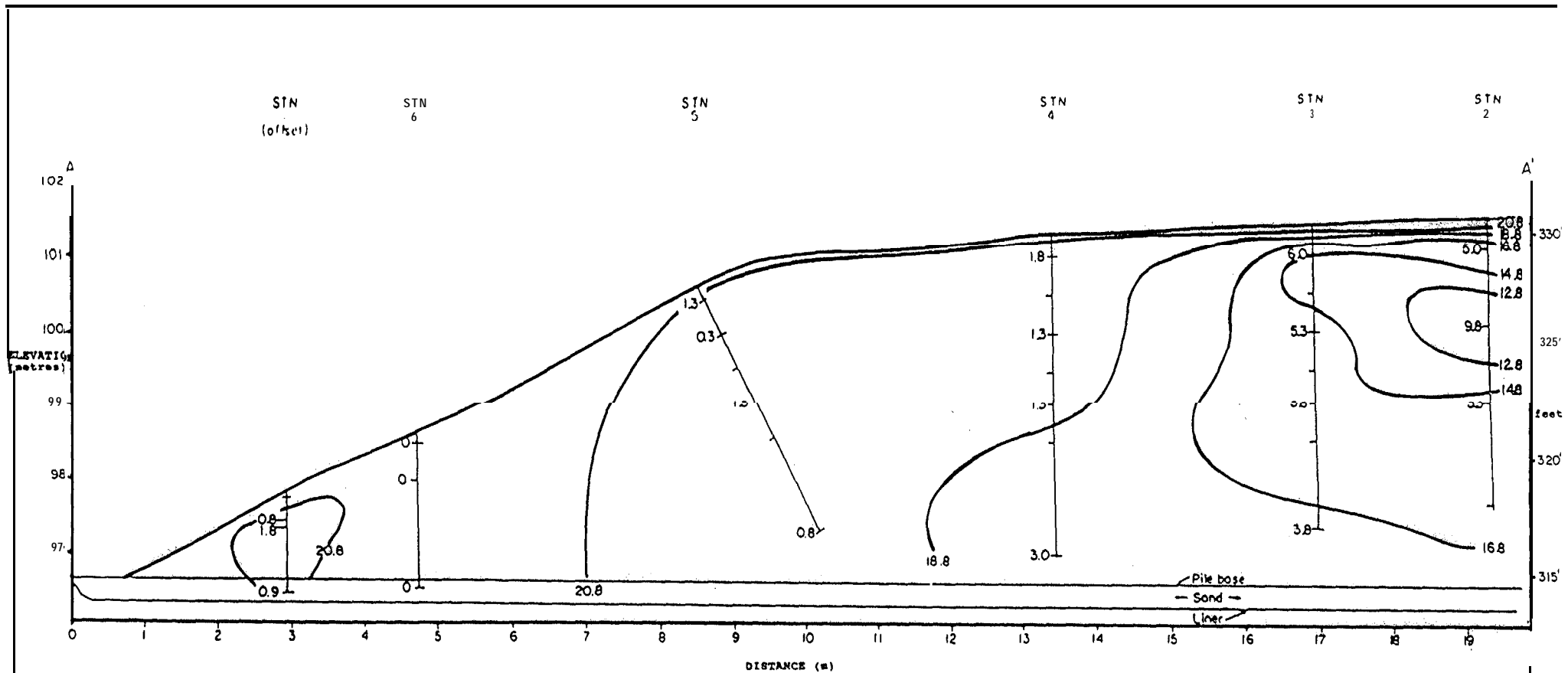
NOLAN, DAVIS
& ASSOCIATES

FIGURE 3-18
TEMPERATURE PROFILE
PILE 7/12 - DEC. 1989
HEATH STEELE MINES



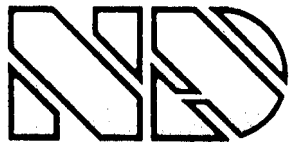
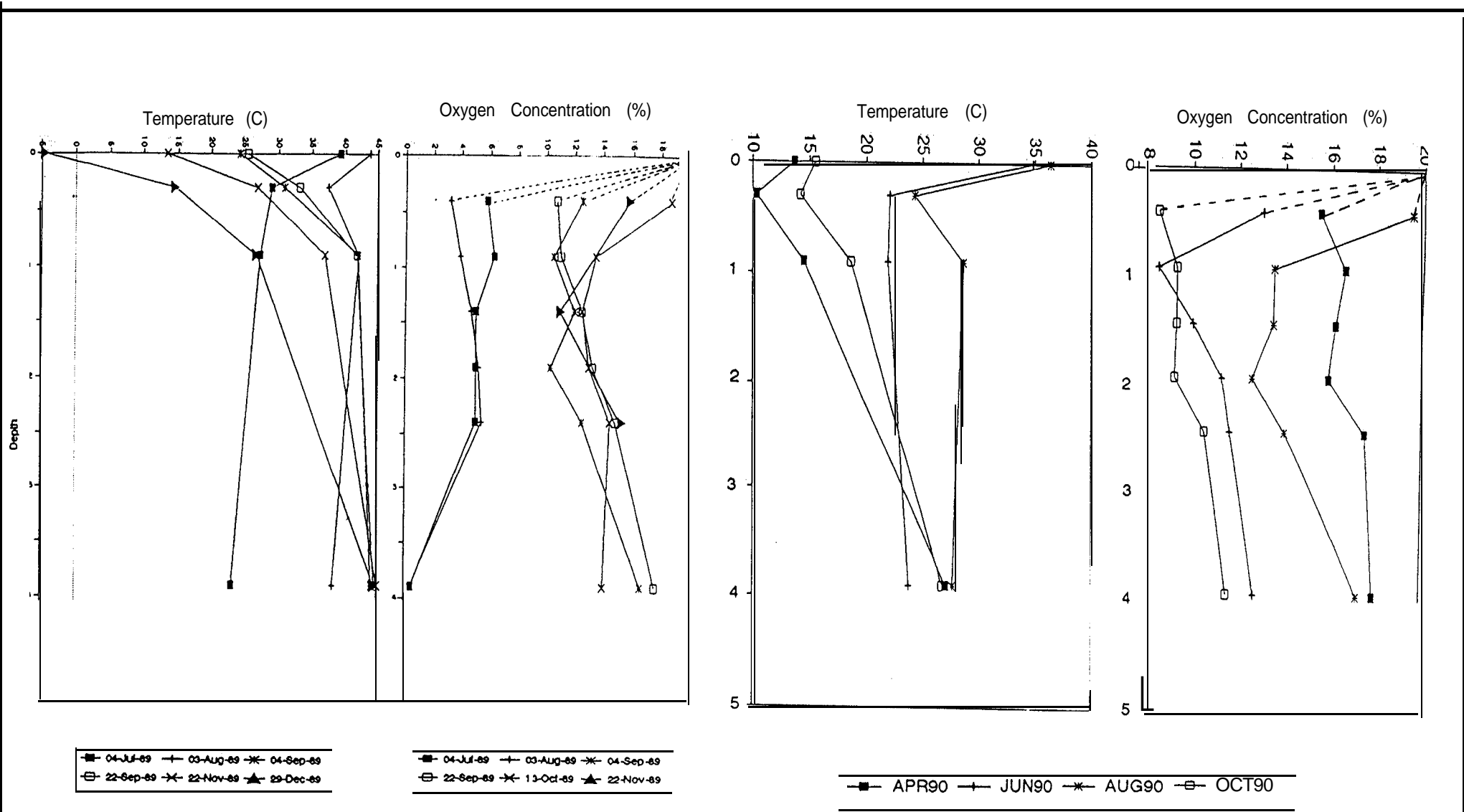
NOLAN, DAVIS
& ASSOCIATES

FIGURE 3-19
EASONAL VARIATION IN TEMPERATURE AND OXYGEN
PILE 7/12
HEATH STEELE MINES



NOLAN, DAVIS
& ASSOCIATES

FIGURE 3-20
OXYGEN PROFILE
PILE 7/12 - NOV. 1989
HEATH STEELE MINES



NOLAN, DAVIS
& ASSOCIATES

FIGURE 3-21

MATCHED TEMPERATURE AND OXYGEN DEPTH PROFILES
PILES 7/12, STATION 2
HEATH STEELE MINES

PART FOUR

COMPARATIVE REVIEW

4.0 COMPARATIVE REVIEW

The objective of this phase of the project was to define the background conditions in each of the four test piles so as to provide a basis for evaluating the performance of the covers to be installed in Phase IV. It is useful, however, to briefly review the findings to date and to compare the baseline conditions with those in other waste rock cover trials, such as those at Rum Jungle in Northern Australia and the Mount Washington Site in British Columbia.

At Heath Steele, 23 data sets have been collected for Piles **18A**, 18B and 17. The data for these **piles** covers a full range of seasons but does not provide for an evaluation of water or contaminant balances due the problems associated with the location of the piles on fractured bedrock. For Pile **7/12**, a total of 17 data sets are currently available and it will be possible to determine contaminant -loadings for this pile once the cover is in place.

The temperature characteristics of the four piles are generally similar in that each pile displays relatively uniform temperature gradients from the surface to the bottom of the pile, with the deeper piles generally showing higher temperatures at depth.

The oxidation of pyrite to sulphuric acid and ferrous sulphate is exothermic and releases 1440 **kJ** per **mol FeS₂** (Bennett et al., 1988). This release of heat results in elevated temperatures in pyritic waste rock dumps and explains the high temperatures measured in each of the waste piles. Similar results were obtained at Rum Jungle, but at Mount Washington temperatures were found to be relatively constant throughout the dump profile (Golder, 1989). In order to fully evaluate the effectiveness of the cover, it will be necessary to calculate the distribution of heat production in the piles using a heat transfer model similar to that applied at Rum Jungle, where this determination provided **a very** definitive demonstration of the effectiveness of the cover in curtailing oxidation in the pile as shown in Figure 4-1. It is therefore recommended that the **thermal** conductivity of the waste rock be measured in order to allow heat values to be determined.

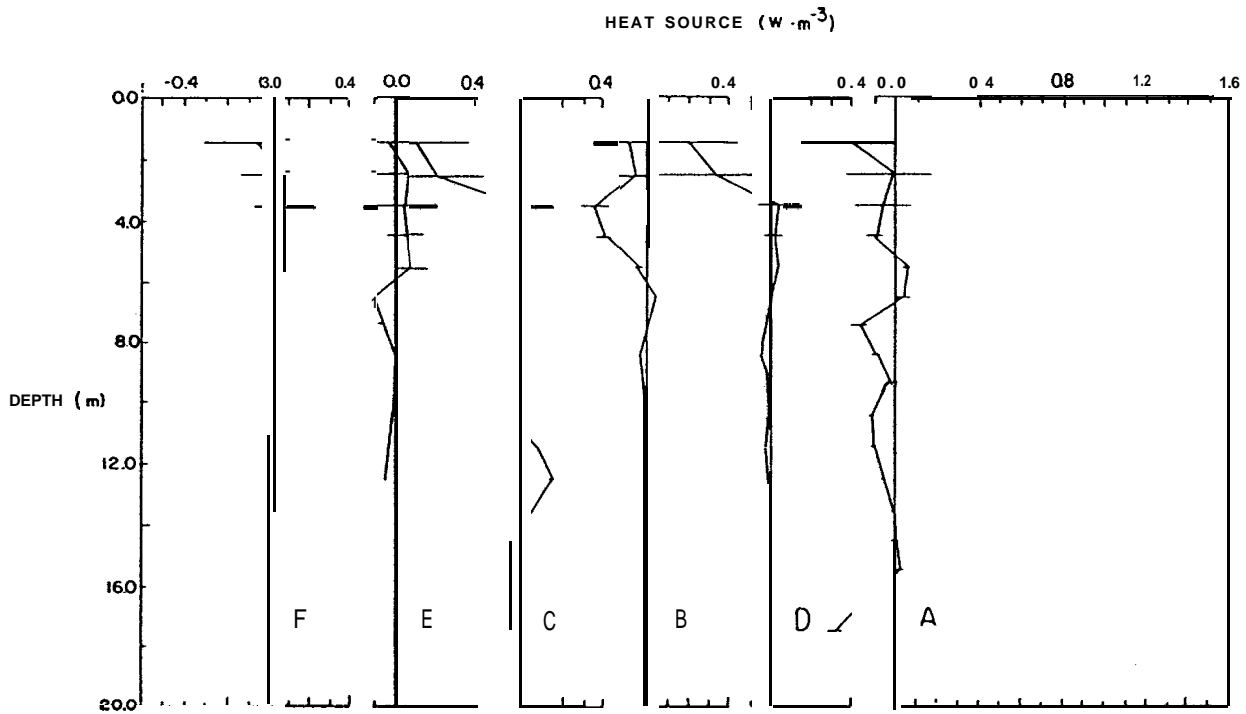
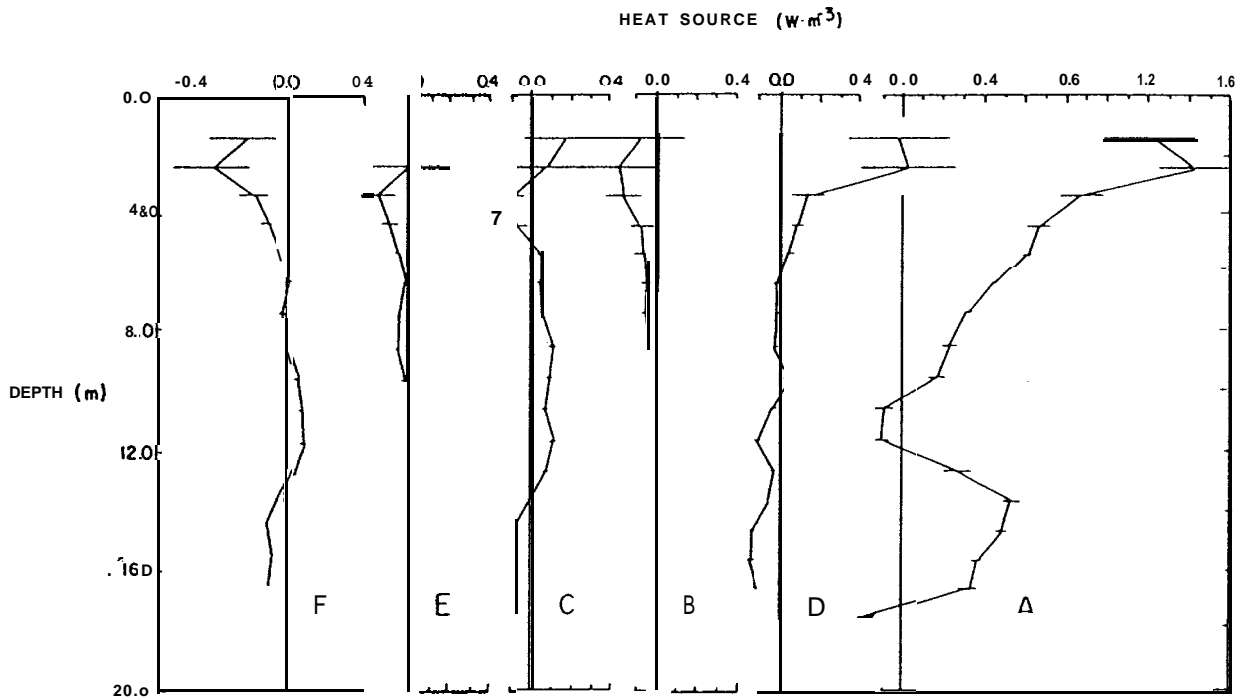
The temperature monitoring shows that the effect of seasonal temperature changes at Heath Steele influences the temperatures at depth within the dumps, and it will be important to ensure that this effect is taken into account when making comparisons between **pre-** and post-cover conditions. At Rum Jungle, the ambient temperature was of influence only to about 6 m depth. At Mount Washington, pre-cover conditions were not monitored for a seasonal cycle, and this has caused problems in the early interpretation of the effectiveness of the cover.

The profiles of oxygen concentrations determined to date at the Heath Steele site vary dramatically. This **may** be due to local variations in the dump permeability, local differences in **mineralogy**, or a combination of the two. **Similar** irregularities were observed at Rum Jungle prior to placement of the cover as shown in Figure 4-2.

Seasonal variations in oxygen concentrations also occur near the surface at many locations. Low oxygen concentrations in the top few metres tended to occur in the summer when the temperature of the waste rock was above about **10°C**. This suggests that the oxidation process, which consumes oxygen, was greatly reduced by low temperatures during the winter.

A contributing process to the higher oxygen concentrations in winter could be thermal convection which can transport oxygen into the piles. In winter **there** is a larger difference between temperatures in the piles and those in the surrounding air and this increases the driving pressure for thermal convection. However the air flow due to thermal convection will depend on how much the air flow is restricted by snow and frozen ground.

Winds at the site are predominately from the northwest which increases pressures on the northwest side of piles and reduces pressures on the southeast side. The wind effects could contribute to the asymmetry which occurs in the oxygen concentrations in the section across pile **18B**. Is it possible that some of the spatial variability evident in the temperature and oxygen distributions could be due to differences in the levels of pyrite and other properties in the waste rock.

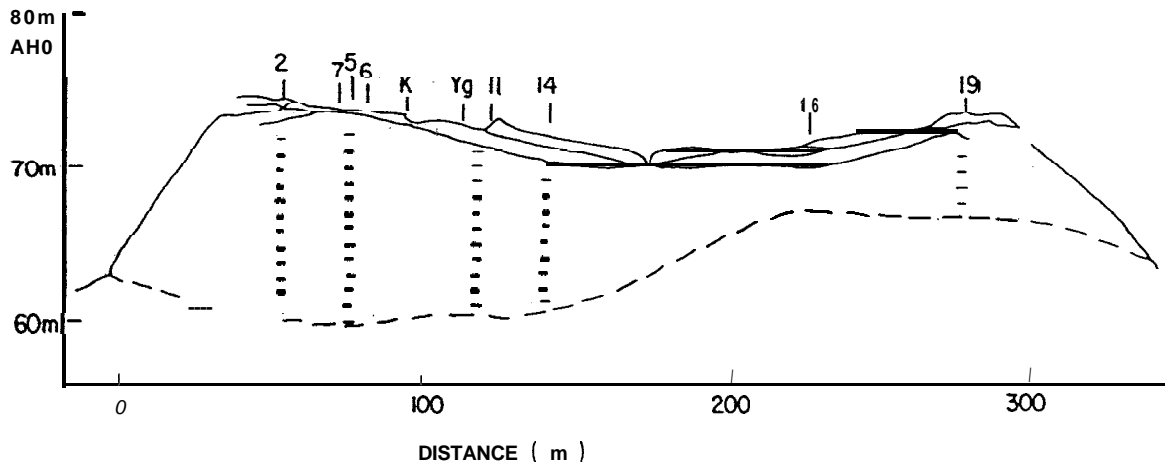
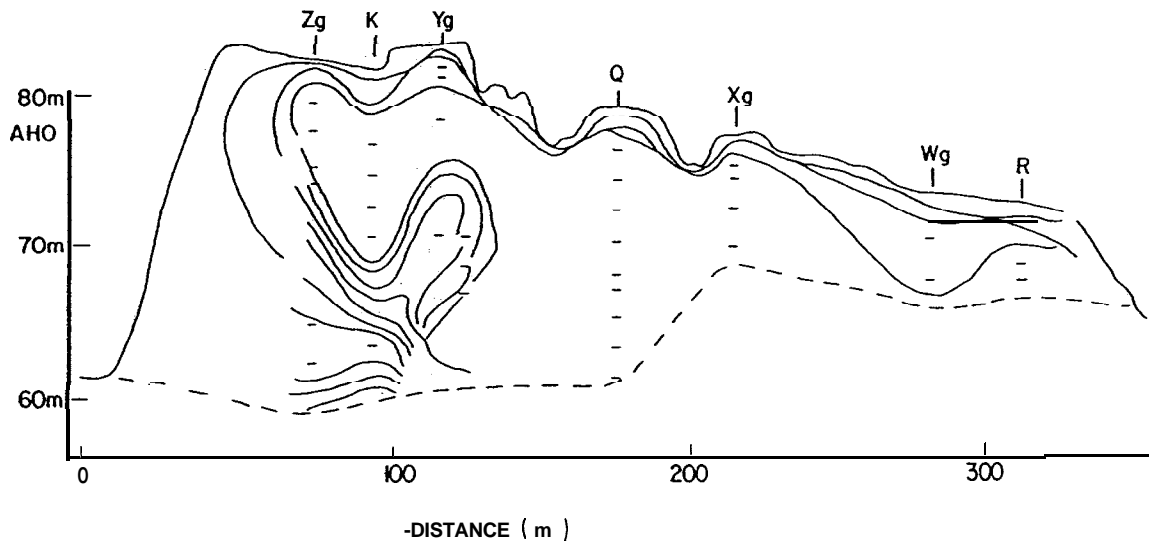


FROM : BENNETT ET AL ,1988



NOLAN, DAVIS
& ASSOCIATES

FIGURE 4-1
HEAT SOURCE PROFILES
WHITE'S DUMP
RUM JUNGLE, AUSTRALIA



From : BENNETT ET AL , 1988



**NOLAN, DAVIS
& ASSOCIATES**

**FIGURE 4-2
OXYGEN PROFILE
INTERMEDIATE DUMP
RUM JUNGLE, AUSTRALIA**

At Rum Jungle, there do not appear to be such marked seasonal changes but the effect of diurnal atmospheric pressure changes on oxygen concentrations in the dump during the Australian wet season was quite marked and was well documented in that project (NTDME, 1986).

Figure 4-3 shows a comparison of the oxygen/depth profiles in each of the piles at Heath Steele. It is quite striking that, while there is a reasonable consistent pattern within each pile, the depth profile differs significantly between piles. In 18A for example there is a depletion of oxygen at depth, whereas in 18B the maximum depletion tends to occur at about 1m below the surface, while in 17 the profile is generally linear yet moves laterally with the seasons.

Harries and Ritchie, 1985, report that there are three mechanisms by which oxygen can be transported to reaction sites within a waste dump: diffusion, thermal convection, and advection driven by wind or atmospheric pressure variations. Thermal convection causes the oxygen concentration to be higher at the base of the dump due to the effect of the temperature differences drawing in air through high permeability layers caused by segregation during dumping. Diffusion causes the oxygen concentration to decrease monotonically with depth, while advection can cause more uniform changes in concentration throughout the dump. Evidence of these three oxygen transfer mechanisms can be drawn from the data collected at Heath Steele. What is not well understood at this time is the interaction of the three mechanisms and the reasons as to why the balance between them appears to differ dramatically between piles with similar general characteristics other than size. Is it therefore recommended that further investigative work be carried out on the piles using tracer gas techniques and that an attempt be made to develop a computer model of the gas transfer mechanisms as a tool to better understanding the factors influencing gas transfer and their interaction.

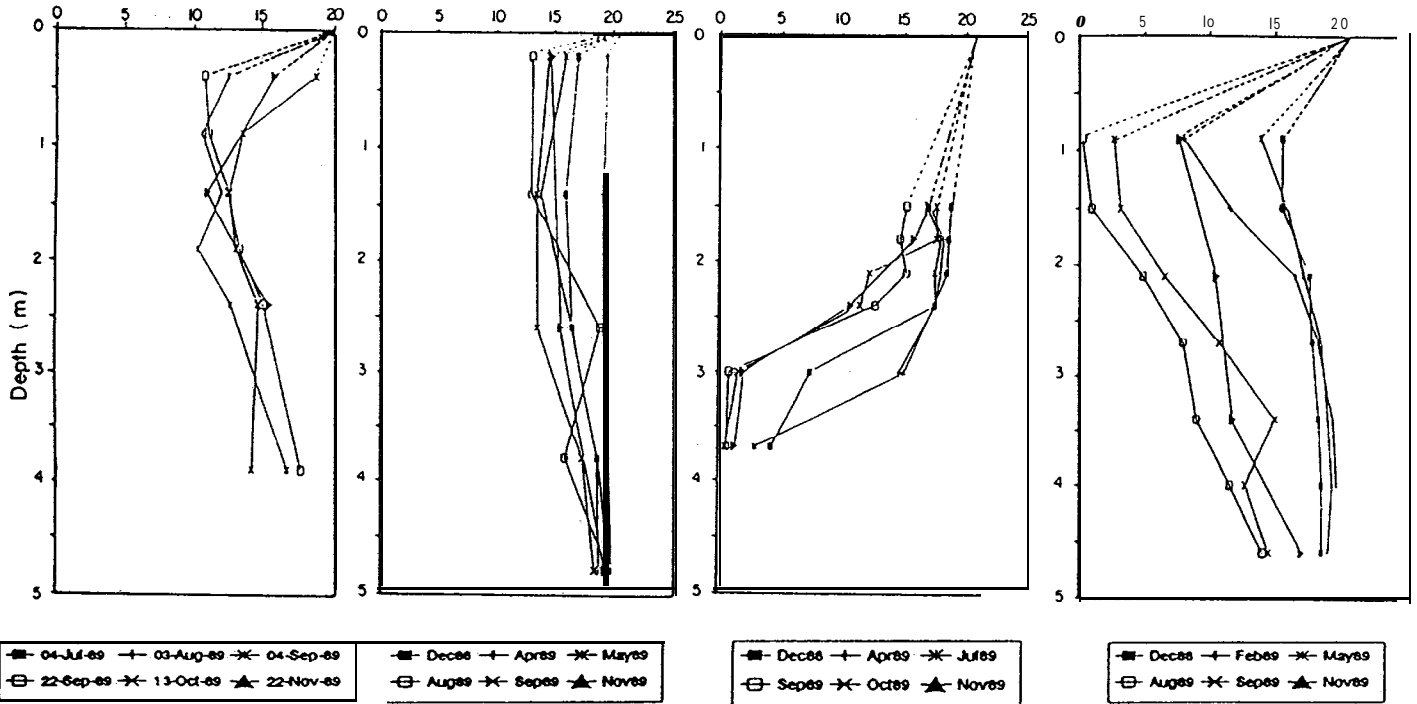
PILE 7/12

PILE 17

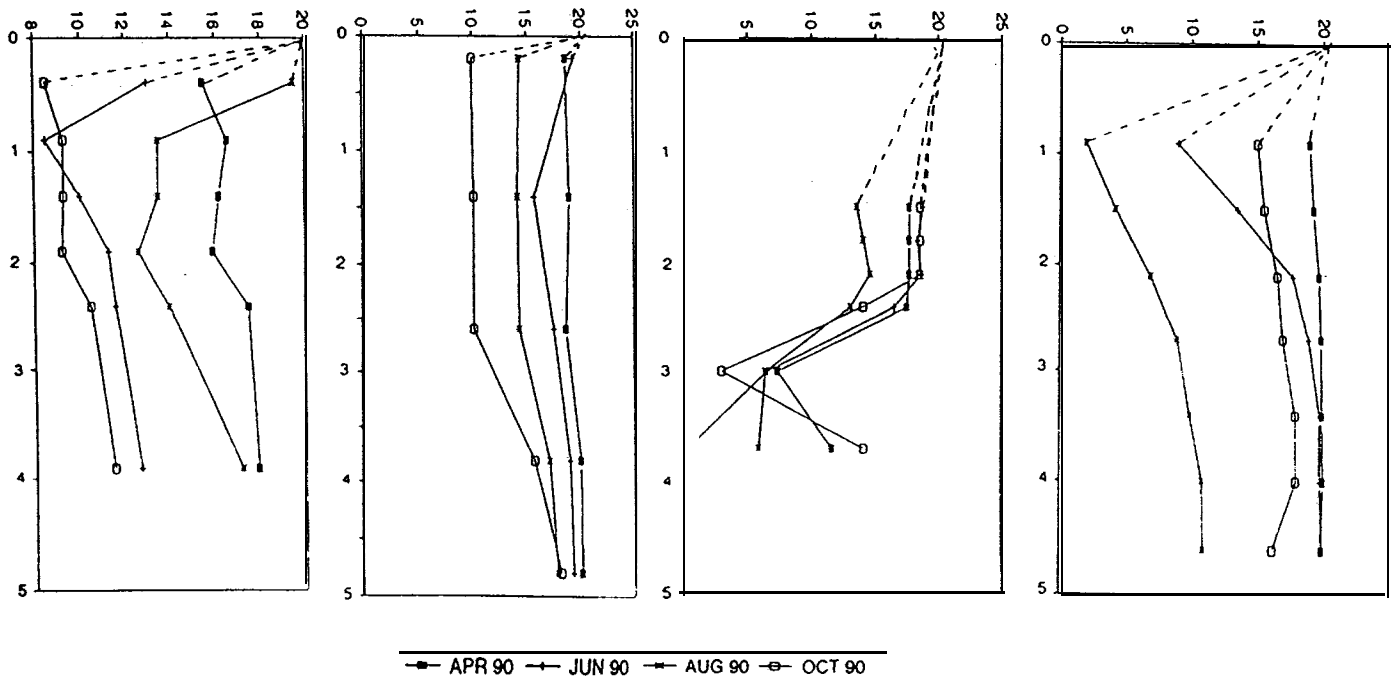
PILE 18A

PILE 188

Oxygen Concentration (%) - 1989



Oxygen Concentration (%) - 1990



**NOLAN, DAVIS
& ASSOCIATES**

FIGURE 4-3
COMPARISON OF OXYGEN/ DEPTH PROFILES
HEATH STEELE MINES

4.1 Comparison to Rum Jungle

As previously mentioned the work on monitoring **cover** performance on pyritic waste rock dumps at the Rum Jungle mine site in Australia provides a valuable basis of comparison for the Heath Steele results.

The two dumps at Rum Jungle for which temperature and oxygen data have been collected contain about two and seven million tonnes. The largest pile at Heath Steele contains about a quarter of a million tonnes. This means that the behaviour of the Heath Steele piles was more strongly affected by surface conditions and particularly the air temperatures. The smaller distance for transferring heat out of the dump means that a higher oxidation rate is necessary at Heath Steele than at Rum Jungle to achieve the same waste rock temperatures.

The climates at the two sites are very different, Rum Jungle is in the tropics at latitude **13°S** and Heath Steele is subject to cold Canadian maritime winters at **47°N**. The mean daily air temperature at Rum Jungle varied from a minimum of **25.1°C** in July to a maximum of **29.6°C** in November. In contrast, at Heath Steele the mean daily air temperature varied from **17.9°C** in July to **-12.5°C** in January. The piles at Heath Steele were thus subject to a much greater seasonal variation and a much lower winter temperatures.

Despite the differences in climate and sizes of the piles and dumps, there are many similarities between conditions in the piles at Heath Steele and in the dumps at Rum Jungle before they were rehabilitated. The similarities include:

pore gas through most of the piles had high enough oxygen concentrations to allow oxidation to occur,

decreased oxygen concentrations at many locations was indicative of oxygen consumption,

elevated waste rock temperatures tended to occur at locations where there were low oxygen concentrations,

at some locations oxygen concentrations near the base were higher than concentrations nearer the surface, which is characteristic of thermal convection bringing oxygenated air from the side into the pile, and

at other locations oxygen concentrations decreased with depth, which is characteristic of diffusion of oxygen from the top surface into the dump.

It is reassuring that many of the processes occurring in the Heath Steele piles were similar to those that occurred in the Rum Jungle dumps.

There are some processes that occurred on one site but not appear to occur at the other.

The oxidation rate decreased in winter at Heath Steele due to the cold winter temperatures and in the top few metres of the piles oxidation was effectively stopped. In the small piles the reduction in oxidation rate was significant at all depths.

The cold outside air temperature at Heath Steele increased the temperature difference between the outside air and the pore gas in the piles which means that thermal convection could increase in winter. This tendency to increased thermal convection in winter might be offset to some extent by snow cover or frozen ground. It is not clear from the data if the increase in thermal convection was significant.

Advective diurnal transport of oxygen that was driven by atmospheric tides occurred at Rum Jungle but would not be a factor at Heath Steele.

There are differences in the relative importance of the various processes in the piles and dumps at the two sites but most of the differences can be explained by the relative sizes of the dumps and external effects such as atmospheric pressure and air temperatures. Internal factors such as mineralogy and construction techniques appear to be less important.

PART FIVE

CONCLUSIONS AND RECOMMENDATIONS

5.0 CONCLUSIONS AND RECOMMENDATIONS

- The project has achieved the objective of defining pre-cover background conditions in each of the four piles monitored.
- Since it is now expected that placement of the covers will not occur prior to the 1991 construction season, it is recommended that monthly monitoring of all piles be continued through June 1991.
- All instrumentation is functioning according to expectations and reflects the conditions in each pile with reasonable accuracy. The existing instrumentation will continue to serve the needs of the project if properly maintained and protected during the placement of the covers.
- All four piles appear to have temperature, oxygen and, in the case of Piles 17 and 7/12, water quality characteristics representative of wastes undergoing active sulphide oxidation reactions and are, therefore, suitable candidates for the placement and evaluation of covers.
- It is recommended that cover placement on Pile 7/12 be given priority for Phase IV due to the ability to determine contaminant loadings for that pile.
- It is recommended that the thermal conductivity of several waste rock samples be determined and that heat production profiles be determined.
- It is recommended that further investigative work be carried out to determine the air permeability of the piles using tracer gas techniques, and that an attempt be made to develop a computer model of the gas transfer mechanisms as a tool to better understanding the factors influencing gas transfer and the interaction between diffusion, convection and advection in the waste piles.

REFERENCES

- Bennett, J.W.; Harries, J.R.; and Ritchie, A.I.M., 1988. "Rehabilitation of Waste Rock Dumps at the Rum Jungle Mine Site". Proceedings of Mine Drainage and Surface Mine Reclamation. P. 104-108.
- Golder, 1989. Report to Environment Canada on the Drilling Program at the Mount Washington Mine Site, British Columbia.
- Harries, J.R. and Ritchie, A.I.M., 1985. "Pore Gas Composition in Waste Rock Dumps Undergoing Pyritic Oxidation." Soil Sci. 140; p. 143-152.
- Northern Territory Department of Mines and Energy, 1986. "The Rum Jungle -Rehabilitation Project, Final Project Report." NTDME, Darwin, Australia, 1986.
- Nolan, Davis & Associates, 1989. "Heath Steele Waste Rock Study, Phase I - Interim Report.
- Nolan, Davis & Associates, 1987. "Study of Acid Waste Rock Management at Canadian Base Metal Mines." Report to Energy, Mines and Resources Canada (CANMET), Ottawa.

RESEARCH REPORT

EN2-9303-006 : RR 90-1
AN INVESTIGATION OF ENGINEERED
SOIL COVER TECHNOLOGY FOR
HEATH STEELE WASTE PILES

by

Ernest K. Yanful

Submitted as Phase III of
HEATH STEELE WASTE ROCK STUDY

December 1990 ,

Centre de technologie Noranda
240 boulevard Hyrnus
Pointe Claire, Qué., H9R 1G5
C a n a d a

TABLE OF CONTENTS

| | <u>Page</u> |
|--|-------------|
| EXECUTIVE SUMMARY | 1 |
| INTRODUCTION | 2 |
| 1.1 Historical Background | 2 |
| 1.2 Heath Steele Waste Rock Project | 2 |
| 2. OBJECTIVES AND SCOPE | 3 |
| 3. SULPHIDE OXIDATION AND ACID GENERATION IN WASTE ROCK | 3 |
| 3.1 Oxidation Process | 3 |
| 3.2 Oxygen Transport | 5 |
| 3.2.1 Diffusion | 5 |
| 3.2.2 Advection | 7 |
| 3.2.2.1 Barometric Pumping | 8 |
| 3.2.2.2 Wind Currents | 8 |
| 3.2.2.3 Thermal Effects | 8 |
| 3.2.2.4 Transport of Dissolved Oxygen | 9 |

| | | |
|-------|--|----|
| 3.3 | Role of Temperature | 10 |
| 4. | ENGINEERED SOIL COVER APPLICATIONS ON WASTE ROCK PILES | 10 |
| 4.1 | State of the Art | 10 |
| 4.2 | Case Studies | 11 |
| 4.2.1 | Mount Washington Site, British Columbia | 11 |
| 4.2.2 | Rum Jungle Mine, Australia | 12 |
| 5. | CANDIDATE SOIL COVER MATERIALS FROM HEATH STEELE MINE | 13 |
| 5.1 | Sampling of Soil Materials | 13 |
| 5.2 | Laboratory Investigation. | 14 |
| 5.2.1 | Index Tests | 14 |
| 5.2.2 | Mineralogy | 15 |
| 5.2.3 | Compaction | 15 |
| 5.2.4 | Consolidation Tests | 16 |
| 5.2.5 | Hydraulic Conductivity | 16 |

| | <u>Page</u> |
|---|-------------|
| 5.2.6 Freeze-thaw Tests | 17 |
| 5.2.7 Hydraulic Characteristics of a Cover | 18 |
| 5.2.8 Oxygen Diffusion Measurements | 18 |
| 5.3 Results of Laboratory Investigation | 19 |
| 5.3.1 Mineralogy | 19 |
| 5.3.2 Geotechnique | 20 |
| 5.3.3 Prediction of Cover Performance | 26 |
| 6. COVER DESIGN SCENARIOS FOR HEATH STEELE WASTE ROCK | 27 |
| 6.1 Theoretical Concepts | 27 |
| 6.2 Single Cover | 29 |
| 6.3 Composite Cover | 30 |
| 6.3.1 Diffusion Model. | 30 |
| 6.3.2 Two-Layer System | 30 |
| 6.3.3 Three-Layer System | 31 |

| | |
|----------------------------|----|
| 7. SUMMARY & CONCLUSIONS | 32 |
| REFERENCES | 34 |
| APPENDIX FREEZE-THAW TESTS | |

LIST OF TABLES

| | | <u>Page</u> |
|-----------|--|-------------|
| Table 3.1 | Parameters used in flux calculations | 7 |
| Table 5.1 | Location of Heath Steele Soils | 14 |
| Table 5.2 | Index Properties of Candidate Heath Steele Soils | 20 |
| Table 5.3 | Consolidation Spreadsheet, Heath Steele Soil HS-C1 | 24 |
| Table 5.4 | Consolidation Spreadsheet, Heath Steele Soil HS-C2 | 24 |
| Table 5.5 | Results of Hydraulic Conductivity Tests for Compacted Heath Steele Till, HS-C | 25 |
| Table 6.1 | Water Content versus Pressure Head | 27 |
| Table 6.2 | Calculated Capillary Heads for Heath Steele Soils | 28 |
| Table 6.3 | Calculated Oxygen Fluxes for Different Cover Scenarios | 32 |

LIST OF FIGURES

- Figure 3.1 The variation of radon gas diffusion coefficient with moisture saturation.
- Figure 3.2 The variation of a) oxygen solubility and b) Henry's law constant with temperature.
- Figure 4.1 A location map of **the Mount** Washington mine site on Vancouver Island, B.C.
- Figure 4.2 Typical gas concentrations and temperature profiles in Mount Washington waste dumps before and after placement of cover.
- Figure 4.3 Location of White's and Intermediate Dumps, Rum Jungle Mine, Australia.
- Figure 4.4 Temperature distributions in White's Dump before and after rehabilitation (directly from Bennett et al., 1989).
- Figure 4.5 Temperature distributions in Intermediate Dump before and after rehabilitation (directly from Bennett et al., 1989).
- Figure 4.8 Oxygen distribution in White's dump before and after rehabilitation. Contours indicate pore gas concentration (vol.%). Directly from Bennett et al., (1989).
- Figure 4.7 Oxygen distribution in Intermediate dump before and after rehabilitation. Contours indicate pore gas oxygen concentration (vol.%). Directly from Bennett et al., (1989).
- Figure 5.1 Triaxial panel and cell used in the hydraulic conductivity tests.
- Figure 5.2 Moisture content (defined as V_w/V_T) and pressure head for a sand and a silt loam (from Nicholson et al., 1989).

LIST OF FIGURES (Cont'd).

- Figure 5.3 A schematic representation of the column used for investigating the hydraulics of a two-layer cover system.
- Figure 5.4 A schematic representation of the set up used in oxygen diffusion measurements.
- Figure 5.5 A random X-ray powder diffractogram of soil HS-C.
- Figure 5.6 Oriented X-ray diffractograms of soil HS-C.
- Figure 5.7 Grain size distribution of till HS-A.
- Figure 5.8 Grain size distribution of till HS-B.
- Figure 5.9 Grain size distribution of till HS-C.
- Figure 5.10 Grain size distribution of till HS-E.
- Figure 5.11 Grain size distribution of till HS-D.
- Figure 5.12 Modified Proctor compaction curve for tills HS-A and HS-B.
- Figure 5.13 Modified Proctor compaction curve for tills HS-C and **HS-E**.
- Figure 5.14 Modified Proctor compaction curve for till **HS-D**.
- Figure 5.15 Moisture density relationship for till HS-B, showing different degrees of saturation.
- Figure 5.16 Void ratio-pressure relationship for till HS-C (test # 1, HS-C1).
- Figure 5.17 Void ratio-pressure relationship for till HS-C (test **#2, HS-C2**).

LIST OF FIGURES (Cont'd).

- Figure 5.18 Variations of compression index, C_c , and coefficient of consolidation, c_v , with applied stress.
- Figure 5.19 The hydraulic conductivity of compacted soil HS-C permeated with distilled water at a hydraulic gradient of 18.
- Figure 5.20 The hydraulic conductivity of compacted soil HS-C permeated with distilled water at a hydraulic gradient of 60.
- Figure 5.21 Hydraulic conductivity and laboratory temperature versus time.
- Figure 5.22 Hydraulic conductivity and change in sample volume versus time.
- Figure 5.23 Profiles of a) pressure and b) moisture content **observed** in laboratory column.
- Figure 5.24 A schematic representation of demonstration column for assessing the effectiveness of a composite cover system.
- Figure 5.25 Transient moisture content profiles observed in soil HS-C in demonstration column.
- Figure 6.1 Moisture Drainage Curve for Heath Steele Sand HS-D
- Figure 6.2 Variation of Oxygen Flux with Cover Thickness
- Figure 6.3 Variation **of** Flux with Diision Time for Different Diffusion Coefficients
- Figure 6.4 Oxygen Profiles in a Conceptualized Single and Two-Layer Cover Systems
- Figure 6.5 Oxygen Profiles in a Conceptualized Single and Three-Layer Cover Systems

EXECUTIVE SUMMARY

Soils located in the vicinity of Heath Steele Mines have been sampled and tested for their potential **use as** engineered covers for the waste rock piles located at **the** site. The soils are mostly sandy silt **tills** with only about 10 percent of clay-sized materials. When compacted slightly wet of the optimum water content, the tills are found to be nearly fully saturated with a low hydraulic conductivity. This suggests that if properly designed, a cover system incorporating any of the tills could be both an effective oxygen and water barrier. A 3-layer composite soil cover system, consisting of an uppermost coarse-grained soil, a middle saturated till layer and an underlying coarse layer is proposed for the decommissioning of the waste rock piles. Computer modelling indicates that much lower oxygen fluxes can be expected from this composite system than from a single till layer.

It is recommended that other important factors such as frost heaving, selection and grading of slopes, erosion, and availability of abundant tills in the vicinity of the mine be considered prior to actual design **and implementation.**

I. INTRODUCTION

1.1 Historical Background

The Heath **Steele** mine site is located approximately 50 km northwest of Newcastle, New Brunswick, and about 60 km southwest of Bathurst. The massive ore deposits at the site were discovered in 1953. Mine development commenced in **1955** and ore beneficiation in 1957. Operations ceased in May 1968 as a result of low metal prices and difficulties encountered in the processing of oxidized portions of the ore. Production was resumed in 1960 and the mill capacity increased to 3000 tonnes/day in 1969 and then to 4000 tonnes/day in 1977. Production was suspended in May 1983, again, as a result of low metal prices. Milling, however, continued with modification of the concentrator to process silver-gold gossan ore which had been stockpiled on site. Processing of the gossan ore continued until October 1984. Since closure, surface water and mine drainage from the site have been collected by means of a comprehensive site drainage collection system and either pumped to the mill or to the tailings pond for treatment.

Production commenced at the new Stratmat mine and the existing B-Zone underground mine.

In total, some 750,000 tonnes of pyritic waste rock and reject ore are currently stockpiled in more than 20 piles at the Heath Steele site. The total projected waste rock inventory at closure (including waste rock from the Stratmat, E-Zone and B-Zone, operations) is 2.3 million tonnes.

1.2 Heath Steele Waste Rock Project

During the fall of **1986/spring** 1987, Brunswick Mining and Smelting Corporation Limited proposed to various federal and provincial agencies the possibility of using several of the waste rock piles at the Heath Steele mine site to develop and test strategies for long-term management of acid-generating waste rock. Following favourable responses from these agencies, Brunswick Mining developed and submitted a four-phase program for possible funding. An agreement to fund the initial three phases was signed on December 16, 1988 by the New Brunswick Department of Natural Resources and Energy, the New Brunswick Department of Commerce and Technology, and Brunswick Mining and Smelting Corporation.

The four phases of the program are as follows:

- | | |
|-----------|---|
| Phase I | Selection of four waste rock piles to be used for specific field trials. |
| Phase II | Installation of monitoring equipment to define the characteristics and background data for the four piles identified in Phase I. |
| Phase III | Geotechnical and column testing to evaluate the performance characteristics of potential soil covers, including oxygen diffusion. |

Phase IV Application of covers (designed on the basis of the results of Phase III) and performance monitoring under field conditions.

This report addresses Phase III.

2. **OBJECTIVES AND SCOPE**

The principal objective of the Heath Steele Waste Rock Phase III Study was to determine the performance characteristics of natural soils in the vicinity of the Heath Steele mine site as potential engineered covers for the waste rock piles. It was also the intent of the study to develop the most appropriate cover design scenario for the waste rock piles.

The study involved site exploration for natural soil materials (such as tills, clays, and sand), laboratory geotechnical testing, column fabrication, testing of the soils for their hydraulic characteristics, and measurements of oxygen diffusion coefficients. Laboratory geotechnical testing consisted of measurements for grain size distribution, specific gravity, compaction and consolidation characteristics, and hydraulic conductivity. The hydraulic characteristics (moisture drainage curves) of these natural soils were also determined in order to assess the potential for their inclusion in composite or layered cover systems. The exploration for the soils was restricted to a 15-km radius of the Heath Steele site, since soils located at greater distances would not be useful in economical cover design considerations.

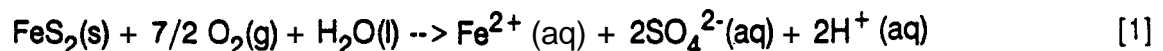
Although advection is a major component of gas transport in waste rock piles, this study was restricted to diffusion for two main reasons. Firstly, diffusion is the dominant transport mechanism in a fine-grained, compacted soil cover, such as the one envisaged for the waste rock. Secondly, advection and hence air permeability would be more reliably evaluated in the field than in the laboratory because of scale and the complex distribution of pore spaces in real waste rock piles.

3. **SULPHIDE OXIDATION AND ACID GENERATION IN WASTE ROCK**

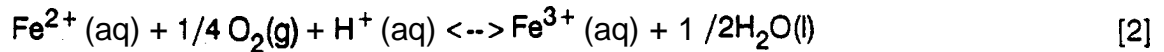
3.1 **Oxidation Process**

Acid generation in waste rock is caused by the exposure of rock containing sulphide minerals (principally pyrite and pyrrhotite) to air and water during mining, resulting in the production of acidity and high concentrations of dissolved sulphate (SO_4^{2-}) and metals. These sulphide minerals are generally found in ore or surrounding rock in most base metal, precious metal and uranium mines.

The first important reaction in acid generation is the oxidation of pyrite into dissolved iron, sulphate and hydrogen ion (H^+):

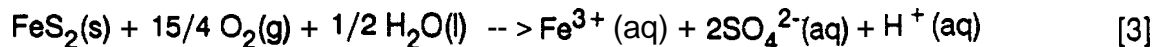


The dissolved Fe^{2+} , SO_4^{2-} , and H^+ represent an increase in total dissolved solids and acidity of the water and, hence, a decrease in pH, unless the water is neutralized. For a low-pH environment (that is, pH 1.5 to 3.5) in which oxygen is readily available, subsequent oxidation of ferrous iron, Fe^{2+} , will occur, producing ferric iron, Fe^{3+} , as follows:

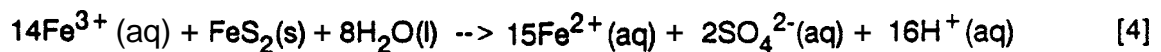


Ferrous oxidation to ferric iron in the pH range 1.5 to 3.5, Equation [2], is sometimes catalyzed by the iron bacteria, Thiobacillus ferrooxidans.

The reactions in Equations [1] and [2] can be combined to yield:

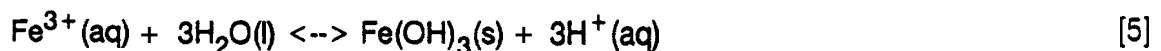


The reaction in Equation [3] indicates that during pyrite oxidation both Fe^{2+} and S_2^{2-} of $\text{FeS}_2(\text{s})$ can oxidize, resulting in the formation of two moles of SO_4^{2-} and one mole of H^+ for each mole of FeS_2 oxidized. Ferric iron, Fe^{3+} , released as either in Equation [2] or Equation [3], will further oxidize pyrite, thereby generating additional acidity and dissolved ferrous iron, according to the following reaction:



A comparison of Equations [1] and [4] indicates that, at low pH, dissolved ferric iron will oxidize pyrite and generate more acidity than that produced from pyrite oxidation by gaseous oxygen.

At slightly higher pH values (say 3.5 or greater), hydrolysis of Fe^{3+} will occur, resulting in the precipitation of ferric hydroxide and leaving little Fe^{3+} in solution while lowering pH (through release of additional H^+) at the same time:



Thus, the oxidation and the subsequent acidification processes, once started, are self-perpetuating.

As shown in the preceding discussions, the primary ingredients for acid generation are: 1) sulphide minerals, 2) water or a humid atmosphere, and 3) oxidants, principally oxygen from the atmosphere or from chemical sources and dissolved ferric iron. Thus, the exclusion of oxygen and moisture will stop sulphide oxidation and acid generation. Although ferric iron is an important oxidant, examination of Equations [1] and [2] indicates that if oxygen is not available, ferric iron will not form and the oxidation process will not occur. Thus, the role of the ferric iron is intermediate. Oxygen availability and transport therefore appears to be the most important consideration in any reactive waste rock management strategy.

In addition to oxygen and water, other factors found to influence pyrite oxidation are sulphide content, pore characteristics (pore size distribution, porosity and grain size) of the waste rock, bacterial population density, and ferric iron concentration. Carbon dioxide enhances bacterial activity and therefore its concentration in the gas phase can have an effect on rate of oxidation. Carbon dioxide, like oxygen and other gases, is initially derived from the atmosphere. The gaseous CO₂ concentration in the pile could, however, be higher than atmospheric if the rate of acid generation in the pile is high enough to result in the dissolution of available carbonate minerals.

3.2 Oxygen Transport

Oxygen is a key requirement for sulphide oxidation and acid generation. The principal modes of gaseous oxygen transport within a waste rock pile are diffusion and advection.

3.2.1 Diffusion

Gas transport by diffusion occurs when gas molecules move in response to concentration gradients. The movement of the molecules occurs in random patterns due to the kinetic energy of the molecules and inter-molecular collisions. Gas movement by diffusion is generally slow and tends to be unimportant when there is significant movement by wind currents.

Gas diffusion in a waste rock pile can be assumed to be Fickian in behaviour so that the diffusive flux of oxygen into the pile can be described by Fick's first law, as follows:

$$J = -D \frac{\delta C}{\delta Z} \quad [6]$$

where J = flux of oxygen (moles/m²s)
 D = diffusion coefficient (m²/s)
 C = concentration (moles/m³)
 Z = depth in the pile (m)

The rate at which the oxygen concentration changes is given by Fick's second law:

$$\frac{\delta C}{\delta t} = D \frac{\delta^2 C}{\delta Z^2} \quad [7]$$

where t is the time variable in seconds and C, D and Z have the same meanings as before.

The concentration gradient required for diffusion in waste rock piles results from differences between gas concentrations in the pore spaces and the atmosphere. For example, gaseous oxygen concentrations in the pores that are lower than atmospheric values result from consumption in the pore spaces due to geochemical reactions which generally occur following the construction of the pile. The resulting gradient drives gaseous oxygen into the pile at a rate which is governed by the diffusion coefficient. For example, the diffusion coefficient of oxygen

in air is $0.178 \text{ cm}^2/\text{s}$, compared to a value of $2 \times 10^{-5} \text{ cm}^2/\text{s}$ in water. Oxygen diffusion from the atmosphere into a waste rock pile can occur through air-filled cracks and pores in the rock fragments as well as through water-filled pores. The relative magnitudes of the diffusion coefficients indicate that diffusion through the **water-filled** cracks and pores is less important.

Generally, when oxygen transport into a waste rock pile is controlled by diffusion through air-filled pores in the pile, high (close to atmospheric values) gaseous oxygen concentrations are observed at or near the surface of the pile. These values decrease rapidly with depth to the zone where the oxygen is consumed by sulphide mineral oxidation.

The effective diffusion coefficient is highly dependent on the pore characteristics of the rocks in the pile. For oxygen, the effective diffusion coefficient, D_e , can be written as a function of the rock porosity, n , and a tortuosity, τ , as follows:

$$D_e = D_o n \tau \quad [8]$$

where D_o is the diffusion coefficient of oxygen in air. The tortuosity is introduced to account for obstructions caused by the presence of solids and liquids in the pathway. It is generally defined as the inverse of the normalized path length (Taylor, 1949; Nielsen et al. 1984; Nicholson et al. 1989).

To illustrate the calculation of flux, a waste rock pile with a thickness of 1 m and a porosity of 5% is assumed. If the tortuosity, τ , is taken to be 0.2, then the effective diffusion coefficient of gaseous oxygen is calculated from Equation (8) to be $1.78 \times 10^{-3} \text{ cm}^2/\text{s}$. The flux of gaseous oxygen across the 1 m thick pile is 4.3×10^{-4} grams per square centimeter per month. On the other hand, if the rock is fully saturated, the effective diffusion coefficient of oxygen in water is calculated to be $2 \times 10^{-7} \text{ cm}^2/\text{s}$, using the parameters in Table 3.1 and Equation (8). The flux of oxygen through the water-saturated pores is 4.4×10^{-5} grams per square centimeter per month. Thus, the flux of oxygen as a result of aqueous diffusion is lower than by gaseous diffusion.

Gaseous diffusion is particularly important in the reclamation of waste rock dumps and piles because it is the mechanism by which oxygen enters piles covered with engineered soils. If the cover is designed to have a high water content, the flux of oxygen into the pile can be very small. Figure 3.1 shows the relationship between the diffusion coefficient of a gas (radon) and the water content of a soil expressed as the moisture saturation. The data indicate that the diffusion **coefficient** decreases as the water content increases. The diffusion coefficient decreases by about two orders of magnitude and **as moisture saturation increases** from 75 to 95 **percent**, the pores are effectively blocked by water molecules. Since the diffusion **coefficient** of a gas (**for** example, oxygen, Table 3.1) is about 10,000 times higher in a gas phase than in water and the solubility of gases in general is low in water, the soil voids are effectively blocked by water molecules at these high moisture saturation states. This leads to the low, effective diffusivities and therefore diffusive fluxes at the high water contents.

The foregoing discussions suggest that properly designed engineered soil covers may be an attractive option for reclamation of waste rock piles or dumps.

TABLE 3.1

PARAMETERS USED IN FLUX CALCULATIONS

| | | |
|--|------------------------|--------------------|
| Diffusion coefficient of oxygen in air | 0.178 | cm ² /s |
| Diffusion coefficient of oxygen in water | 2x 10 ⁻⁵ | cm ² /s |
| Concentration of oxygen in air | 2.8 x 10 ⁻⁴ | g/cm ³ |
| Concentration. of oxygen in water | 8.6 x 10 ⁻³ | g/cm ³ |
| Porosity of rock, n | 5% | |
| Tortuosity, τ | 0 . 2 | |

3.2.2. Advection

Advective transport of oxygen into a waste rock pile represents the bulk movement of the gas through the existing pore spaces under a pressure gradient. Gas advection is controlled by the gas permeability of the pile and the magnitude of the gradient. Gaseous oxygen can be transported deep into a waste rock pile as a result of advection. Parizek (1985) noted that advection was the major mechanism by which oxygen was transported in spoils and that it could carry oxygen to depths greater than 20 meters in spoils.

Harries and Ritchie (1985) have noted that, for a given pressure gradient, the volume of gas transported by advection through a particular pore is a function of the fourth power of the pore diameter. They further noted that the advective velocity in the pore depends on the square of the diameter. This implies that the presence of a few large pores in a waste rock pile could facilitate advective transport.

Advective transport of gas in a porous medium can be represented by an expression similar to Darcy's law for water transport:

$$Q = \frac{-k \delta P}{\mu \delta Z} \quad (9)$$

where Q is the volumetric flow rate ($L T^{-1}$), k the gas permeability (L^2), μ the dynamic viscosity ($M L^{-1} T^{-1}$), and $\frac{\delta P}{\delta Z}$ the pressure gradient ($M L^{-2} T^{-2}$).

The viscosity is practically independent of pressure and depends upon temperature **only**. Gas viscosity increases with temperature. The viscosity of air increases only slightly **from** about 1.2×10^{-5} at $-10^\circ C$ to 1.8×10^{-5} Pa.s at $60^\circ C$ with a value of about 1.6×10^{-5} Pa.s at $20^\circ C$ (Streeter and Wylie, 1981). Gaseous oxygen will have viscosities similar to those of air.

The permeability is a function of the pore size distribution of the medium. It is usually expressed in units of darcies or m^2 (1 **darcy** = $9.87 \times 10^{-13} \text{m}^2$).

As already mentioned, advection also occurs in response to pressure gradients. There are three principal processes which cause pressure gradients to form in and around waste rock piles. These are barometric pumping, wind currents, and internal heat production. Gas removal by plant roots could also lead to the ingress of atmospheric gas at the surface of waste rock piles to replenish removed volumes.

3.2.2.1 Barometric Pumping

Advective transfer of oxygen in the gas phase can occur in response to pressure adjustments within pore spaces of waste rock piles resulting from changes in the external atmospheric pressure. Increase in atmospheric pressure leads to the compression of internal gases. The compression results in the movement of air from the atmosphere into the pile. Decrease in the atmosphere pressure will conversely result in the expansion and migration of the internal gases out of the pile. The contribution of barometric pumping to the overall process of gas advection could be relatively minor, in comparison to wind currents and thermal effects. Two main reasons account for this: 1) barometric pumping will affect gas concentrations in the peripheries of waste rock piles where the gases are entering and exiting, and 2) normal changes in atmospheric pressure, with the exception of occasional hurricanes and tornadoes, may not be large enough to induce significant volume changes in gases entering or exiting waste rock piles. Although the volume of air entering a pile by barometric pumping may be small, it could lead to extensive sulphide mineral oxidation (Morin et al., 1990).

3.2.2.2 Wind Currents

Gaseous oxygen can enter waste rock piles as a result of turbulent flow of air due to wind action. **Wind** currents can result in the development of high pressures on the sides of waste rock piles. In response, air moves into the pile to **flush** out resident gases from the pore spaces. It is conceivable that wind advection could be an important transport mechanism in waste rock piles located at high elevations above the surrounding land surface (Morin et al., 1990).

3.2.2.3 Thermal Effects

Exothermic geochemical reactions, such as pyrite oxidation, generate heat in waste rock piles. This heat could lower the density of the surrounding gases which causes them to move upwards and out of the upper surfaces of the pile. In response, gases from more distant locations in the pile, and ultimately from the atmosphere, move in to the heated area, sometimes called a 'hot spot'. The movement of oxygen into the 'hot spot' could accelerate sulphide mineral oxidation and, therefore, heat production. Thermal advection is considered to be the dominant form of gas advection (Morin et al., 1990). Parizek (1985) has noted that the volume of acid products observed in acid-generating spoils could only be adequately explained by gas advection.

3.2.2.4 Transport of Dissolved Oxygen

Oxygen and the other gases dissolved in precipitation will be transported through waste rock piles by aqueous advection. This type of advection is the bulk movement of water through the pore spaces in piles in response to a hydraulic gradient. The hydraulic conductivity of the pile is a very important factor in advection. The flux of gas through the pile due to advection can be calculated as follows :

$$F = kiC \quad [10]$$

where k is the hydraulic conductivity (LT^{-1}), i the hydraulic gradient (dimensionless) and C the concentration (ML^{-3}) of the gas in water.

The above equation indicates that the advective flux of oxygen through a pile is also a function of the rate of dissolution in water. This rate will attain a maximum value at the solubility limit. The solubility of oxygen in water decreases with increase in temperature but increases with increase in pressure. Figure 3.2a shows the relationship between the concentration of dissolved oxygen in water in equilibrium with air at a total pressure of 1 atmosphere, plotted from the data of Truesdale et al. (1955). The dissolved oxygen concentration at $10^{\circ}C$ is about 11 mg/L or 0.34 mmoles/L . For a waste rock pile with a hydraulic conductivity of 10^{-3} cm/s , the advective flux of oxygen at a unit hydraulic gradient is calculated from Equation [10] to be 8.8 moles of O_2 per square meter per month.

The partial pressure of oxygen in equilibrium with the 0.34 mmoles/L at $10^{\circ}C$ can be estimated from Henry's law :

$$kP_{O_2} = [O_2(aq)] \quad [11]$$

where k is Henry's law constant, P_{O_2} the partial pressure of oxygen and $[O_2(aq)]$ the concentration of dissolved oxygen. Values of Henry's law constant for oxygen in ($\text{mmoles/L}/\text{atm}$) for various temperatures is presented in Figure 3.2b. At $10^{\circ}C$, Henry's law constant for oxygen is $1.70 \text{ (mmoles/L)/atm}$. Using this value in equation, the partial pressure of gaseous oxygen in equilibrium with 0.34 mmoles/L of dissolved oxygen is estimated to be 0.20 atmosphere or $8.6 \times 10^{-4} \text{ mmoles/litre}$, assuming ideal gas behaviour.

The flux of oxygen that reaches the waste rock pile by advection is high, compared to the diffusive flux calculated in Section 3.2.1. Consequently, aqueous advection can be a major means of transport of oxygen into waste rock piles, unlike tailings deposits.

3.3 Role of Temperature

The oxidation of pyrite to sulphuric acid and ferrous sulphate is an exothermic reaction which produces 1440 kJ mole⁻¹ (FeS₂) of heat. This can be verified by performing enthalpy change calculations for the reactions describing pyrite oxidation (Yanful et al., 1990a). Consequently, temperature profiles in waste rock piles can give an indication of oxidation. Daniel et al. (1980) and Harries and Ritchie (1981, 1985) used temperature profiles to identify oxidation sites in waste rock dumps at the Rum Jungle mine in the Northern Territory of Australia.

Unlike acidity and drainage metal concentration, temperature provides a very good indication of the location of oxidation sites and also of rates of oxidation in waste rock piles.

Temperatures in waste rocks tend to be elevated (50 to 60°C) in zones where sulphide mineral oxidation is occurring. These high temperatures derive from the fact that sulphide oxidation is exothermic. The quantity of heat released can be calculated from the temperature observed in the waste rock pile, as was done for the Rum Jungle site in Australia (Harries and Ritchie, 1981). The elevated temperatures can increase the rate of oxidation by promoting bacterial activity. Iron oxidizing bacteria Thiobacillus ferrooxidans catalyze the oxidation of ferrous to ferric iron which is the rate-determining step in the sulphide oxidation process. These bacteria have optimal activity in the temperature range of 30 to 35°C.

4. ENGINEERED SOIL COVER APPLICATIONS ON WASTE ROCK PILES

4.1 State of the Art

Engineered soil covers have a potential for reducing acid generation in waste rock piles. Abundant tills or clays located in the vicinity of piles offer the most attractive option for reclamation. These soils are generally fine-grained and can yield low hydraulic conductivities when compacted. If they are placed at near-saturated conditions, the reduced air-filled porosity leads to low diffusive oxygen fluxes. Consequently, the rates of sulphide oxidation and acid production are reduced. Thus the cost of treating acidic seepage is substantially reduced. The greatest advantage offered by engineered soil covers is their low maintenance. It should, however, be mentioned that soil cover applications may not be suitable for all situations. For example, their cost could be prohibitive if soil materials are not readily available and have to be transported from distant places. Thus, each situation has to be assessed on the basis of logistics and economics.

Canada's MEND (Mine Environment for Neutral Drainage) program is currently sponsoring projects on applications of engineered soil covers. These projects, which include the Heath Steele Waste Rock Study, are described elsewhere (Filion and Ferguson, 1989).

Soil covers have also been applied over waste rock piles at the Mount Washington site in British Columbia, Canada, and the Rum Jungle site in the Northern Territories of Australia. At both sites, the piles have been monitored for gaseous oxygen fluxes, temperatures, and seepage water concentrations as a means of evaluating the effectiveness of the covers.

4.2 Case Studies

4.2.1 Mount Washington Site, British Columbia

Mount Washington mine is an abandoned porphyry copper mine located in south-central Vancouver Island, British Columbia, Canada. Open pit mining was in operation from 1964 to late 1966. The remains of mining activity at the present site include two open pits containing waste dumps called West and East Dumps. The East Dump gives rise to acid drainage causing detrimental effects on salmon stocks in the nearby Tsolum River (Kwong and Nordstrom, 1989). The West Dump does not generate acid and reports to Oyster River. A location map of the Mt. Washington mine site is shown in Fig 4.1.

As part of the reclamation work undertaken by the British Columbia Department of Mines and Energy, a compacted till cover was placed on the East Dump between 1988 and 1989. The purpose of the till cover was to prevent the infiltration of water and ingress of oxygen into the waste rock. Prior to the placement of the cover, all waste rock and overburden in the North Pit area were scraped and placed in the East Dump. The total thickness of the completed cover was 1 m. In the initial design requirements, the lower 50 cm (barrier layer) was to be compacted at 93% modified Proctor and the upper at 99% modified Proctor. The results of post-compaction density and water content measurements showed that these requirements were exceeded.

A soil compacted at a moisture content above its optimum moisture content is less permeable and more resistant to cracking (less brittle) than a soil with the same density compacted at a moisture content below optimum. Therefore, both the upper and lower layers were compacted at the natural moisture content which was thought to be slightly higher than optimum. However, personal communications with the staff of the Engineering Department of the B.C. Dept. of Mines and Energy indicate that the upper layer of the till cover may have been placed at a water content slightly less than optimum. Thus, the upper layer of the cover could dry and crack during the hot summer months. Long-term monitoring of the integrity of the cover will therefore be beneficial.

Figure 4.2 presents typical gaseous oxygen, carbon dioxide and temperature profiles in the waste dumps before and after placement of the till cover. The results indicate slightly reduced oxygen and elevated carbon dioxide concentrations after placement of the till cover.

The temperature profiles show more stable values at the base of the dump and vary near the top of the dump according to atmospheric conditions. The placement of the till cover also appears to have had an insulating effect on the dump temperatures.

The data represent conditions only a few months after placement of the cover and might therefore not be conclusive. Continuous monitoring for longer periods will provide the basis for assessing the effectiveness of the cover.

4.2.2 Rum **Jungle** Mine, Australia

The Rum Jungle mine is an abandoned uranium and copper open cut mine in the Northern Territory, Australia. Mining was carried out between 1954 and 1964 and the site was abandoned in 1971, leaving three large open cuts and their associated overburden dumps. The physical, chemical and microbiological aspect of two of the dumps, White's and Intermediate, have been studied in detail (Harries and Ritchie, 1981; 1985). The locations of the two dumps is shown in Fig 4.3. Both waste rock dumps are about 20 m high, with White's dump, the larger of the two dumps, being about 500 m wide and containing $4 \times 10^6 \text{ m}^3$ of material. Intermediate dump has a width of about 300 m and contains $6.5 \times 10^5 \text{ m}^3$ of material. The average sulphur content of both dumps is about 3 percent. Both the ore and the overburden contained significant amounts of pyrite (Daniel et al., 1980; Harries and Ritchie, 1985).

The major sources of pollution from the site were identified to be the waste rock dumps and an abandoned experimental copper heap leach pile (Davy, 1975). The continued release of pollutants from the site led to the establishment of a rehabilitation program to reduce the level of pollutants in the local river system. The program also aimed at reducing the risk to public health and improving the general appearance of the site.

The rehabilitation work was initially confined to White's dump. Work on Intermediate dump started later in 1985. The principal intent of rehabilitation was to reduce the infiltration of water through the dumps. The work consisted of the application of a composite soil cover system on the dumps. Prior to the application of the cover, the tops of the dumps were reshaped to give a maximum slope of 5° with a central drainage system. The sides of the dumps were also reworked to provide a maximum slope of 1 : 3 with a berm halfway down the slope. Engineered drop structures were also provided to take water from the berms to the base of the dumps.

The cover system applied on top of the dumps comprised a compacted clay layer of at least 225 mm thickness overlain by a sandy clay loam (minimum thickness 250 mm) which was, in turn, overlain by a layer of gravelly sand (minimum thickness 150 mm). The functions of these layers were as follows: the compacted clay to minimize water infiltration, the sandy clay loam to retain moisture for support of vegetation and to prevent the clay from drying out, and the gravelly sand to provide erosion protection and to restrict moisture loss by evaporation in the dry season. The sides of the dumps were also covered with a similar but thicker three-layer cover system composed of minimum thicknesses of 300 mm compacted clay, 300 mm of sandy clay loam and 150 mm crushed rock. The top surfaces of the covers were vegetated to provide additional protection against erosion and to improve the appearance of the dump.

The dumps were instrumented to measure temperature, gaseous oxygen and carbon dioxide before and after the application of the covers. The infiltration of water through the cover layers was monitored using lysimeters installed in the dumps before emplacement of the compacted clay layer.

Figures 4.4 and 4.5 show temperature distributions in White's and Intermediate dumps before and after rehabilitation. Before rehabilitation, the temperatures at several locations within both dumps exceeded 50°C. The temperatures decreased following rehabilitation with the highest in either dump in June 1988 being 41°C. The elevated temperatures in the dumps have been attributed to the heat released in the oxidation of sulphidic materials in the dump. The oxidation of pyrite, for example, to sulphuric acid and ferrous sulphide is exothermic and can be shown to release 1440 kJ per mole of FeS_2 (Bennett et al., 1989).

The placement of the composite soil covers on the dumps was observed to have greatly reduced the level of oxygen in most regions of the dumps (Figures 3.8 and 3.9). Bennett et al., (1989) have observed that, since rehabilitation, the oxygen concentrations at depth have been low at all measuring points, with the exception of a few isolated portions of the dumps where the pyritic content was low. These authors note that the clay cover was effective in stopping oxygen transport into the dumps by thermal convection. Further monitoring, however, indicated that oxygen distribution in the top few meters of the dumps was diurnal. The oxygen concentrations were observed to increase in the mornings and evenings in the wet season. This behaviour was found to be similar to that observed even prior to rehabilitation. Bennett et al., (1989) attributed this diurnal behaviour to advection driven by changes in atmospheric pressure. Since the elevated oxygen concentrations were observed only in the wet season, the authors attributed the diurnal behaviour observed in the covered dumps to seasonable changes in the hydraulic conductivity of the compacted clay layer. Presumably, the clay near the monitoring hole was not as well compacted as the clay further away, resulting in greater air flow following an increase in the atmospheric pressure. In the dry season, no diurnal variation was observed and the oxygen concentrations were low. Bennett et al., (1989) infer that cracking of the clay in the dry season provided additional flow paths for air. This resulted in increased advection of air by atmospheric pressure variations. They note further that, early in the wet season, most of the cracks located further away from the monitoring holes closed as the moisture content of the clay increased. The clay near the holes probably did not seal as well as those further away, resulting in the re-appearance of the diurnal variations.

5. CANDIDATE SOIL COVER MATERIALS FROM HEATH STEELE MINE

5.1 Sampling of Soil Materials

During the summer of 1989, samples of soils were collected from trenches excavated in the vicinity of Heath Steele mines. These trenches were excavated for the construction of pipelines for the mine and were all covered up by late fall 1989. The soils were glacial tills with fair amounts of stones. The locations of the samples are presented in Table 5.1. In one trench near Austin Brook, the face of the trench revealed a layer of medium sand between two till

layers. The two layers were examined in detail for grain size distribution and stone content and found to be similar. A sample of the sand was also obtained. One of the tills (soil HS-B) was collected from an exploration pit on the property of CNE Stratabound belonging to one Mr. Ken Whaley, located about 20 km from Heath Steele Mines.

TABLE 5.1

LOCATION OF HEATH STEELE SOILS

| Soil | Type | Location | Depth |
|------|--------------|---|---------------|
| HS-A | Glacial Till | Stratmat Area | 0.61 • 1.83 m |
| HS-B | Glacial Till | Captain North Extension (CNE) Stratabound Exploration Pit | 1.22 m |
| HS-C | Glacial Till | Otterbrook Road | 0.40 m |
| HS-D | Sand | Otterbrook Road | 1.52 m |
| HS-E | Glacial Till | Otterbrook Road | 1.52 m |

The samples were obtained by excavating fresh trench faces with a shovel and pick and then put in large plastic bags. The bags were sealed immediately and transported to the laboratory within two weeks for investigation.

5.2 Laboratory Investigation

5.2.1 Index Test8

The soil samples were tested for geotechnical index properties (grain size distribution, Atterberg limits, and specific gravity). These tests were all performed in accordance with standard geotechnical procedures (Sowies, 1986).

The grain size distribution provides information for predicting the water retention and drainage characteristics of a soil. These characteristics control the performance of a saturated soil cover. The grain size also influences gas diffusion coefficients in soils. The Atterberg limits (liquid and plastic) describe the plasticity characteristics of a soil and reflect on mineralogy and water-holding capabilities.

5.2.2 Mineralogy

Mineralogical characterization of a fine-grain soil provides useful information on its geotechnical behaviour. For example, the swelling and shrinking potential of a soil can be predicted from its mineralogy. This information is useful in considering soils for inclusion in cover systems.

The soils obtained from the site were characterized for mineralogy using X-ray diffraction and chemical techniques. X-ray methods involved random powder diffraction and oriented diffraction analysis of <math><2\ \mu\text{m}</math> fraction. The oriented diffraction work included air-dry, wet and potassium-saturated analyses of the <math><2\ \mu\text{m}</math> fraction of the tills. This work was conducted in order to define the clay mineral composition of the tills. Carbonate contents were obtained by gasometric analysis using the Chittick apparatus (Dreimanis, 1962). In addition, glycol retention and total potassium were measured to provide estimates of vermiculite and illite contents.

5.2.3 Compaction

In geotechnical engineering, compaction is performed in order to densify soils through removal of air from the pores. Laboratory compaction tests yield two important parameters: the optimum moisture content (OMC) and maximum dry density (MDD). These parameters are normally specified for placement of soils in field applications. Generally, the shear strength of the soil increases as water is added to the soil and compacted until the OMC is reached. The shear strength begins to decrease beyond the OMC. The hydraulic conductivity (K) varies differently. As the soil is compacted, K decreases through a decrease in the void ratio and continues to decrease, although only slightly, beyond the OMC (Lambe, 1958; Mitchell, 1976; Daniel et al., 1986). Therefore, the hydraulic conductivity of a compacted soil attains its minimum value at a water content higher than the OMC.

Laboratory compaction tests were performed on the -No. 4 mesh fraction of the soils to provide information on the OMC and MDD. This information is needed for specifying field compaction densities if any of the soils are to be used as cover materials. The soils were all compacted using the modified Proctor energy of $42.5\ \text{kJ/m}^3$ with an automatic mechanical compactor. The procedure used is described in (ASTM D 1557-78).

5.2.4 Consolidation Tests

The compressibility of a soil can be determined from the results of a consolidation test. Consolidation is a process by which a soil is **densified** through removal of water from the pores. The densification occurs through a decrease in void ratio which, in most cases, results from the application of an external load. Consolidation can also occur through loss of water due to osmosis (Barbour, 1987).

The most popular consolidation test used in geotechnical engineering is the oedometer test, the principles of which are based on Terzaghi's one-dimensional theory of consolidation. A consolidation test can also provide information on the rate at which water moves through a soil and therefore provides an estimate of the hydraulic conductivity. Since the compressibility of coarse-grained soils is low, oedometer tests are only carried out on fine-grained soils (clays and silts).

The oedometer tests were performed on two till samples initially compacted at water contents of about 2 percent higher than the OMC. After compacting in 100 mm diameter split moulds, the soils were carefully removed and trimmed into **50** mm diameter and 20 mm thick oedometer rings. The rings containing the soils were immediately weighed to provide the mass of the test specimens and then loaded in a front-loading Control **T302** consolidometer using a load increment ratio (LIR) of unity from 0 to 1600 **kPa**. The standard procedure used is described in standard texts on soil mechanics (for example, Taylor, 1948; Bowles, 1986).

5.2.5 Hydraulic Conductivity

The hydraulic conductivity, **K**, of a soil is a measure of the rate at which a liquid flows through it. Unlike the intrinsic permeability, **k**, it takes into account the density and viscosity of the flowing liquid. The two **are** related as follows:

$$K = \frac{\rho g k}{\mu} \quad [12]$$

where **p** is the density, **μ** the viscosity of the liquid and **g** the acceleration due to gravity. Hydraulic **conductivity**, **K**, is usually reported in cm/s or m/s. From Equation [12], using **appropriate** dimensions for **p**, **g**, and **μ**, the corresponding units for the permeability will be **cm²** or **m²**.

Hydraulic conductivity can vary by several orders of magnitude, depending on how it is measured. Several factors, such as gradient, confinement, type of permeating liquid, length of testing time, size of sample and type of equipment influence the magnitude of **K**. The different roles played by these factors have been discussed in detail by several authors (Mitchell and Younger, 1967; Olson and Daniel, 1981; Fernandez and Quigley, 1985; Yanful et al., 1990b).

Laboratory measurements of hydraulic conductivity generally yield values which are 2 to 3 orders of magnitude lower than those measured in the field. This discrepancy has been attributed to the presence of micro and macro fissures or cracks in field soils. These cracks are normally absent in laboratory specimens. Consequently, researchers and practicing engineers consider field measured values of K more reliable than laboratory values. However, field tests tend to be more complicated and therefore costly. In fine-grained soils, in particular, field tests can take a long time because of the slow rate at which liquids such as water move through these soils. In addition, the use of certain liquids (for example, **organics**) in field tests may not be desirable because of the serious environmental implications. Well-controlled laboratory tests offer the best methods for obtaining K values associated with such liquids.

A laboratory K test was performed to measure the rate at which water will infiltrate a cover constructed from any of the tills. Although the K obtained from the test is only a rough estimate of what a cover constructed from the compacted till will attain in the field, it nevertheless provides important data for calculating potential water flux through the cover. One till sample was compacted at two percent wet of the optimum water content in a 102 mm diameter split mould using the modified Proctor energy. The specimen was carefully trimmed on the top and sealed with rubber membranes and then assembled in a triaxial cell for testing.

A photograph of the Geostore Brainard Kilman triaxial panel and cell used in the test is presented in Figure 5.1. The sample was initially consolidated to a stress of 24 kPa and then permeated with deionized distilled water at a gradient of 18.0 for 70 days which corresponded to only 0.58 pore volume.. The gradient was then increased to 60 and the sample permeated to 1.25 pore volumes, or for 42 days. A pore volume is the total volume of pore spaces in the sample and is calculated as a product of q/VT , the ratio of the flow rate (q) to the total sample **volume** (VT), and the time of flow, t . Testing a sample to at least one pore volume ensures that all the resident pore water has been displaced. by the permeating liquid. This makes it possible to assess the effects, if any, of the permeating liquid on the hydraulic conductivity of the soil.

52.6 Freezethaw Tests

Several authors (**Yong** et al., 1984; Konrad; 1989) have shown that the physical and mechanical properties of fine-grained soils can change when subjected to freezing and thawing **cycles**. Of particular importance to engineered soil cover technology is the pore size distribution and the swelling and shrinking potential of the soil. For instance, the development of fissures or cracks in a soil cover after one or several freeze-thaw cycles will not be desirable since such a cover will no longer be effective.

The results of the grain size tests indicated that the tills had large proportions of silt-sized materials which are generally regarded as prime candidates for frost heaving. Normally, if other soils with less silt-sized components were available, they would have been selected. The tills constitute the only fine-grained soils located in the vicinity of Heath Steele Mines. Therefore, the only altefnative was to assess the extent of any potential frost heaving and, if possible, design against it.

5.2.7 Hydraulic Characteristics of a Cover

The application of saturated soil covers on sulphide tailings appears to be one of the best ways of reducing acid generation. A saturated soil cover is one whose pores are all nearly filled with water so that the rate of movement of gaseous oxygen by diffusion through the few air-filled pores is very low (see Section 3.2.1). Unfortunately, however, any saturated soil cover placed on tailings will drain during dry climatic conditions unless it is specially designed. One way of reducing drainage is to design the cover to incorporate an underlying coarser-grained soil material. Figure 5.2 shows the moisture drainage curves for a fine-grained soil (silt) and a coarse-grained soil (sand). None of these soils will drain until the pressure head becomes more negative than the respective air-entry pressure, U_a . This air entry pressure is the pressure head required to overcome the capillary forces that can be exerted by the largest pore in the medium (Nicholson et al., 1989). Once the pressure head falls below U_a , the soil will drain until residual saturation (ϕ_{res}) is attained. It is clear from Figure 5.2 that the sand will reach ϕ_{res} at a much lower negative pressure head than the silt.

The principle of maintaining a saturated fine-grained soil layer above a coarse-grained layer which has drained to residual saturation was investigated for a possible application to a cover design for the waste rock piles at Heath Steele mines. The laboratory methodology and equipment used were adapted from those developed under a separate project involving Noranda **Technology Centre** (NTC) and the University of Waterloo.

A laboratory column evaluation was conducted at NTC to define the water content and pressure head developed in a fine-grained soil and an underlying coarse-grained layer. The soils were initially saturated and then allowed to drain, keeping the water table at a distance of about 50 cm below the the column. This was designed to simulate the commonest situations in waste rock piles where the water table is at substantially great depths. This case represent unsaturated conditions in the cover system; the suction developed was therefore measured with a system of specially designed tensionmeters and pressure transducers. Soil water content was measured in place by time domain reflectometry using a Tektronix 15028 cable tester and 3 mm diameter stainless steel rods inserted into the soil. Figure 5.3 is a schematic representation of the column and the monitoring units.

5.2.8 Oxygen Diffusion Measurements

In fine-grained geologic materials such a clay or till cover, oxygen is transported by means of gas diffusion. An accurate prediction of oxygen fluxes across such a cover system on a waste rock pile requires a precise knowledge of the diffusion coefficient of oxygen in the soil. The diffusion coefficient can be measured in the laboratory. There are several empirical relationships which relate the diffusion coefficient to the gas-filled porosity. An example of such a relationship is given by Troeh et al. (1982) is:

$$D_e/D_o = [(S-u)/(1-u)]^V \quad [13]$$

in which D_e is the effective gas diffusion coefficient, D_o the diffusion coefficient of gas in air, S the gas-filled porosity (V_{gas}/V_{total}) and u and v are dimensionless parameters that are determined experimentally for a specific medium.

In the present investigation, a transient diffusion method was used for measuring the diffusion coefficient of oxygen. The technique essentially involved allowing a constant source of gaseous oxygen to diffuse freely through a column packed with soil to a known density and water content. The oxygen concentration in the soil is directly measured in ports located along the column with a Teledyne 340 BS portable oxygen analyzer. The oxygen concentration at the bottom of the column can be measured on a trace oxygen analyzer in a stream of nitrogen gas. A schematic of the experimental set up is illustrated in **Figure 5.4**.

The effective diffusion coefficient, D_e , is obtained in two ways: (1) matching the experimental concentration profile with a theoretical profile, and (2) equating the theoretical oxygen flux through the column to the observed flux and back-calculating the diffusion coefficient. Both of these methods are currently being used at NTC and results will be reported later when they become available.

5.3 Results of Laboratory Investigation

5.3.1 Mineralogy

Mineralogical analyses of the Heath Steele tills indicated that they are composed of abundant quartz, feldspar(both orthoclase and plagioclase), illite, chlorite, and probably a trace of carbonate. A typical random X-ray powder diffractogram is presented in Figure 5.5 for soil HS-C. Although a carbonate content of about 3 percent was obtained from gasometric analysis, this amount was too small to yield an X-ray peak on the diffractogram.

The distribution of exchangeable cations in soil HS-C in milliequivalents per 100 gram of dry soil was found to be Na^+ (0.28), K^+ (2.37), Ca^{++} (1.44), and Mg^{++} (2.21). This distribution gives a rather low cation exchange capacity of 8.36 meq/100 g, which probably suggests that the clay minerals are either present only in a very small amount or are inactive.

Figure 5.6 shows the natural and K^+ -saturated oriented X-ray diffractograms obtained on the $< 2 \mu m$ fraction of soil HS-C. The traces indicate the presence of abundant illite. The strong peaks at 0.72 and 1.45 nm on Figure 5.6a suggest chlorite; however, heat treatment did not produce a strong 1.4 nm in confirmation. As shown, K^+ -saturation seemed to greatly modify the traces without increasing the size of the 1.0 nm illite peak. This suggests the 1.42 and 0.72 nm peaks are produced by a smectite that actually expanded on contact with KCl solutions to produce the rather ragged traces on Figure 5.6b.

5.3.2 Geotechnique

Index Properties

Figures 5.7 to 5.10 present the grain size distributions of the tills, indicating that they are mostly sandy silts with varying clay size fractions (5 to 14 percent). Till samples HS-B and HS-E have the highest amounts of clay-size fractions of 14 and 11 percent, respectively. Sample HS-B also has the highest amount of **-200 mesh (75 μm)** size fraction (approximately 52 percent). The **amounts of silt-size** materials present in **Samples HS-A, HS-B, HS-C and HS-E** are 33, 36, 46, and 37 percent respectively. These high contents have important implications for their potential use as covers in a temperature. climate like New Brunswick which experiences long periods of frost during the winter months. The grain size distribution of the sand, HS-D, is presented in Figure 5.11. Based on the MIT soil classification system (Taylor, **1948**), soil HS-D is a medium to coarse sand with an appreciable fine gravel content. The potential benefits of including such a sandy material in a composite cover design are fully discussed in Section 5.3.3. These nearly linear grain size curves are similar to those obtained on a few samples from the general Heath Steele mine area by Gemtec consultants of Fredricton, N.B. (G.R.E. Dickinson, 1989, personal communication).

Atterberg limits (liquid and plastic) obtained for the tills are presented in Table 5.2, along with a summary of the grain size data. The values of the limits confirm that soils HS-B and HS-E have the highest clay content. The grain size data and the Atterberg limits indicate that the tills have low activities. As shown in Table 5.2, the specific gravities of the tills range from 2.69 to 2.73.

TABLE 5.2

INDEX PROPERTIES OF CANDIDATE HEATH STEELE SOILS

| Soil | HS-A | HS-B | HS-C | HS-D | HS-E |
|--|----------|---------------------------|----------------------------|---------------------|---------------------|
| <2 μm (%) | 6 | 14 | 8 | 0 | 11 |
| <75 μm (%) | 42 | 52 | 37 | 4 | 42 |
| Liquid limit (%) | 24.5 | 27.1 | 30.2 | Nonplastic | 28.9 |
| Plastic limit (%) | 28.2 | 17.2 | 17.5 | Nonplastic | 18.6 |
| Specific gravity | 2.83 | 2.73 | 2.72 | 2.68 | 27.1 |
| Location | Stratmat | CNE Stratabound | Otterbrook Stn 2 | Otterbrook Stn 2 | Otterbrook Stn 3 |

Compaction Parameters

Modified **Proctor** compaction curves for the tills are presented in Figs 5.12 and 5.13. Optimum water contents range from 9 to 11 percent and maximum dry densities from 1.91 to 2.10 Mg/m^3 . Standard Proctor compaction dry densities and optimum water contents obtained by Gemtec Consultants for similar tills from the area range from 1.80 to 1.82 Mg/m^3 and 15 to 17 percent, respectively. The higher densities and lower water contents obtained in the present investigation are due to the greater compaction effort used and are similar to those reported in the literature for inorganic clayey sandy silts (Craig, 1974; Holtz and Kovacs, 1981). The compaction parameters for soil **HS-D** (maximum dry density of 2200 kg/m^3 and optimum water content of 8 percent) as well as the shape of the curve (Fig 5.14) are characteristic of medium to coarse sands.

As an illustration of the utility of the compaction data, the curve for soil **HS-B** is replotted in Figure 5.15. with lines for three different degrees of saturation. The plot suggests that this till could be compacted at 2 percent wet of the optimum water content to yield approximately 95 percent of the maximum modified Proctor density. The resulting degree of water saturation will be close to 95 percent. The diffusion coefficient of gaseous oxygen at this degree of saturation will be **very** low. The hydraulic **conductivity** of the till compacted wet of optimum will also be very low. The low hydraulic conductivity will result in low amounts of water infiltration. This suggests that if any of the tills could be properly and efficiently compacted and placed as a cover in the field, it could function as an effective diffusional and water barrier. Several other factors have to be considered in an actual design and field placement. For example, the effects of freeze-thaw on the soil pore structure and hydraulic conductivity should be fully evaluated and incorporated into any design and construction protocol. These effects were assessed for soils **HS-C** and **HS-E** and the results are discussed below.

Freeze-thaw Behaviour

Freeze-thaw evaluation of the tills samples showed a frost heave of 15 to 20 mm on 100 mm after only 2 cycles. Scanning electron photomicrographs of the samples taken at the end of the freeze-thaw cycles revealed the formation of ice lenses in the samples. The hydraulic conductivity, **K**, of the soils, however, did not change significantly after 8 freeze-thaw cycles. The **K** for soil **HS-C** increased only slightly from 2.9 to 3.2 x 10^{-7} cm/s, and that of soil **HS-E** from 2.1 to 2.7 x 10^{-7} cm/s. It appears the soils heaved upon freezing and thawing without a significant change in the volume of void spaces. Water intake into soil **HS-C** was about 5 mL at the end of the first freezing cycle, compared to about 16 mL at the end of the second freezing cycle. Soil **HS-E**, on the other hand, showed an increase of only about 2 mLs in water intake at the end of the second cycle. The results of the freeze-thaw tests are presented in the Appendix.

The water intake characteristics of the soils noted above support the observation of Konrad (1989) that soil samples compacted at a water content of about 2 percent higher than optimum, unless saturated by a back pressure technique, will absorb water during the first freezing cycle to attain full saturation. This may explain why, in the soils under investigation, the total frost heave during the first freezing cycle was less than the total frost heave at the end of the second

second cycle. A similar behaviour can be expected in an actual field cover application since these soils will not be fully saturated. It should also be mentioned that freeze-thaw effects vary with soil type. Chamberlain and Gow (1979) found that soil with high plasticity may develop shrinkage cracks during freezing. The development of these cracks will result in changes in internal volume. The amount of shrinkage is a function of the water content and degree of saturation (Penner, 1969). Less plastic soils, such as clayey silts, do not develop shrinkage cracks upon freezing (Konrad, 1989). The soils investigated in the present study are all sandy silts of low **plasticity** (with clay-sized fraction of only 5 to 14 percent) and are not likely to crack upon freezing.

Consolidation Characteristics

The results of oedometer consolidation tests are presented in Tables 5.3 and 5.4 for two identical samples HS-C1 and HS-C2. The coefficient of consolidation, c_v , at low average stresses (6 to 38 kPa) range from $3.5 \times 10^{-3} \text{ cm}^2/\text{s}$ to $7.9 \times 10^{-3} \text{ cm}^2/\text{s}$, with the exception of the value for HS-C1 at 6 kPa. The tests were performed using a load increment ratio equal to one. Each applied load was maintained until most of the primary consolidation was deemed to have occurred.

Figures 5.16 and 5.17 show plots of void ratio versus log pressure curves obtained from the tests. The curves indicate essentially linear virgin behaviour between 100 and 1600 kPa. An average compression index, C_c , of about 0.13 is estimated from the virgin compression. The preconsolidation pressure, σ_c' , of this compacted till estimated from a Casagrande construction technique is about 80 kPa.

The variations of the compression index and the **coefficient** of consolidation with applied stress are shown in Figure 5.18. The compression index, C_c , increases with stress until the preconsolidation pressure is substantially exceeded and then begins to fall slightly. This suggests that the soil may have undergone some structural or fabric changes at these high stresses. The wavy shape of the c_v versus **applied** stress curve may be attributed to quasi-preconsolidation. Each applied load was maintained until there was no change in dial gauge readings or sample compression. The elapsed time for this phenomenon to occur was different for each applied load. Therefore, it was possible that some secondary compression occurred, resulting in a quasi-preconsolidation pressure that is larger than the maximum previous consolidation pressure (Leonards and Ramiah, 1959; Das, 1983).

Hydraulic Conductivity

The results of the hydraulic conductivity, K , tests obtained on soil HS-C are summarized in Figures 5.19 and 5.20. and then also in Table 5.4. The K value decreased only slightly from 2.0 to $1.7 \times 10^{-8} \text{ cm/s}$ when the hydraulic gradient was increased from 18 to 60. This decrease is due to a decrease in void ratio resulting from increased effective stress at the outflow end of the sample (Table 5.4). An average effective stress of 24 kPa was applied to the sample at the lower hydraulic gradient of 18. This stress will correspond to that due to the weight of about

80 cm thick capillary barrier and vegetated top soil placed above the compacted till. Thus, a hydraulic conductivity of 2.0×10^{-8} cm/s **can** be used for preliminary flux calculations for a **composite** cover on the waste rock piles at the **Heath Steele** mines site.

TABLE 5.3

CONSOLIDATION SPREADSHEET
HEATH STEELE - COVERS #1

| APPLIED STRESS (KPA) | FINAL DIAL (mm) | DIAL CHANGE (mm) | SPEC. HEIGHT (mm) | MACH. CORR. (mm) | CORR. SPEC. HEIGHT (mm) | AVG. SPEC. HEIGHT (mm) | VOID HEIGHT (mm) | VOID RATIO | FITTING TIME (sec) | | COEF. OF CONSOL. Cv (cm ² /s) | AVERAGE PRESSURE (kPa) | ds (mm) | | | PRIMARY CONSOL. RATIO | CHANGE VOID RATIO | COMPRES. INDEX Cc | COEFFIC. COMPRES. Hv (kPa-1) | AVG. VOID RATIO | PERMEABILITY (cm/s) | | |
|----------------------|-----------------|------------------|-------------------|------------------|-------------------------|------------------------|------------------|------------|--------------------|----------|--|------------------------|-----------|----------|----------|-----------------------|-------------------|-------------------|------------------------------|-----------------|---------------------|--------|--------|
| | | | | | | | | | t90 | t50 | | | SORT TIME | LOG TIME | d90 (mm) | | | | | | d100 (mm) | (cm/s) | (cm/s) |
| 0.00 | 12.000 | 0.000 | 20.000 | 0.000 | 20.000 | | 6.3127 | 0.461 | | | | | | | | | | | | | | | |
| 12.50 | 11.836 | 0.164 | 19.836 | 0.010 | 19.846 | 19.923 | 6.1587 | 0.450 | 67.20 | 0.012522 | 6.25 | 11.89 | 11.87 | 0.135501 | 0.011251 | 0.037380 | 0.002602 | 0.455583 | 3.2E-06 | | | | |
| 25.00 | 11.723 | 0.113 | 19.723 | 0.009 | 19.732 | 19.789 | 6.0447 | 0.442 | 105.10 | 0.007899 | 18.75 | 11.78 | 11.76 | 0.127827 | 0.008329 | 0.027671 | 0.000642 | 0.445793 | 5.0E-07 | | | | |
| 50.00 | 11.545 | 0.178 | 19.545 | 0.022 | 19.567 | 19.650 | 5.8797 | 0.430 | 193.10 | 0.004239 | 37.50 | 11.62 | 11.59 | 0.205993 | 0.012055 | 0.040050 | 0.000465 | 0.435601 | 1.9E-07 | | | | |
| 100.00 | 11.219 | 0.326 | 19.219 | 0.033 | 19.252 | 19.410 | 5.5647 | 0.407 | 90.49 | 0.008826 | 75.00 | 11.39 | 11.28 | 0.357873 | 0.023014 | 0.076459 | 0.000443 | 0.418066 | 3.8E-07 | | | | |
| 200.00 | 10.707 | 0.512 | 18.707 | 0.041 | 18.748 | 19.000 | 5.0607 | 0.370 | 128.20 | 0.005970 | 150.00 | 10.90 | 10.78 | 0.271267 | 0.036822 | 0.122334 | 0.000355 | 0.388148 | 2.1E-07 | | | | |
| 400.00 | 10.082 | 0.625 | 18.082 | 0.048 | 18.130 | 18.439 | 4.4427 | 0.325 | 126.02 | 0.005720 | 300.00 | 10.29 | 10.16 | 0.231111 | 0.045151 | 0.150004 | 0.000218 | 0.347161 | 1.2E-07 | | | | |
| 800.00 | 9.537 | 0.545 | 17.537 | 0.046 | 17.583 | 17.857 | 3.8957 | 0.285 | 276.95 | 0.002441 | 600.00 | 9.75 | 9.59 | 0.326198 | 0.039964 | 0.132771 | 0.000096 | 0.304604 | 2.3E-08 | | | | |
| 1600.00 | 8.993 | 0.544 | 16.993 | 0.066 | 17.059 | 17.321 | 3.3717 | 0.246 | 196.00 | 0.003245 | 1200.00 | 9.26 | 9.06 | 0.418709 | 0.038284 | 0.127188 | 0.000046 | 0.265480 | 1.5E-08 | | | | |
| 800.00 | 9.035 | -0.042 | 17.035 | 0.011 | 17.044 | 17.053 | 3.3587 | 0.245 | | | | | | | | | | | | | | | |
| 400.00 | 9.104 | -0.069 | 17.104 | 0.025 | 17.129 | 17.088 | 3.4417 | 0.251 | | | | | | | | | | | | | | | |
| 200.00 | 9.176 | -0.072 | 17.176 | 0.041 | 17.217 | 17.173 | 3.5297 | 0.258 | | | | | | | | | | | | | | | |
| 50.00 | 9.324 | -0.148 | 17.324 | 0.088 | 17.412 | 17.315 | 3.7247 | 0.272 | | | | | | | | | | | | | | | |
| 12.50 | 9.461 | -0.137 | 17.461 | 0.051 | 17.512 | 17.462 | 3.8247 | 0.279 | | | | | | | | | | | | | | | |

c:\heathste\conscov1.wk3

TABLE 5.4

CONSOLIDATION SPREADSHEET
HEATH STEELE - COVERS #2

| APPLIED STRESS (kPa) | FINAL DIAL (mm) | DIAL CHANGE (mm) | SPEC. HEIGHT (mm) | MACH. CORR. (mm) | CORR. SPEC. HEIGHT (mm) | AVG. SPEC. HEIGHT (mm) | VOID HEIGHT (mm) | VOID RATIO | FITTING TIME (sec) | | COEF. OF CONSOL. Cv (cm ² /s) | AVERAGE PRESSURE (kPa) | ds (mm) | | | PRIMARY CONSOL. RATIO | CHANGE VOID RATIO | COMPRES. INDEX Cc | COEFFIC. COMPRES. Hv (kPa-1) | AVG. VOID RATIO | PERMEABILITY (cm/s) | | |
|----------------------|-----------------|------------------|-------------------|------------------|-------------------------|------------------------|------------------|------------|--------------------|----------|--|------------------------|-----------|----------|----------|-----------------------|-------------------|-------------------|------------------------------|-----------------|---------------------|--------|--------|
| | | | | | | | | | t90 | t50 | | | SORT TIME | LOG TIME | d90 (mm) | | | | | | d100 (mm) | (cm/s) | (cm/s) |
| 0.00 | 11.000 | 0.000 | 20.000 | 0.000 | 20.000 | | 6.370 | 0.467 | | | | | | | | | | | | | | | |
| 12.50 | 10.943 | 0.057 | 19.943 | 0.011 | 19.954 | 19.977 | 6.324 | 0.464 | 256.800 | 0.003295 | 6.25 | 10.971 | 10.956 | 0.292398 | 0.003375 | 0.011212 | 0.000780 | 0.465664 | 2.5E-07 | | | | |
| 25.00 | 10.895 | 0.048 | 19.895 | 0.009 | 19.904 | 19.929 | 6.274 | 0.460 | 129.800 | 0.006487 | 18.75 | 10.927 | 10.920 | 0.162037 | 0.003668 | 0.012187 | 0.000283 | 0.462142 | 1.8E-07 | | | | |
| 50.00 | 10.826 | 0.069 | 19.826 | 0.016 | 19.842 | 19.873 | 6.212 | 0.456 | 240.000 | 0.003489 | 37.50 | 10.868 | 10.854 | 0.225443 | 0.004549 | 0.015112 | 0.000175 | 0.458034 | 6.0E-08 | | | | |
| 100.00 | 10.580 | 0.246 | 19.580 | 0.027 | 19.607 | 19.725 | 5.977 | 0.439 | 178.400 | 0.004623 | 75.00 | 10.785 | 10.638 | 0.663957 | 0.017241 | 0.057280 | 0.000332 | 0.447139 | 1.5E-07 | | | | |
| 200.00 | 10.000 | 0.580 | 19.000 | 0.041 | 19.041 | 19.324 | 5.411 | 0.397 | 126.000 | 0.006283 | 150.00 | 10.200 | 10.084 | 0.222222 | 0.041526 | 0.137960 | 0.000400 | 0.417755 | 2.5E-07 | | | | |
| 400.00 | 9.339 | 0.661 | 18.339 | 0.057 | 18.396 | 18.719 | 4.764 | 0.350 | 233.100 | 0.003187 | 300.00 | 9.556 | 9.417 | 0.233653 | 0.047322 | 0.157216 | 0.000228 | 0.373331 | 7.1E-08 | | | | |
| 800.00 | 8.799 | 0.540 | 17.799 | 0.077 | 17.876 | 18.136 | 4.246 | 0.312 | 264.400 | 0.002637 | 600.00 | 9.100 | 8.870 | 0.473251 | 0.038151 | 0.126748 | 0.000092 | 0.330594 | 2.4E-08 | | | | |
| 1600.00 | 8.240 | 0.559 | 17.240 | 0.086 | 17.326 | 17.601 | 3.696 | 0.271 | 290.100 | 0.002264 | 1200.00 | 8.865 | 8.335 | 1.053468 | 0.040352 | 0.134060 | 0.000049 | 0.291343 | 1.1E-08 | | | | |
| 800.00 | 8.276 | -0.036 | 17.276 | 0.020 | 17.296 | 17.311 | 3.666 | 0.269 | | | | | | | | | | | | | | | |
| 400.00 | 8.327 | -0.051 | 17.327 | 0.031 | 17.358 | 17.327 | 3.728 | 0.274 | | | | | | | | | | | | | | | |
| 200.00 | 8.394 | -0.067 | 17.394 | 0.037 | 17.431 | 17.395 | 3.801 | 0.279 | | | | | | | | | | | | | | | |
| 50.00 | 8.538 | -0.144 | 17.538 | 0.058 | 17.596 | 17.513 | 3.966 | 0.291 | | | | | | | | | | | | | | | |
| 12.50 | 8.676 | -0.138 | 17.676 | 0.028 | 17.704 | 17.650 | 4.074 | 0.299 | | | | | | | | | | | | | | | |

c:\heathste\conscov2.wk3

As shown in Fig 5.26, the outflow hydraulic conductivity at a gradient of 60 decreased initially and then increased slowly until the inflow and outflow conductivities equalized at steady state. Fluctuations in laboratory temperature recorded during the tests, presented in Fig 5.21, do not show the same trends as the variations in K . Thus temperature changes cannot account for the observed variations in K . The decrease in sample volume observed in the tests is plotted in Figure 52.2. The plot shows a substantial decrease in sample volume after 1000 minutes which appears to correspond to the decrease in outflow K .

TABLE 5.5

RESULTS OF HYDRAULIC CONDUCTIVITY TESTS
FOR COMPACTED HEATH STEELE TILL. HS-C

| | <u>Hydraulic Gradient</u> | |
|---|---------------------------|----------------------|
| | 18 | 60 |
| Cell Pressure | 275.6 | 275.6 |
| Inflow Pressure | 261.8 | 261.8 |
| Outflow Pressure | 241.1 | 192.9 |
| Effective Stress (Inflow) | 13.8 | 13.8 |
| Effective Stress (Outflow) | 34.5 | 82.7 |
| Pore Volumes | 0.58 | 1.25 |
| Final Hydraulic Conductivity, K , (cm/s) | 2.0×10^{-8} | 1.7×10^{-8} |

- Notes:
- (1) All pressures and stresses in **kPa**
 - (2) Dimensions of compacted test specimen = 102 mm diameter and
= 116 mm length
 - (3) Initial water content = 13.1%
Initial bulk density = 1.96 Mg/m^3
 - (4) **Permeant** = distilled water

5.3.3 Prediction of Cover Performance

The waste rock piles at the Heath Steele Mines site have already oxidized and presumably contain large **volumes** of stored acidity. There is still a substantial amount of unoxidized sulphide minerals left in the pile, as shown in the mineralogical data (Nolan Davis, 1990). Therefore, the two key aspects of an effective cover system is the control or mitigation of water infiltration and oxygen ingress into the piles. High infiltration rates would flush out large volumes of stored acid, resulting in high treatment costs. Residual sulphide minerals left in the pile will oxidize upon contact with oxygen and water.

The design of a saturated cover requires development of methodologies for predicting its long-term hydraulic and diffusive behaviour. Figure 5.23 presents pressure and moisture profiles observed in the two-layer column described in Figure 5.2.7. The interface between the fine and coarse layers is represented by I in the figures. The coarse layer drains within 7 days to residual saturation at a suction of -50 cm. At residual saturation, the coarse layer has minimum hydraulic conductivity and is not able to transmit any more suction. The fine layer does not drain and after 14 days, the pressure profile is observed to be nearly parallel to the static equilibrium line. This means that the hydraulic gradient across the fine layer is essentially zero so that there can be no flow of water from the fine layer to the underlying coarse layer. The moisture content profile confirms these observations and show further that the fine layer remains saturated at a moisture content of nearly 32 percent. The slight decrease in the moisture content at the top of **fine** layer can be attributed to loss of moisture by evaporation.

The column observations described above confirm the results of transient state numerical modelling conducted by Akindunni et al., (1990). These authors showed that a fine layer overlying a coarse layer will remain saturated for 50 days without the need for infiltration. These results are encouraging and suggest that an effective composite soil cover could be designed for the Heath Steele waste rock piles. This system, however, needs further assessment prior to field application. For example, the long-term drainage characteristics of a cover on a waste pile with a deep water table should be assessed with full consideration given to climatic conditions at the site. This assessment may be carried out by means of computer modelling using a number of models, such as HELP (Schroeder et al., **1984**), and a coupled diffusion-flow model developed by Collin (1987) for the Swedish Environmental Protection Board. Another important consideration would be the ability to predict the effect of heat generated in the pile on the overlying cover.

A second **aspect** of accurate prediction of cover performance is estimating diffusive fluxes across soil covers. A special column was developed to demonstrate the effectiveness of the two-layer system described above, in terms of potential reductions in oxygen fluxes. The essential features of the column are presented in Figure 5.24, In a laboratory evaluation, a composite system consisting of 10 cm of Heath Steele soil HS-C overlying 30 cm of medium sand HS-D was initially saturated and allowed to drain. Moisture content profiles observed in the column at different times are presented in Figure 5.25. These results show transient moisture fluxes in the column as the sand layer drains towards residual saturation. It is

anticipated that the fine **layer** will remain saturated and therefore substantially reduce oxygen flux in the column. Flux measurements in progress at NTC will provide data for back-calculating the diffusion coefficients of soil **HS-C** at **full** saturation.

6. COVER DESIGN SCENARIOS FOR HEATH STEELE WASTE ROCK PILES

6.1 Theoretical Concepts

An initially saturated single soil layer placed as cover on waste rock pile will ultimately desaturate by drainage and moisture losses due to evaporation. The diffusion coefficient of oxygen for such a system, although initially low, will increase with time resulting in large oxygen fluxes into the pile. The cover can be compacted during placement to have a low hydraulic conductivity. However, as it desaturates, it could dry out and develop cracks, especially if it has high clay content. Moisture fluxes resulting from infiltration across this cover will be high. Another complication is the upward flow **of** heat generated in waste rock pile into the overlying cover.

Table 6.1 presents the drainage characteristics of the Heath Steele soils under investigation. The tests were conducted by the Department of Land Resource Science, University of Guelph. The data suggest that residual saturation occurs at volumetric water contents of about 15 and 6 percent for till HS-E and sand HS-D, respectively. The gap in the results for till **HS-B** makes it difficult to estimate its water content at residual saturation. The moisture drainage curve for sand HS-D was also obtained by separate measurements at the Noranda Technology **Centre**. Figure 6.1 presents the **curve** indicating that the volumetric water content at full saturation (Or the porosity) is 0.33 while residual saturation occurs at about 0.11. These results are similar to those reported in the literature for medium to coarse sands **Gillham** (1984). It appears that both the residual and saturation water contents have been underestimated in the Guelph work.

TABLE
WATER CONTENT VS. PRESSURE HEAD.

| Pressure Head (m) | Volumetric Water Content (%) | | |
|-------------------|------------------------------|-----------|-----------|
| | Till HS-B | Sand HS-D | Till HS-E |
| 0.00 | 29.72 | 26.02 | 29.11 |
| -0.20 | 23.50 | 6.57 | 19.36 |
| -0.71 | 20.46 | 6.78 | 17.11 |
| -1.02 | | 6.68 | 16.65 |
| -2.04 | | 6.42 | 15.52 |
| -3.06 | | 5.92 | 15.02 |
| -4.08 | | 5.87 | 14.67 |
| -5.10 | | 5.71 | 14.43 |
| -6.12 | | 5.55 | 14.44 |
| -7.14 | | 5.46 | 13.95 |
| -8.15 | | 5.44 | 13.68 |
| -9.17 | | 5.38 | 13.54 |
| -10.19 | | 5.32 | 13.35 |
| -15.29 | | 5.19 | 12.88 |
| -17.04 | 13.66 | 5.01 | 12.70 |
| -20.39 | 13.64 | 4.82 | 12.60 |

Table 6.2 shows capillary heads for the soils, calculated using the correlation between the head, h_e and D_{10} , the particle sizes below which 10 percent of the material is finer:

$$h_e = -0.01 (-21.9 - 85.12 \log (D_{10})) \quad [14]$$

In Equation [14] h_e is in meters and D_{10} in millimeters. The above correlation is based on data from **Lambe** and Whitman (1969). The capillary head, h_e is the height above the water table at which air entry can occur by gravity drainage. The D_{10} is the particle size corresponding to the 10 percentile point on a grain size distribution **curve** (see Figures 5.7 to 5.11).

The influence of the drainage characteristics, saturation and grain size in the selection of any of the soils for various cover design scenarios is discussed.

TABLE 6.2
CALCULATED CAPILLARY HEADS FOR
HEATH STEELE SOILS

| Soil | Type & Gradation | D_{10} (mm) | Capillary head h_e (m) |
|------|-----------------------|---------------|--------------------------|
| HS-A | Sandy, siltfill | 0.0035 | -1.a7 |
| HS-B | Sandy, siltfill | 0.0036 | -1.86 |
| HS-C | Sandy, siltfill | 0.0026 | -1.98 |
| HS-E | Sandy, siltfill | 0.001 | -2.14 |
| HS-D | Medium to coarse sand | 0.2 | -0.38 |

Note: Capillary fringe, h_e was estimated from:

$$h_e = -0.01 (-21.9 - 65.12 \log (D_{10}))$$

The above correlation is based on data from Lamb and Whitman (1969).

6.2 Single Cover

In order to calculate oxygen flux across a single cover, the solution to the transient diffusion equation or Fick's second law (described by Equation [7.1], section 3.2.1), given by Crank (1975) is used. For a cover on a sulphide-rich waste rock pile, the following boundary conditions are applicable:

- a) Constant source oxygen concentration, C_0 .
- b) Initial oxygen concentration is zero throughout the cover of thickness L .
- c) Oxygen concentration at the base of the cover is assumed to be Zero at all time to simulate rapid oxygen consumption by sulphide minerals in the waste rock. In other words, the oxygen is consumed as fast as it is transported through the cover.

The solution for the flux at time t , using these boundary conditions is given by Crank (1975) as follows:

$$F(t) = \left(D \frac{\partial C}{\partial x} \right)_{x=L} = 2C_0 \sum_{n=0}^{\infty} \left(\frac{D}{\pi t} \right)^{1/2} \exp \left[-\frac{(2n+1)^2 L^2}{4Dt} \right] \quad [15]$$

The solution for the series is implemented in a computer program developed by the University of Waterloo under a subcontract from Noranda (Gillham and Nicholson, 1990).

Figure 6.2 presents oxygen fluxes computed using the program. Two important conclusions can be drawn from the plots: (i) the most beneficial cover will be the one with a very low diffusion coefficient ($< 1.0 \times 10^{-8} \text{ m}^2/\text{s}$), (ii) for covers with low diffusion coefficients ($< 2.5 \times 10^{-7} \text{ m}^2/\text{s}$), only a thickness of 1m is required to provide the maximum reductions in oxygen fluxes, (iii) a thickness of about 2m is required for a single cover with a higher diffusion coefficient (about $1.0 \times 10^{-6} \text{ m}^2/\text{s}$) to provide maximum benefits.

The time rate of diffusion in a single cover is illustrated in Figure 6.3. For relatively effective higher diffusion coefficients (between 2.5×10^{-7} and $1.0 \times 10^{-6} \text{ m}^2/\text{s}$), steady state is attained rather quickly within 10 to 25 days. When the diffusion coefficient is low (about $1.0 \times 10^{-8} \text{ m}^2/\text{s}$), it is shown that the time required to attain steady state is much longer, reaching nearly 2 years.

The diffusion coefficient of $2.5 \times 10^{-7} \text{ m}^2/\text{s}$ used in the above discussions was estimated for till **HS-C** using the empirical equation proposed by Troeh et al (1982) (see Equation [13]). Values of the empirical coefficients, u and v used were 0.05 and 1.10, respectively. This diffusion coefficient corresponds to only 70 percent degree of saturation. For the till compacted at 2 percent wet of optimum, Figure 5.15 suggests that a much higher degree of saturation (about 95 percent) would be attained. In this case, the lower diffusion coefficient of $1.0 \times 10^{-8} \text{ m}^2/\text{s}$ would apply. However if this till is placed as a single cover, drainage and subsequent drying will occur resulting in lower degrees of saturation and hence higher diffusion coefficients, probably, of the order of $1.0 \times 10^{-6} \text{ m}^2/\text{s}$. An intermediate coefficient of $5 \times 10^{-7} \text{ m}^2/\text{s}$,

representing moderate degrees of saturation is therefore used for calculation of the depth of oxygen penetration in a 1 m thick single cover. This depth is then compared to those attained in two and three-layer composite covers.

6.3 Composite Cover

6.3.1 Diffusion model

The flux of oxygen through a multi-layered cover system was calculated using a steady state diffusion model. The flux is a direct indication of the potential maximum rate of oxidation of sulphide minerals that may occur below a cover. For practical purposes, it is assumed that the time-dependent nature of diffusion in this composite cover system can be ignored. The mass flux F for steady state diffusion is described mathematically by the equation:

$$F = -D \frac{\partial C}{\partial x} \quad [16]$$

For a multi-layered system, the flux can be equated at the interface for any two adjacent layers with the resulting general equation:

$$\left(\frac{D_i}{L_i}\right) C_{i+1} + \left(\frac{D_{i+1}}{L_{i+1}} - \frac{D_i}{L_i}\right) C_i + \left(\frac{D_{i+1}}{L_{i+1}}\right) C_{i+1} = 0 \quad [17]$$

where i represents the i th layer. Evaluating the fluxes in this manner results in a system of equations (equal to the number of layers minus one) which can then be solved simultaneously.

It is assumed that a constant source oxygen concentration exists at the surface of the cover, equal to atmospheric value, and that the concentration at the base of the deepest layer is zero. The solution of the resulting system of independent equations, using a decomposition matrix routine, is implemented in the University of Waterloo model described in Section 6.1 This model was adopted for the conceptual design scenarios presented in the next sections.

6.3.2 Two-layer System

The P-layer composite cover under consideration consists of a 400mm thick compacted Heath Steele till overlying a 600mm medium to coarse sand. It is envisaged that the till is compacted wet of optimum so that it is nearly fully saturated (about 95 percent). In its natural state, the sand would conceivably be at its residual saturation so that no further drainage will occur immediately after **placement**. Under these conditions, effective diffusion coefficients of 1.0×10^{-6} and $1.0 \times 10^{-6} \text{ m}^2/\text{s}$ are proposed for the till and sand, respectively. The resulting gaseous oxygen distribution in this composite system, calculated from the steady state diffusion model, is presented in Fig.6.4. For comparison, the oxygen profile in a 1m thick single till cover is also presented. An intermediate diffusion coefficient of $5.0 \times 10^{-7} \text{ m}^2/\text{s}$ is used for the single till cover to reflect potential drainage and moisture loss by evaporation.

The results shown in Fig. 6.4 indicate that oxygen penetration is effectively contained in the till cover overlying the sand so that the concentration at the interface is nearly zero. In comparison, a much deeper profile is observed in the single cover. The composite system incorporates an underlying coarse layer which would drain faster and reach residual saturation long before the till cover. At residual saturation, the hydraulic conductivity of the coarse layer is minimum so that it is no longer able to transmit the negative pressures required to drain the till cover. The till cover is therefore expected to remain saturated even in summer dry conditions. The work done by Akindunni et al (1990) suggests that, for a composite system consisting of silt and a underlying medium to coarse sand, full saturation can be expected for at least 50 days. This length of time probably represents the longest period in the year during which there will be no moisture flux into the cover by infiltration. After 50 days, infiltration resulting from precipitation and spring melt will occur so that the cover can be expected to remain saturated most part of the year.

A major factor which should be considered is the loss of moisture from the surface of the cover as a result of evaporation. It is conceivable that incorporating a top coarse layer (such as sand) on the cover will reduce evaporative losses because of the poor capillarity of the coarse layer. Steady state diffusion through such a 3-layer composite system is presented.

6.3.3 Three-Layer System

The 3-layer composite cover under consideration is a system consisting of 30 cm of a coarse capillary barrier, a 40 cm thick saturated till layer and an underlying coarse layer of thickness 30 cm. The steady state gaseous oxygen profile calculated for such a system is shown in Fig.65 along with the profile for the single cover. Again, the depth of oxygen penetration terminates in the fine-grained till layer because of its lower diffusion coefficient. The uppermost coarse layer does very little to oxygen penetration, as shown in the figure.

Table 6.3 presents calculated oxygen fluxes for the three scenarios discussed. A flux of 0.21 kg/m².a is calculated for both the two and three layer systems. The flux for the single cover system is about 20 times higher than for the composites.

TABLE 6.3

CALCULATED OXYGEN FLUXES FOR DIFFERENT COVER SCENARIOS

| Cover | Layer | Thickness (m) | Diffusion Coefficient (m ² /s) | Flux (kg/m ² .a) |
|-----------|-------|---------------|---|-----------------------------|
| Single | till | 1.0 | 5.0 x 10 ⁻⁷ | 4.32 |
| Composite | till | 0.4 | 1.0 x 10 ⁻⁸ | 0.21 |
| | sand | 0.6 | 1.0 x 10 ⁻⁶ | |
| Composite | sand | 0.3 | 1.0 x 10 ⁻⁶ | 0.21 |
| | till | 0.4 | 1.0 x 10 ⁻⁸ | |
| | sand | 0.3 | 1.0 x 10 ⁻⁶ | |

7. SUMMARY AND CONCLUSIONS

Samples of glacial till and sand collected from the Heath Steele mine site have been evaluated for their geotechnical properties and soil cover characteristics. The four tills investigated are similar and consist of sandy silts of low activities. The laboratory hydraulic conductivity of the compacted till permeated with distilled water is about 2.0 x 10⁻⁸ cm/s.

The hydraulic behaviour of a P-layer cover system is evaluated. It is inferred that an initially saturated till layer overlying a coarse-grained layer can be expected to remain saturated during most parts of the year. Under dry conditions, the coarse layer will be the first to drain. When it has drained to residual saturation, the resulting low hydraulic conductivity will prevent further transmission of negative pressures required to drain the overlying till layer. The hydraulic performance of this composite system can be improved by incorporating a coarse-grained layer on top of the till. This upper capillary breaking layer prevents upward transport of moisture and minimizes losses from the till.

Steady state diffusion modelling is conducted for single and composite cover systems. Results indicate gaseous oxygen penetrates to a shallower depth in the composite system than in the single cover. As expected, the gas flux in the composites is also lower.

It is proposed that a **3-layer** composite cover, consisting of a fine-grained saturated till, sandwiched between two coarse-grained layers, will be an effective oxygen barrier. If the till is compacted at a water content slightly wet of optimum, it can be expected to have a low hydraulic conductivity and be an effective water barrier as well.

Several other factors have to be taken into account during design and application of the composite system. For example, since the tills are observed to undergo appreciable frost heaving, the depth of the **fine** layer should be carefully selected based on the frost penetration index for the Heath Steele mine area. Proper grading of side slopes, surface water and erosion control must also be taken into account.

A final important consideration is the availability of abundant till and sandy materials in the vicinity of the mine. The exploration work conducted at the beginning of this study showed that the most promising location is the property belonging to CNE Stratabound where till HS-B was sampled. A detailed material inventory should be conducted prior to full-scale implementation.

REFERENCES

- ASTM **D1557-78** (1978) Standard methods for moisture-density relations of soils and soil-aggregate mixtures. In: Soil and Rock; Building Stones; Geotextiles, Vol. 04.08, Annual ASTM Standards, Section 4 Construction, pp. **280-286**.
- Akindunni, F.F., R.W. **Gillham**, and R.V. Nicholson (1990) Numerical simulations to investigate moisture retention characteristics in the design of oxygen-limiting covers for reactive mine tailings. Submitted to the Canadian Geotechnical Journal.
- Barbour**, S.L. (1987) Role of physiochemical effects on the behaviour of clay soils. Proceedings of the **40th** Canadian Geotechnical Conference, Regina, Sask., pp. 323-342.
- Bennett, J.W., J.R. Harries, G. Pantelis, and **A.I.M.** Ritchie (1989) Limitations on pyrite oxidation rates in dumps set by air transport mechanisms. In: International Symposium on Biohydrometallurgy, Jackson Hole, Wyoming, August 13-18.
- Bowles, J.E. (1986) Engineering properties of soils and their measurement. McGraw-Hill Book Company, New York.
- Chamberlain, E.J., and A.J. Gow (1979) Effect of freezing and thawing on the permeability and structure of soils. Engineering-Geology (Amsterdam), **13:73-92**.
- Collin**, M. (1987) Mathematical modelling of water and oxygen transport in layered soil covers for deposits of pyritic mine tailings. Licentiate Treatise. Department of Chemical Engineering, Royal Institute of Technology, Stockholm. 189p.
- Craig, R.F. (1974) Soil mechanics. 1st edition, Van Nostrand Reinhold Co. Ltd., England.
- Crank, J. (1975) The mathematics of diffusion. 2nd. edition. Clarendon Press, Oxford, U.K.
- Daniel, D.E., D.C. Anderson, and **S.S** Boynton (1985) Fixed-wall versus flexible-wall permeameters. In: Hydraulic barriers in soil and rock. ASTM Special Technical Publication 874, pp: 107-123.
- Daniel, J.A., **J.R.** Harries, A.I.M. Ritchie (1980) Water movement caused by monsoonal rainfall in an overburden dump undergoing pyritic oxidation. pp. 623-629.

- Das, **B.M.** (1983) Advanced soil mechanics. McGraw-Hill Book Company, New York.
- Davy, **D.R.** (Ed.) (1975) Rum Jungle environmental studies. Australian Atomic Energy Commission report **AAEC/E365**, Chapter 6.
- Dreimanis, A. (1962) Quantitative gasometric determination of calcite and dolomite by using **Chittick** apparatus. Journal of Sedimentary Petrology, **32:520-529**.
- Fernandez, F., and R.M. Quigley (1985) Hydraulic conductivity of natural clays permeated with simple liquid hydrocarbons. Canadian Geotechnical Journal, **22:205-214**.
- Filion, M.P. and K. Ferguson (1989) Acid mine drainage research in Canada. Proceedings of the international symposium on tailings and effluent management, **Halifax**. Tailings and Effluent Management. pp. 61-72.
- Gillham**, R.W. (1984) The capillary fringe and its effects on the water-table response. Journal of Hydrology, Vol. 67: 307-324.
- Gillham**, R.W. and R.V. Nicholson (1990) Development of a laboratory procedure for evaluating the effectiveness of reactive tailings covers. Final Report to Centre de technologie Noranda., December.
- Harries, J.R. and A.I.M. Ritchie (1981) The use of temperature profiles to estimate the pyritic iron oxidation rate in a waste rock dump from an open cut mine. Water, Air and Soil pollution, 16: **405-423**.
- Harries, J.R. and A.I.M. Ritchie (1985) Pore gas composition in waste rock dumps undergoing pyritic oxidation. Soil Science, 140, pp. 143-152.
- Holtz, R.D. and W.D. Kovacs (1981) An introduction to geotechnical engineering. Prentice-Hall, Inc., New Jersey.
- Konrad, J.-M. (1989) Effect of freeze-thaw cycles on the freezing characteristics of a clayey silt at various overconsolidation ratios. Canadian Geotechnical Journal, Vol. 26, No. 2, pp. **217-226**.

- Kwong, **Y.T.J.** and **D.K.** Nordstrom (1989) Copper-arsenic mobilization and attenuation in an acid mine drainage environment. Proceedings of the 6th. International Symposium on Water-Rock interaction, U.K.
- Lambe, T.W.**, (1958) The structure of compacted clay. Journal of the Soil Mechanics and Foundation Division, ASCE, **Vol 84**, No. SM2, 1654-1 to 1654-34.
- Lambe, T.W.**, and R.V. Whitman, (1979) Soil mechanics. John Wiley and Sons inc., New York.
- Leonards, G.A.** and B.K. Ramiah (1959) Time effects in the consolidation of clay. Papers on soils • 1959 Meeting, American society for Testing and Materials, Special Technical Publication No. 254, pp. 116-130.
- Mitchell J.K. (1976) Fundamentals of soil behaviour. John Wiley & Sons Inc., New York., 422p.
- Mitchell, J.K.** and J.S. Younger (1967) Abnormalities in hydraulic flow through fine-grained soils. ASTM Special Technical Publication 417, pp. 106-139.
- Morin, K.A., E. Gerencher, C.E. Jones, D.E. Konasewich, and J.R. Harries (1990) Critical literature review of acid drainage from waste-rock.
- Nicholson, R.V., R.W. **Gillham**, J.A. Cherry, and E.J. **Reardon** (1989) Reduction of acid generation in mine tailings through the use of moisture-retaining cover layers as oxygen barriers. Canadian Geotechnical Journal, Vol. 16, No. 1, pp. 1-8.
- Nielson, **K.K.**, V.C. Rogers, and G.W. Gee (1984) Diffusion of radon through soils: a pore distribution model. Soil Science Society of America Journal **48:482-487**.
- Nolan, Davis and Associates (N.S.) Limited (1990) Heath Steele waste rock study phase II report. Submitted to Brunswick Mining and Smelting Corporation Limited. File No. **H88113**.
- Olson, R.E. and D.E. Daniel (1981) Measurement of the hydraulic conductivity of fine-grained soils. Permeability and groundwater contaminant transport, ASTM Special Technical Publication 746, pp. 18-64.

- Parizek, **R.R.** (1985) Exploitation of hydrogeologic systems for abatement of acidic drainages and wetland protection. In: Wetlands Water Management Mined Lands Conference, Pennsylvania State University, October 23-24, pp. 19-53.
- Penner, E. (1969) Frost heaving forces in **leda** clay. Canadian Geotechnical Journal, Vol. 7, pp. 8-16.
- Rogers, V.C., K.K. Rich, G.M. Sandquist, and M.L. **Mauch** (1962) Radon attenuation with earthen covers. RAE-33-14. Annual Report to US. Department of Energy UM-TRAP Project Office, Rogers and Associates Engineering Corp., Salt Lake City, Utah.
- Shroeder, P.R., A.C. Gibson, and M.D. Siden (1984) The hydrologic evaluation of landfill performance (HELP) model, **Vol.II**. Documentation for Version I. **EPA/530-SW-84-010**, U.S. Environmental Protection Agency, Office of Solid Waste and Emergency Response, Washington, D.C., **256p**.
- Silker, W.B. and D.R. Kalkwarf (1983) Radon diffusion in candidate soils for covering uranium mill tailings. NUREG/CR-2924. U.S. Nuclear Regulatory Commission, Washinton D.C.
- Streeter, V.L. and E.B. Wylie (1981) Fluid mechanics. First **SI** metric edition, McGraw-Hill Ryerson Limited, Toronto.
- Taylor, D.W. (1948) Fundamentals of soil mechanics. Wiley, New York.
- Taylor, S.A. (1949) Oxygen diffusion in porous media as a measure of soil aeration. Soil Sci. **Soc. Am. Proc.**, Vol. 14, pp. **55-61**.
- Troeh, F.R., J.D. Jabro, and D. **Kirkham** (1982) Gaseous diffusion equations of porous materials. Geoderma 27: **239-253**.
- Truesdale, G.A., **A.L.** Downing, and G.F. **Lowden** (1955) The solubility of oxygen in pure water and sea-water. J. appl. Chem., 5, February, pp. 53-62.
- Yanful, **E.K.**, L St-Arnaud, and R. Prairie (1999) Generation and evolution of acidic pore waters at the Waite Amulet tailings. Final Report. DSS Contract **09SQ.23440-8-9162**.

Yanful, E.K., M.D. Haug, and L.C. Wong (1990) The impact of synthetic **leachate** on the hydraulic conductivity of a **smectitic** till underlying a landfill near Saskatoon, Saskatchewan. Canadian Geotechnical Journal 27: 509-519.

Yong, R.N., P. Booninsuk, and A.E. Tucker (1984) A study of frost-heave **mechanics** of high-clay content soils. Journal of Energy Resources Technology, Vol. 106, December, pp. **502-508**.

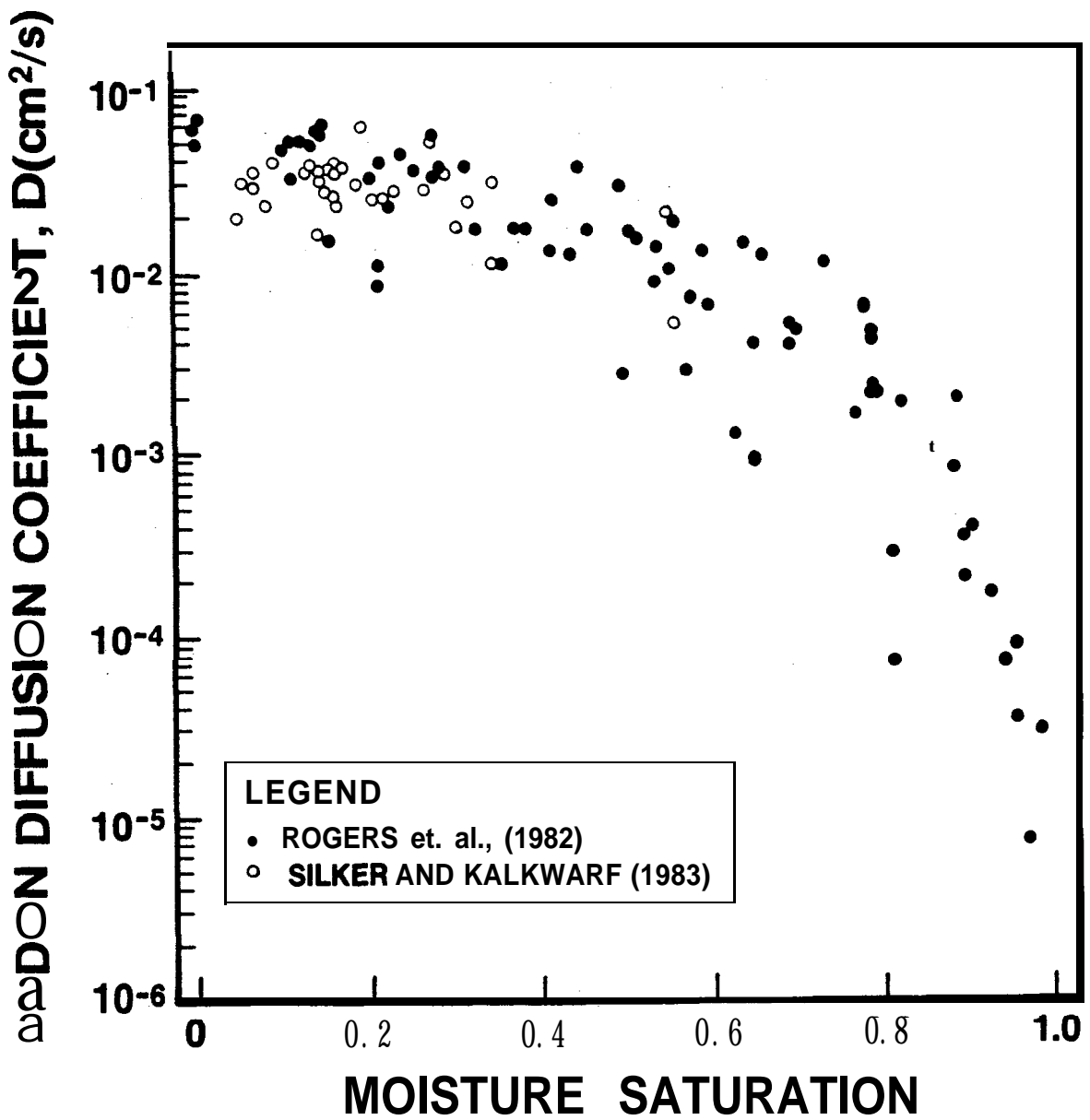


Figure 3.1 The variation of radon gas diffusion coefficient with moisture saturation.

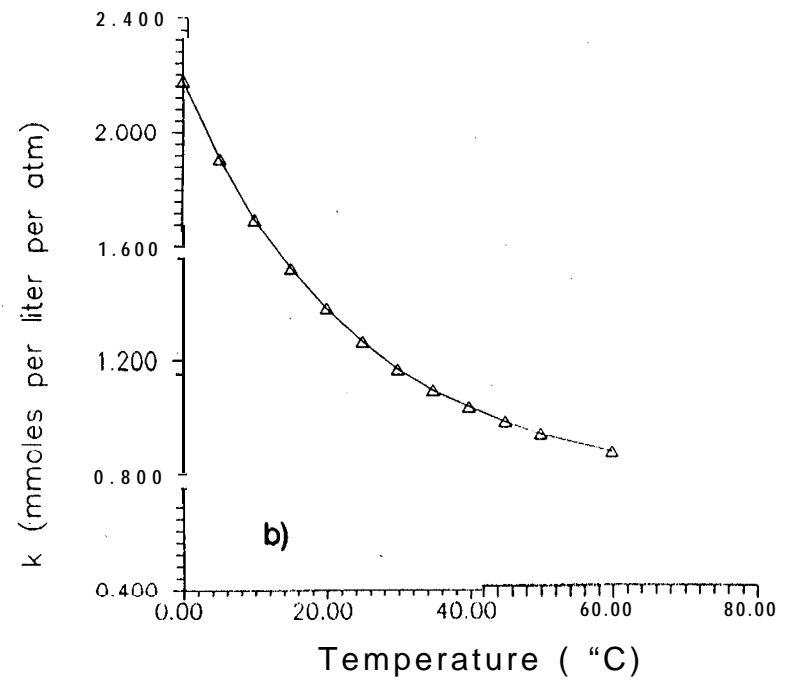
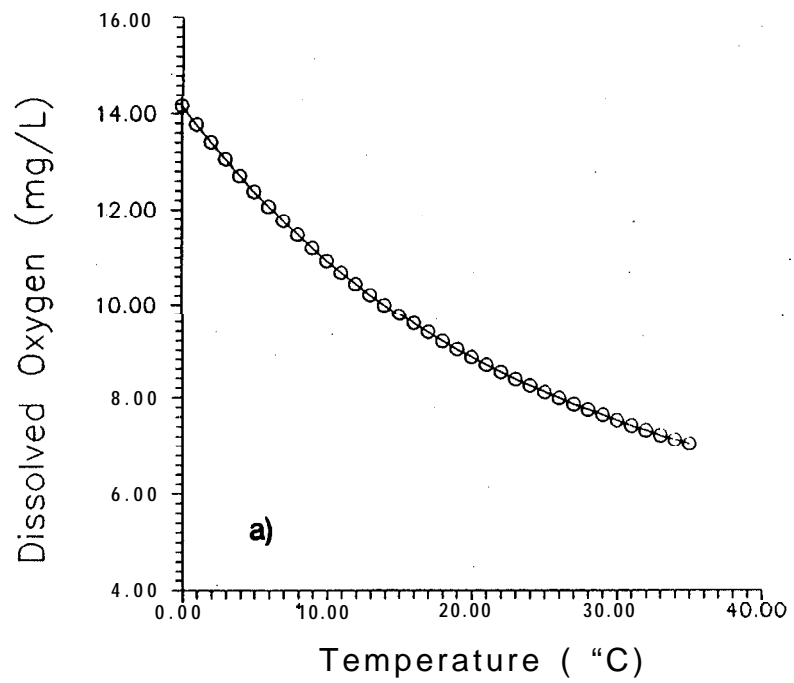


Figure 3.2 The variation of a) oxygen solubility and b) Henry's law constant with temperature.

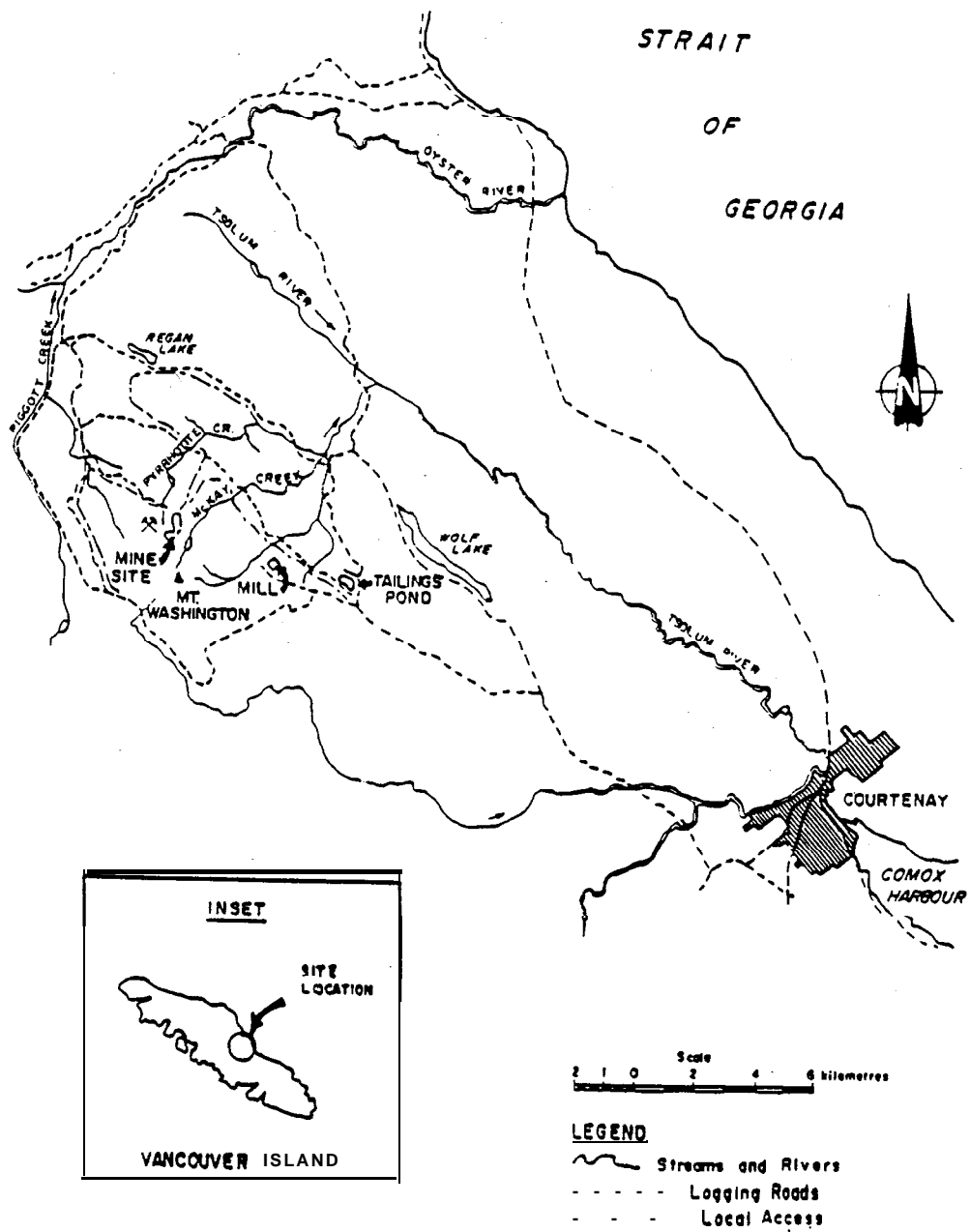


Figure 4.1 A location map of the Mount Washington mine site on Vancouver Island, B.C.

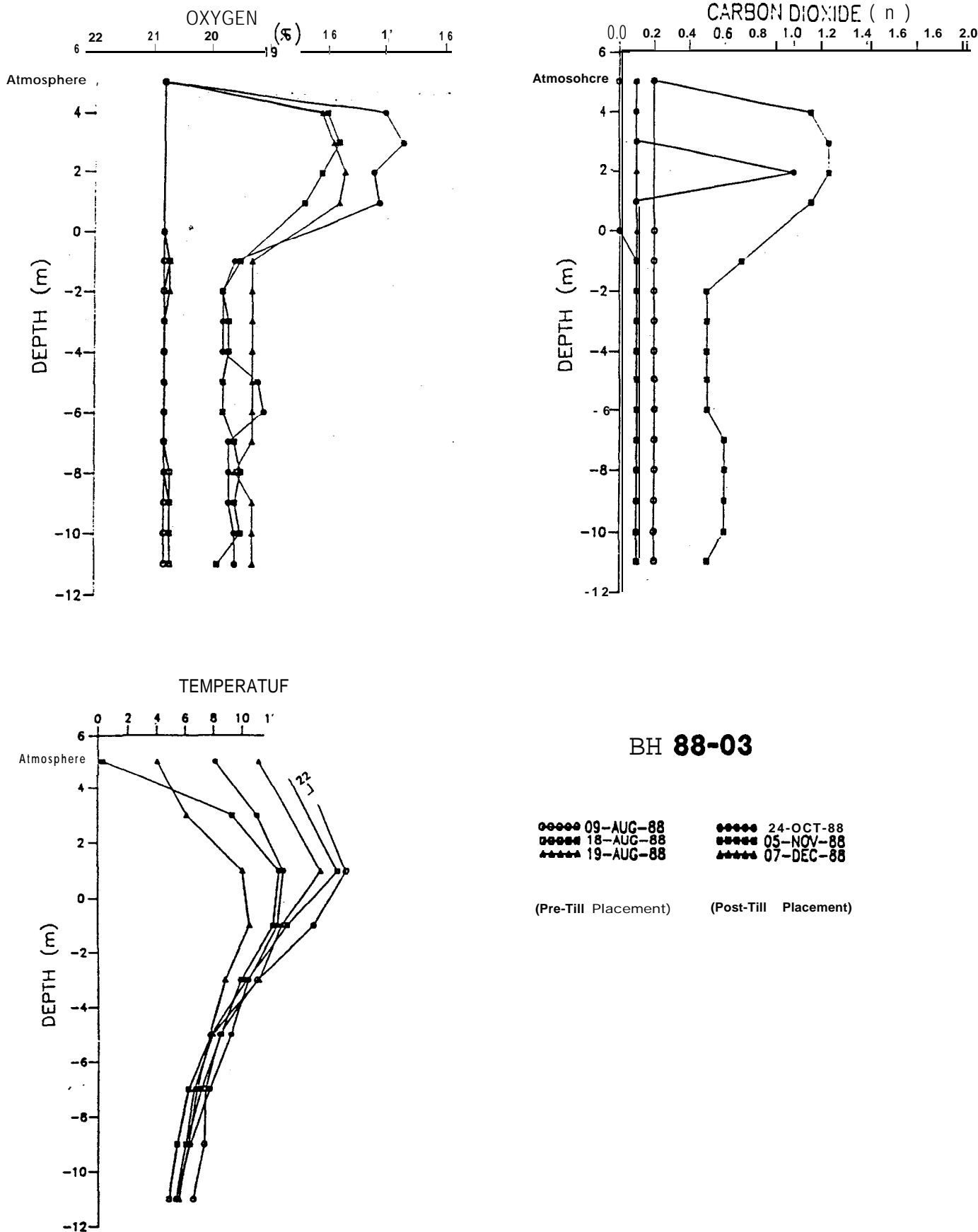


Figure 4.2 Typical gas concentrations and **temperature profiles** in Mount Washington waste dumps before and after placement of cover.

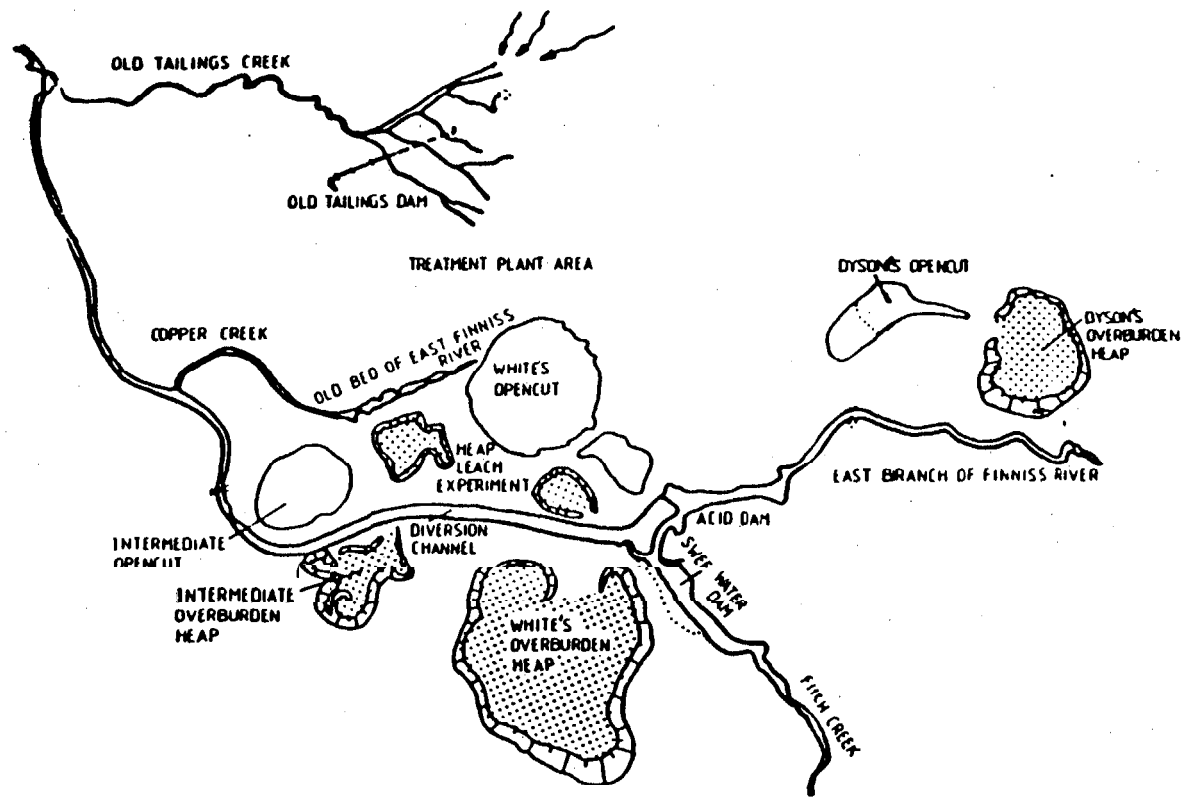


Figure 4.3 Location of White's and Intermediate Dumps, Rum Jungle Mine, Australia.

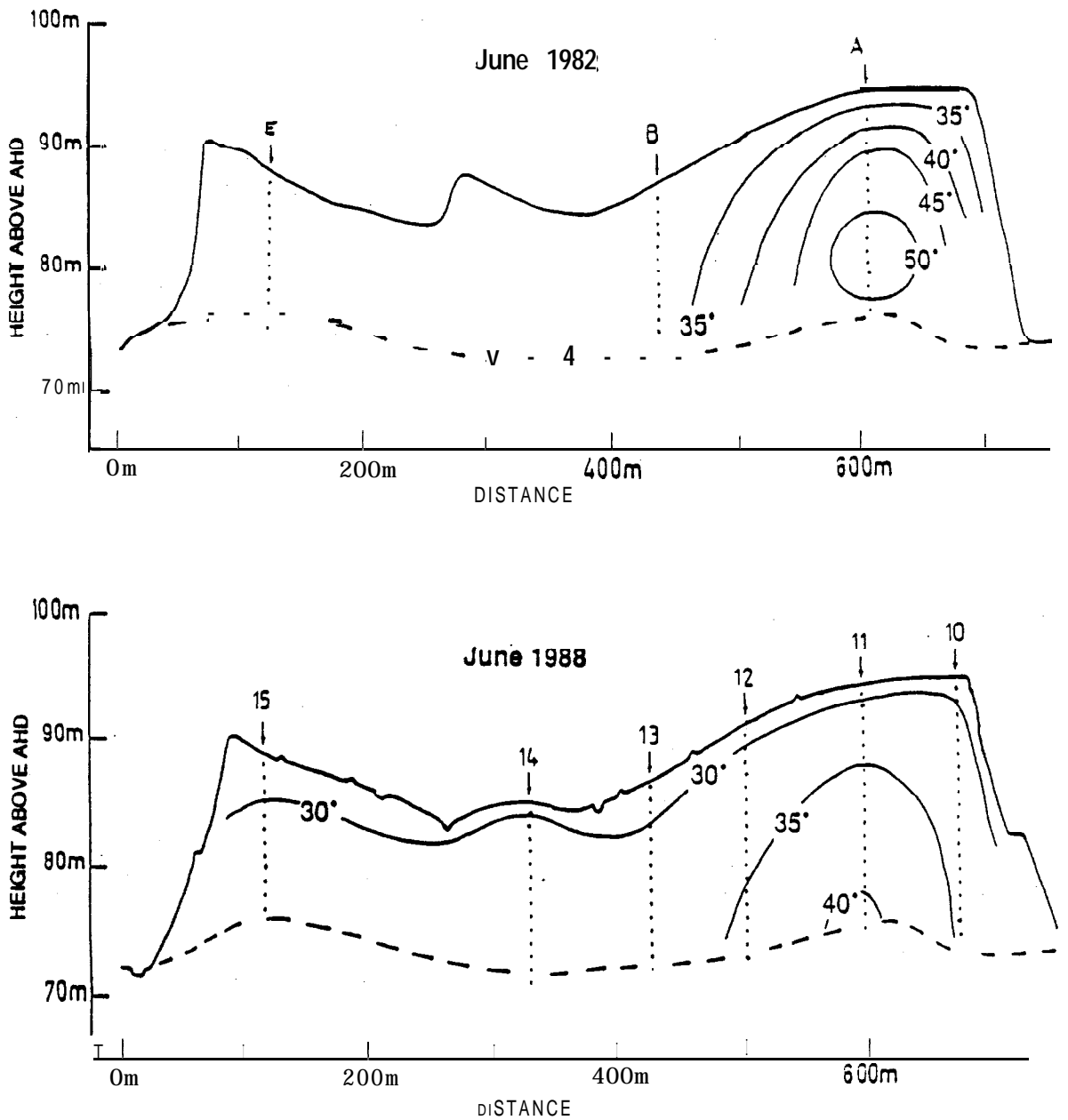


Figure 4.4 Temperature distributions in White's Dump before and after rehabilitation (directly from Bennett et al., 1989).

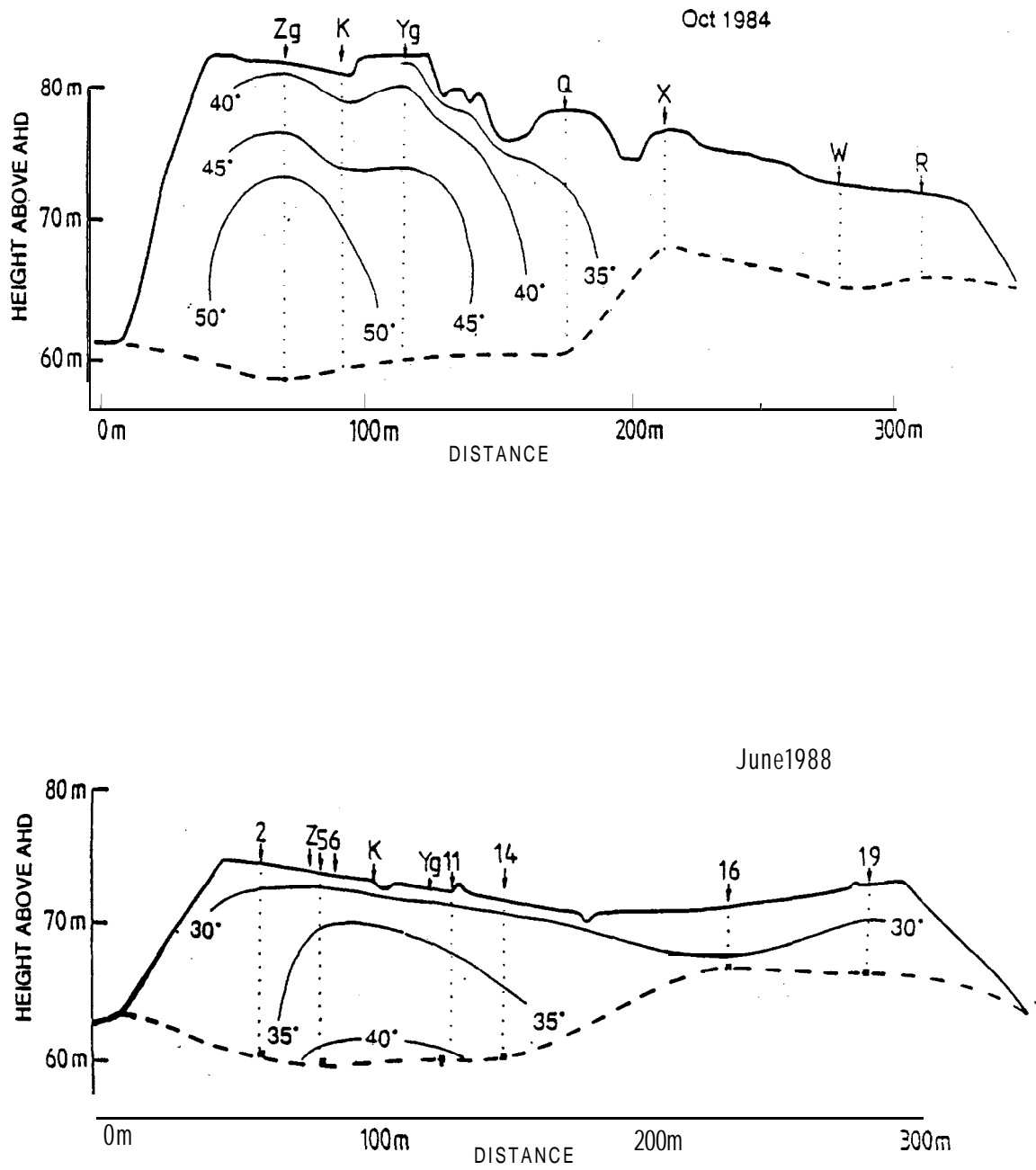


Figure 4.5 Temperature distributions in Intermediate Dump before and after rehabilitation (directly from Bennett et al., 1989).

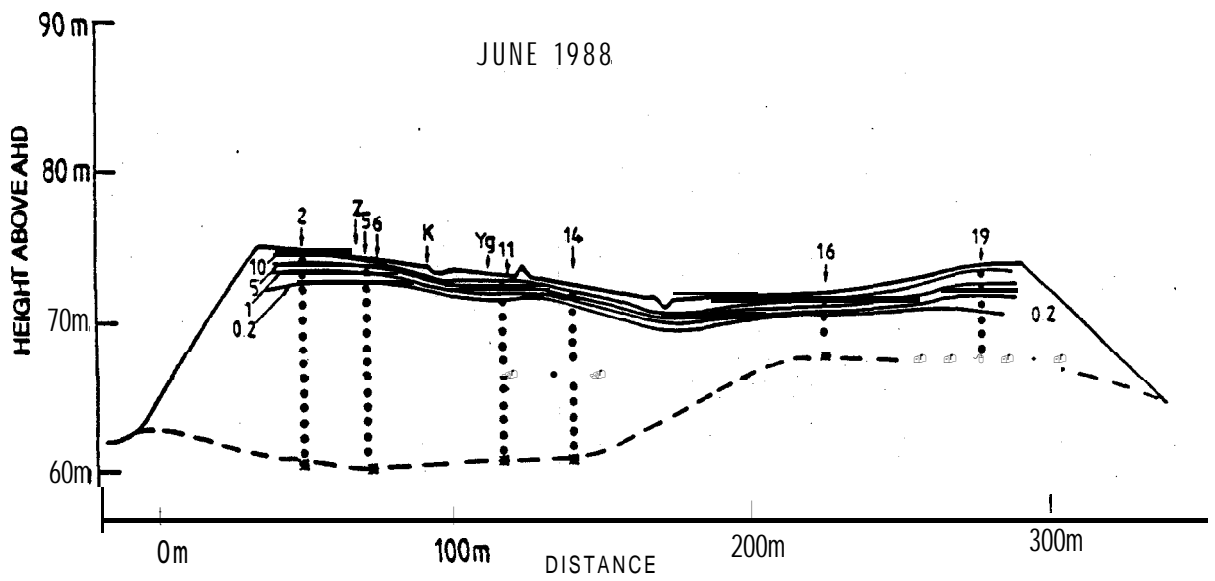
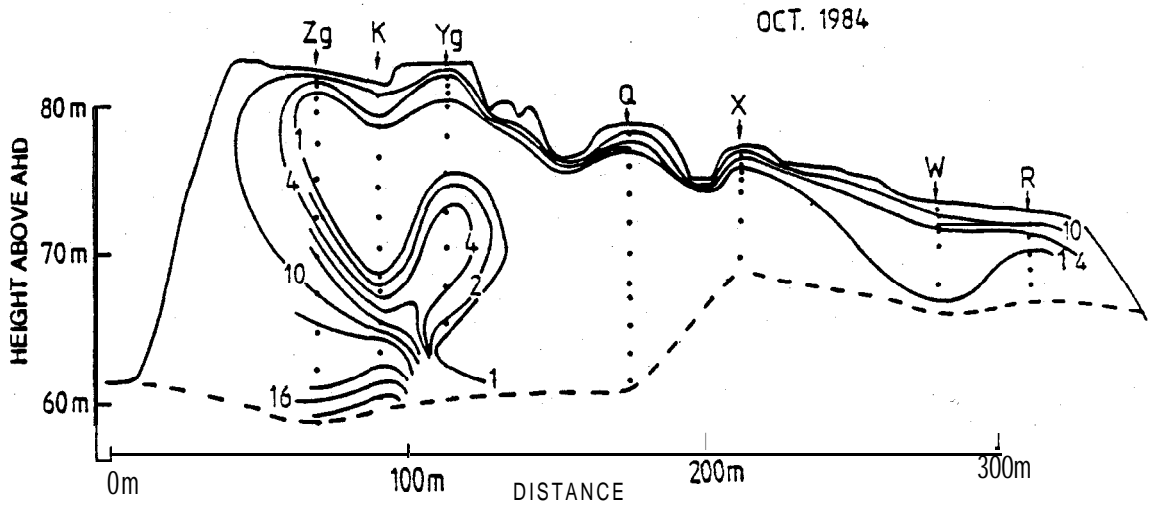


Figure 4.6 Oxygen distribution in White's dump before and after rehabilitation. Contours indicate pore gas concentration (vol.%). Directly from Bennett et al., (1989).

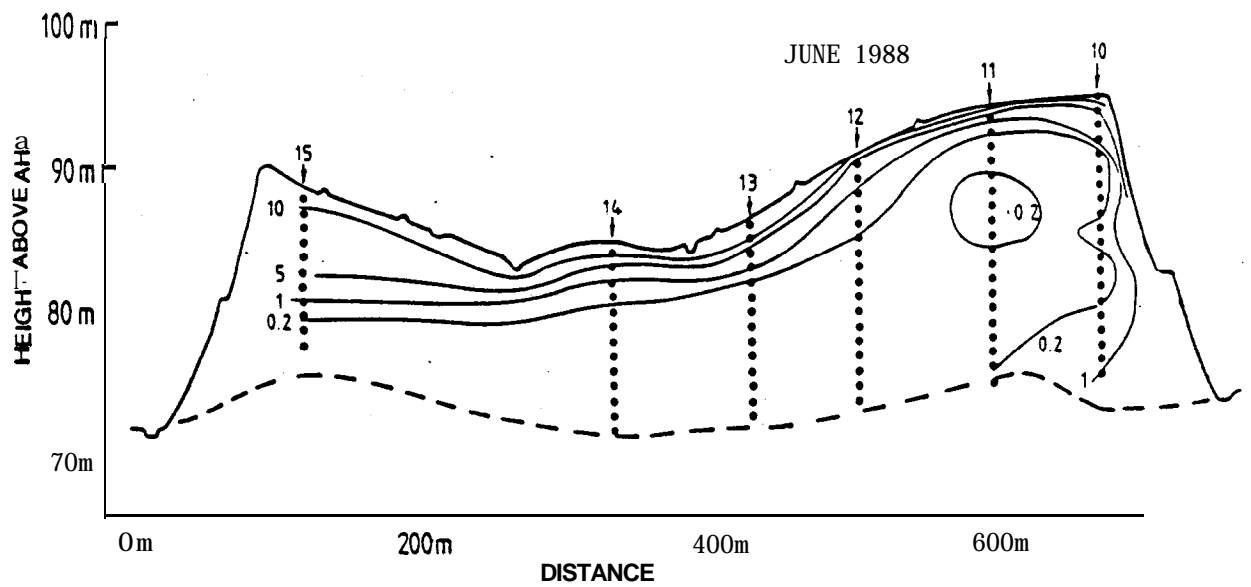
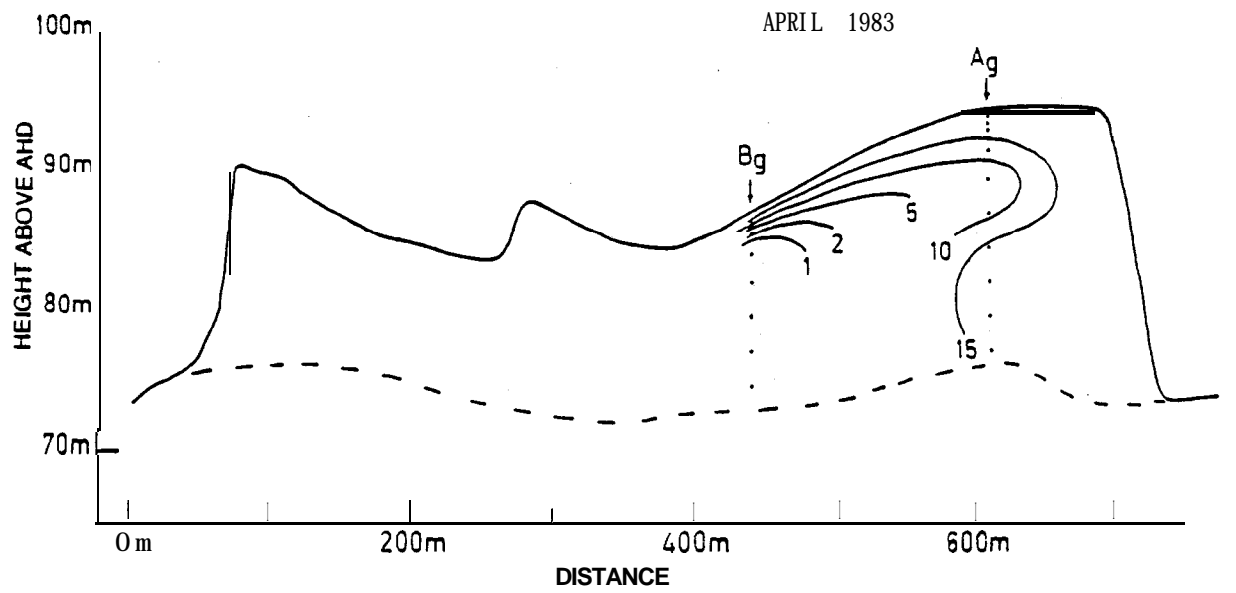


Figure 4.7 Oxygen distribution in Intermediate dump before and after rehabilitation. Contours indicate pore gas oxygen concentration (vol.%). Directly from Bennett et al., (1989).

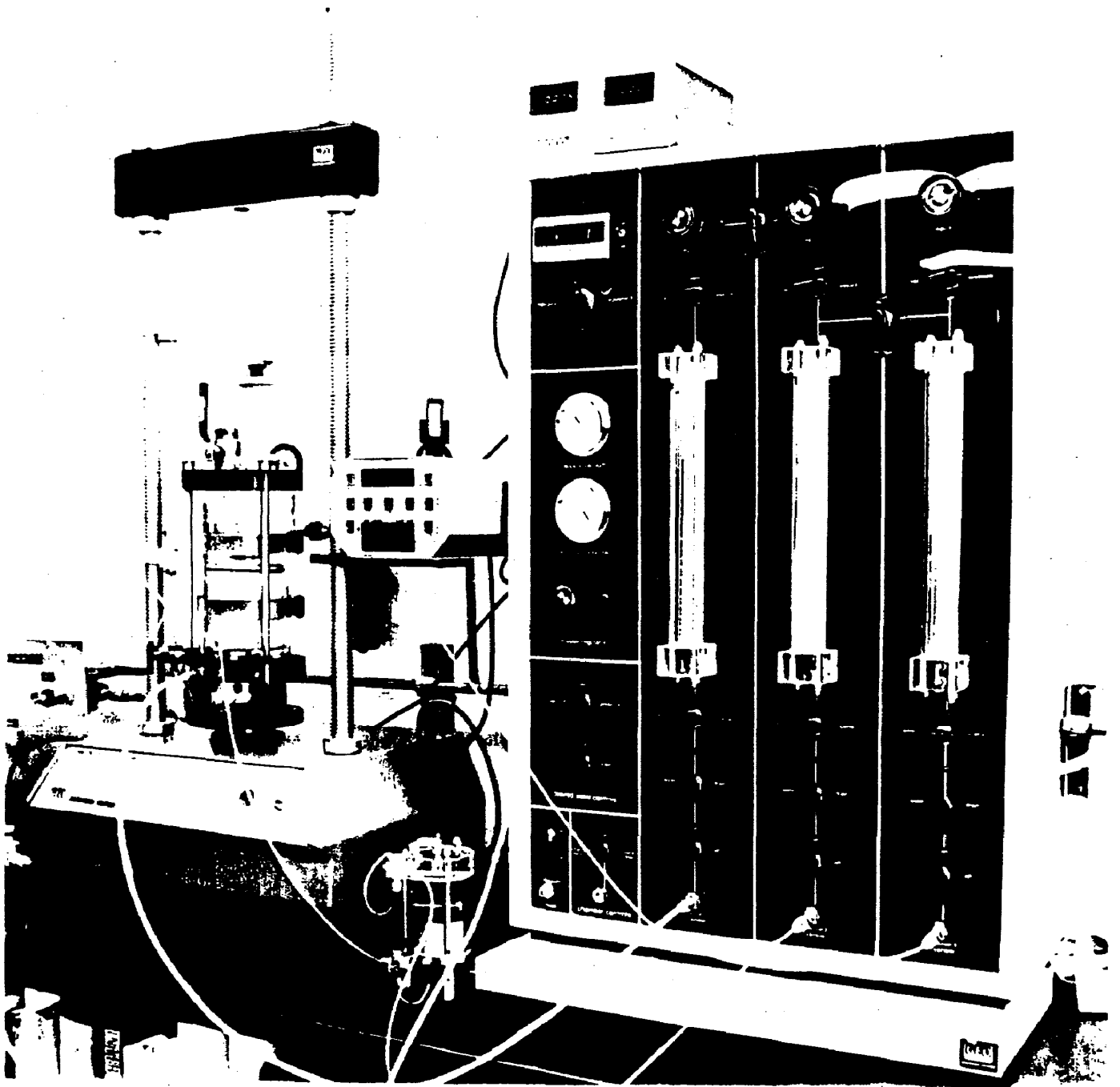


FIGURE 5.1 Triaxial panel and cell used in the hydraulic conductivity tests.

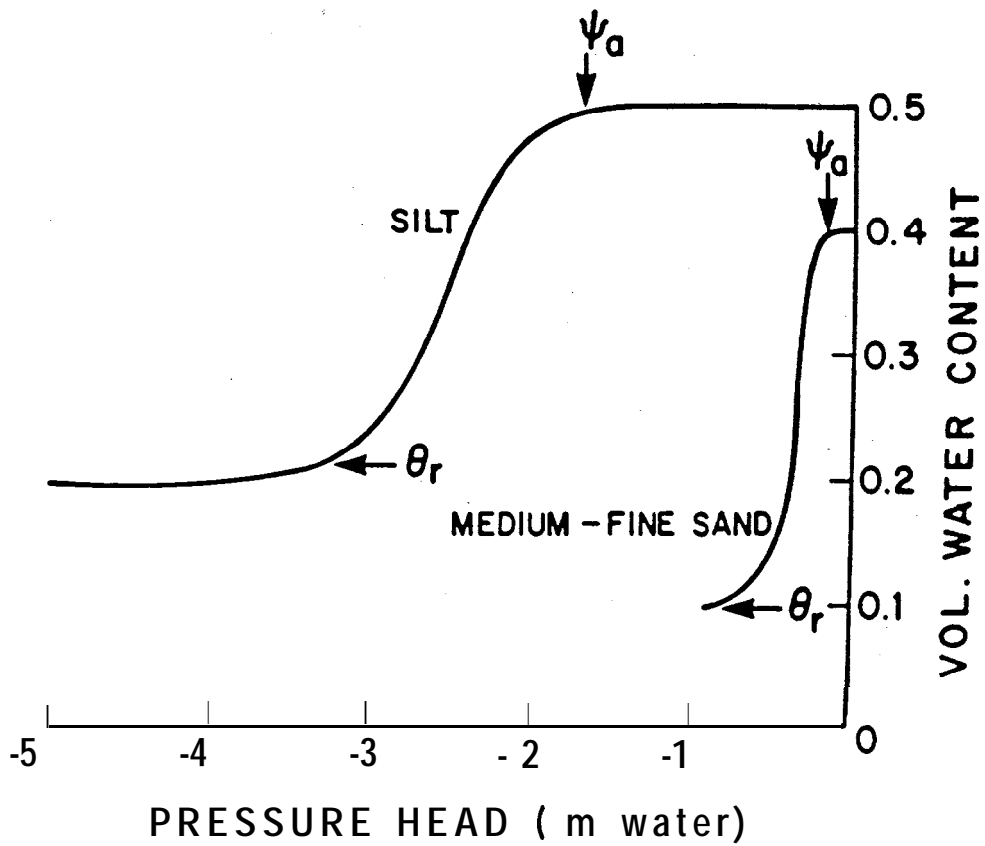


Figure 5.2 Moisture content (defined as V_w/V_T) and pressure head for a sand and a silt loam (from Nicholson et al., 1989).

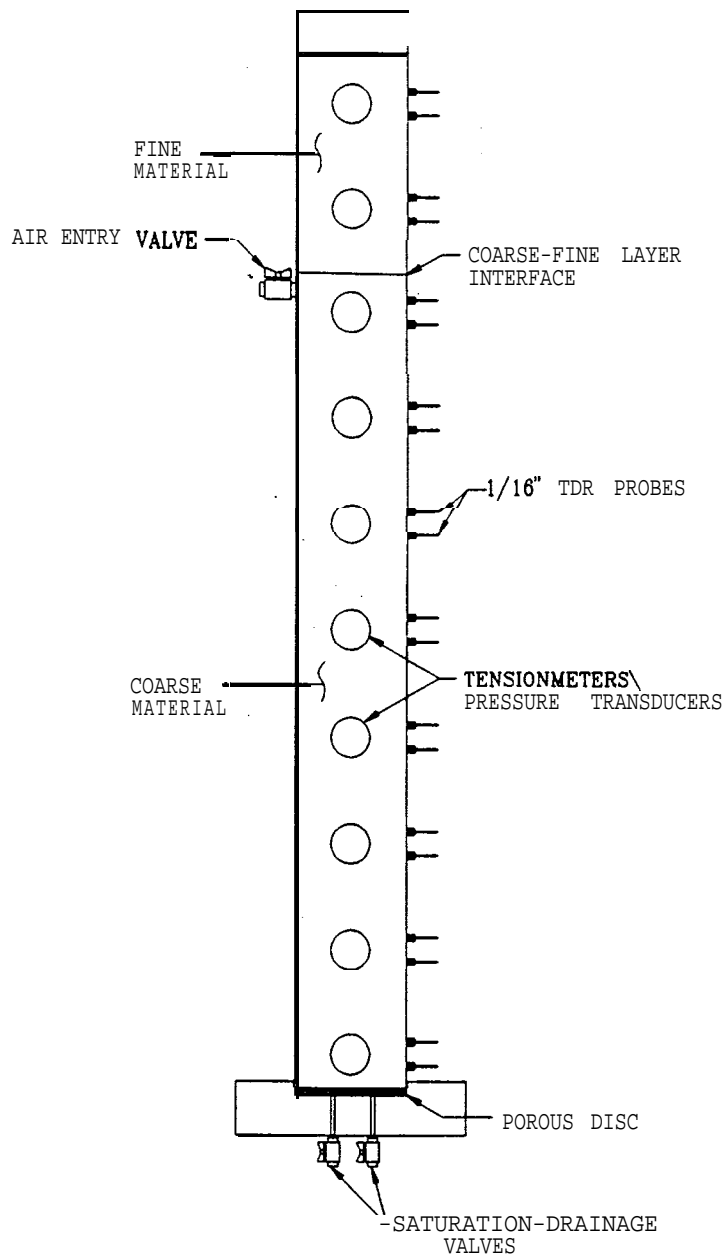


Figure 5.3 A schematic representation of the column used for investigating the hydraulics of a two-layer cover system.

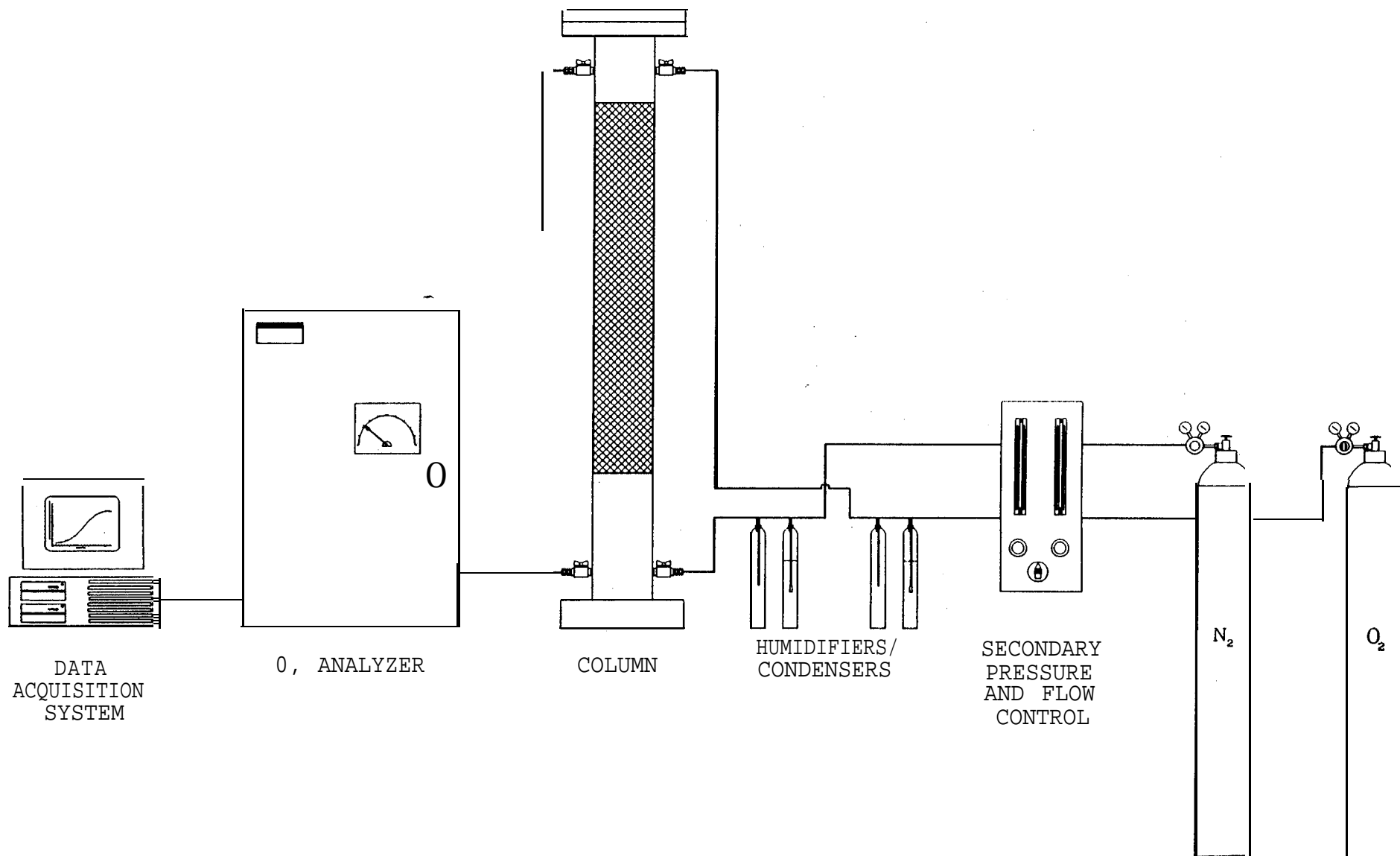


Figure 5.4 A schematic representation of the set up used in oxygen diffusion measurements

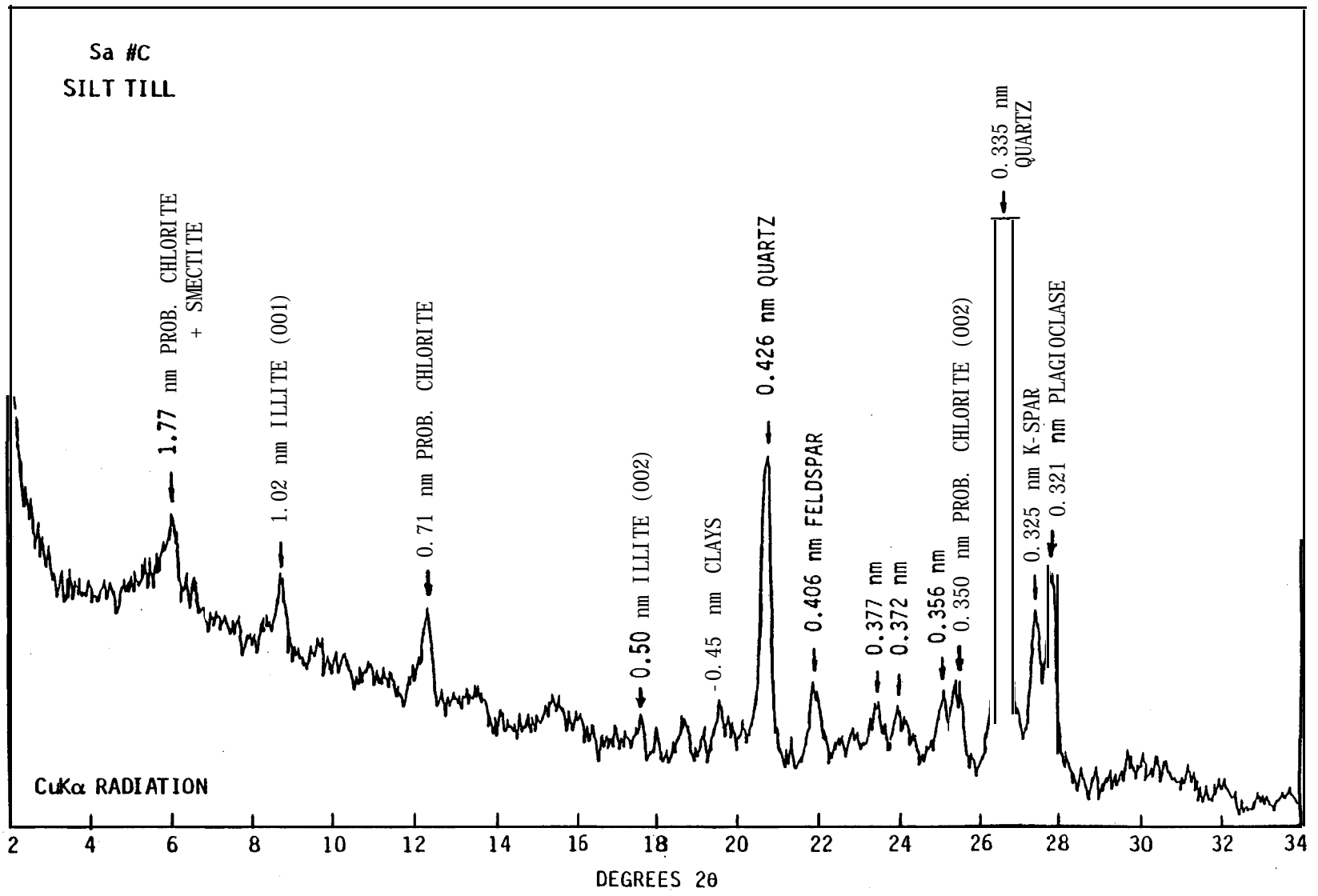


Figure 5.5 A random X-ray powder diffractogram of soil-S.C.

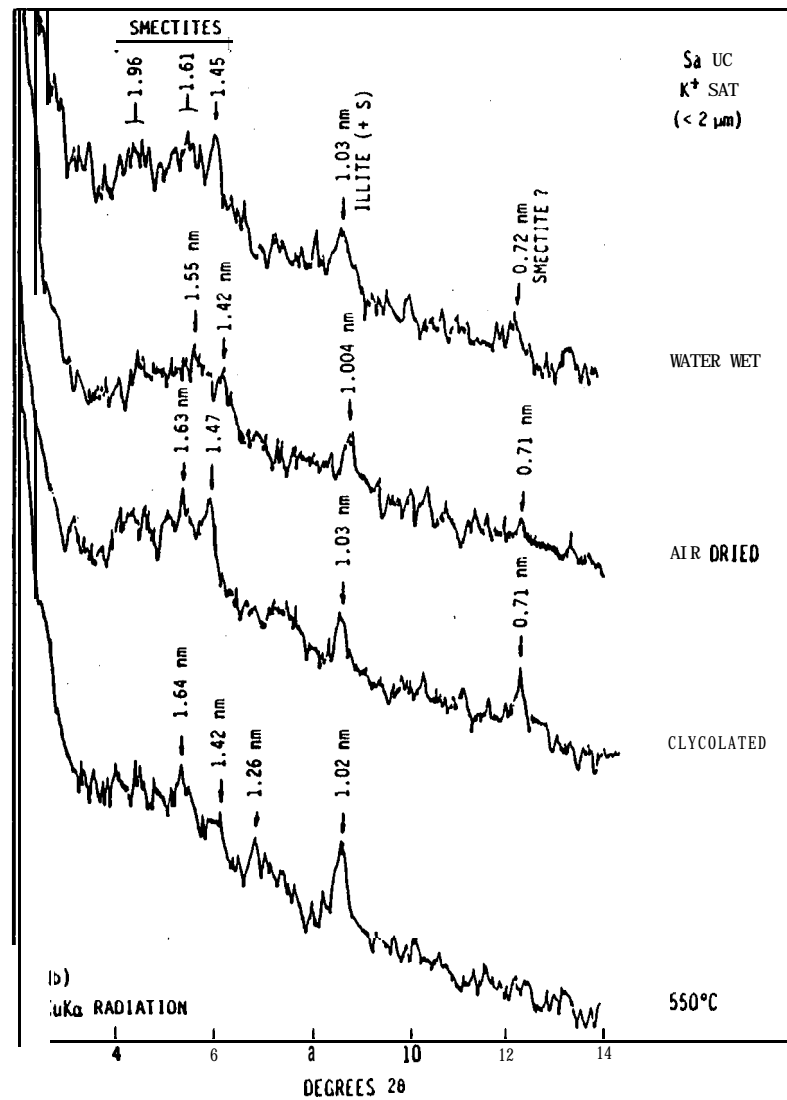
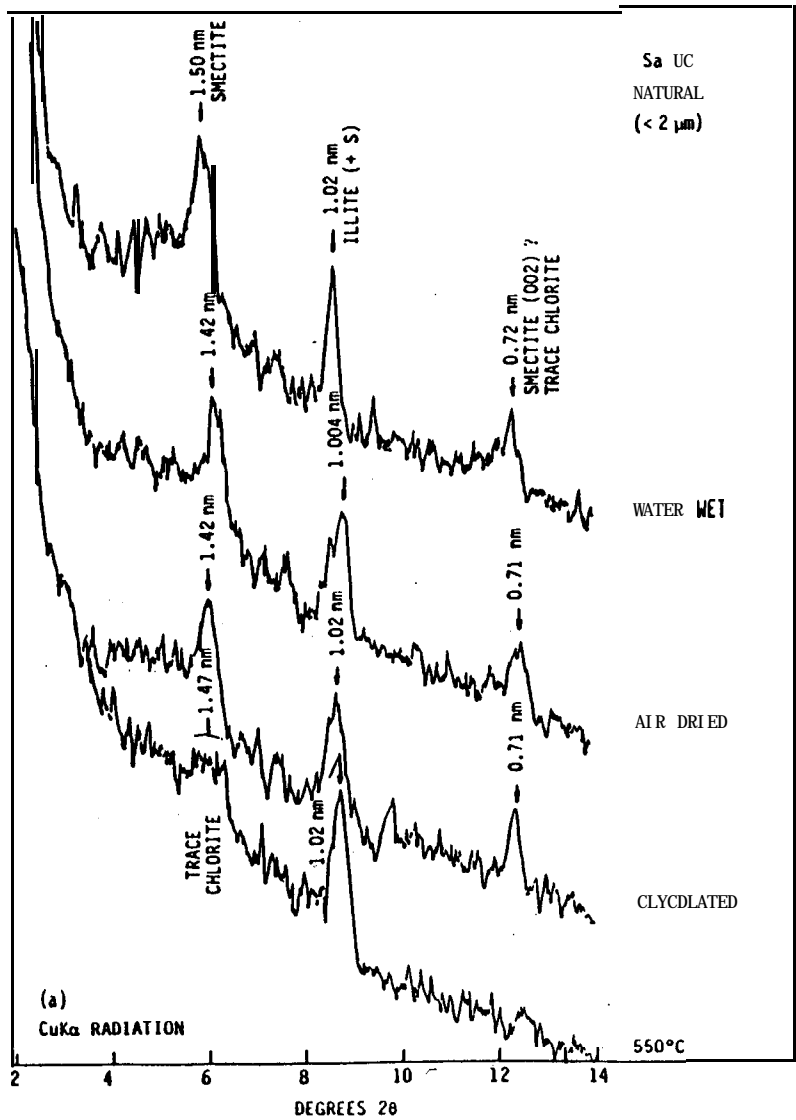


Figure 5.6 Oriented X-ray diffractograms of soil HS-C.

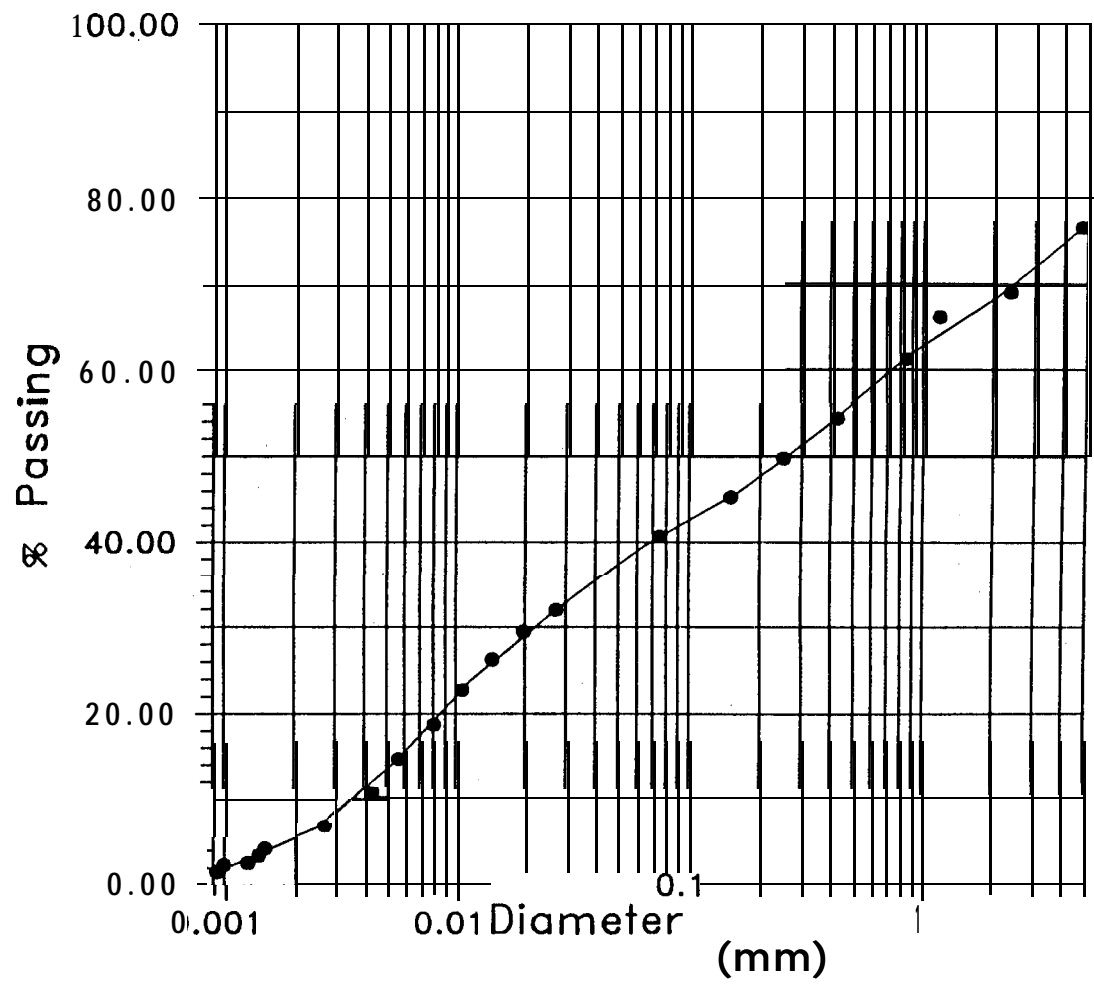


Figure 5.7 Grain size distribution of till HS-A.

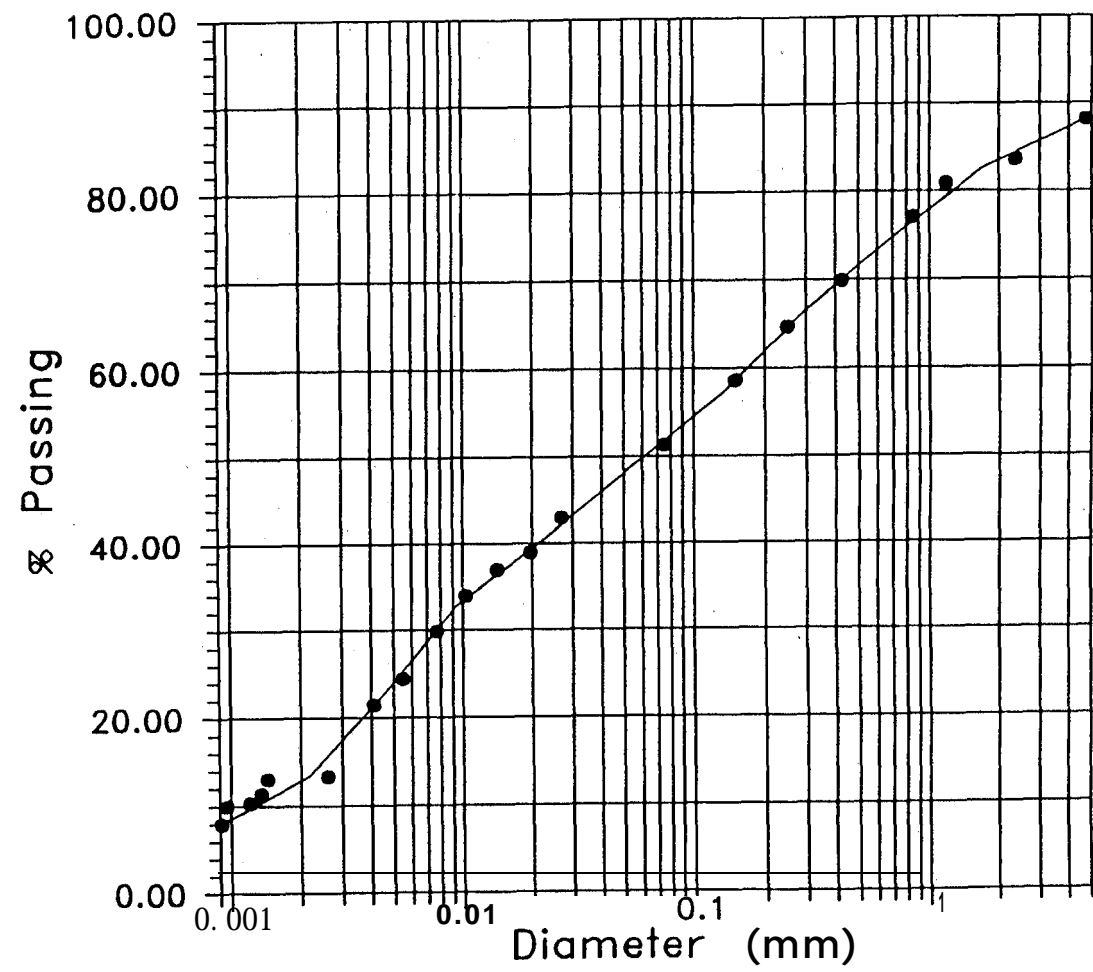


Figure 5.8 Grain size distribution of till HS-B.

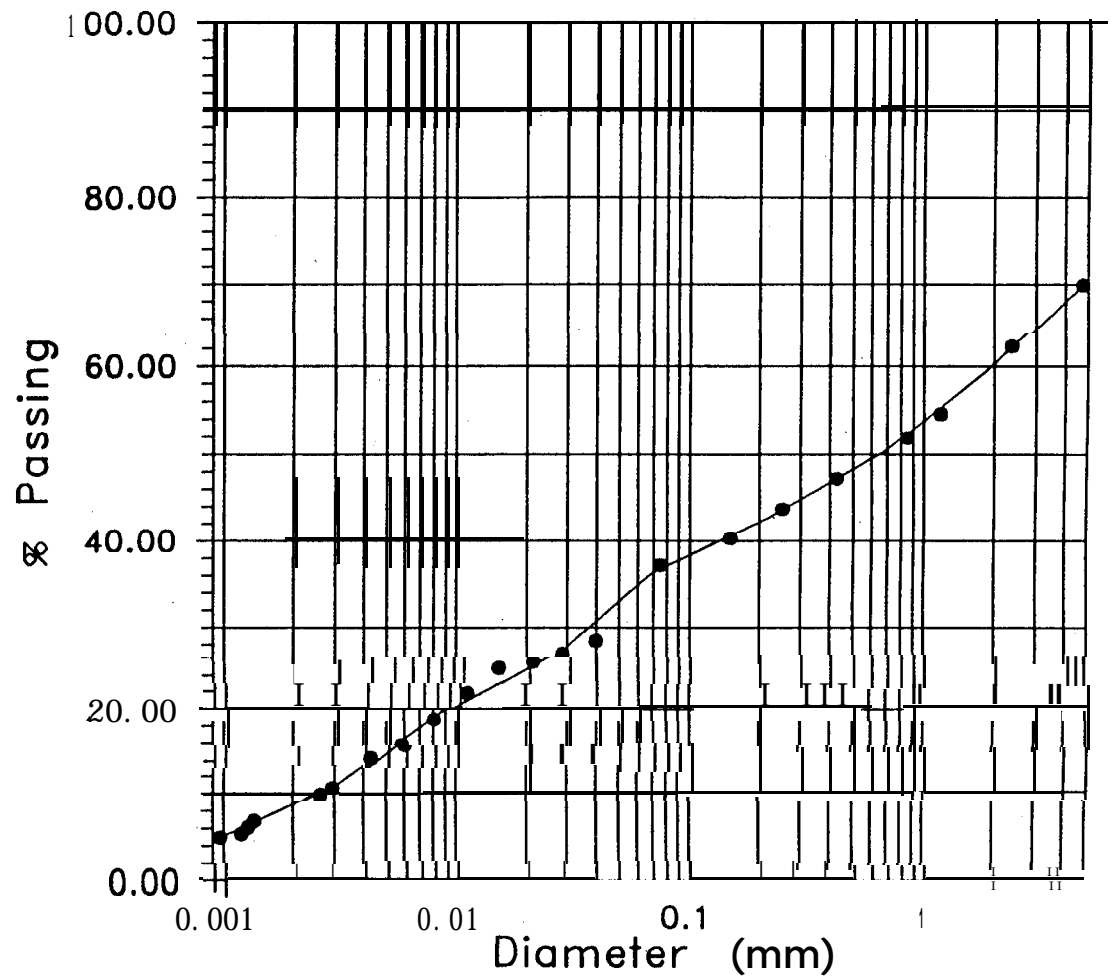


Figure 5.9 Grain size distribution of till HS-C.

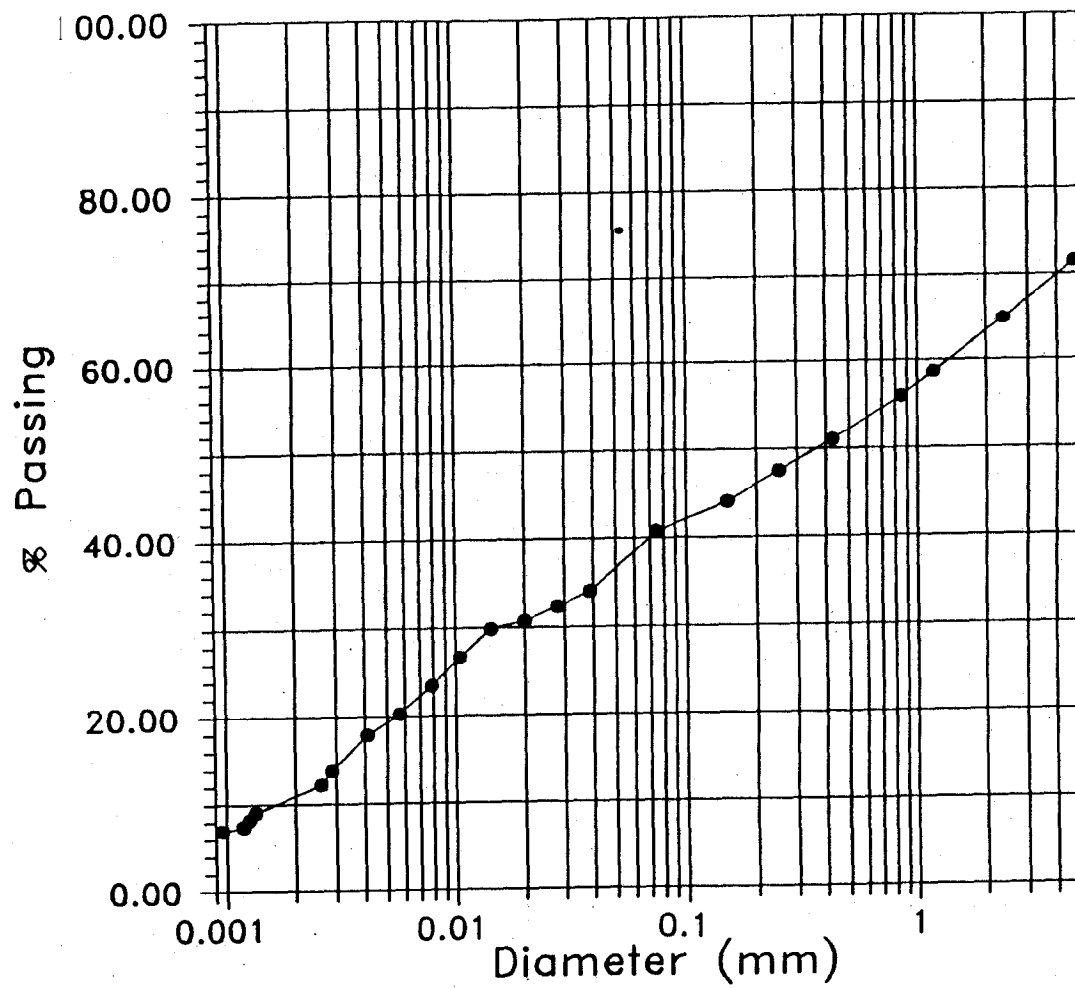


Figure 5.10 Grain size distribution of till HS-E.

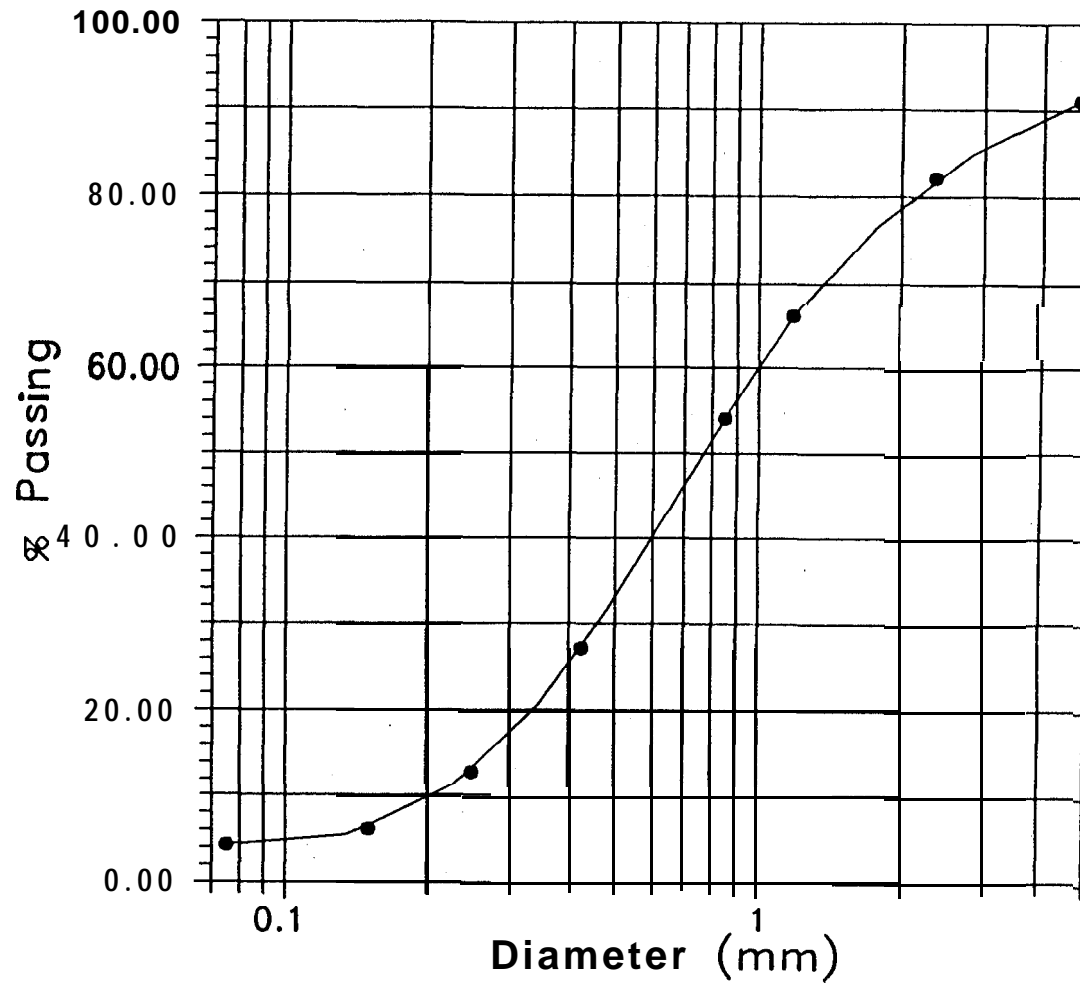


Figure 5.11 Grain size distribution of till HS-D.

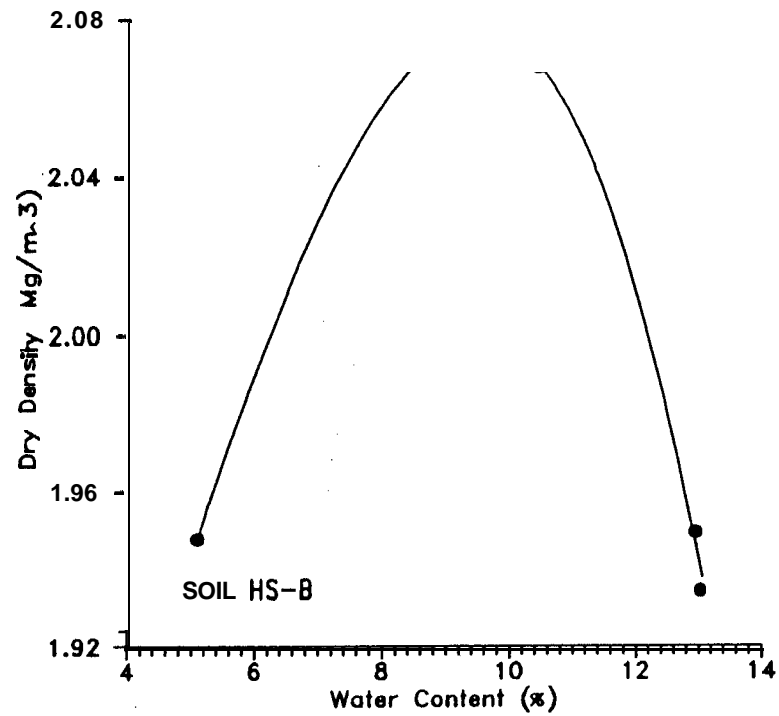
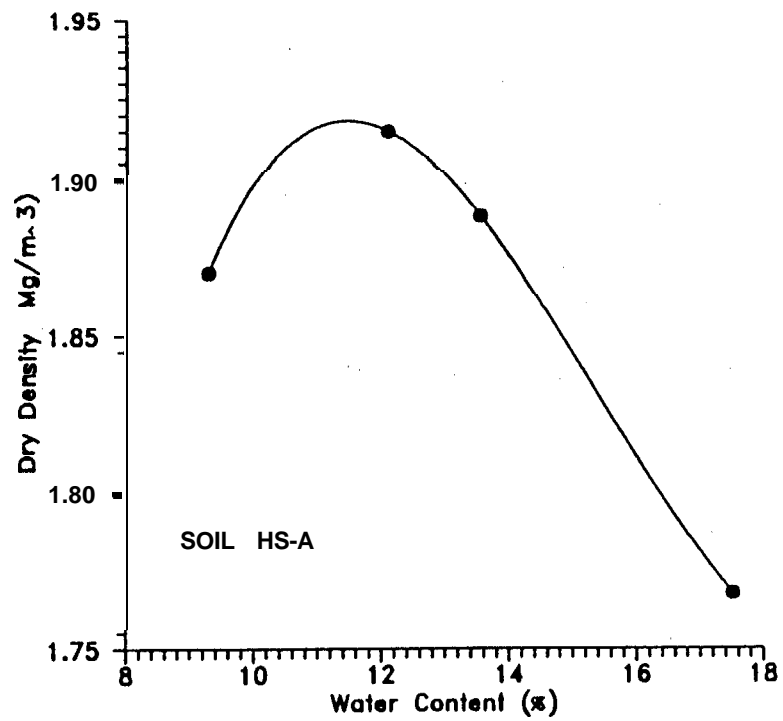


Figure 5.12 Modified Proctor compaction curve for tills HS-A and HS-B.

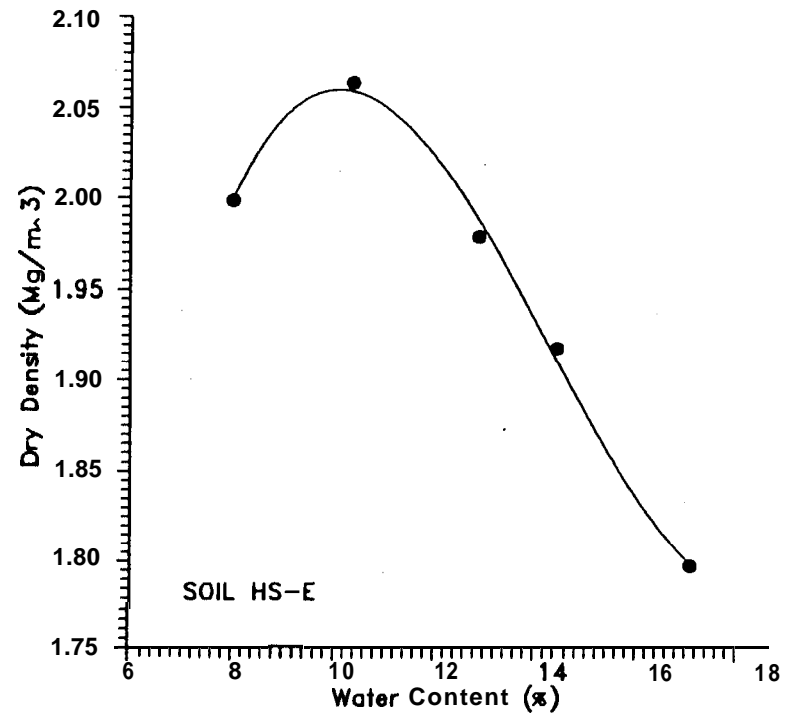
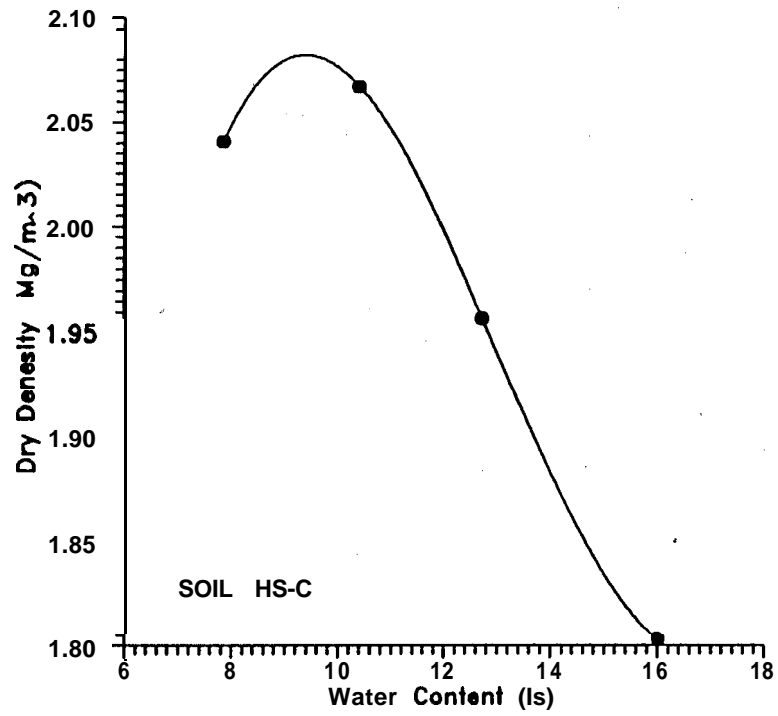


Figure 5.13 Modified Proctor compaction curve for tills HS-C and HS-E.

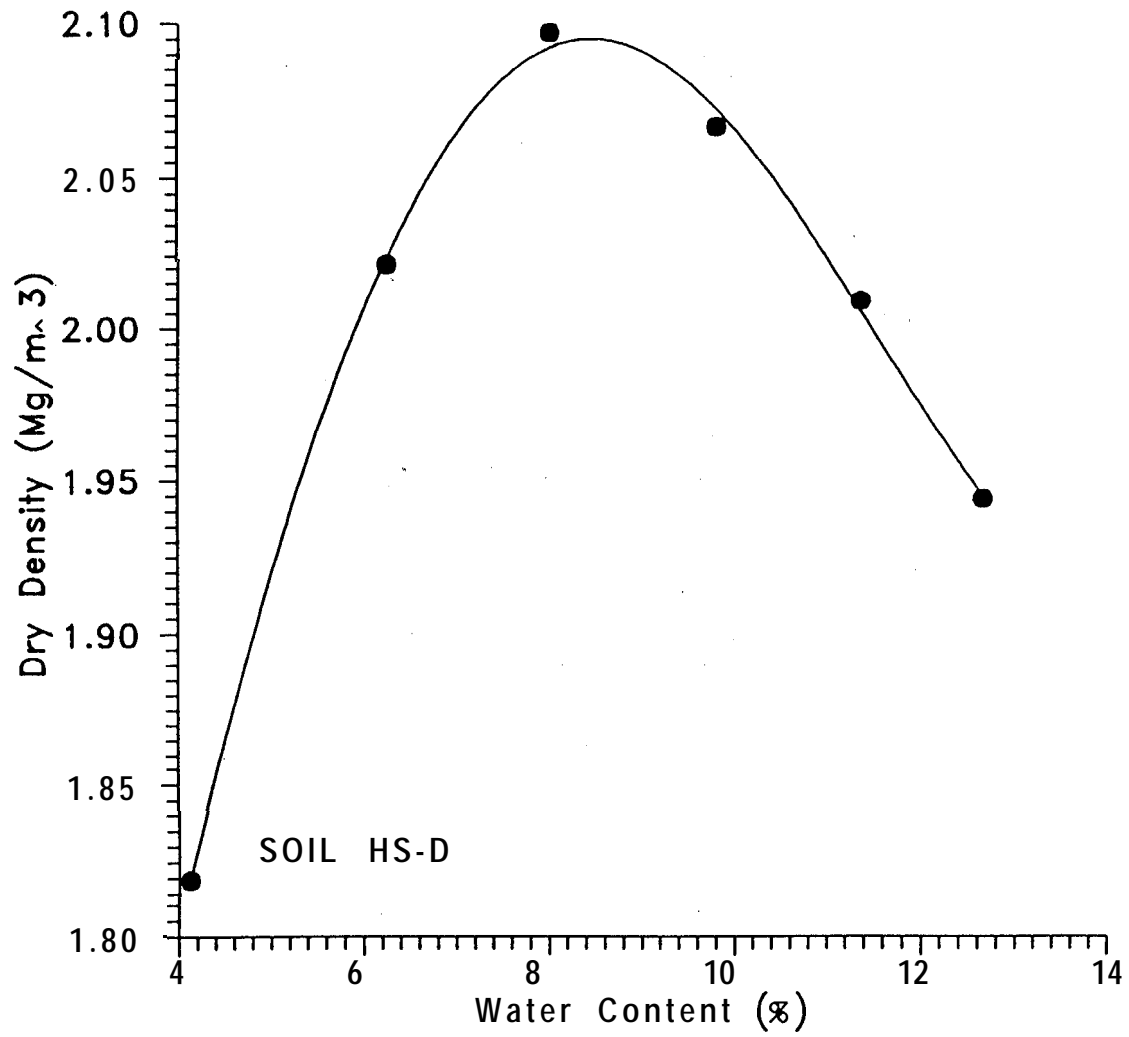


Figure 5.14 Modified Proctor compaction curve for till HS-D.

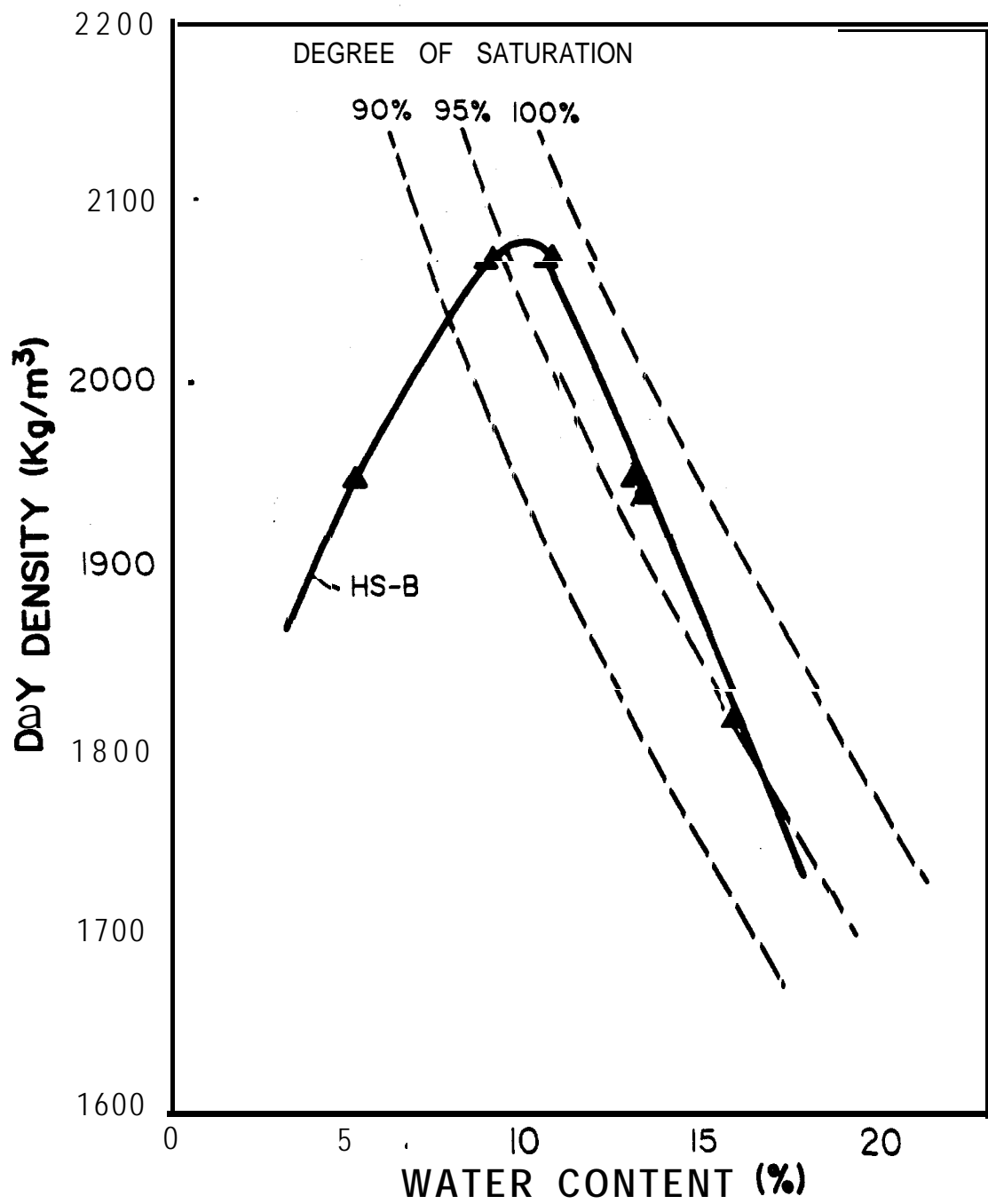


Figure 5.15 Moisture density relationship for till **HS-B**, showing different degrees of saturation.

HEATH STEELE

COVERS - #1

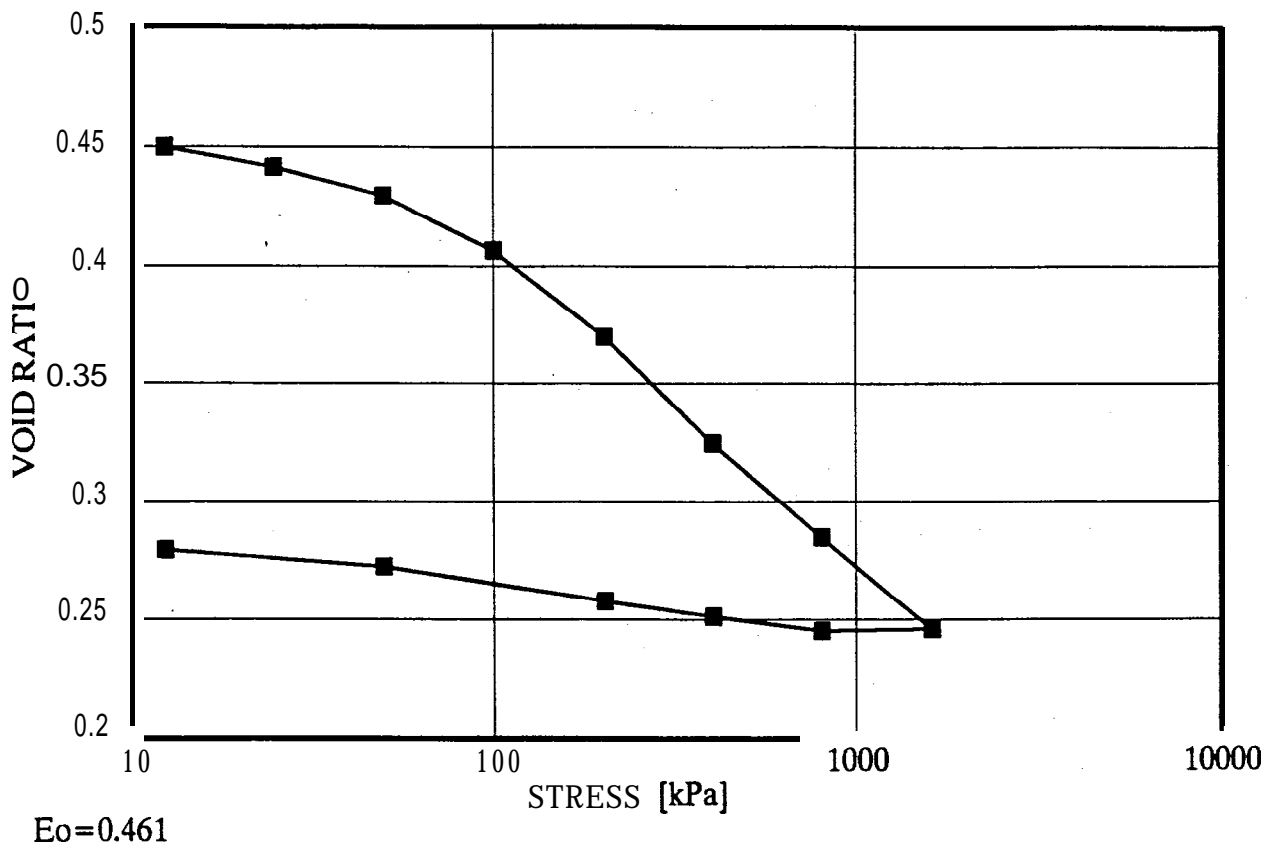


figure 5.16 Void ratio-pressure relationship for till HS-C (test #1, HS-CI).

HEATH STEELE COVERS - #2

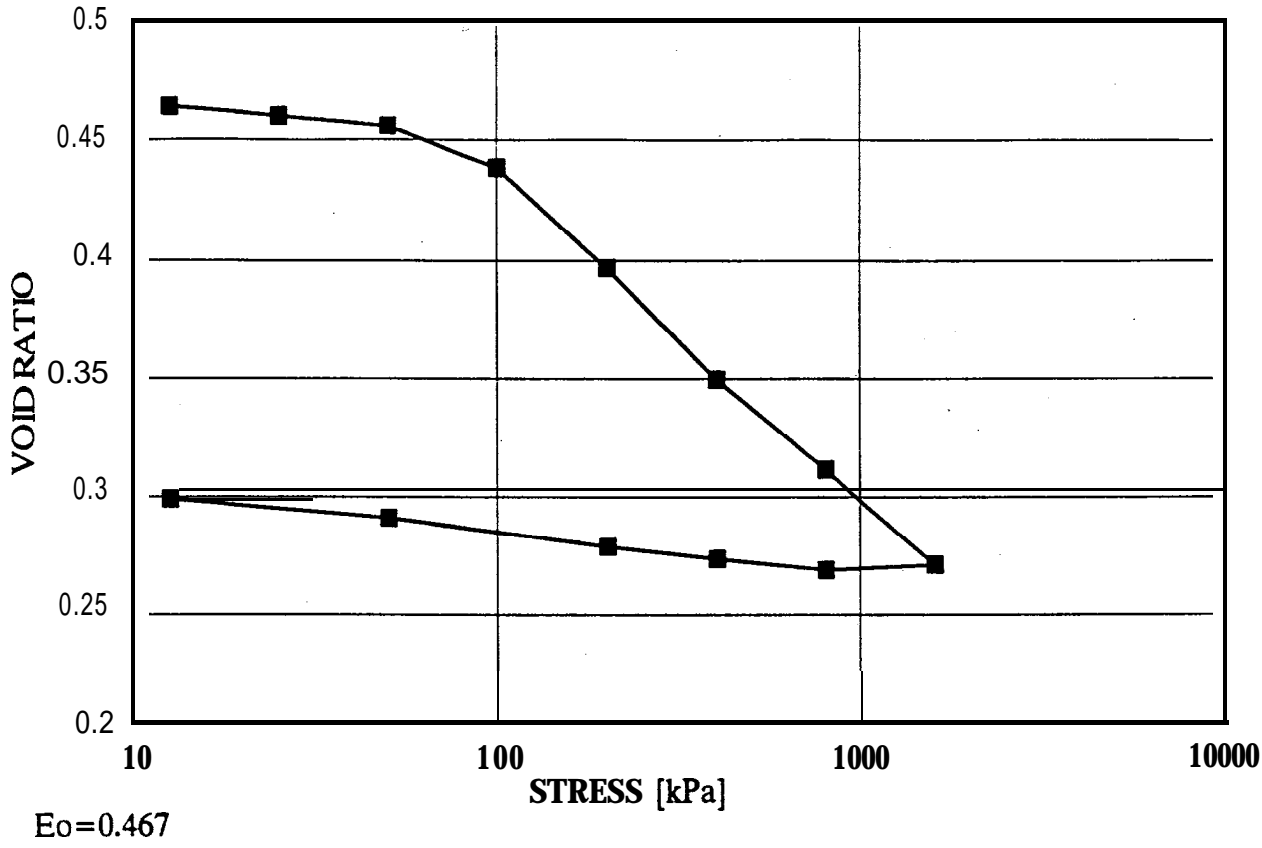


Figure 5.17 Void ratio-pressure relationship for till HS-C (test #2, HS-C2).

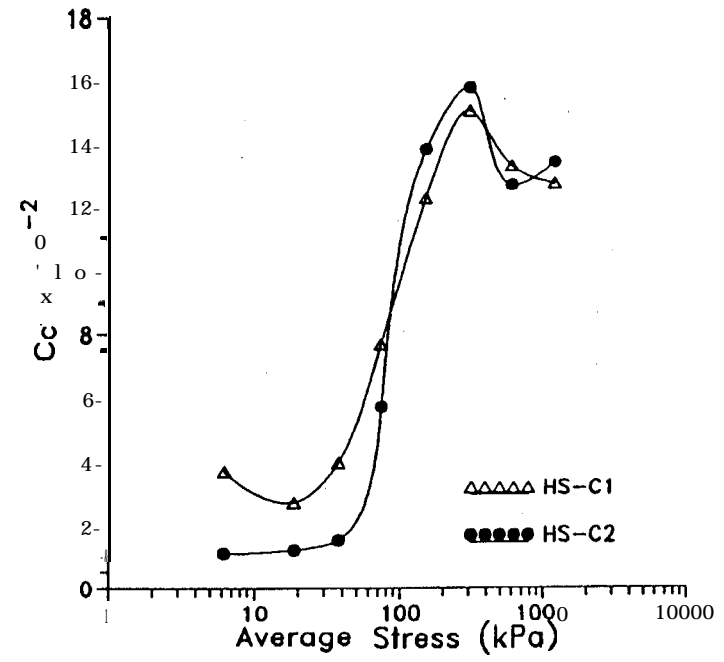
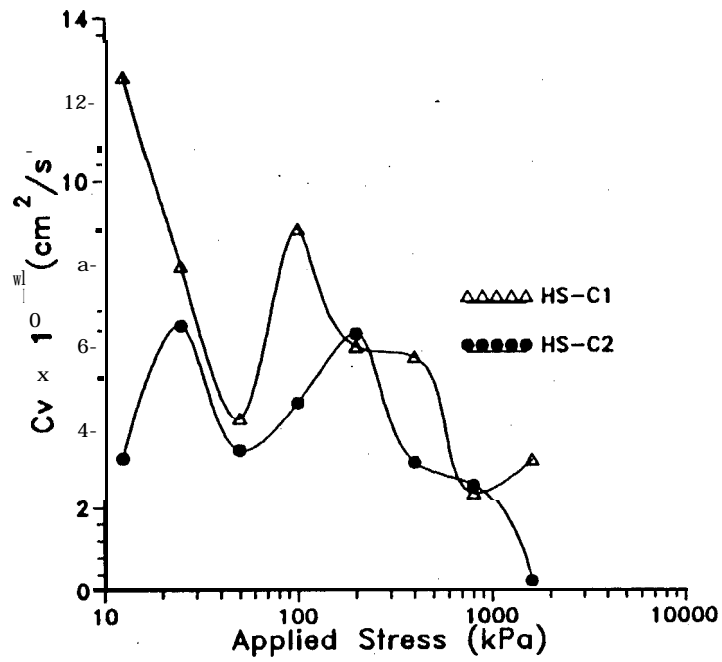


Figure 5.18 Variations of compression index, C_c , and coefficient of consolidation, c_v , with applied stress.

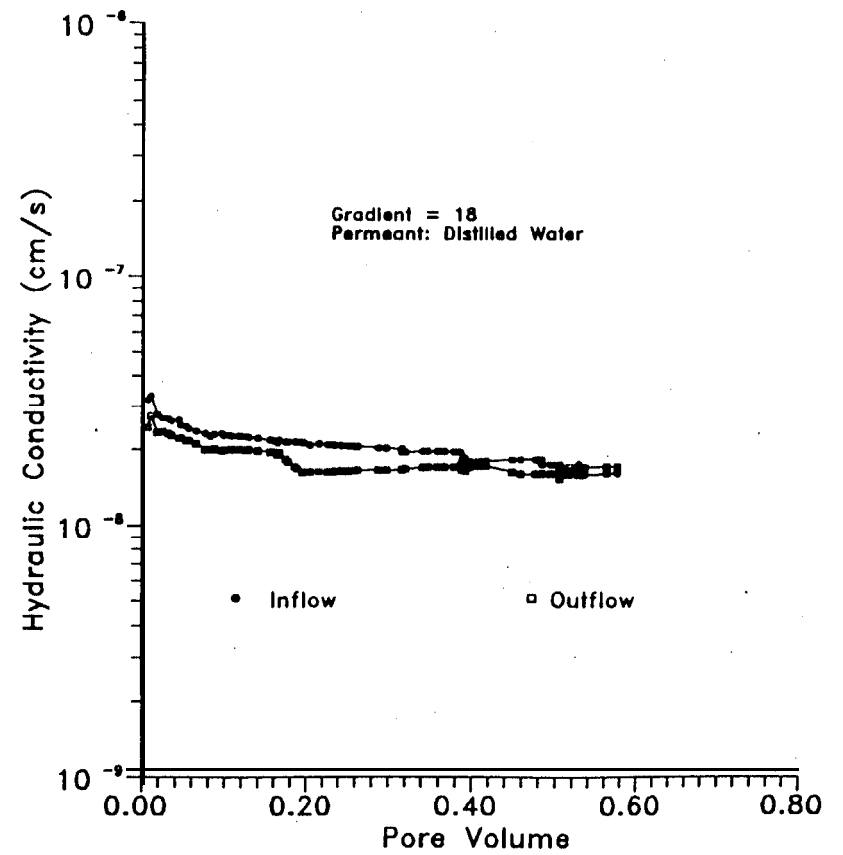
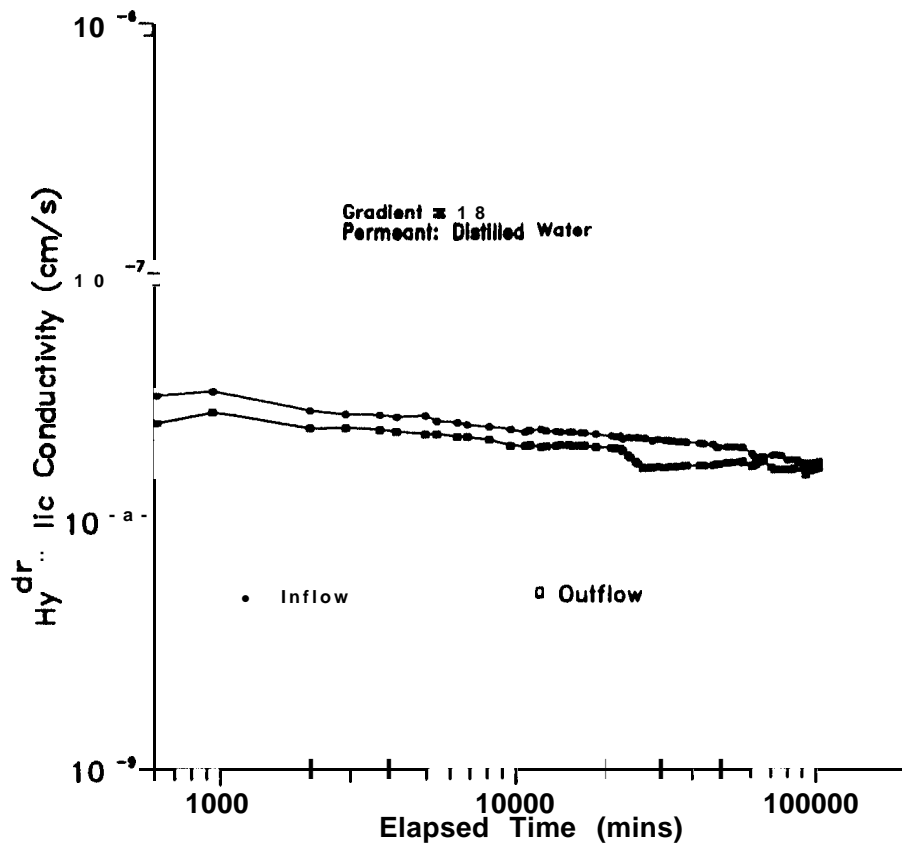


Figure 5.19 The hydraulic conductivity of compacted soil HS-C permeated with distilled water at a hydraulic gradient of 18.

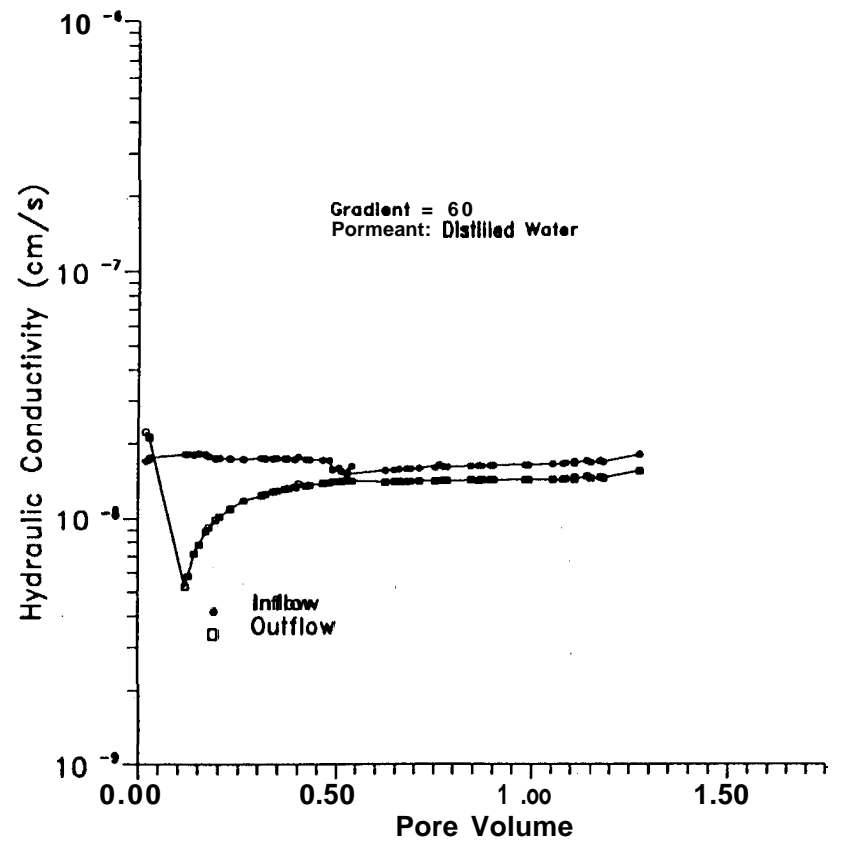
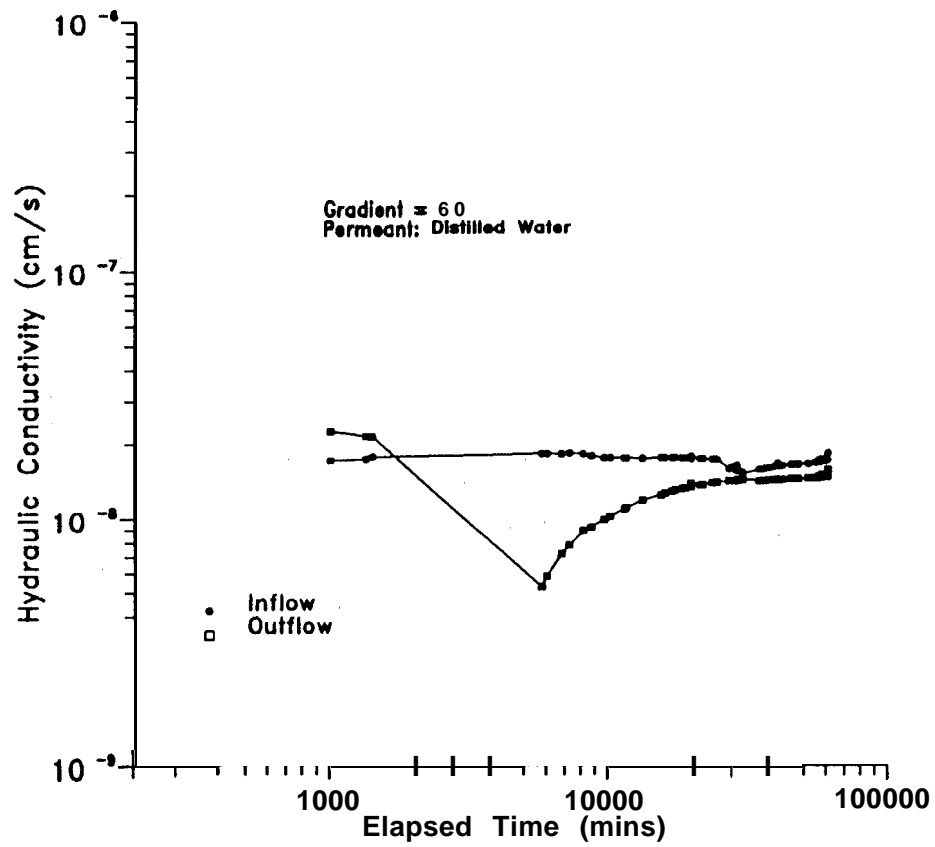


Figure 5.20 The hydraulic conductivity of compacted soil HS-C permeated with distilled water at a hydraulic gradient of 60.

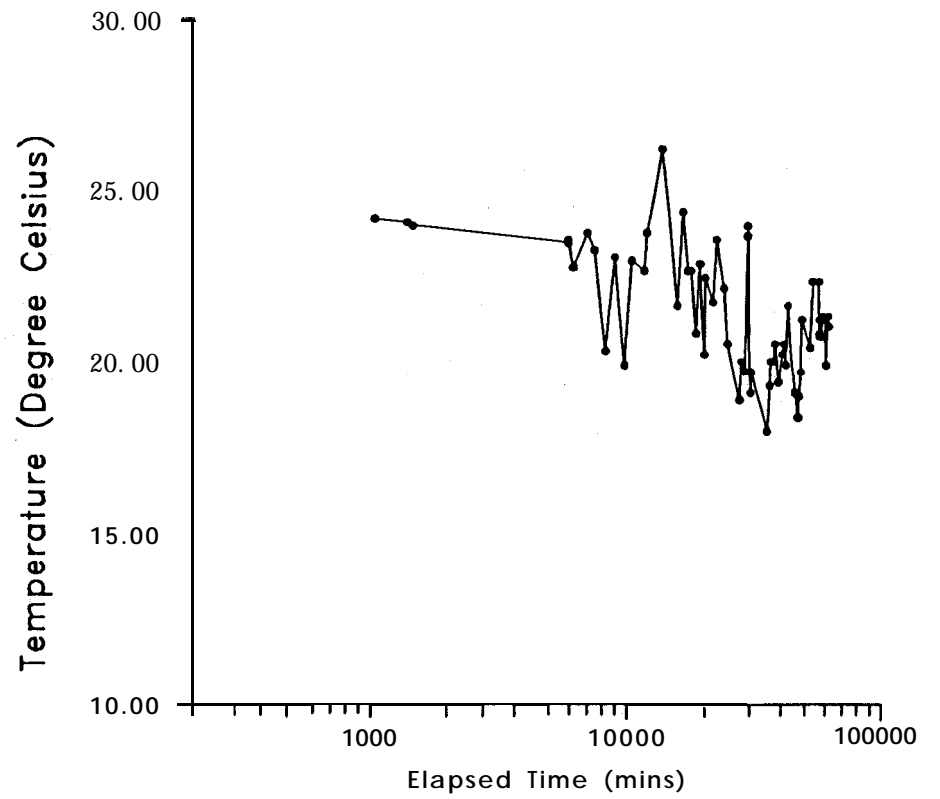
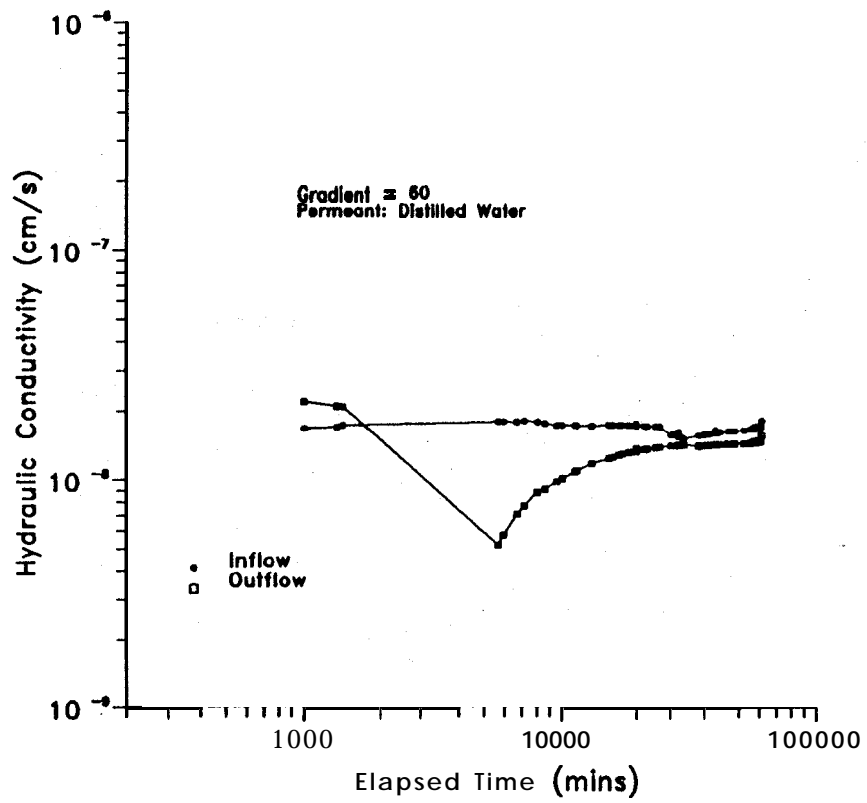


Figure 5.21 Hydraulic conductivity and laboratory temperature versus time.

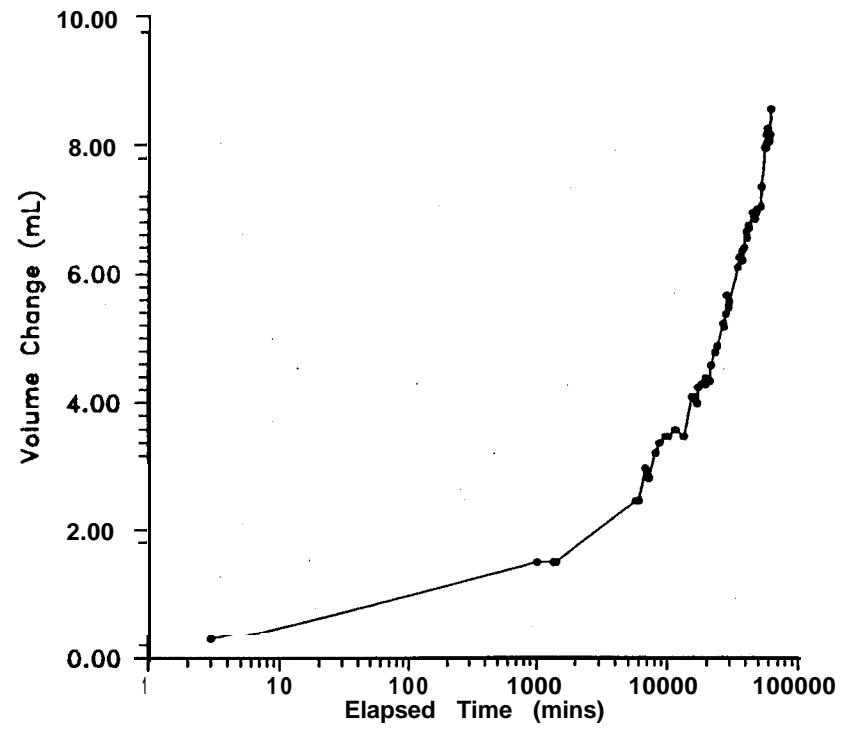
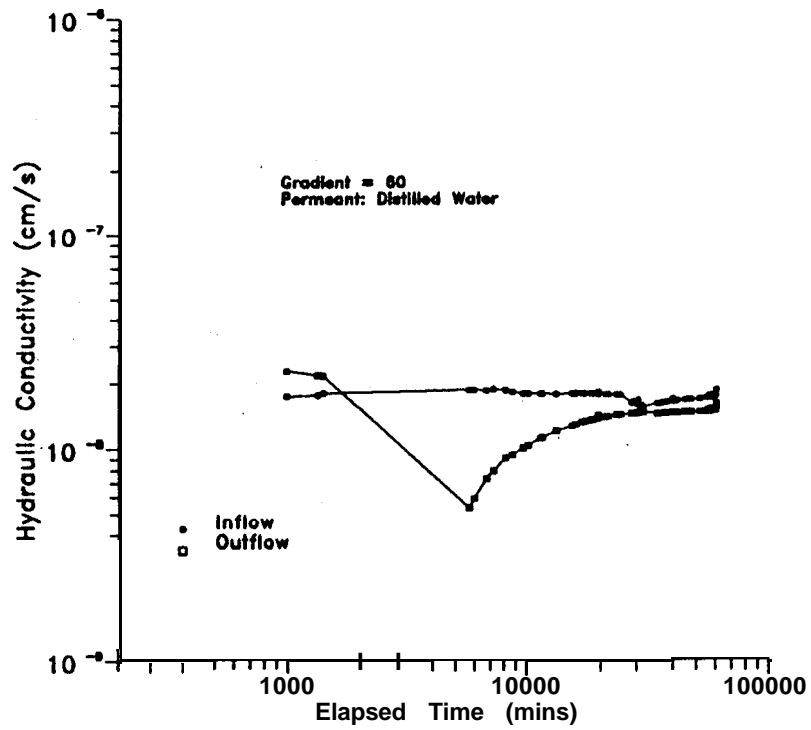


Figure 5.22 Hydraulic conductivity and change in sample volume versus time.

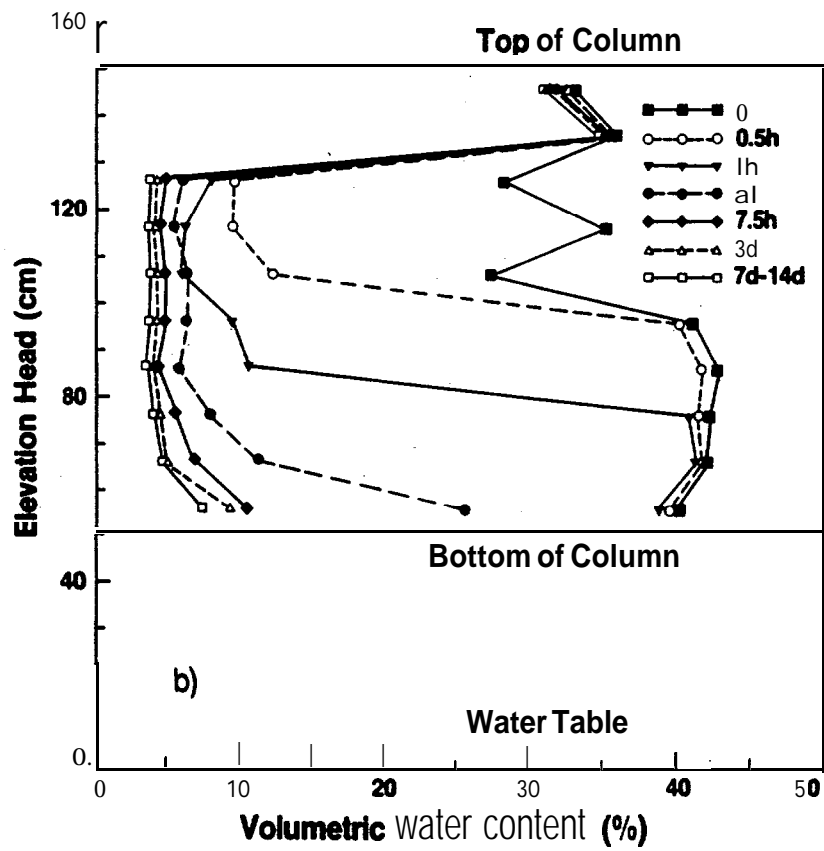
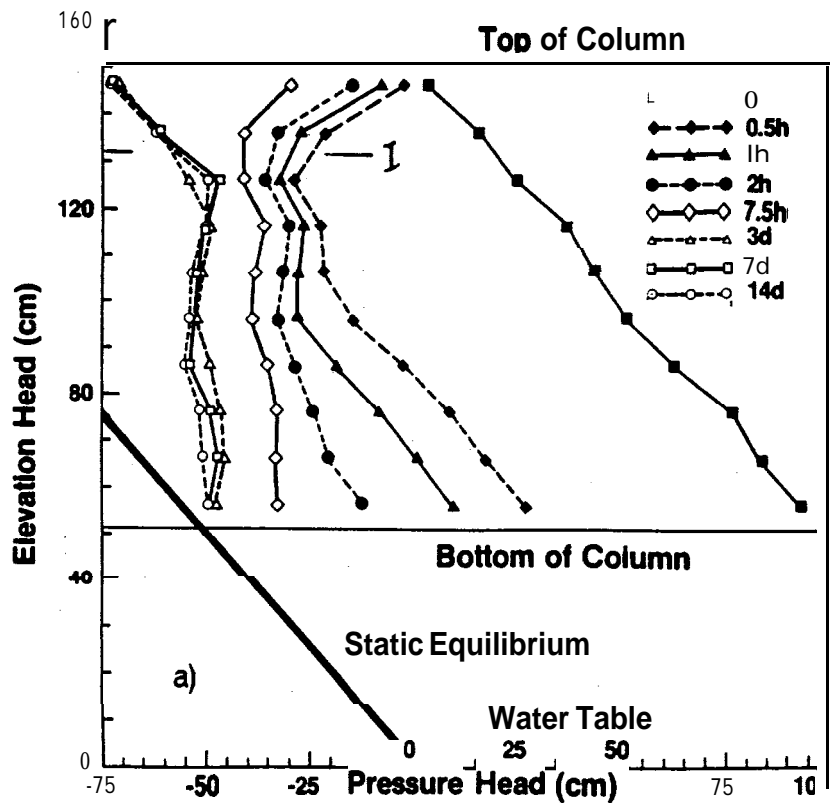


Figure 5.23 Profiles of a) pressure and b) moisture content observed in laboratory column.

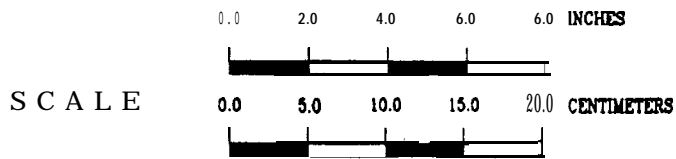
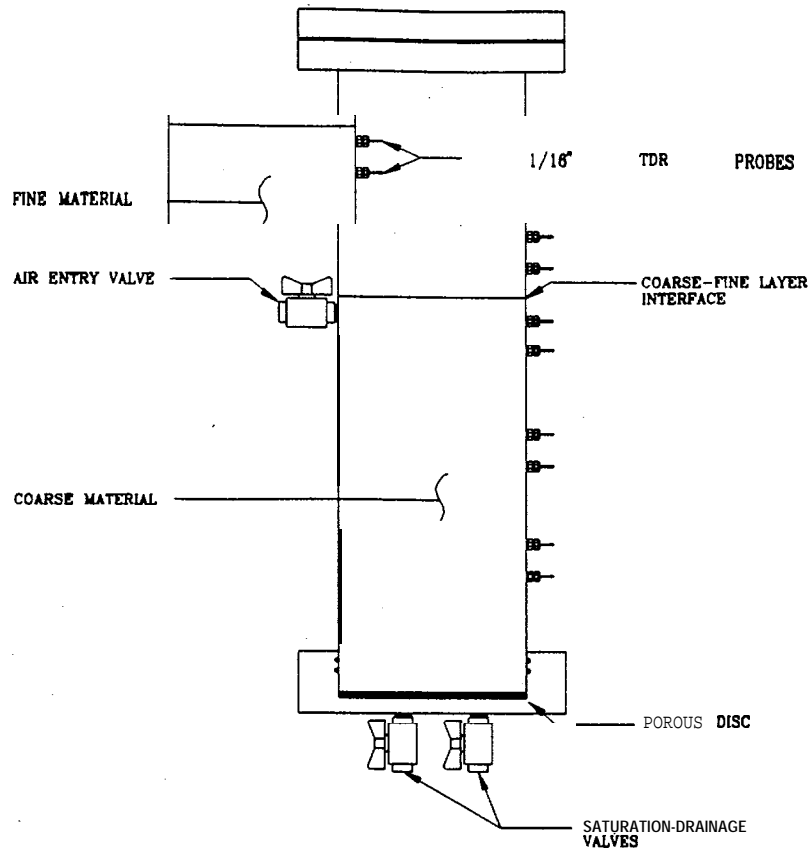


Figure 5.24 A schematic representation of demonstration column for assessing the effectiveness of a composite cover.

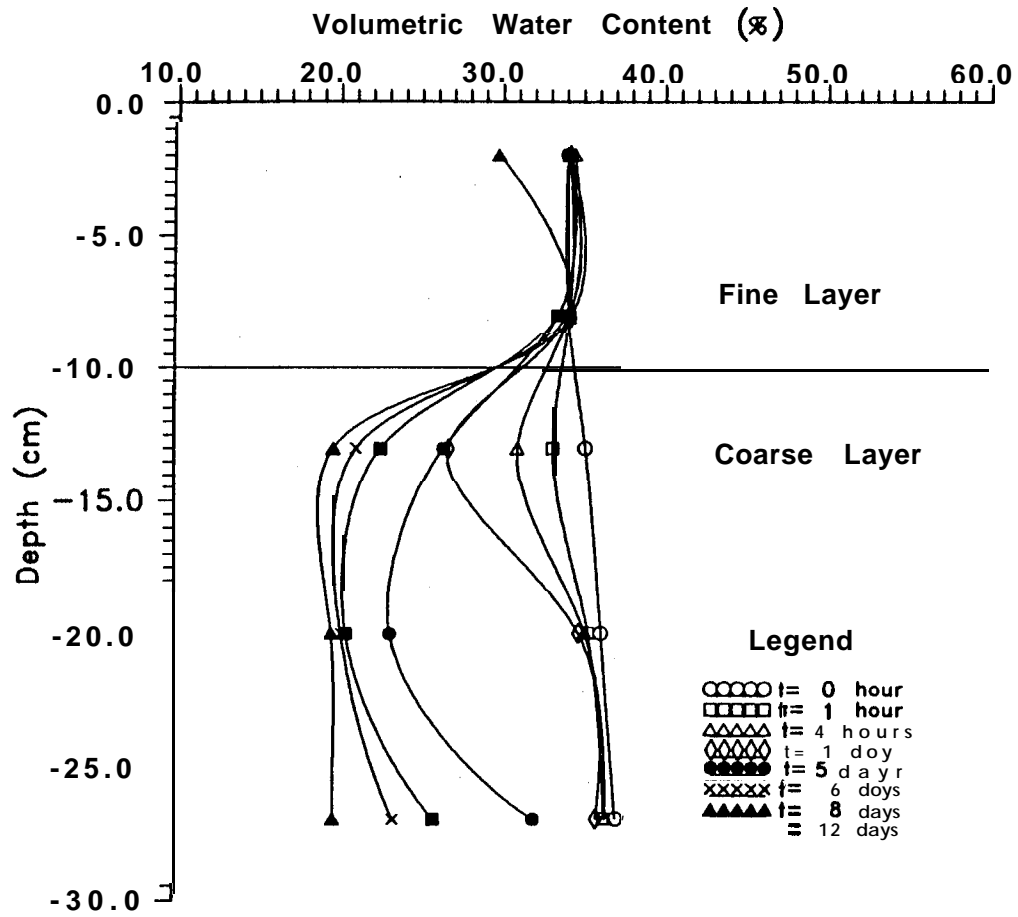


Figure 5.25 Transient moisture content profiles observed in soil HS-C in demonstration column.

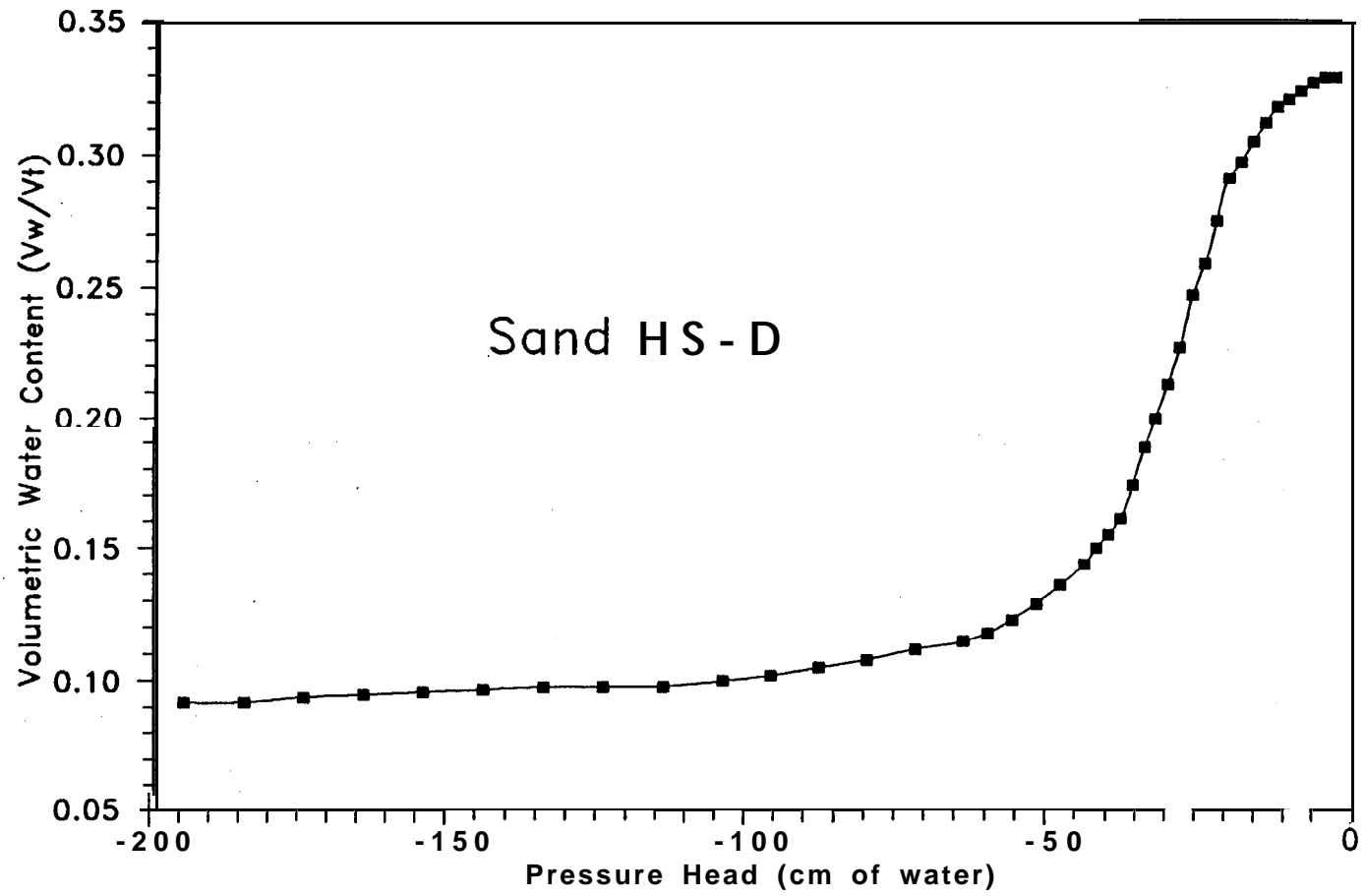


Figure 6.1 Moisture Drainage Curve for Heath Steele Sand HS-D

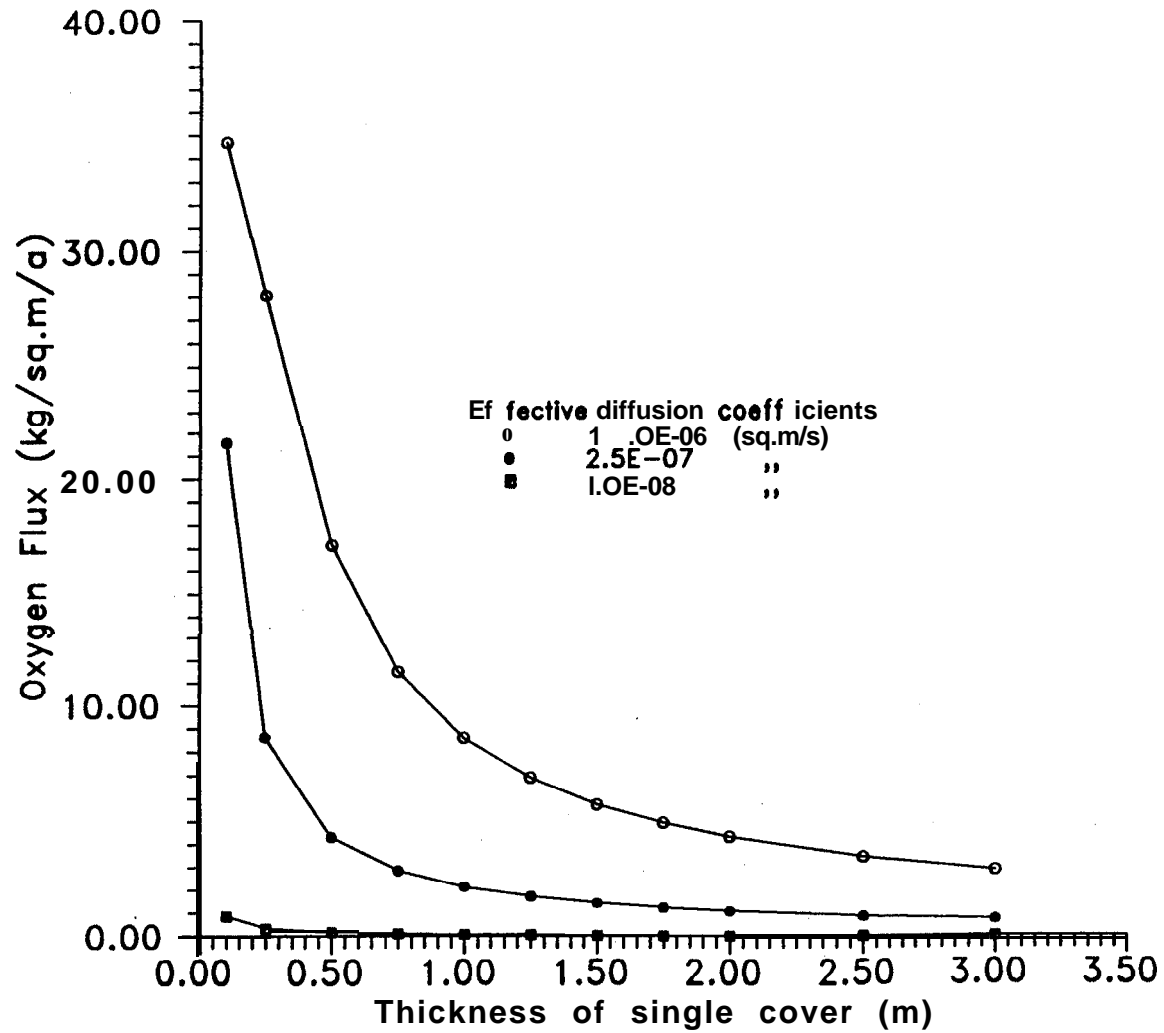


Figure 6.2 Variation of Oxygen Flux with Cover Thickness

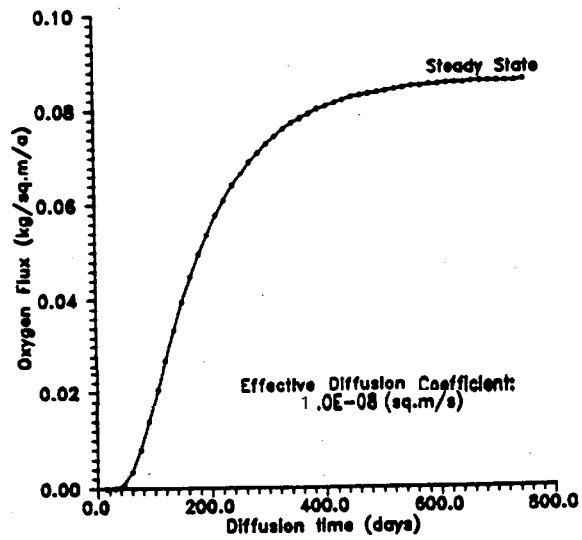
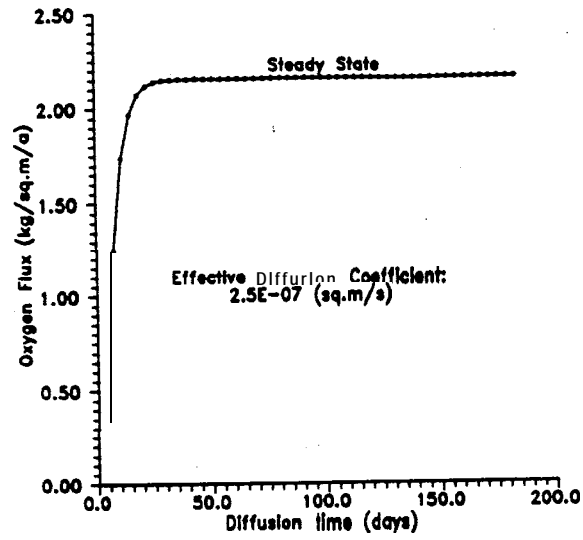
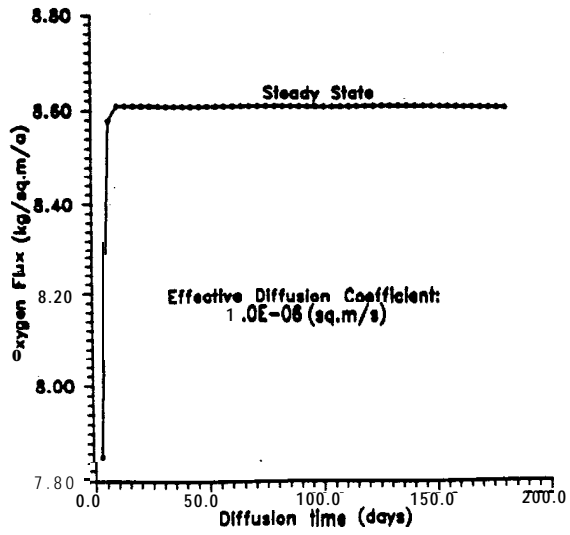


Figure 6.3 Variation of Flux with Diffusion Time for Different Diffusion Coefficients

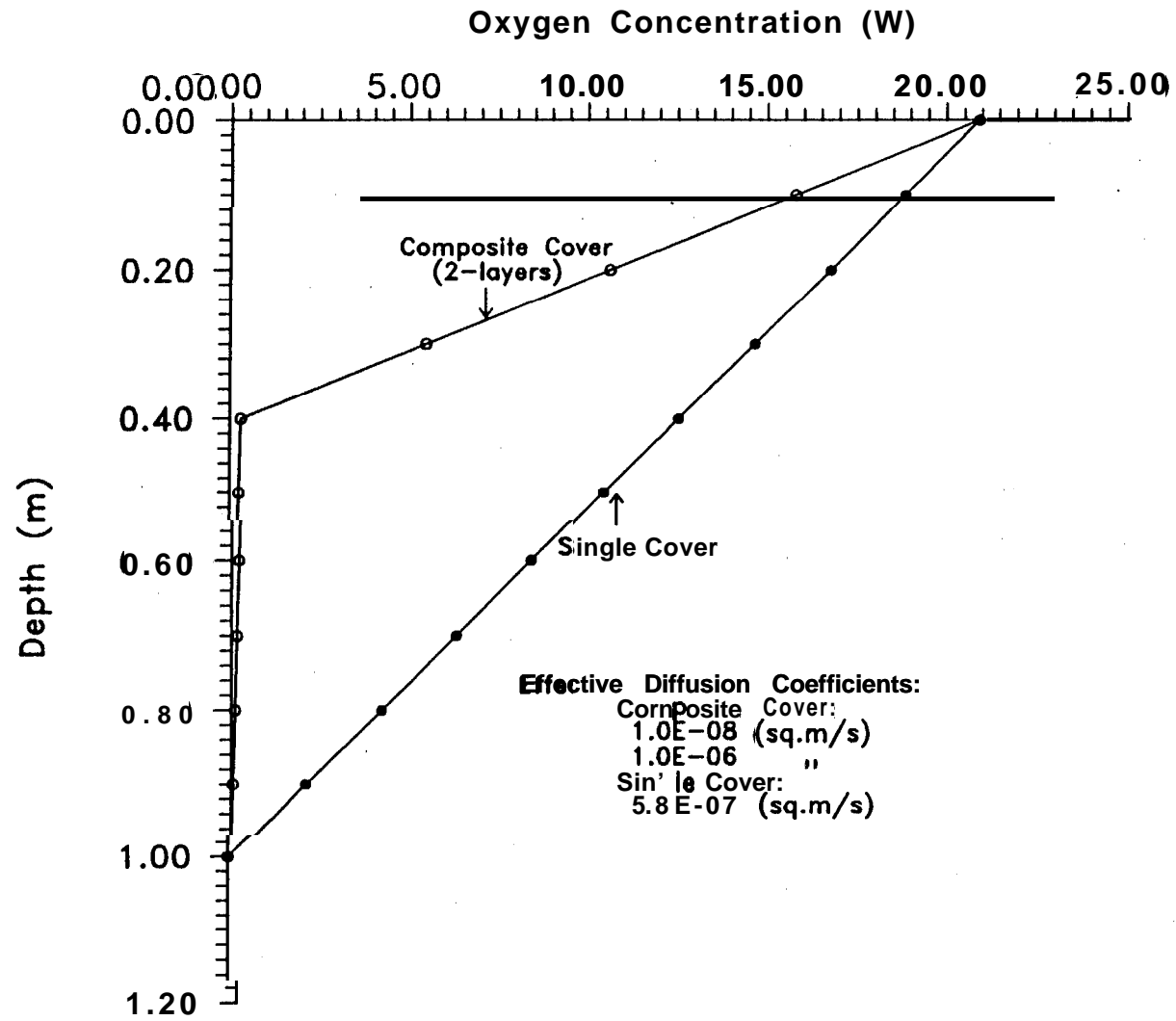


Figure 6.4 Oxygen Profiles in a Conceptualized Single and Two-Layer Cover Systems

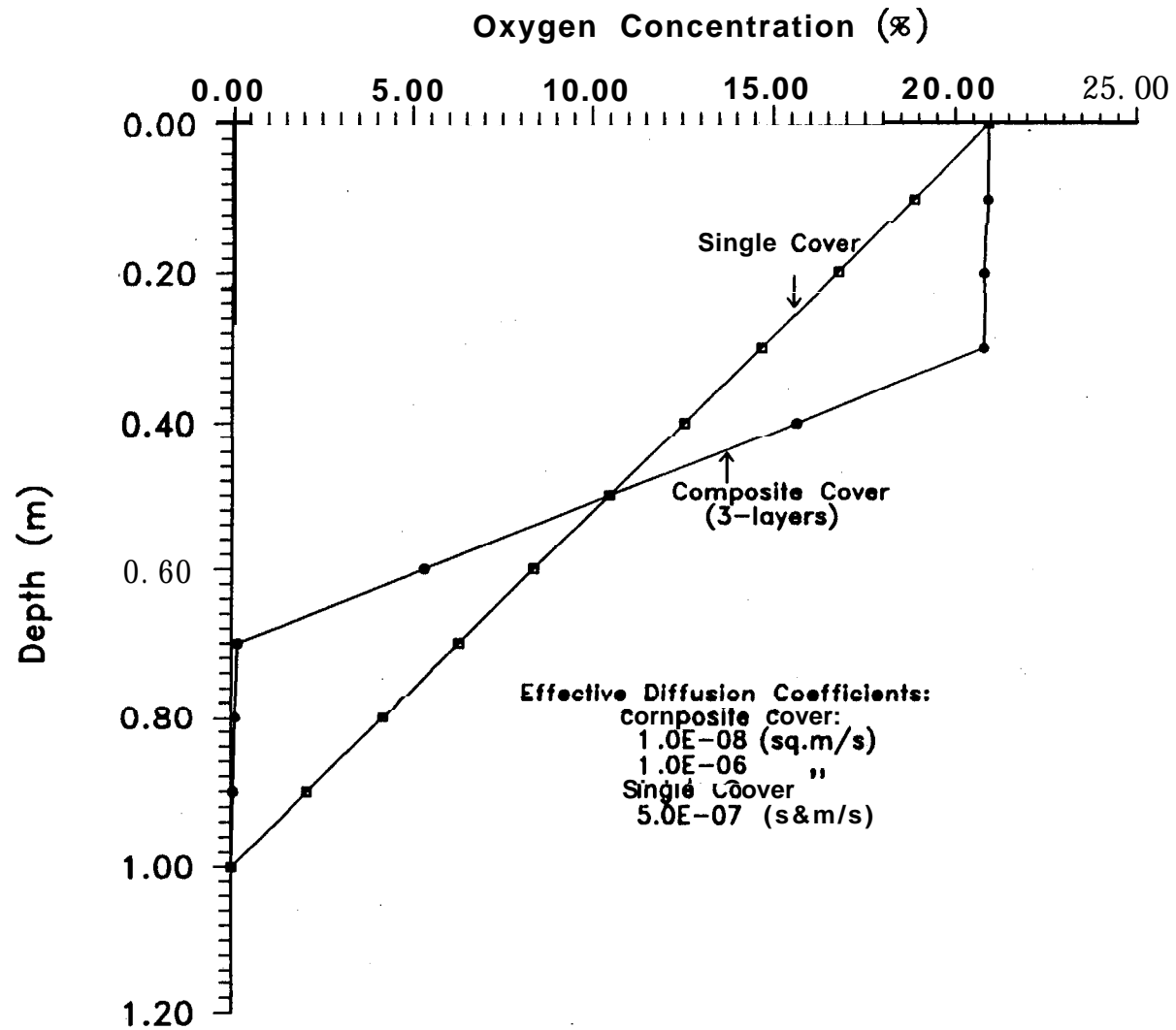


Figure 6.5 Oxygen Profiles in a Conceptualized Single and Three-Layer Cover Systems